MOLECULAR STUDY OF CELL CULTURE MODELS OF PARKINSON'S DISEASE AND HUNTINGTON'S DISEASE

by

Michael Orth, MD

Department of Clinical Neurosciences

Royal Free and University College Medical School

University of London

A thesis submitted, in fulfilment, for the degree

of Doctor of Philosophy

September 2004

ProQuest LLC
789 East Eisenhower Parkway
P.O. Box 1346
Ann Arbor, MI 48106-1346

Abstract

The discovery of the genetic basis of neurodegenerative disorders has enabled the generation of models to study their pathogenesis.

In part one, human embryonic kidney cells with inducible expression of wild-type or mutant G209A α-synuclein modelled increased α-synuclein expression and a familial form of Parkinson's disease, respectively. Both wild-type and mutant α-synuclein were localised to vesicles, some of which were catecholaminergic. Over-expression of wild-type or mutant (G209A) α-synuclein alone did not reduce cell viability, cause oxidative stress or impair mitochondrial function. However, mutant α-synuclein expression enhanced the susceptibility to dopamine toxicity causing increased oxidative stress and cell death. This effect was similar to that of reserpine, an inhibitor of vesicular monoamine uptake, in controls. These results suggest that α-synuclein may play a role in dopamine compartmentalisation. Loss of function conferred by the G209A mutation could therefore increase cytoplasmic dopamine concentrations with subsequent cell damage or death.

In part two, myoblast cell lines were established, and characterised, from the R6/2 mouse model of Huntington's disease (HD). Mutant N-terminal huntingtin transgene over-expression was associated with significantly greater numbers of myotubes suggesting a role of huntingtin in muscle differentiation. In long-term culture, differentiated R6/2 myotubes, but not controls, formed nuclear huntingtin inclusions. Inclusion number depended upon culture medium conditions suggesting that environmental factors might be relevant. This model of HD in non-neuronal post-mitotic cells may be useful to study the pathophysiology of, and possibly the effect of therapeutics on, huntingtin aggregate formation.

The third part examined the suggestion that codon 129 homozygosity of the prion protein (PrP) gene may predispose to sporadic inclusion body myositis (sIBM).

Codon 129 zygosity in 41 sIBM muscle biopsies was not significantly different to results published in population studies in several Western countries suggesting sIBM is not linked to homozygosity at codon 129 of the PrP gene.

Declaration

All of the experimental work in this thesis was performed by the author and the majority of this thesis is published (see Publications).

Acknowledgements

There are many people who I am indebted to in one way or another. These include my supervisors, Tony Schapira and Mark Cooper, who have inspired and encouraged me each in their own way. I am grateful to Tony particularly for helping me to keep an eye on the "bigger picture" beyond the work necessary for this degree and for his ongoing support. To Mark I am grateful for teaching me patiently about scientific thinking and critical appraisal of my own work. Many insights came only after years on this educational path on which he led with great spirit and always in good humour.

This work would have been very difficult without the help of Sarah Tabrizi. Not only did she welcome me with a warm heart but also she had laid some of the foundations for some of this work. And let's not forget the encouraging "tannoy-DAAARLINGS" that brightened up the day! A special thanks has to go to Jan-Willem Taanman for always being there to answer questions and give advice, without him I would have struggled more! And then there were the "fellow strugglers" competing in the number of tissue culture plates and incubator space needed such as Paul Hart and Sion Williams, and later Pras and Chris. Thanks also to Ross King, Michelle and Jane W for help and their companionship, and to the secretary team who are always there to help and always have a friendly word. Last but not least I want to thank my family and friends, some far away "in Europe", for their encouragement, and most of all Maria for her love and support even though this "thing" was taking up a sheer endless amount of time and energy. Without her I would most certainly have become even more of a recluse towards the end. Moltes gracies!

Dedication

To my family; my parents, Hans and Heidi, and my sister, Meike

Index **page**

CHAPTER 2. Material and Methods

List of Tables

List of Figures

Abbreviations

6-OHDA: 6-hydroxydopamine
ADP: adenosine diphosphate
ATP: adenosine triphosphate
AIF: apoptosis inducing factor
Apaf: apoptosis associated factor
APES: 3-aminopropyltriethoxysilane
ARJPD: autosomal recessive juvenile PD
BCA: bicinchoninic acid copper assay
BID: BCl_2-interacting domain
BSA: bovine serum albumine
BSE: bovine spongiform encephalopathy
CCCP: m-chlorophenylhydrazone
CDNA: complementary DNA
CJD: Creutzfeld-Jacob disease
CoA: coenzyme A
CoQ_1: coenzyme Q
CRE: cAMP response element
CS: citrate synthase
DAPI: 4',6-diamidine-2-phenylindol
DAT: dopamine uptake transporter
$DiOC_{6(3)}$: 3,3'-dihexyloacarbocyanine
DMEM: Dulbecco's modified Eagle medium
DOPAC: 3,4-dihydroxyphenylacetic acid
DOPAL: 3,4-dihydroxyphenylacetaldehyde
DOPET: 3,4-dihydroxyphenylethanol
DRPLA: dentatorubropallidolysian atrophy
DTNB: 5-5'-dithiobisnitrobenzoic acid
FACS: fluorescence associated cell sorter
FADD: Fas associated death domain
EcRE: Ecdysone response element
E2: ubiquitin conjugating enzyme
E3: ubiquitin ligase
FAPyG: 2,6-diamino-4-hydroxy-5-formidopyrimidine
FITC: Fluorescein
FSC: forward angle light scatter
FTDP: fronto- temporal dementia with parkinsonism
FasL: Fas ligand

G49, G50, G65, G66: Department of Clinical Neuroscience, RFH+UCLMS, internal code for oligonucleotide primers

GSH: glutathione

HA: haemagglutinin

HAP1: huntingtin-associated protein 1

HEAT: huntingtin elongation factor

HEK 293: human embryonic kidney 293 cells

HD Huntington's disease

HIP1: huntingtin-interacting protein 1

IAF: inhibitor of apoptosis

ICAD: inhibitory protein of the caspase activated DNAase

KCN: potassium cyanide

LB: Lewy body

LDH: Lactate Dehydrogenase

MAB: mouse monoclonal antibody

MEF: mitochondrial enriched fraction

MEM: Minimal Essential Medium

MOA: monoamine oxidase

MOMP: mitochondrial outer membrane permeabilisation

MPP+: N-methyl-4-phenylpyridinium

MRC: mitochondrial respiratory chain

MPTP: 1-methyl-4-phenyl-1,2,3,6 tetrahydropyridine

MtDNA: Mitochondrial DNA

NAT: noradrenalin transporters

NF-κB: nuclear factor kappa B

NMDA: N-methyl-D-aspartate

NOS: nitric oxide synthases

PARP: poly(ADP)ribose polymerase

Par-4: prostate apoptosis response-4 protein

Paraquat: N,N'-dimethyl-4-4'biperidinium

PBS: physiologically buffered saline

PCR: Polymerase chain reaction

PD: Parkinson's disease (PD

peroxyl radical (-COO·-)

PI: propidium iodide

PINK1: PTEN induced kinase

PNS: post-nuclear supernatant

PolyQ: polyglutamine

PRNP: Prion protein gene

PrP: prion protein

PT: permeability transition pore

PUVA: polyunsaturated fatty acids

PVDF: polyvinylidene difluoride

RNS: reactive nitrogen species

ROS: Reactive oxygen species

RxR: retinoid X receptor

SBMA: spinobulbar muscular atrophy

SCA: spinocerebellar ataxia

SIBM: sporadic inclusion body myositis

SOD: superoxide dismutase

Sp1: specificity protein-1

SSC: right angle light scatter

TBE: Tris borate EDTA buffer

TH: tyrosine hydroxylase

TNFR: tumour necrosis factor receptor

TRADD: tumour necrosis factor receptor associated death domain

TRNA: transfer RNA

TSE: transmissible spongiform encephalopathies

UCH-L1: Ubiquitin carboxyhydrolase -L1

UPS: ubiquitin-proteasome system

VAMP: vesicle associated membrane protein

VgEcR: Ecdysone receptor from *drosophila* modified with the VP16 transactivation domain

VMAT: Vesicular monoamine transporters

Δp: protonelectrochemical gradient

$\Delta\Psi_m$: mitochondrial membrane potential

ρ^0 : mtDNA-less cells

CHAPTER 1: General introduction

1.1. Introduction

Neurodegenerative diseases are common diseases; in the United States an estimated 4 million people have the most common neurodegenerative disease, Alzheimer's disease, and about 1 million suffer from Parkinson's disease (Kawas and Katzman, 1999; Lilienfeld, 1994), with a similar prevalence in Europe (de Rijk et al., 2000). Other neurodegenerative diseases such as Huntington's disease, Amyotrophic Lateral Sclerosis, prion disease, or fronto-temporal dementia are less common.

The increase in life expectancy across the world has raised further concern about the incidence of neurodegenerative diseases, in particular Alzheimer's disease and Parkinson's disease. The incidence of these diseases rises with age so that the prevalence of Alzheimer's disease is about 1 in 10,000 at the age of 60 and 1 in 3 among individuals at the age of 85 (Evans et al., 1989; Katzman, 1986). It has been estimated that in the United States by 2025 more than 10 million people will suffer from Alzheimer's disease and this number may rise to 20 million by 2050 (Kawas and Katzman, 1999). Age was also found to be the most important risk factor for Parkinson's disease with an estimated prevalence of 1 to 2% in the population over 65 years of age (de Rijk et al., 2000). Close to 50% of individuals at the age of 85 in the community showed at least one symptom or sign of Parkinson's disease (Bennett et al., 1996).

The death of neurones characterises many neurodegenerative diseases including Parkinson's disease, Huntington's disease, stroke, prion disorders, and amyotrophic lateral sclerosis. Since the capacity of the central nervous system for regeneration is severely limited it is paramount to prevent neuronal death. Research into what causes neuronal cell death in neurodegenerative diseases promises

valuable insight into their pathogenesis, which may ultimately help design treatments. This is important not only because it would help treat millions of patients but also because of the socio-economic burden associated with neurodegenerative diseases.

This thesis investigated the molecular pathology of 3 neurodegenerative diseases. The first part describes a cell culture model of Parkinson's disease using a stable inducible system, the Ecdysone Mammalian Expression system. This model allowed the investigation of α-synuclein gene expression, both wild-type and G209A mutant, and it's relationship to cellular dysfunction, in particular oxidative stress, dopamine toxicity and mitochondrial function. The second part of the thesis describes a cell culture model of Huntington's disease established in myoblast cell cultures from transgenic Huntington's disease mice (R6/2). In this model, the relevance of over-expression of the human transgene for protein aggregation and myotube differentiation was examined. Finally, the last part of the thesis tested the hypothesis that homozygosity at the common polymorphism at codon 129 of the prion protein gene might be more common in sporadic inclusion body myositis.

This introductory chapter reviews basic mechanisms underlying, and pathways leading to, neuronal cell death. These include mitochondrial function, oxidative stress and excitotoxicity, and protein aggregation and the ubiquitin-proteasome pathway.

1.1.1. Mitochondrial function

Mitochondria are present in every cell. The mitochondrial respiratory chain and oxidative phosphorylation provide the majority of energy in the form of ATP. The mitochondrial respiratory chain complexes are located on the inner mitochondrial membrane. Of the five complexes, complex I (NADH CoQ10 reductase) is the

largest with 41 subunits, complex III (ubiquinol cytochrome c reductase) has 11 subunits, complex IV (cytochrome oxidase, COX) has 13 subunits and complex V (ATPase) has 14 subunits. Complex II (succinate ubiquinone oxidoreductase) with 4 subunits is the only complex completely encoded by the nucleus.

Tissues with high energy demands such as brain, skeletal and cardiac muscle contain the greatest number of mitochondria. Mitochondria contain the only source of extranuclear DNA. Each mitochondrion harbours 2 to 10 molecules of mitochondrial DNA (mtDNA), which is a 16.5 kilobase circular double-stranded molecule consisting of a heavy (H) and a light (L) chain. Mt DNA encodes 22 transfer RNAs (tRNAs) and 12S and 16S ribosomal RNA as well as 13 proteins all part of the respiratory chain and oxidative phosphorylation system. Of these13 polypeptides 7 are subunits of complex I, one is a subunit of complex III, three are subunits of complex IV and 2 are subunits of complex V. The remaining 70 subunits of mitochondrial respiratory chain are encoded by the nucleus and imported into mitochondria. Nuclear DNA also encodes proteins for mtDNA replication, transcription, translation, repair and regulation of mitochondrial respiratory chain assembly.

MtDNA is very compact, with 93% of the sequence encoding genes and virtually no introns. There is no protective histone coat and mtDNA repair may be slower than nuclear DNA repair with subsequent accumulation of base damage (Yakes and Van Houten, 1997). Mitochondria are highly active metabolically. Fuel molecules such as carbohydrates, fatty acids and amino acids are oxidised in the citric acid cycle within the mitochondrial matrix leading to the production of NADH and $FADH_2$. Glycolysis and fatty acid oxidation are other sources of NADH and $FADH_2$, which contain a pair of electrons with high transfer potential. The transfer of these electrons from NADH or $FADH_2$ to O_2 through protein complexes located in the inner mitochondrial membrane generates a pH gradient and a transmembrane

electric potential. Subsequently ADP is phosporylated to ATP when electrons flow back to the mitochondrial matrix. This process is called oxidative phosphorylation. The citric acid cycle and oxidative phosphorylation also generate free radicals in the form of superoxide ions. Reactive oxygen species are thought to contribute to the high mutation rate of mtDNA (Shenkar et al., 1996).

Mitochondria serve a variety of functions within the cell other than the oxidative phosphorylation of ADP to ATP. A number of metabolic processes take place in the mitochondrial matrix including fatty acid oxidation, amino acid metabolism, heme synthesis, iron-sulfur synthesis, ubiquinone syntheses, and mitochondrial DNA replication and repair. Mitochondria play a critical role in the regulation of programmed cell death with pro- and antiapoptotic proteins being localised at the outer mitochondrial membrane and proapoptotic cytochrome c and apoptosis inducing factors (AIFs) located in the mitochondrial matrix (see next section). In addition, free radicals are produced within mitochondria, which also contain anti-oxidant defences. An excess of free radical production or diminished anti-oxidant defences can lead to oxidative stress within cells (see section 1.1.3). Mitochondria maintain a protonelectrochemical gradient (Δp) across their inner membrane and serve to buffer cellular calcium levels, key factors for ATP production and mitochondrial integrity (see section 1.1.5).

1.1.2.Types of cell death

1.1.2.1. Necrosis

Neuronal necrotic cell death occurs with abrupt cessation of the supply of oxygen and/or glucose, for example in anoxia, ischaemia, or associated with trauma (Emery et al., 1998; Linnik et al., 1993). Cells are unable to produce the ATP necessary to maintain their integrity and function; histologically, nucleus and mitochondria swell

followed by rapid lysis of cellular organelles. The DNA is degraded enzymatically at random.

1.1.2.2. Programmed cell death

Programmed cell death occurs following the activation of an intrinsic cellular programme. In multicellular organisms development, organ morphogenesis, and the regulation of defence mechanisms to remove infected or otherwise damaged cells require programmed cell death. Apoptosis describes one morphological form of cells undergoing programmed cell death. It is characterised morphologically by reduced cell volume, condensation of chromatin and fragmented nuclei with preservation of cellular membranes. Apoptotic cells exhibit "apoptotic bodies" containing cellular material and are recognised and removed by phagocytes.

Programmed cell death needs to be tightly regulated. Diseases such as neurodegenerative diseases and immunodeficiency may be linked to an excess of programmed cell death with the untimely death of important cells such as neurones or lymphocytes. Indeed, evidence to suggest involvement of programmed cell death has been provided for diseases such as Alzheimer's disease, Amyotrophic Lateral Sclerosis, Parkinson's disease and Huntington's disease (for a review see (Vila and Przedborski, 2003), and sections 3.1.10 and 4.1.9). Understanding the mechanisms of programmed cell death in neurodegeneration may be relevant to the development of treatment for these devastating diseases.

The caspase family

Key to programmed cell death is the activation of a cascade of proteolytic enzymes called caspases. Caspases exist in almost all cells. Intracellular signalling processes triggered by intracellular damage or lack of trophic factors can activate caspases. In mammals, 15 members of the caspase family have been identified; procaspases 2,

8, 9 and 10 are known as initiators whereas procaspases 3, 6 and 7 are known as effectors. Initiator caspase activation precedes effector caspase activation. Eventually, activated caspase-3 cleaves an inhibitory protein of the caspase activated DNAase (ICAD), which can then act as an endonuclease to digest DNA (Enari et al., 1998; Sakahira et al., 1998). This is followed by mitochondrial damage, chromatin condensation, DNA fragmentation and nuclear membrane disruption, and ultimately cell death.

Mitochondrial involvement

Mitochondria play a pivotal role in programmed cell death (Green and Kroemer, 2004) (Figure 1.1). One mechanism involves the inner mitochondrial membrane while the other involves the Bcl 2 family of programmed cell death regulating proteins situated at the outer mitochondrial membrane. In the first mechanism a pore in the inner mitochondrial membrane, the permeability transition pore (PT) opens and allows the flow of water and molecules smaller than about 1.5kD. This leads to an equilibration of ions across the inner mitochondrial membrane and thus to a loss of the mitochondrial membrane potential ($\Delta\Psi_m$). The entry of water leads to swelling of the mitochondrial matrix, and subsequently the outer mitochondrial membrane may become permeable. Situated at the outer mitochondrial membrane, the Bcl 2 family helps regulate programmed cell death. Some of its members promote programmed cell death (Bax and Bak) whereas others have anti-programmed cell death activities (Bcl 2 and Bcl X_L) (Gross et al., 1999). They play an important part in the regulation of mitochondrial integrity, particularly mitochondrial outer membrane permeabilisation (Green and Kroemer, 2004), and the release of mitochondrial pro-apoptotic factors such as cytochrome c, apoptosis-inducing factor (AIF) or Smac/Diablo (Gross et al., 1999).

Initiation of programmed cell death

Programmed cell death can be initiated following extracellular or intracellular signals (Figure 1.1). In the extrinsic pathway activation of cell surface receptors such as Fas/CD95 or tumour necrosis factor receptor 1 (TNFR 1) are activated when they bind their respective ligands (Fas ligand for Fas/CD95 or tumour necrosis factor α for TNFR 1). This leads to the association of an intracellular death domain that is part of the receptor with a death effector domain (FADD, Fas associated death domain, and TRADD, tumour necrosis factor receptor associated death domain respectively). Subsequently, procaspase 8 is activated followed by downstream caspase activation and cell death. In the intrinsic, receptor independent pathway, in response to e.g. oxidative stress or the formation of toxic aggregates pro-apoptotic molecules such as Bax translocate to mitochondria to induce mitochondrial outer membrane permeabilisation and release of mitochondrial pro-apoptotic cytochrome c, AIF, or Smac/Diablo. In the cytosol cytochrome c and AIF form a complex with procaspase 9 and Apaf 1 and then activate the effector caspase 3. Endoplasmatic reticulum stress induced by abnormal calcium homoeostasis or increase in the concentration of unfolded proteins within the endoplasmatic reticulum can also induce programmed cell death by activation of caspase 12 and subsequent activation of caspase 9 (Morishima et al., 2002; Nakagawa et al., 2000).

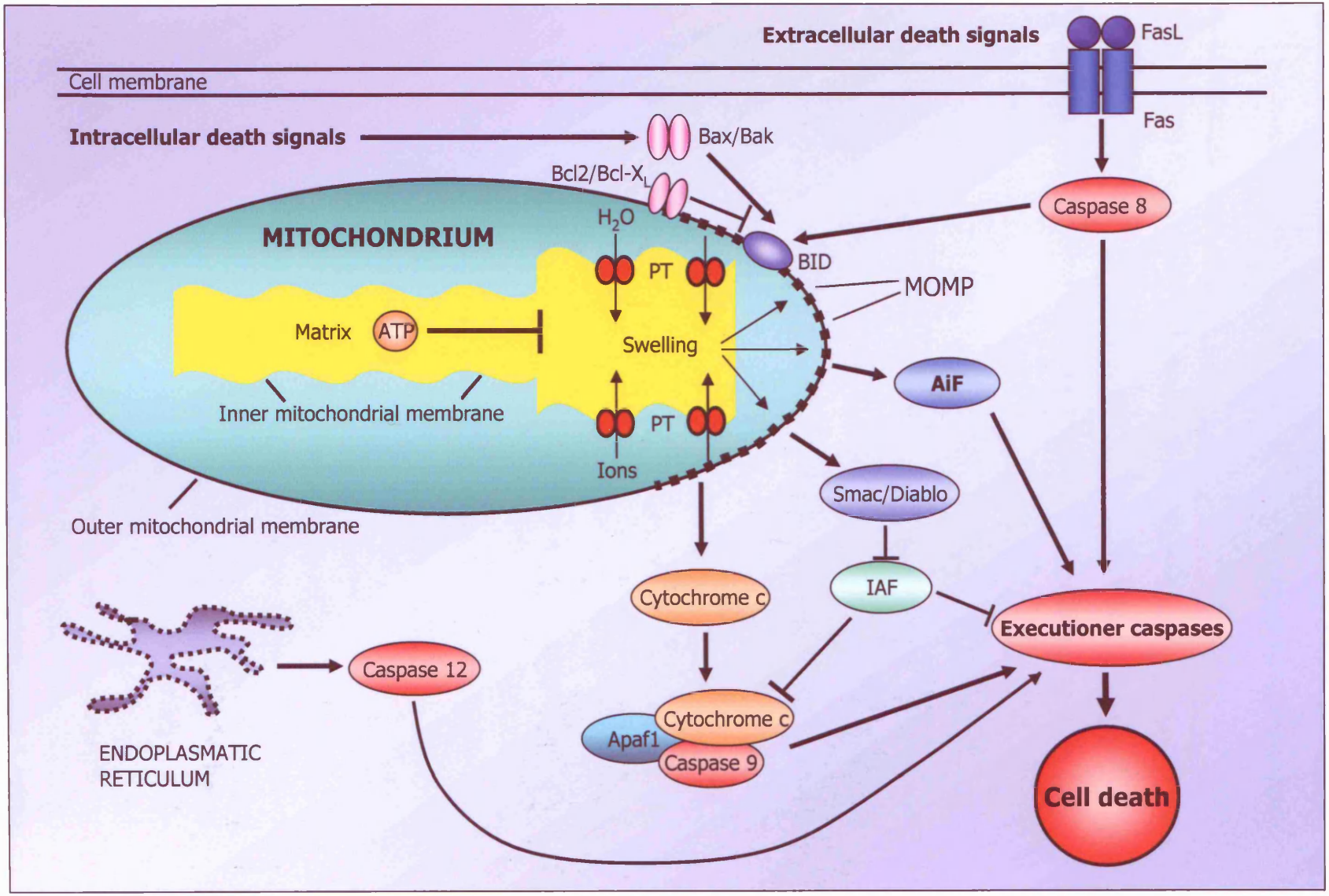
Extracellular death signals
FasL
Cell membrane
Fas
Intracellular death signals
Bax/Bak
Bcl2/Bcl-X$_L$
Caspase 8
H_2O
MITOCHONDRIUM
BID
PT
MOMP
Matrix
ATP
Swelling
AiF
Inner mitochondrial membrane
PT
Ions
Smac/Diablo
Outer mitochondrial membrane
Cytochrome c
IAF
Executioner caspases
Caspase 12
Cytochrome c
Apaf1
Caspase 9
ENDOPLASMATIC
RETICULUM
Cell death

Figure 1. Mitochondria and programmed cell death

Figure 1.1. Mitochondria and programmed cell death.
Mitochondria play a central part in pathways leading to programmed cell death. Intracellular death signals (e.g. oxidative damage or toxic aggregates) can initiate a cascade of events including transfer of pro-apoptotic Bax or Bak to the outer mitochondrial membrane, opening of the permeability transition pore (PT) and loss of the mitochondrial transmembrane potential. This leads to the entry of water and ions into the mitochondrial matrix, swelling and subsequent mitochondrial outer membrane permeabilisation (MOMP). Cytochrome c, apoptosis inducing factor (AiF) and Smac/Diablo can then leak into the cytoplasm activating executioner caspases, which leads to programmed cell death. Extracellular death signals activate cellular death receptors such as Fas with subsequent activation of caspase 8 and then executioner caspases leading to programmed cell death. Apaf: apoptosis associated factor. BID: BCl_2-interacting domain. IAF: inhibitor of apoptosis. FasL: Fas ligand.

1.1.3. Free radicals and anti-oxidant cellular defence systems

Any independent species that contains one or more unpaired electron is a free radical. Free radicals are generally unstable and therefore highly reactive with a half-life of only nanoseconds (Halliwell and Gutteridge, 1999). They are normal by-products of cellular aerobic metabolism (Halliwell and Gutteridge, 1999). The most prominent biological free radicals are the reactive oxygen species (ROS) superoxide ($O_2^{\bullet-}$), hydroxyl ($OH^{\bullet}$), and hydrogen peroxide (H_2O_2), and the reactive nitrogen species (RNS). These result from nitric oxide ($NO^{\bullet}$), which also possesses an unpaired electron and can either via a series of reactions give nitrous oxide (N_2O) and hydroxyl radical ($OH^{\bullet}$) or, following one-electron reduction to nitroxyl anion, react with O_2 to give peroxynitrite ($ONOO^-$). $NO^{\bullet}$ reacts with O_2 on exposure to air to form the gas nitrogen dioxide ($NO_2^{\bullet}$), which is a more reactive free radical than $NO^{\bullet}$. $NO^{\bullet}$, $ONOO^-$ and $NO_2^{\bullet}$. Nitric oxide is synthesised in living organisms by enzymes called nitric oxide synthases (NOS). Three different types of NOS, neuronal NOS (nNOS), endothelial NOS (eNOS) and inducible NOS (iNOS) help regulate $NO^{\bullet}$ synthesis. NOS and $NO^{\bullet}$ production serve physiological functions, e.g. blood vessel

tonus and thus blood pressure regulation. Apart from iNOS NOS are dependant on Ca^{2+} levels, which links free radical production to mitochondria, which buffer cytoplasmic calcium.

Experiments on isolated mitochondria exposed to high levels of oxygen indicate that mitochondria convert 1-2% of oxygen into ROS (Boveris and Chance, 1973). The main source of free radical production is the mitochondrial respiratory chain complex I and particularly complex III (ubiquinone-cytochrome c reductase) (Turrens, 1997). In the regeneration of co-enzyme Q the intermediate free radical semiquinone (·Q-) is formed. ·Q-can transfer electrons non-enzymatically to oxygen thus generating $O_2^{\bullet-}$. Cytosolic enzyme systems contribute to ROS production, in particular the NADPH oxidase family (Suh et al., 1999).

Free radicals can be counteracted by the cellular antioxidant defence systems, which are particularly strong in mitochondria. These defence systems include the enzymatic scavengers superoxide dismutase (SOD), catalase and glutathione peroxidase. SOD exists in three forms: a cytoplasmic copper/zinc (Cu/Zn) form (SOD 1), a mitochondrial manganese form (SOD 2) and an extracellular form (SOD 3)(Fridovich, 1995). All forms catalyse the rapid conversion of $O_2^{\bullet-} + 2H^+$ to H_2O_2. Catalase and glutathione peroxidase convert H_2O_2 to water. Other non-enzymatic low molecular weight compounds contribute to ROS scavenging. These include ascorbate (vitamin C), pyruvate, flavonoids (vitamin E), carotenoids (vitamin A), co-enzyme Q and glutathione (GSH). The latter is likely the most important of this group and present in all cells with high metabolic demands such as neurones in combination with glutathione peroxidase and glutathione reductase. Glutathione can reduce H_2O_2 and lipid hydroperoxides, which results in oxidised glutathione (GSSG). Subsequently, GSSG is reduced to GSH by glutathione reductase in a NADPH dependent conversion.

1.1.4. Cellular consequences of oxidative stress

If ROS/RNS production is not balanced by the cellular defence mechanisms oxidative stress occurs. Consequently this can result in oxidative damage to lipids, proteins and DNA with subsequent functional impairment. If oxidative stress is severe it may cause cell death by necrosis or by programmed cell death. This may involve oxidative damage to mitochondria with Ca^{2+} release, opening of the mitochondrial permeability transition pore and release of pro-apoptotic factors (see section 1.1.2.2. and Figure 1.1.). ROS/RNS damaged proteins may be more prone to ubiquitination and degradation within the ubiquitin-proteasom system (UPS, see section 1.1.6.). Additional abnormal function of the UPS can further promote accumulation of damaged proteins leading to the formation of aggregates and possibly triggering the initiation of programmed cell death (see section 1.1.2.2. and Figure 1.1.).

Lipid peroxidation

The decomposition of H_2O_2 produces $OH^{\bullet}$, which can react with polyunsaturated fatty acids (PUVA) abstracting a hydrogen atom from a methyl group. This results in an unpaired unstable electron on the carbon atom (-HC˙-) that stabilises itself through electron re-arrangements forming a conjugated diene radical in the process. This can react with O_2 to form a peroxyl radical (-COO˙-) that can abstract an electron from another lipid molecule creating a cycle of lipid peroxidation and the generation of lipid hydroxyperoxide products such as malonaldehyde (Gutteridge and Halliwell, 1990). Functionally, lipid peroxidation can affect membranes leading to loss of membrane fluidity, reduced membrane potential or changes in permeability to ions such as Ca^{2+} (Simonian and Coyle, 1996).

Oxidative damage to DNA

Hydroxyl radicals can react with sugars, purins and pyrimidines of DNA. For example, $OH^{\bullet}$ can add on to guanine at positions 4,5 or 8 in the purine ring; addition at position 8 leads to a C-8 OH-adduct radical that can be reduced to 8-hydroxy-7,8-dihydroguanine; it can also be oxidised to 8-hydroxyguanine or the imidazol ring may be opened with subsequent one-electron reduction and protonation resulting in 2,6-diamino-4-hydroxy-5-formidopyrimidine (abbreviated as FAPyG). In a similar manner $OH^{\bullet}$ can add on to adenine, cytosine or thymine (Halliwell and Gutteridge, 1999). Deoxyribose sugars are vulnerable to fragmentation by $OH^{\bullet}$ where hydrogen abstraction by $OH^{\bullet}$ can result in carbon centred-radicals, which in the presence of O_2 convert rapidly into sugar peroxyl radicals followed by the generation of carbonyl products in subsequent reactions. Consequences of ROS damage to DNA include base and sugar modifications, single- and double-strand breaks, and, if there is additional damage to proteins, DNA-protein cross links within the chromatin. This can interfere with chromatin unfolding, DNA repair, replication and transcription. In addition, the generation of single-strand breaks can activate poly(ADP)ribose polymerase (PARP) a process that requires ATP and can lead to depletion of NAD+ with subsequent impairment of mitochondrial function, glycolysis and ATP synthesis.

Oxidative damage to proteins

Proteins are particularly vulnerable to attacks by reactive nitrogen species such as $ONOO^{-}$, $NO_2^{\bullet}$ and NO_2Cl; an attack upon tyrosine leads to the production of 3-nitrotyrosine. In addition, peroxides can be generated on the peptide backbone and side-chains of aminoacid residues, and carbonyls can also form. The consequences of oxidative damage to proteins can be widespread depending on the protein involved. It can change the function of enzymes including those involved in DNA replication and repair, receptors, signal transduction pathways and transport

proteins. In addition, protein alterations may trigger an immune response with antibody formation, which has been hyothesised for example in scleroderma (Peng et al., 1997).

1.1.5. Excitotoxicity

Mitochondria maintain a protonelectrochemical gradient (Δp) across their inner membrane. This gradient consists of a transmembrane potential of about 150mV ($\Delta\Psi_m$) and a small pH gradient, which controls ATP synthesis through oxidative phosphorylation (see section1.1.2). The mitochondrial membrane potential ($\Delta\Psi_m$) is the component of the proton electrochemical potential (Δp), which determines Ca^{2+} sequestration and also the generation of reactive oxygen species.

Abnormal mitochondrial respiratory chain function may affect the energy dependent maintenance of the cellular transmembrane resting potential. Depolarisation of the cell membrane from the normal -90mV to between -60 and -30mV relieves the voltage dependent block of N-methyl-D-aspartate (NMDA) receptors by magnesium (Nicholls and Ward, 2000) and leads to their activation by ambient levels of glutamate. Calcium influx follows NMDA receptor activation. Mitochondria serve to buffer intracellular calcium. Failure of cytoplasmic Ca^{2+} homeostasis in the wake of mitochondrial dysfunction represents an early step towards excitotoxicity and necrotic cell death (for a review see Nicholls and Ward, 2000). Increased levels of cytoplasmic Ca^{2+} trigger the activation of nitric oxide synthase (NOS), and the ensuing increase in superoxide and nitric oxide potentially leads to the generation of peroxynitrite (Dawson et al., 1991). Both intra-mitochondrial calcium accumulation followed by mitochondrial depolarisation and peroxynitrite formation have been demonstrated to be associated with excitotoxic cell death (Schinder et al., 1996; White and Reynolds, 1995).

1.1.6. The ubiquitin-proteasome system (UPS)

The UPS degrades intracellular proteins in a highly specific, complex and tightly regulated process. The UPS plays an important role in a variety of cellular processes such as the regulation of immune responses, regulation of the cell-cycle, growth and cell differentiation (Pickart, 2001; Voges et al., 1999). It also serves as a quality control instrument to ensure that abnormal, e.g. misfolded or damaged (e.g. by ROS) proteins are disposed of to prevent the formation of potentially toxic aggregates (Pickart, 2001; Voges et al., 1999). Abnormalities of the UPS have been linked to neurodegenerative diseases such as Parkinson's disease, Huntington's disease, Amyotrophic Lateral Sclerosis or Prion Diseases (for a review see (Ciechanover and Brundin, 2003), and also sections 3.1.9 and 4.1.7.2). It is not always clear whether abnormal UPS function is a primary cause of disease or involved secondary to another pathological process. For example mutations of Parkin, a ubiquitin ligase, that cause autosomal recessive Parkinson's disease may be considered a primary cause (see section 3.1.11.2) whereas ubiquitin mediated aggregate formation and its consequences in Huntington's disease could be considered secondary involvement of the UPS (see sections 4.1.7.2 and 4.1.7.3).

In the first step of the degradation process, in an ATP-dependent reaction a ubiquitin activating enzyme, E1, activates ubiquitin monomers. A ubiquitin conjugating enzyme (E2) binds activated ubiquitin which is then in an ATP-dependent reaction covalently linked to the targeted protein by a ubiquitin ligase (E3). This is repeated until several ubiquitin molecules are tagged onto the abnormal protein. It is not fully understood how abnormal proteins are recognised. Clearly, the E3-ligase family plays an important role but there may be other factors that contribute to the specificity of substrate recognition.

The UPS degrades poly-ubiquitinated proteins and non-ubiquitinated proteins are degraded in the 26S and 20S proteasome. These multicatalytic

proteases are present in the cytoplasm, endoplasmatic reticulum, perinuclear region and within the nucleus of eukaryotic cells. The 20S proteasome (700kDa) forms the 28-subunit catalytic core of the 26S proteasome. The 20S proteasome consists of two outer and two inner heptameric rings which assume the shape of a hollow cylinder. Within this structure 7β subunits of each of the two inner rings catalyse proteolysis at the C-terminus of acidic, hydrophobic and basic residues; they are referred to as peptidylglutamyl-, chymotrypsin- and trypsin-peptide hydrolytic activities. Seven α-subunits without proteolytic activity compose the outer ring of the 20S proteasome. Here the 700kDa multisubunit ATPase containing PA700 activator (19S) is anchored to form the larger 26S proteasome. Upon binding of the PA700 activator to the 20S proteasome the gate to the inner channel opens so that proteins destined for degradation can enter. Before proteins enter the proteolytic core of the 20S proteasome C-terminal hydrolases detach and recycle the polyubiquitin chains so that single ubiquitin molecules again become available for E1 mediated ubiquitination (Pickart, 2001; Voges et al., 1999).

The degradation process in the proteasome generates small peptides, which can be re-used as building blocks in the synthesis of proteins, or can be presented on major-histocompatibility-complex I molecules as antigens to cells of the immune system. If the function of the proteasome or the ubiquitin labelling system is compromised abnormal proteins can accumulate and may aggregate to form insoluble inclusion bodies. This may disrupt cellular homeostasis and integrity, and may even lead to apoptosis (Sherman and Goldberg, 2001).

1.1.7. Models of neurodegenerative diseases

Disease models are a useful tool to help further our understanding of the pathogenesis of the respective disease, in particular, causes of the relative selective loss of dopaminergic neurones in PD or medium spiny striatal neurones in HD at the

molecular level. Ultimately, these models may aid the development of therapeutic strategies. Models can be generated by using toxins, either in animals or in cell culture, or by genetically modifying animals or cells, or a combination of both.

Ideally, an animal model should reproduce the characteristic clinical and pathological features of a disease; for example in PD this should include a L-Dopa responsive movement disorder, a chronically progressive loss of dopaminergic neurones, and LB-like inclusions. This may simplify the complexity of human diseases, and no animal or cell culture model is likely to be an exact phenocopy of the human disease. Nonetheless, these models are vital in helping to dissect the many different molecular and biochemical pathways that converge on the final clinico-pathological phenotype of a given disease.

1.1.7.1. Toxin models

Toxins models utilise a specific toxin to model a disease, e.g. if mitochondrial involvement in a given disease is thought to play a role in the pathogenesis of this disease a mitochondrial toxin can be used. Toxins can be applied systemically to animals or injected under stereotactical guidance directly into the area of interest, e.g. the substantia nigra in PD. In addition, toxins can be used in cell culture models to investigate their effects at a subcellular level.

1.1.7.2. Knock-out models

In 'knock-out' mouse lines the genome is manipulated to remove or alter DNA sequences so a gene cannot function. For the generation of knock-out mouse lines, firstly embryonic stem (ES) cells are genetically modified in culture to introduce the desired changes into the genome, and successfully transformed ES cells are selected. Secondly, these ES cells are injected into recipient blastocysts from wild-type mice, which results in a mixture of normal and genetically modified cells

(chimera). Thereafter, the chimeric blastocysts are implanted into the reproductive tracts of normal mice that subsequently give birth to a number of chimeric mice. If these chimeric mice have incorporated the modified genes into their germ line, then a new strain of mice can be created that carries the targeted mutation. Knock-out mice model recessive disorders where the phenotype results from the loss of the protein encoded by the dysfunctional gene. In addition, the pathological consequences of the absence of the protein of interest may indirectly help to understand its function.

1.1.7.3. Transgenic animal models

Transgenic animals express a gene of interest foreign to their own DNA. DNA of the gene of interest under the control of a promoter sequence is constructed with recombinant DNA techniques and injected into the male pronucleus of fertilised uncleaved eggs from a donor animal. At the two-cell stage the injected eggs are transferred into the reproductive tract of a female animal. After confirmation of the successful incorporation of the transgene, heterozygous offspring are re-mated to generate a homozygous transgenic animal. The quality of the animal model is reflected in the expression of the gene of interest in the appropriate anatomical site, e.g. the substantia nigra in PD models. This depends upon the intrinsic efficiency of the promoter of the transgene, the number of transgene copies introduced into the host genome, and possibly upon the site of incorporation of the transgene into the host genome (for a review see Shuldiner, 1996).

1.1.7.4. Cell culture models

Cells can be genetically modified to express specific genes of interest, and the structural, biochemical and functional consequences of gene expression can be analysed at the level of the individual cell. Genes of interest are introduced into the

host cell by a process called transfection. Most commonly, the cDNA of the gene of interest is inserted into a plasmid or viral cloning vector, and following transfection into a host cell line, the gene may be expressed transiently (transient transfection) or becomes incorporated into the host cell genome (stable transfection). Cells can also be modified to loose expression of a gene of interest, e.g. by using anti-sense mRNA.

Cell models of diseases can be generated in several ways:

Transient transfection. A plasmid of interest is transfected into cells and the gene of interest is transiently expressed. This type of model is useful for morphological analysis of protein expression in individual cells. However, the disadvantages are that the level of protein expression cannot be controlled, only a proportion of cells (usually 20-30%) express the protein and protein expression is short-lived (about 7-10 days).

Constitutive and stable expression. In these models the protein of interest is expressed permanently. However, often the transfected gene is markedly over-expressed so that the physical load of over-expressed protein may be harmful for the cells. In addition, the continuous expression of the transfected gene may lead to a selection of cells that are able to grow in its presence thus introducing an important confounding factor.

Inducible and stable expression. In these models not only is the transfection stable but the inducing agent allows for more control over the amount of protein expressed from the transgene. Contrary to constitutive and stable expression systems, cells grow unselected for their ability to grow in the presence of the expressed protein and the comparison of the same cells with and without protein

expression can identify relatively small differences. This can be more problematic with constitutive protein expression in particular because clonal cell lines, even when derived from the same precursor cell line, may show important differences per se. This could be an important confounding factor for comparisons between clones that express different proteins. A problem with inducible models is that the inducing agent itself can introduce artefactual changes compared with the non-induced controls. Using as inducer for example an insect hormone, which has no homologue in mammalian cells, can circumvent this.

Cell culture models are useful to selectively investigate pathological and biochemical aspects of diseases at the sub-cellular level. The quality of a cell culture model depends on the cell line in which the model was established. This should ideally reflect properties of the cell type affected in the disease it models, e.g. dopaminergic neurones in PD. Other factors that determine the quality of a cell culture model include the number of cells successfully transfected, the amount of protein expressed from the transfected cDNA and the control over the levels of protein expression. These factors may limit the types questions that can be addressed with a given model. With transient transfection, for example, only about 30% of cells will be successfully transfected (this may be higher with viral vectors) and the cells may not contain the transfected cDNA for longer than 10 days. This means that experiments are limited to those cells that have been transfected and will have to be short.

CHAPTER 2

Material and Methods

2.1 Materials

Unless otherwise stated the following equipment was used.

Tissue culture and human tissue handling equipment

ICN-Flow Automatic CO_2 Incubator model 320 (ICN-Flow Ltd., High Wycombe, Bucks, UK); Gelair (ICN-Flow) for tissue culture; Class I ICN Flow hood.

Centrifuges

Beckman GPR bench-top centrifuge with GH-3.7 horizontal rotor (Beckman Ltd., High Wycombe, Bucks, UK), Kontron T-124 high-speed centrifuge with 8.24 8 x 50ml fixed angle rotor (Kontron Instruments, Watford, Herts, UK), Biofuge 13 with 18 x 1.5ml fixed angle rotor (Heraeus, Germany), Fresco Microcentrifuge (Heraeus).

Molecular Biology equipment

Hybaid mini hybridisation oven (Hybaid Ltd., Middx, UK), Perkin-Elmer 2400 thermal cycler (Perkin-Elmer, Warrington, Cheshire UK), Infors-HAT orbital shaker (Infors Ltd., Crewe, UK), G25 Incubator shaker (New Brunswick Scientific Co. Inc. Edison, NJ, USA), Gel Dryer (BioRad Lab. Ltd., Hemel Hempstead, Herts, UK).

Electrophoresis equipment

BioRad 200/2.0 constant voltage power packs (BioRad Lab. Ltd.), BRL horizontal system for agarose gel electrophoresis (Bethesda Res Lab, Life Technologies Inc., Gaithsburg, MD, USA), BioRad vertical system for polyacrylamide gel

electrophoresis (BioRad), UV transilluminator (GRI Ltd., Dunmow, Essex, UK), Polaroid camera.

Cell homogenisers

Uni-form 5ml and 10ml glass/Teflon homogeniser (Jecons Ltd., Leighton Buzzard, Bedforshire, UK), 5ml glass homogeniser and Glass-Col stirrer (CamLab Ltd., Cambridge, UK).

Spectrophotometers

Hitachi U-3210 (Hitachi Scientific Instruments, Wokingham, Berks, UK) and Kontron Uvikon 940 (Kontron Instruments, Watford, Herts, UK) split beam spectrophotometers.

Microscopy and photography

Zeiss Axiophot fluorescence microscope with FITC, UV and rhodamine filters (Carl Zeiss Microscope Division, Oberkochen, Germany), MRC 600 confocal microscope (BioRad Microscience Division, Herts, UK), Kodak Ektachrome 400ASA for immunofluorescence.

Flow cytometer

FACScalibur (Becton Dickinson, UK) flow cytometer using an argon 488nm laser and 500nm long-pass filter (FL1 channel) for $DiOC_{6(3)}$ and 578nm (FL2 channel) for propidium iodide. This flow cytometer runs on a MAC computer platform using Cellquest 4 (Becton Dickinson) software.

PCR equipment

Peltier Thermal Cycler (PTC 200), MJ Research Inc., Watertown, Mass, USA or GeneAmp PCR Systems 2400, Perkin Elmer, Norwalk, CT, USA.

UV-transilluminator

Chromato-UVE, transilluminator model TM-20, San Gabriel, CA, USA.

Chemicals

Unless otherwise stated all chemicals were purchased from Sigma (Poole, Dorset, UK) or Merck Ltd. (Dagenham, Essex, UK).

2.2. Cell lines and cell culture

2.2.1. EcR 293 cell line (Invitrogen, UK)

Human embryonic kidney cells (HEK293) with stable transfection of the pVgRxR plasmid (EcR 293) were purchased from Invitrogen (Invitrogen, UK). This plasmid confers resistence to the antibiotic Zeocin (400μg/ml).

Cells were grown at 37°C in a humidified atmosphere containing 5% $C0_2$ in growth medium consisting of Dulbecco's modified Eagle medium (DMEM, Life Technologies, Paisley, UK) and 4.5 μg/L glucose, 10% fetal calf serum, 50 units/ml penicillin, 50 μg/ml streptomycin (all Life Technologies), 400 μg/ml Zeocin (Invitrogen), 50 μg/ml uridine and 110 μg/ml sodium pyruvate.

2.2.2. NT2 cells (Ntera2/D1)(Stratagene, UK)

NT2 cells are neuronal precursor stem cells derived from a human teratocarcinoma. They differentiate into post-mitotic mature neurones (hNT2 neurones) following treatment with retinoic acid (Pleasure and Lee, 1993; Pleasure et al., 1992).

Cells were grown at 37°C in a humidified atmosphere containing 5% $C0_2$ in growth medium consisting of Dulbecco's modified Eagle medium (DMEM) and 4.5 µg/L glucose, 10% fetal calf serum, 50 units/ml penicillin, 50 µg/ml streptomycin.

2.2.3. SH-SY5Y neuroblastoma cells

SH SY5Y neuroblastoma cells (Ross et al., 1983) were purchased from ECACC (Wiltshire, UK). SH SY5Y cells were grown in growth medium consisting of Minimal Essential Medium (MEM)/F12 supplemented with 15% foetal calf serum, 50 units/ml penicillin and 50 µg/ml streptomycin. For differentiation, SH-SY5Y cells were plated out at about 10% confluency (approximately 5000 cells/ml); 10 µM retinoic acid (all-trans retinoic acid, Sigma) was added to SH SY5Y cells every 2-3 days for 14 days.

2.2.4. R6/2 transgenic mice and myoblast cell lines

Transgenic mice, and littermate control mice, were bred by Professor Gillian Bates, Department of Medical Genetics, UMDS, London. Mice were maintained on a SDS No.3 breeders diet. The R6/2 transgenic mouse colony was maintained by backcrossing with C57BL/6 X CBA) F1 mice. Genotyping and CAG repeat sizing was performed by Professor Bates as described previously (Mangiarini et al., 1996).

Mice were sacrificed at 12 weeks of age by cervical dislocation. Quadriceps and gastrocnemius muscles were dissected under sterile conditions from 6 transgenic R6/2 mice and 6 normal littermate mice. Muscle tissue was teased apart on 10cm Petri dishes using sterile needles and incubated for 12 minutes in 10ml filter sterilised dissociation medium (40ml DMEM with 12000 units of collagenase, 40mg bovine serum albumin and 3.2 ml trypsin solution (2.5% diluted 1/20 in Versene, Gibco) at 37°C in a humidified atmosphere containing 8% $C0_2$. Growth medium (10ml, DMEM supplemented with 4.5 g/L glucose, 20% foetal calf serum, 50 units/ml penicillin, 50 µg/ml streptomycin, 50 µg/ml uridine, 110 µg/ml sodium

pyruvate) was added and the suspension was triturated repeatedly through a 10ml tissue culture pipette. The supernatant was filtered through a cell strainer (40µm mesh, Falcon) and spun at 1000rpm for 10 minutes. The supernatant was aspirated and the cell pellet resuspended in growth medium. The entire procedure was repeated three times and the combined cell pellets were cultured on a plastic dish coated with laminin (Sigma, 10µg/ml physiologically buffered saline (PBS)) in growth medium at 37°C in a humidified atmosphere containing 8% $C0_2$. The medium was changed daily until cells were 50-70% confluent when they were harvested with trypsin solution and plated out on laminin (10µg/ml PBS) coated glass coverslips at 70% confluency (Melo et al., 1996; Vachon et al., 1996). After 24 hours growth medium was replaced with differentiation medium (growth medium with either 2% horse serum instead of foetal calf serum or no serum). Once myotubes formed (usually within one week of differentiation) coverslips were examined weekly for 6 weeks by immunocytochemistry.

2.2.5. Myotube desmin stain and myotube counts

For semi-quantitative analysis myoblast cultures were differentiated for 1 week and stained with desmin and DAPI. On each cover-slip, 4 randomly selected representative areas were photographed using a times 20 objective. Images were digitised and the total number of nuclei stained with DAPI, the number of desmin positive cells and the number of nuclei stained with DAPI within desmin positive cells were counted using Sigma Scan Pro5 image analysis software package (Jandel Scientific, San Rafael, CA, USA). For semi-quantitative analysis of inclusions myoblast cultures (n=3 for controls, and R6/2 cultured with and without serum) were differentiated for 6 weeks, and immunostained with ubiquitin and huntingtin with DAPI nuclear stain, followed by analysis as described above.

2.3. Cell culture

All cell lines were grown on 10cm plastic culture dishes (Life Technologies Ltd., Paisley, UK). Growth medium was changed at least twice weekly following a wash in sterile phosphate buffered saline (PBS, Sigma, UK, consisting of 137mM NaCl, 2.7mM KCl, 10mM $Na_2 HPO_4$ and 1.8mM $KH_2 PO_4$ pH 7.4). Cells were harvested and subcultured once they had become confluent. First, they were washed in PBS. Then, 1ml of 2.5 % trypsin (25g trypsin and 8.5g NaCl per litre, Gibco) solution (10% v/v in Versene) was added for 1-2 minutes at 37°C in a humidified atmosphere until cells could be dislodged easily by gentle tapping of the plate against the bench. The trypsin was then inactivated by the addition of 9ml of fresh growth medium and the cells divided for further growth onto new culture dishes or frozen down for storage.

2.3.1. Cell freezing and defrosting

A confluent plate of cells was harvested as described above. Cells were then centrifuged at 350g for 10 minutes at room temperature. The medium was aspirated and the cell pellet resuspended in freezing medium. This consisted of 90% growth medium and 10% filter sterilised DSMO except for hNT2 and EcR 293 cells where the growth medium was substituted with fetal calf serum. Cells resuspended in freezing medium in 1ml cryotubes were placed in a sealed polystyrene rack and frozen slowly overnight at –70°C before they were transferred into liquid nitrogen for long term storage.

Vials of frozen cells were defrosted rapidly at 37°C in a water bath. The cells were transferred to 10ml of pre-warmed growth medium in a 20ml universal container. Cells were pelleted by centrifugation at 300g for 10 minutes. The medium was aspirated, the cells resuspended in 8ml of fresh growth medium and plated onto a fresh culture dish. 24 hours later the cells were washed in PBS and the growth medium renewed.

2.4. Molecular biology

2.4.1. The Ecdysone Mammalian Expression System

The Ecdysone-Inducible Mammalian Expression System (Figure 2.1) utilises the ability of the insect hormone 20- OH Ecdysone to induce gene expression via the ecdysone receptor. The system uses a heterodimer consisting of the ecdysone receptor (VgEcR from *drosophila* modified with the VP16 transactivation domain) and the retinoid X receptor (RxR from mammalian cells). This receptor contains a modified "Ecdysone response element" (EcRE), which is activated in the presence of a ligand such as ecdysone or its analogue ponasterone A. Binding of the heterodimer to the EcRE activates transcription. Mammalian cells do not contain the ecdysone receptor and therefore do not usually respond to ecdysone or its analogs and do not express the ligand. Therefore, there is no basal gene transcription. The plasmid pVgRxR contains the VgEcR and RxR genes while the pIND plasmid contains the modified ecdysone response element and the "multiple cloning site". PIND confers resistence against the antibiotic Zeocin, pVgRxR confers resistence against the antibiotic G418.

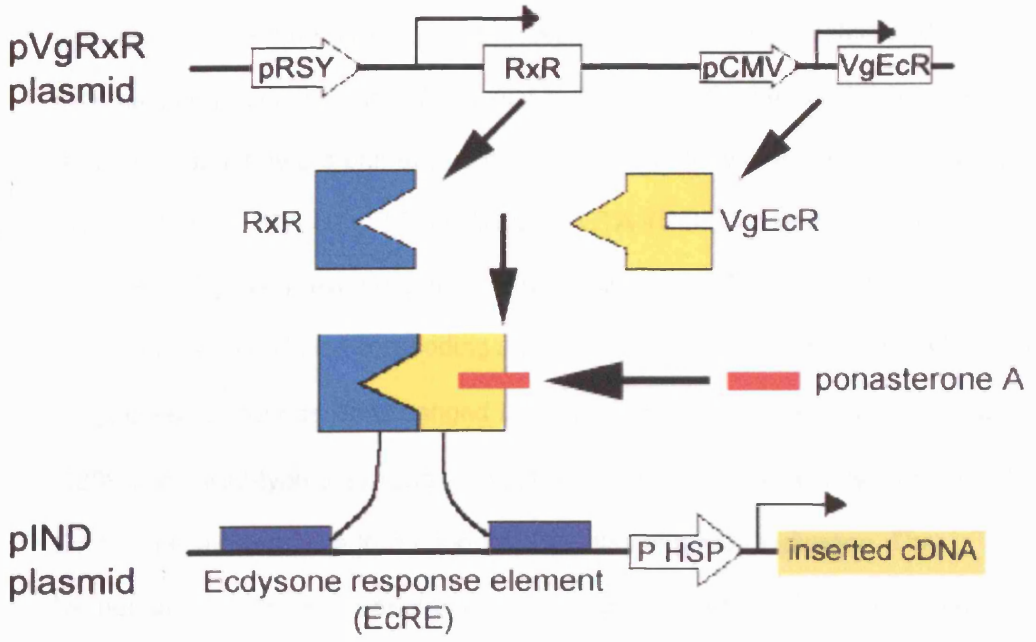

Figure 2.1. Schematic illustration of the Ecdysone Mammalian Expression system. For an explanation of abbreviations see the main text.

2.4.2. Generation of vectors

The pIND constructs for transfection, containing wild-type α-synuclein or G209A mutant α-synuclein, were generated by Dr. Sarah Tabrizi (Department of Clinical Neurosciences, Royal Free and University College Medical School London). In brief, total RNA was isolated from lymphoblasts from a male PD patient with the G209A α-synuclein mutation (kind gift from M. Polymeropoulos, NIH, Bethesda, USA) and control lymphoblasts with wild-type α-synuclein (from ECACC, Wiltshire, UK) as described by (Chomczynski and Sacchi, 1987). cDNA was generated by RT-PCR using the cDNA Cycle Kit (Invitrogen, The Netherlands) according to the manufacturer's instructions. The High Fidelity system (Boehringer Mannhein, Germany) was used for all subsequent PCR. Alpha-synuclein cDNA was amplified

using 5'-CAT TCG ACG ACA GTG TGG TGT (nucleotide 16-37) as a forward primer and 5' CTG CTG ATG GAA GAC TTC GAG (nucleotide 586-607) as a reverse primer. In a subsequent PCR the open reading frame of α-synuclein and its 31-nt 5' untranslated region was amplified using 5'-AAG GTA CC GAC AGT GTG GTG TAA AGG AAT as a forward primer (G65; nucleotide 26-44 with a 5' *Kpn* I site) and 5'-AA TGA TCA AGC GTA GTC TGG GAC GTC GTA TGG GTA GGC TTC AGG TTC GTA GTG T 3' as a reverse primer (G66; nucleotide 456-478 with a 3'-haemagglutinin (HA) epitope coding sequence and *Bcl* I site, the stop codon of the α-synuclein sequence was changed to allow translation of HA). Both mutated G209A and wild-type α-synuclein amplified fragments were digested with *Kpn* I and *Bcl* I and ligated into the *Kpn* I and *BamH* I sites of pIND (Invitrogen, The Netherlands). The correct sequence was confirmed by BIG DYE automated sequencing (AB1 310, Perkin Elmer, UK).

This yielded two vector constructs for transfection: pIND containing wild-type α-synuclein with a haemagglutinin tag (pIND. α-syn-HA) and pIND containing G209A mutant α-synuclein with an haemagglutinin tag (pIND. α-syn/G209A-HA).

2.4.3. Transfection of cDNA

CDNA was transfected using the Escort™ lipofection method according to the manufacturer's instructions (Sigma). Two days before the transfection a confluent plate of cells was harvested and split 1:1. One day before the transfection, the cells were harvested, counted using a haemocytometer and seeded at a concentration of 2×10^5 per well in a 6 well plate (35mm well diameter). Just before the transfection 15μl of the Escort™ reagent were mixed with 230μl of DMEM and 5μg of vector cDNA and incubated for 15 minutes at room temperature. Thereafter, 2ml of growth medium was added to the Escort™-vector cDNA solution. Following aspiration of growth medium from each well containing the cells 0.7ml of Escort™-vector cDNA

solution was added to each well. Cells were incubated for 5-6 hours at 37°C in a humidified chamber with 5% CO_2. The Escort™-cDNA solution was then removed and replaced by growth medium; after a further 24 hours cells from each well were harvested, plated out onto a 10cm Petri dish and grown in growth medium containing the selection antibiotics Zeocin (400μg/ml), if the pVgRxR plasmid was transfected, or G418 (400μg/ml) if the pIND plasmid was transfected. Varying concentrations of antibiotics (0, 50, 125, 250, 300, 400, 500, 750 and 1000μg/ml) were used to determine the minimum concentration required to kill (as assessed visually under a light microscope) all untransfected HEK293 cells after 7 days in culture when cells were plated out at 25% confluency with change of selection medium every 3 days.

Individual clones were generated as described (see section 2.4.4.) and grown in selection antibiotics.

2.4.4. Ring cloning

Cells were plated out at very low density so that clones could grow from individual cells. Sterile plastic rings were cut from the tops of 0.5ml Eppendorf tubes and then autoclaved. After clones were observed by microscopy the medium was aspirated and the cells washed in PBS. A sterile plastic ring dipped into UV sterilised high vacuum silicone grease was placed around a given clone creating a well, and 100μl of trypsin solution was added to this well. Subsequently, 100μl of growth medium was added to the well and the cells were transferred to a 35mm culture dish.

2.4.5. DNA extraction from cells

Cells were grown on 10cm tissue culture dishes, harvested by trypsinisation and washed in PBS. DNA was extracted using the Nucleon I DNA extraction kit (Scotlab, UK) following the manufacturer's instructions. In brief, cell lysis was followed by

deproteinisation with sodium perchlorate. Then, DNA was extracted using chloroform treatment and recovered with cold absolute ethanol. The DNA was then washed using 70% ethanol, centrifuged at 15000g, dried in a heating block at 37°C and dissolved in $T_{10}E_1$ buffer (10mM Tris-HCl and 1mM K_2-EDTA, pH 7.4) at room temperature.

2.4.6. DNA extraction from muscle tissue

The method described here follows that previously described (Sambrook et al., 1989). In a class I hood, muscle tissue the size of 1-3 matchstick heads was chopped up on a microscope slide with a scalpel. The tissue was transferred to a 1.5ml Eppendorf tube that contained 600µl of 0.1M Sodium EDTA, 0.01M Tris-HCl (pH 8), 40µl of 10%SDS and 100µl proteinase K (20mg/ml). Tissue was left to digest for 3 hours at 56°C rotating in a Hybaid incubator. The samples were then stored at –20°C until further processing.

All the following steps were performed at room temperature. 750µl of phenol (commercially available liquefied phenol washed in Tris buffer, PhiBio, Loughborough, UK) were added to each sample in a class I hood and samples were rotated for 15 minutes. Thereafter, the samples were centrifuged at 15000g for 15 minutes and then the upper, aqueous phase was carefully pipetted to a new 1.5ml Eppendorf tube. This was followed by adding 700µl of phenol/bromo-chloropropane/isoamyl alcohol (ratio 25:24:1) to each sample and rotation for 15 minutes. Samples were then centrifuged at 15000g for 15 minutes with subsequent transfer of the upper aqueous phase into a new 1.5ml Eppendorf tube. This step was repeated 3 times on the upper aqueous phase; the last aqueous phase was pipetted into a fresh Eppendorf tube, 650µl of bromo-chloropropane/isoamyl alcohol (ratio 24:1) were added and samples rotated for 15 minutes. Samples were

centrifuged at 15000g for 15 minutes and 500µl of the aqueous phase were pipetted into a new 1.5ml Eppendorf tube.

To each of these samples, 50µl of 3M sodium acetate (NaOAC, pH 4.8) and 1ml ethanol were added in order to precipitate DNA. The precipitate was hooked out using a clean plastic stick and transferred into a new 1.5ml Eppendorf tube containing 1ml of 70% ethanol. If the precipitate was small the original tube was centrifuged at 15000g for 5 minutes and the supernatant aspirated. Then, 1ml 70% ethanol was added to the tube. This was repeated twice. The pellet was then dried in a heat block (37°C) for about 5 minutes and dissolved in 30-100µl of $T_{10}E_1$ at room temperature for several hours.

2.4.7. Estimation of DNA concentration and purity

Once the DNA was fully dissolved the DNA concentration and purity was estimated. For this purpose, 5µl of DNA solution was added to 995µl of ddH_2O in a 1ml silica quartz cuvette and mixed by inverting. The solution was scanned on a spectrophotometer to measure the absorbance pattern between 310nm and 210nm. The DNA concentration (µg/µl) was calculated assuming that a 1mg/ml DNA solution has an absorbance of 20 at 260nm. The purity of the DNA was accepted when the A260/A280 ratio was between 1.7 and 2.0.

2.4.8. Polymerase chain reaction (PCR)

DNA primers, dATP, dGTP, dCTP, dTTP, *Taq* polymerase and polymerase buffers were obtained from Perkin-Elmer Ltd (Buckinghamshire, UK). All reactions were carried out in 0.3ml thin walled PCR tubes.

2.4.8.1. Amplification of cDNA in pIND constructs

The multiple cloning site of pIND plasmid was amplified using the Ecdyson Forward and Reverse primers (Invitrogen).

Ecdysone Forward (G49): 5'CTC TGA ATA CTT TCA ACA AGT TAC 3'

Ecdysone Reverse (G50): 5' TAG AAG GCA CAG TCG AGG 3'

The PCR mixture consisted of 1μg DNA extracted from samples, 40pmol of each oligonucleotide primer, 50mM KCl, 10mM Tris-HCl (pH 8.3), 1.5mM $MgCl_2$, 200μM of each deoxynucleoside triphosphate, 5% dimethylsulphoxide and 2.5U *Taq* polymerase in a total volume of 25μl (all concentrations are final concentrations). PCR conditions were: 94°C for 4 minutes, 72°C for 1 minute, followed by 35 cycles of 94°C (1 minute), 56°C (1 minute, 72°C (1 minute), final extension at 72°C for 10 minutes. The PCR product was then stored at -20°C until further analysis.

2.4.8.2. Prion protein gene (*PRNP*) PCR

The *PRNP* gene open reading frame was amplified as described by Palmer et al (Palmer Nature 1991). The PCR mixture consisted of 1μg DNA extracted from samples, 25pmol of each oligonucleotide primer, 50mM KCl, 10mM Tris-HCl (pH 8.3), 1.5mM $MgCl_2$, 200μM of each deoxynucleoside triphosphate, 5% dimethylsulphoxide and 2.5U *Taq* polymerase in a total volume of 50μl (all concentrations are final concentrations). PCR cycling conditions were 94°C for 30 seconds, 57°C for 30 seconds, and 72°C for 1 minute for a total of 35 cycles. The PCR product was then stored at -20°C until further analysis.

The following primers were used: forward 5'-ACT GAG AAT TCT CTG ACA TTC TCC TCT CTT CA and reverse 5'TAC TGA GGA TCC CTC AAG CTG GAA AAA GA.

2.4.9. PCR clean-up and sequencing

PCR products were cleaned using a commercially available kit following the manufacturer's instructions (QIAquick PCR purification kit, Qiagen, UK). This kit utilises spin-column technology and the selective binding properties of a silica-gel membrane designed by Qiagen. DNA adsorbs to these silica membranes in the presence of high salt concentrations while contaminants pass through the column. Impurities are washed away and the DNA is eluted with Tris buffer or water. The purified DNA was dried and stored at –20°C until further analysis.

DNA was sequenced by the company MWG (MWG, Germany).

The sequence of the samples was compared with the sequence of human α-synuclein (SNCA, NM 000345, gi 6806896) obtained from www.ncbi.nlm.nih.gov/LocustLink/ website. Sequences were aligned using SeqMan II software (DNASTAR Inc., USA).

2.4.10. DNA digestion by restriction endonucleases

All enzymes and buffers were from Promega (Chilworth Science Park, Southampton, UK). PCR products were digested with the restriction endonucleases *Mae*II (2 units, MBI, Fermentas, Lithuania) at 56°C or *Nsp*I (2 units, Boehringer-Mannheim, Germany) at 65°C for two hours. All reactions were performed in SuRE/Cut buffer M (Boehringer-Mannheim) in a total volume of 25μl.

2.4.11. Detection of DNA

PCR reaction or restriction digests were separated on agarose gels using the BRL horizontal system for agarose gel electrophoresis (Bethesda Res Lab., Life Technologies Inc., USA). Agarose gels (0.8-2% (w/v)) were prepared in 1 x Tris borate EDTA buffer (TBE, 0.9M Tris borate, 1mM EDTA, pH8) containing 1μg/ml ethidium bromide. The DNA and the DNA size markers (Smartladder containing

DNA size markers from 200bp to 10kB, Eurogentic, Belgium) were diluted in 6 x loading buffer (Promega UK Ltd., Hants, UK) and loaded onto the gel. DNA was separated by electrophoresis in 1 x TBE buffer at 100V for 1 hour. The DNA bands on the gel were visualised using a UV transilluminator and then photographed with a Polaroid camera.

2.5. Cytochemical staining

2.5.1. Histochemical staining

Histochemical analyses were conducted on muscle tissue mounted on a piece of cork so that the muscle fibres were orientated perpendicular to the cork. Samples were immediately snap-frozen in isopentane chilled in liquid nitrogen and stored in liquid nitrogen. 7-9 μm sections were cut at -25°C with a cryotome (Reichert-Jung 2800 Frigocut, Germany).

2.5.1.1. Haematoxylin and eosin

The staining protocol followed established histological staining techniques (Dubowitz, 1985; Engel, 1994). Sections were stained for 5 minutes in Meyer's haemalaun (Merck, UK), rinsed carefully under running water and left in tap water for 10 minutes. Sections were then stained in 0.1% (w/v) eosin for 1 minute followed by dehydration in 70-100% ethanol, clearing in xylene and mounting in DPX (Agar Scientific Ltd, Cambridge, UK).

2.5.1.2. Gomori Trichrome

The Gomori Trichrome stain is an established histological staining technique (Dubowitz, 1985; Engel, 1994). The staining protocol followed the method described by Engel (Engel and Cunningham, 1963). Sections were first stained in haematoxylin for 5 minutes, rinsed thoroughly under running tap water and left in tap

water for 10 minutes. Sections were then briefly rinsed in distilled water and stained in Gomori solution (0.6g chromotrope, 0.3g Fast Green, 0.6g tungstophosphoric acid, 1ml glacial acetic acid in a total volume of 100ml with tap H_2O, pH 3.4). Sections were dipped into 0.2% (v/v) glacial acetic acid, dehydrated in 70-100% ethanol, cleared in xylene and mounted in DPX.

2.5.1.3. Modified Congo red stain

This method followed the method described by Mendell et al (Mendell et al., 1991). Frozen sections were cut onto glass slides washed with methanol. After air-drying they were stained for 10 minutes with haematoxylin followed by three washes in distilled water for 5 minutes each. Sections were then placed in 80% isopropanol (saturated with NaCl, pH 10.5-11) for 5 minutes. Thereafter, sections were stained for 60 minutes with Congo red solution (0.2g Congo red in 80% isopropanol saturated with NaCl pH 10.5-11). Sections were dehydrated in 70-100% ethanol, cleared in xylene and mounted in DPX.

2.5.2. Immunocytochemistry

Irrespective of cell line, cells were grown on glass coverslips in a 35 mm dish with 2 ml of growth medium. Myoblasts were grown on glass coverslips coated with laminin (10μg/ml in PBS) overnight at 37°C. The medium was aspirated and the coverslips were washed in PBS. Cells were fixed for 20 minutes in 4% (w/v) paraformaldehyde in PBS and then for 15 minutes at –20°C in methanol. All the following incubations took place in a humid chamber at 37°C. Fixation was followed by blocking with 10% normal goat serum in PBS for 1 hour; PBS was removed followed by incubation with the primary antibody (see section 2.5.4. for dilutions) for 3 hours. After 3 washes in PBS, primary antibodies raised in mouse were developed for 1 hour with goat anti-mouse Alexa 488 conjugates respectively (Molecular

Probes, Oregon, USA, dilution 1/200 in PBS) while the rabbit or goat primary antibodies were detected with goat anti-rabbit or donkey anti-goat Alexa 568 conjugates, respectively (Molecular Probes, Oregon, USA, 1/1000). After 3 washes in PBS, coverslips were mounted on glass slides in Citifluor (Agar Scientific, UK) with 1µg/ml DAPI or 1µg/ml propidium iodide. Dual labeling consisted of incubation with a mouse monoclonal antibody and development with anti-mouse secondary antibody followed by incubation with either rabbit or goat primary antibody and the appropriate fluorescent secondary antibody. In control experiments the primary antibody was omitted.

Cells were also labelled with MitoTracker® (CMXRos-H_2, Molecular Probes, 3µM). To this end cells growing on coverslips were cultured for 45 minutes in prewarmed growth medium containing MitoTracker®; the medium was then replaced by normal growth medium and cells were cultured for a futher 30 minutes. Cells were then fixed and immunostained as described above.

2.5.3. Immunohistochemistry

For immunohistochemical analysis of frozen muscle sections, glass slides were coated in 3-aminopropyltriethoxysilane (APES). Slides were degreased in 100% ethanol, rinsed in ddH_2O and air dried for 10 minutes. The slides were then immersed in 2% APES solution in aceton for 2 minutes followed by two washes in ddH_2O. Slides were then dried overnight at 40°C.

Muscle sections (7µm) were cut on a cryotome (Reichert-Jung 2800 Frigocut, Germany) at -25°C and air-dried for 30 minutes, fixed in aceton at -20°C for 10 minutes and air-dried again for 30 minutes. Immunohistochemical analyses of frozen muscle sections followed the protocol as outlined above. After three washes in PBS, mouse monoclonal antibodies were incubated with biotinylated horse anti-mouse secondary antibodies (Vector Laboratories, Burlingame, USA). After another

three washes in PBS the sections were incubated with an avidin-biotin-complex followed by developing for 5 minutes with 0.5 mg/ml 3,3'diaminobenzidine in PBS and 1µl/ml H_2O_2 using the Vectastain-Kit (Vector Laboratories). Alternatively, alkaline phosphatase conjugates were used and peroxidase demonstrated using alkaline phophatase (Vector SK5100 kit with 0.1M levamisole). Sections were dehydrated in 70-100% ethanol, cleared in xylene and mounted in DPX.

2.5.4. Antibodies

The following primary antibodies were used: α-synuclein either mouse monoclonal antibody (MAB) (Zymed, San Francisco, USA, dilution 1/200) or rabbit polyclonal antibody (Chemicon, 1/2000), haemagglutinin (MAB anti-HA, Boehringer, Germany, 1/200), cytochrome-c-oxidase (MAB anti-COX I subunit, Molecular Probes, Oregon, USA, 1/200), lysosomes (MAB anti-lysosomal associated membrane protein 1, PharMingen, 1/400) or Golgi zone (MAB anti-Golgi zone, Chemicon, 1/200), vesicle associated membrane protein (VAMP) (MAB anti-VAMP, Chemicon 1/200), vesicular monoamine transporter (VMAT) 1 or 2 (goat polyclonal antibody, anti-VMAT 1 and anti-VMAT2 (Santa Cruz Biotechnology, 1/50), desmin (Dako, 1/500), ubiquitin (MAB anti-ubiquitin, Chemicon, 1/300), CD-8 (MAB anti-CD-8, Novocastra, UK, 1/200), tyrosine hydroxylase (rabbit polyclonal antibody, anti-tyrosine hydroxylase, Biogenesis, UK 1/500), neurofilament (MAB anti-neurofilament, Dako, 1/100), and rabbit polyclonal anti-N-terminal huntingtin (675 antibody, gift from Dr L. Jones, Cardiff 1/2000).

2.5.4. Catecholamine stain

Cells were stained for catecholamines using glyoxylic acid fluorescence cytochemistry following the method described by Lindvall and Bjorklund (Lindvall and Bjorklund, 1974). In brief, HEK293 cells were plated out on coverslips at a

density of approximately 25000 cells/ml, washed in PBS and incubated for 5 minutes at 37°C with a solution containing 5% BSA in 0.1M phosphate buffer (pH 7) and 2% glyoxylic acid (Fluka, UK). Coverslips were mounted in PBS and visualised using a fluorescence microscope and FITC filter (see next section).

2.5.5. Image analysis and photography

Slides were evaluated with a Zeiss Fluorescence Axiophot microscope (Carl Zeiss Microscope Division, Oberkochen, Germany) using the appropriate filters to visualise FITC, DAPI and rhodamine with an attached Zeiss MC80 photocamera. For confocal mircroscopy a Krypton-Argon laser (Bio Rad MRC 600, Herts, UK) attached to an Olympus BH2-RFCA fluorescence microscope was used.

Photographs of conventional fluorescence microscopy were taken using a Zeiss Fluorescence Axiophot microscope with an attached Zeiss MC80 photocamera and Kodak Ectachrome film (400 ASA). Slides were digitised using a laser scanner and processed with Adobe Photoshop software version 6.0. Images generated with the confocal microscope were digitally stored and processed using Confocal Assistent™ software and Adobe Photoshop software version 6.0.

2.6. Protein assays

2.6.1. Protein extraction

In general, one plate of confluent cells of the relevant cell line was washed in PBS and harvested using a cell scraper. Cells were washed twice in PBS and solubilised in dissociation buffer containing 50mM TRIS/HCl, 4% (w/v) SDS, 12% (w/v) glycerol, 0.5% (v/v), pH 6.9 containing a cocktail of protease inhibitors (final concentration: 1μg/ml leupeptin, 1μg/ml pepstatin, 1μg/ml antipain, 100μg/ml PMSF, 5μg/ml chemostatin). In order to break up genomic DNA samples were sheared using a 19G needle and 1ml syringe until the viscosity of the sample was reduced.

2.6.2. Protein determination

Protein concentrations were determined with the bicinchoninic acid copper assay (Pierce-Warriner BCA™ kit, USA) kit or with the BioRad kit (Bio-Rad, Munich, Germany).

2.6.2.1. The bicinchoninic acid copper assay (BCA)

Protein concentrations were determined using a commercially available kit (Pierce-Warriner BCA™ kit, USA). Protein reduces Cu^{2+} to Cu^{+} which is detected by bicinchoninic acid (BCA). The purple reaction product is water soluble and exhibits strong absorbance at 562nm. For each assay a set of protein standards was prepared using dilutions of bovine serum albumine (BSA) in the same diluent as the samples. The standards were made to cover the range of protein concentrations expected in the respective samples; typically, 0, 25, 50, 75, 100, 125 and 150μg/ml were used. Assays were performed according to the manufacturer's instructions using the protocol requiring 30 minutes incubation at room temperature. Each assay was performed in triplicate. The readings of the samples were interpolated against the BSA standard curve.

2.6.2.2. The BioRad protein determination kit

This kit determines protein concentrations of samples against an albumin standard curve following the Bradford method. The protein standard curve was prepared using BSA as described above for the BCA assay. The protein solution was diluted 1/50 with the protein assay solution (Bio-Rad, Munich, Germany) according to the manufacturer's instructions, and the absorbance was read at 540nm. The readings of the samples were interpolated against the BSA standard curve.

2.6.3. Protein separation

Proteins were separated using standard techniques (Towbin et al., 1979) on gradient SDS-PAGE gels of varying percentage of acrylamide (between 4-15% w/v) depending on the size of the protein of interest. The recipes and the buffers used are listed in appendix 1. Separating and stacking gels were prepared in BioRad Mini-Protean II gel systems. Samples were heated at 37°C for 10 min and then centrifuged at 6000g for 10 minutes. Prior to loading of the samples onto the gel, 0.01% (w/v) bromophenol blue was added. 20-50μg of protein in dissociation buffer were loaded per well. For small proteins pre-stained low molecular weight markers 3-43kDa (Life Technologies), or for larger proteins rainbow wide range molecular weight markers (2350-46000kDa, Sigma) were used. The gel was run at 100V until the bromophenol blue had run through the stacking gel. Thereafter, the gel was run at 200V until the bromophenol blue had reached the bottom of the separating gel.

2.6.4. Staining of protein gels

Equal protein loading was quantitatively verified on gels stained overnight with 0.1% (w/v) Phastgel blue R250 dye in 40% methanol and 10% (v/v) glacial acetic acid. Gels were then rinsed in ddH_2O for 5-20 hours to destain.

2.6.5. Immunostaining of blots

After separation, gels were equilibrated in transfer buffer (Towbin's buffer, see appendix 1) for 30 minutes. A polyvinylidene difluoride (PVDF, Millipore, Bedford, MA, USA) membrane was "wetted" in methanol and placed onto the gel. This "sandwich" was placed between two sheets of blotting paper (Whatman No1, Whatman Ltd, UK) and then placed in a BioRad mini-blotting tank containing Towbin's transfer buffer. Proteins were blotted for 1 hour at 100V. The post blot gel was stained with Phastgel blue R250 dye as described to control for equal loading of

protein (section 2.6.4.).

The PVDF was blocked for two hours in 10% (w/v) proprietary milk powder in PBS at room temperature. The membrane was washed in 0.3% Tween/PBS for 10 minutes at room temperature and incubated with the primary antibody diluted in 0.3% Tween/PBS overnight. After three washes in 0.3% Tween/PBS for 5 minutes each gels were incubated with the secondary antibody diluted in 0.3% Tween/PBS for 2 hours at room temperature. All blots were developed by chemiluminescence detection (NEN, Life Science Products, Boston, USA) following the manufacturer's instructions. The membranes were then exposed to ECL film (Amersham, UK) for varying times (between 5 seconds and 2 minutes) before development and fixation.

The following antibodies were used: anti-HA rat monoclonal antibody (Boehringer, Mannheim, Germany, 1/3000) as primary and sheep anti-rat Ig-HRP (Fab fragments, Boehringer, Germany, 1/3000) as the secondary antibody; anti-α-synuclein (Zymed, USA, 1/4000) and anti-porin (Calbiochem, USA, 1/25,000) mouse monoclonal antibodies as primary and rabbit anti-mouse HRP (Bio Rad, UK, 1/3000) as secondary antibody; (anti-tyrosine hydroxylase rabbit polyclonal antibody (Biogenesis, UK, 1/500) and donkey anti-rabbit (Dako, UK, 1/200) as secondary antibody.)

2.7. Enzyme analysis

All assays were performed in a final volume of 1ml on either a Hitachi U3210 or a Kontron 940 dual-beam spectrophotometer at 30°C. Enzyme assays were performed in triplicate for each sample. Results were accepted if they were within 15% of each other. The chemicals necessary for the assays were from Sigmal Chemical Company and from Boehringer Mannheim (Boehringer Mannheim, Germany).

2.7.1. Preparation of mitochondrial enriched fractions (MEFs)

MEFs were prepared from 10 X 10cm nearly confluent culture dishes of HEK293 cells according to the method described by Krige et al. (Krige et al., 1992). Cell were harvested, the cell pellet resuspended in 10ml of PBS and centrifuged at 300g for 10 minutes. This procedure was repeated three times. The last cell pellet was frozen at –70°C overnight. The cell pellet was then thawed and resuspended in 2ml ice-cold homogenisation buffer (0.25M sucrose, 10mM Tris-HCl, 1mM EDTA-K_2, pH 7.4). Each sample was homogenised on ice with 20 strokes using a Potter homogeniser at 1000rpm, and then centrifuged at 1500g for 10 minutes at 4°C. The resultant post-nuclear supernatant (PNS) was collected into a fresh tube and kept on ice. The homogenisation and centrifugation steps were repeated twice resulting in three PNSs for each sample. These were combined and centrifuged for another 10 minutes at 1500g; any residual pellet was discarded. The final PNS was centrifuged at 10000g for 12 minutes in a Kontron Centrikon T-124 centrifuge resulting in a brown MEF pellet. This pellet was resuspended in 200-800µl of ice-cold homogenization buffer, aliquoted and snap-frozen in liquid nitrogen and stored at –70°C for up to a week until assaying. Before assaying mitochondrial respiratory chain activities all samples were freeze-thawed in liquid nitrogen three times to brake up mitochondrial membranes.

2.7.2. Mitochondrial respiratory chain activities

2.7.2.1. NADH CoQ reductase (Complex I)

The assay is based on the method described by Ragan et al (Ragan et al., 1987). It measures the rotenone sensitive CoQ_1 dependant oxidation of NADH at 340nm. The CoQ_1 was a gift from the Eisai Chemical Co, Japan. The stock solution of CoQ_1 was diluted in ethanol followed by measuring the absorbance of CoQ_1 at 275nm. To completely reduce quinone to quinol an excess of sodium borohydrate was added to

the reference cuvette. The change in absorbance was used to calculate the concentration of CoQ_1 using a molar extinction coefficient of $2.25x10^3$ (Redfearn, 1967).

The sample and the reference cuvettes contained 20mM K^+ Phosphate buffer with 8mM $MgCl_2$ at pH7.2, 150μM NADH, 1mM KCN 2.5mg/ml BSA in a total volume of 1ml. To the sample cuvette the mitochondrial enriched fraction of the sample was added with the volume depending on the concentration; adjusting for the volume of sample and ubiquinone the volume of H_2O was calculated to give a total volume of 1ml. The test and the sample cuvette were loaded into the photospectrometer followed by the addition of 50μM CoQ_1 to the sample cuvette in order to start the reaction. The linear change of absorbance was recorded for 3-4 minutes. Then, 10μl of rotenone was added to both cuvettes leading to a decrease in the rate of the reaction due to the inhibition of the rotenone sensitive component of the complex I activity. Complex I activity was defined as the rotenone sensitive reaction rate.

The rate was expressed as absorbance units per ml of sample. The molar extinction coefficient of $6.81x10^3$ (adjusted for the concentration of CoQ_1) for NADH was used to calculate the enzyme activity in nmol/min/ml. Enzyme activity was expressed relative to the protein concentration of the sample in nmol/min/mg and as a ratio with citrate synthase activity.

2.7.2.2. Succinate Cytochrome C reductase (Complex II/III)

The assay is based on the method described by King (King, 1967) and measures the antimycin A sensitive, succinate dependant reduction of cytochrome c at 550nm.

The test and the reference cuvette were loaded with 100mM K^+ Phosphate buffer (pH 7.4), 300μM (K_2) EDTA, 100μM cytochrome c and 2.5mg/ml BSA in a total volume of 1ml. In order to activate the enzyme, the sample was incubated in an

Eppendorf tube for 4-5 minutes with 40µl of succinate and 10µl of KCN (to block cytochrome oxidase activity). After 4 minutes of incubation, 10µl of KCN were added to the reference cuvette, both cuvettes were placed into the spectrophotometer and assayed at 550nm. After another minute the entire contents of the Eppendorf tube were added to the test cuvette, which was then thoroughly mixed. After 4-5 minutes, antimycin A (complex III inhibitor) was added to the test cuvette, which was thoroughly mixed again, and the assay was continued for a further 4-5 minutes.

From the recording two reaction rates were calculated. The antimycin A independent rate (usually near zero) was subtracted from the total reaction rate. This resulted in the reaction rate of cytochrome c reductase, which was expressed as absorbance units per ml of sample. Using the molar extinction coefficient of cytochrome c, $19.2x10^3$, the activity was calculated as nmol/min/ml, and related to protein concentration in the sample as nmol/min/mg protein. The activity was also expressed as a ratio with citrate synthase activity.

2.7.2.3. Cytochrome oxidase (Complex IV)

This assay is based on the method described by Wharton et al (Wharton and Tzagoloff, 1967). It measures the oxidation of reduced cytochrome c at 550nm.

Reduced cytochrome c was prepared from 100ml of a 1% solution of cytochrome c from horse heart made up in 10mM K^+ phosphate buffer. Cytochrome c was reduced by adding an excess of ascorbate (13mg). The solution was mixed thoroughly. In order to test whether cytochrome c had been reduced competely 50µl of the cytochrome c solution were added to each of two cuvettes containing 10mM K^+ phosphate buffer in a total volume of 1ml. 10µl of freshly made saturated ascorbate solution were added to the test cuvette and the change in absorbance was noted. A positive change in absorbance indicated that cytochrome c had not been completely reduced and therefore needed further treatment with ascorbate.

Next, in order to remove the ascorbate the solution was dialysed against 5L of 10mM K^+ phosphate buffer pH7 at 4°C overnight using size 1 dialysis tubes (Medicell International Ltd., London, UK). Oxidised cytochrome c was then added to the solution and the absorbance measured. If the ascorbate had been removed completely there should be no change in absorbance.

The volume of cytochrome c needed in the reaction mix to give 50μM reduced cytochrome c (equivalent to an absorbance of 0.96) was calculated from the absorbance with 50μl of stock reduced cytochrome c in a reaction mix of 10mM K^+ Phosphate buffer (pH 7) in a total volume of 1ml against a reference cuvette containing an additional 10μl of K^+ ferricyanide.

Test and reference cuvettes were loaded with 10mM K^+ Phosphate buffer (pH 7), 50μM reduced cytochrome c and H_2O. The volume of H_2O was adjusted to result in a total volume of 1ml. Both cuvettes were placed in the spectrophotometer and after autozeroing 10μl of ferricyanide were added to the reference cuvette. A note of the initial absorbance was made (should be 0.94 – 0.98), the assay was started and then the sample was added and the test cuvette mixed as quickly as possible. The reaction rate was visualised as a decrease in absorbance as a result of oxidation of reduced cytochrome c.

The absorbance at the start of the reaction (t=0) was extrapolated and the change in absorbance determined at several time points. A pseudo-first-order rate constant k was calculated in k/ml using the equation {ln0.96-ln(0.96-change in absorbance at a given time point) X 1000/sample volume in μl X dilution factor}. In this equation 0.96 represents the absorbance of cytochrome c fully reduced at the start of the reaction. The k/min/ml was calculated by plotting the k/ml values for 5 time points (0, 0.5, 1, 1.5 and 2minutes) against time. The gradient was calculated

using a linear regression analysis. The activity of complex IV was expressed as k/min/mg protein and as a ratio with the citrate synthase activity.

2.7.3. Citrate synthase

This assay is based on the method described by Coore et al (Coore et al., 1971). Citrate synthase is a mitochondrial matrix enzyme that catalyses the condensation of oxaloacetate and acetyl CoA in the citric acid cycle. This produces CoA. In the assay, the free thiol group combines with 5-5'-dithiobisnitrobenzoic acid (DTNB) thus increasing the absorbance at 412nm.

The test and the reference cuvettes were loaded with 100mM Tris (pH 8), 100μM acetyl CoA, 100μM DTNB in a total volume of 1ml. The cuvettes were loaded into the spectrophotometer and the assay started at 412nm after autozeroing. Then, 10μl of oxaloacetate (final concentration 100μM) were added to the test cuvette to start the reaction. The reaction rate was expressed as absorbance units per ml of sample, and using the molar extinction coefficient of $13.6x10^3$ for the DTNB-CoA-SH complex as nmol/min/ml. The activity was related to the protein concentration of the sample and expressed in nmol/min/mg protein.

2.7.4. Aconitase

This assay is based on the method described by Gardner et al (Gardner et al., 1994). Following the condensation of oxaloacetae and acetyl CoA to form citrate, in the second step of the citric acid cycle citrate needs to be isomerised in order to undergo oxidative decarboxylation later. Citrate is therefore first dehydrated and then hydrated with cis-aconitate as an intermediate. Both reactions are catalysed by aconitase, an iron-sulfur protein. Since aconitase is very labile sample were assayed immediately.

The test and the reference cuvette contained 50mM Tris/HCl buffer (pH 7.4), 0.4mM NADPH, 5mM sodium citrate, 0.6mM $MgCl_2$, 0.1% Triton X-100, 1-2 units of isocitrate dehydrogenase and H_2O_2 for a total volume of 1ml.

Both cuvettes were loaded into the spectrophotometer, and after autozeroing the assay was started at 340nM and left to run until a linear reaction rate was reached. The reaction rate was expressed as absorption units per ml of sample. Aconitase activity was calculated using the molar extinction coefficient for NADP ($\varepsilon=6.22 \times 10^3$) and expressed in nmol/min/mg protein.

2.8. Flow cytometry

2.8.1. Principles

Flow cytometry allows rapid measurements of cells as they pass individually in a fluid stream past a sensor. This method enables each cell to be measured individually rather than resulting in an average value for the whole cell population in a given sample. In addition, more than one parameter can be measured at the same time. The combination of light scatter and fluorescence yields information on physical properties of cells and allows the use of fluorescent probes to detect specific proteins, nucleic acid content, enzyme activity or membrane potential. It is now very common to combine the measurement of two light scatter (forward and side) and several fluorescent parameters (Ormerod, 2000).

The flow cytometer used in this thesis (FACScalibur, Becton Dickinson, UK) uses lasers as the source of illumination. The scattered and fluorescent light generated by individual cells travelling through the laser beam is collected by photodetectors, which then convert the photon pulses into electronic signals. These signals are amplified and filtered, and finally converted digitally into binary numbers by a computer system. Data generated in this way can be analysed on-line or digitally stored for later, off-line analysis (for details see (Ormerod, 2000).

In this thesis, forward angle light scatter (FSC) and right angle light scatter (S (side) SC) were used to describe cell size and cell surface morphology respectively. Fluorescein (FITC-green) and propidium iodide (PI-red) were used as fluorescence colours. The instrument set up consisted of a set of mirrors (placed at 45° to the incident laser beam) and orthogonally positioned absorption and interference filters. The first mirror was a 500nm long-pass dichroic filter set at right angles to the laser beam path. This mirror reflected wavelengths that were shorter than 500nm towards the SSC detector. Wavelengths above 500nm passed on to the second mirror, a 560nm short-pass dichroic filter so that wavelengths longer than 560nm were reflected towards the PI-red detector passing through a filter centred at 578nm with a 28nm half-peak bandpass. Wavelengths shorter than 560nm and longer than 500nm at the second mirror passed on towards the FITC fluorescence detector through a 530nm filter with a 30nm half-peak band-pass.

The measurement of light scatter parameters was displayed as a dot plot (an example is given in Figure 2.2A). On the grounds of this plot a gate (R1 in Figure 2.2A) was set to exclude cell clumps (as judged by an increase in size) and debris (small size). Next, live and dead cells were distinguished within the cell population in gate R1. If a cell is damaged or dead the integrity of the cell membrane cannot be maintained. The nuclei of these cells become accessible to propidium iodide and fluoresce red when excited at 578nm (FL2 channel). Cells labelled with propidium iodide have therefore been damaged or have died. Further, the lipophylic dye $DiOC_{6(3)}$ (3,3'-dihexyloacarbocyanine, Molecular Probes) can be used to examine the mitochondrial membrane potential. Uptake of this dye depends upon mitochondrial membrane potential and hence identifies viable cells. Therefore, dead cells and viable cells can be differentiated on a dot plot displaying the cell population in gate R1 with red fluorescence indicating propidium iodide uptake in FL2 on the x axis and green fluorescence indicating $DiOC_{6(3)}$ uptake in FL1 (488nm laser and

500nm long-pass filter) on the y axis (Figure 2.2B). Measurements of other parameters, e.g. involving fluorescent dyes, can then be focused on the cell population of interest that has been selected by setting the appropriate gate. Figure 2.2C gives an example of the fluorescence intensity of $DiOC_{6(3)}$ displayed as a histogram from the viable cell population gated in Figure 2.2B (R2).

A

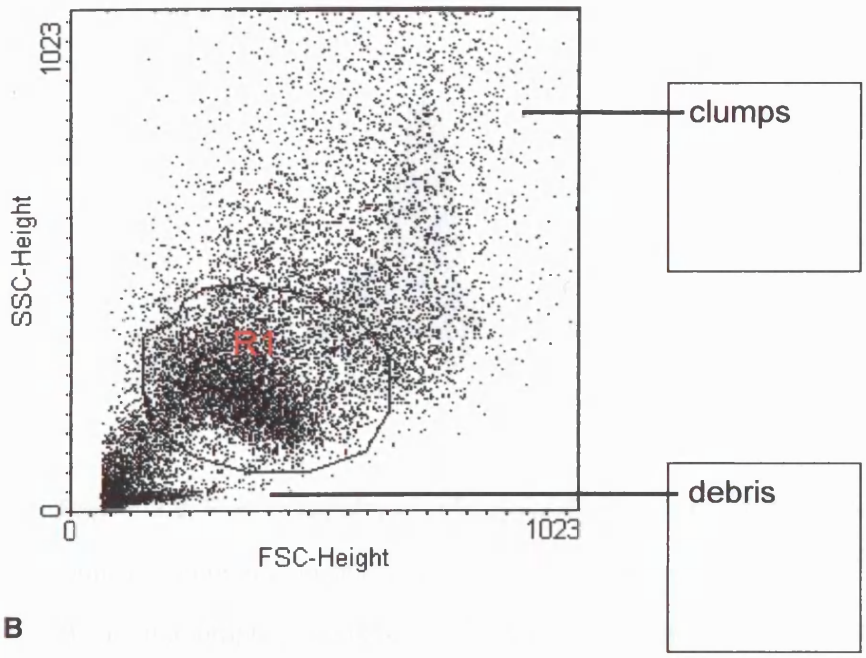
1023
SSC-Height
0
R1
0
1023
FSC-Height
clumps
debris

B

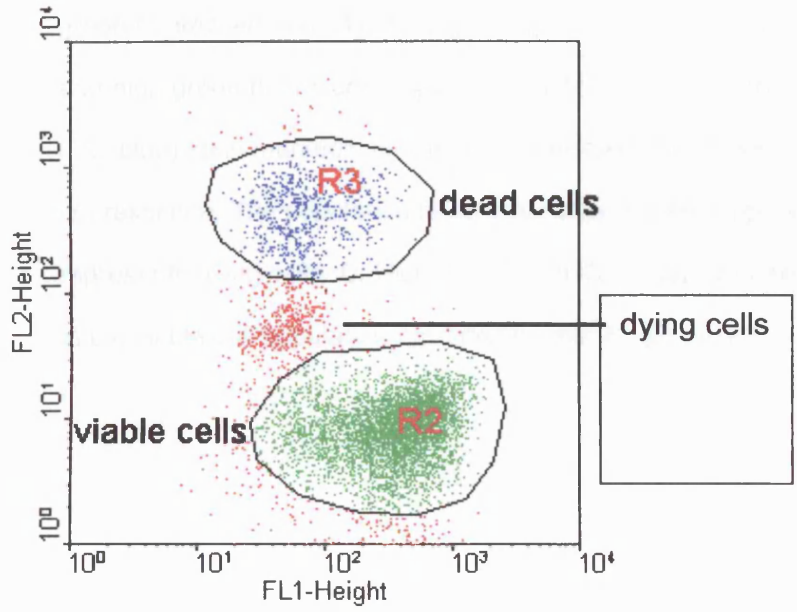
10^4
10^3
10^2
10^1
10^0
FL2-Height
R3
dead cells
dying cells
viable cells
R2
10^0
10^1
10^2
10^3
10^4
FL1-Height

C

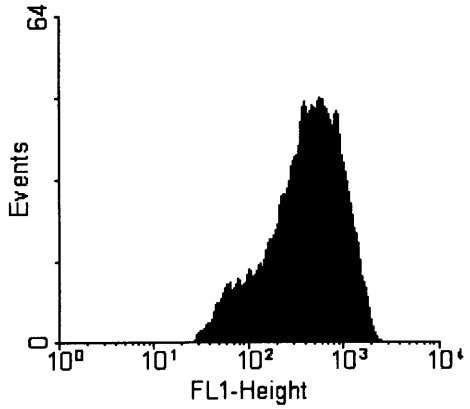

Figure 2.2. Flow cytometry of cells stained with PI and $DiOC_{6(3)}$. **A.** Exclusion of cell clumps and debris on side scatter (SSC) and forward scatter (FSC) dot plot graphs. **B.** Dot plot graph of fluorescence staining for PI red fluorescence (FL2) and $DiOC_{6(3)}$ green fluorescence (FL1) of the gated population in A (R1). Low red fluorescence and high green fluorescence indicated viable cells (R2, green) whereas dead cells (R3, blue) stain markedly for the red fluorescent dye PI and have little $DiOC_{6(3)}$ green fluorescence. The population of cells between the two regions presumably represents dying cells. **C.** Histogram of $DiOC_{6(3)}$ median green fluorescence intensity in the viable cell population indicated by the R2 gate in B.

2.8.2. Sample preparation for flow cytometry

Cells were plated out on 12 well plates at a density of 62500 cells/ml. Following the respective experiment, cells were harvested by trypsinisation, resuspended in PBS and transferred to FACS tubes containing 5mM EDTA to avoid cell clumping. The cells were incubated with 50nM $DiOC_{6(3)}$ for 20 minutes at 37°C. Propidium iodide (1µg/ml) was added for two minutes and FACS analysis performed immediately on a FACScalibur (Becton Dickinson) flow cytometer.

2.8.3. Mitochondrial membrane potential

2.8.3.1. $DiOC_{6(3)}$ staining and fluorescence microscopy

Cells were plated in quadruplicate in 12 well plates at a density of 62500 cells/ml. At the end of the experiment, cells were harvested by trypsinisation, resuspended in PBS and transferred to FACS tubes (Becton Dickinson, France). EDTA was then added (5mM final concentration). $DiOC_{6(3)}$ was added for 15 minutes, and propidium iodide (1µg/ml) was added for two minutes while samples were kept on ice and protected from light; FACS analysis was performed immediately on a FACScalibur (Becton Dickinson) flow cytometer using the instrument set up described in section 2.8.1.). 10^4 events were acquired, and debris and cell clumps excluded on a forward scatter and side scatter dot plot as described (see section 2.8.1.). Within the included events (R1 in figure A), live cells were defined by propidium iodide exclusion (see section 2.8.1.). In viable cells $DiOC_{6(3)}$ fluorescence intensity was measured as described in section 2.8.1. The instrument settings were standardized, and identical gate settings were used for all experiments performed at the same time.

2.9. Cell viability studies

Cell death can be detected by monitoring plasma membrane lysis either by measuring the release of cytosolic lactate dehydrogenase or or detecting the uptake of the membrane impermeable dye propidium iodide (PI). Both methods were used in this thesis. PI uptake measurements by flow cytometry have the advantage that the numbers of vable and dead cells can be quantitated. In addition, cells can be stained with PI and another fluorescent dye, e.g. $DiOC_{6(3)}$ to probe mitochondrial membrane potential on the respective cellular subpopulations, e.g. viable cells. However, all assessments using flow cytometry rely on samples in which there is minimal cell clumping. With some toxins, e.g. dopamine it was very difficult to prepare samples without some degree of cell clumping. In this case, the LDH assays were used.

2.9.1. Lactate Dehydrogenase (LDH) assay

When cells die by necrosis, their membranes leak LDH into the medium. The activity of LDH in the medium of a cell culture dish thus represents a measure of cell death and can be related to the activity of LDH in the total cell fraction of the same culture. The total LDH activity of a given sample is the combined activity of LDH acitivity in the "dead" and the "live" fraction. Viable cells (= LDH activity of the "live" fraction) were expressed as a percentage of the total LDH activity in a given sample.

Cells were plated out in triplicate at a density of circa 62,500 cells per well of a 12 well plate using phenol-red free medium. At the end of the experiment, the medium of each well was pipetted into a screw top container. This container was centrifuged at 13.000 rpm for 5 minutes at 4°C and the supernatant pipetted into a fresh container (dead fraction). The cell pellet was added to the live fraction. Cells were washed in PBS, harvested by flushing them off the dish with PBS and transferred into another screw top container (live fraction). Pairs of supernatant and

cells of the same well were stored at –20 C until they were assayed for LDH acitivity. The ratio of LDH activity in the supernatant to the total LDH activity was taken as the percentage of cell death.

The assay is based on the method of Clark and Nicholas (Clark and Nicklas, 1970) and measures the activity of LDH, a cytoplasmic enzyme catalysing the reduction of pyruvate to lactate and the oxidation of NADH to NAD^+. As NADH is converted to NAD^+ the absorbance at 340nm decreases. The test and the reference cuvette were loaded with K^+ Phosphate buffer (pH 7.4; final concentration 50mM), NADH (final concentration 200μM), Triton X-100 (final concentration 0.5% (v/v)) and H_2O for a total volume of 1ml, depending on the volume of sample added to the test cuvette. Cuvettes were loaded into the spectrophotometer, and the assay was started at 340nm after autozeroing. The reaction was initiated by adding Na pyruvate (final concentration 1mM) to the test cuvette. The reaction rate was expressed as absorbance units per ml of sample.

Alternatively, for large numbers of samples a LDH Cytotoxicity Detection Kit (TaKaRa Biomedicals, Japan) was used. This is a colorimetric assay where the LDH catalysed conversion of lactic acid to pyruvate leads to the reduction of NAD^+ to $NADH/H^+$. In the second step diaphorase transfers H/H^+ from $NADH/H^+$ to the tetrazolium salt INT (yellow), which is reduced to formazan (red). The formazan dye is water-soluble and shows the maximum absorption at 500nm whereas the tetrazolium salt INT does not absorb at these wavelengths. The change in colour from yellow to red, and the respective change in absorption at 500nm, is proportionate to the amount of LDH present in the sample. Assays were set up on 96-well plates at room temperature and ambient air. Samples and controls were assayed in quadruplicate. Controls consisted of phenol-red free medium alone in the same dilution in PBS as the samples. Care was taken to ensure that reactions were read while the rates were in the linear range. First, the change in absorption

measured in the controls was subtracted from that of the samples. Then, the change in absorption in the respective sample pairs, i.e. dead and live fraction, was combined to give the total LDH activity per sample. Finally, the ratio of LDH activity in the live fraction and total LDH activity was taken as the percentage of viable cells.

2.9.2. Flow cytometry

Cells were plated in quadruplicate in 12 well plates at a density of 62500 cells/ml. At the end of the experiment, cells were harvested by trypsinisation, resuspended in PBS and transferred to FACS tubes (Becton Dickinson, France). EDTA was then added (5mM final concentration). $DiOC_{6(3)}$ was added for 15 minutes, and propidium iodide (1µg/ml) was added for two minutes while samples were kept on ice and protected from light; FACS analysis was performed immediately on a FACScalibur (Becton Dickinson) flow cytometer using the instrument set up described in section 2.8.1.). 10^4 events were acquired, and debris and cell clumps excluded on a forward scatter and side scatter dot plot as described (see section 2.8.1.). Within the included events (R1 in figure A), live cells were defined by propidium iodide exclusion (see section 2.8.1.). Viable cells were expressed as a percentage of the total number of included events. The instrument settings were standardized, and identical gate settings were used for all experiments performed at the same time.

2.10. GSH assays

These experiments were performed in collaboration with C Tomlinson, Department of Clinical Neuroscience, Royal Free and University College London Medical School. Cells were plated out at a density of 62.500 cells/ml on 10cm Petri dishes. At the end of the experiment, cells were harvested with Versine and the cell pellet resuspended in 500µl 5% metaphosphoric acid, mixed for 3 min and centrifuged at 10 000 x g for 5 min at 4°C. The supernatant was used to determine glutathione

levels using the Calbiochem GSH assay kit according to the manufacturers instructions (Calbiochem, La Jolla, USA) using a GSH standard curve. The GSH standard was quantitated spectrophotometrically at 412nm following its reaction with DTNB.

2.11. Dopamine Uptake

The ability of the HEK293 cells to take up dopamine was examined in collaboration with Drs P Korlipara, K Messmer and JM Cooper, Department of Clinical Neuroscience, Royal Free and University College London Medical School using [2,5,6-^{3}H]-dopamine. HEK293 cells were grown to 80% confluency on 10cm plates. Cells were washed in PBS, which was replaced by HEK293 growth medium containing 2μCi/ml [^{3}H]-dopamine (Amersham, UK) and 20μM pargyline (Sigma). The plates were incubated at 37°C in a humidified incubator. At various time points (0 - 60 minutes) a plate of cells was removed and washed three times in 10ml of ice-cold PBS. The cells were harvested by scraping in 4ml of PBS, pelleted for 10min at 1000 x g and resuspended in 0.5ml of PBS followed by analysis on a liquid scintillation counter (Beckman, UK). The number of cells was determined by cell counting and the data corrected for cell number.

2.12. Statistical analysis

Data was analysed first to assess whether it was normally distributed (data display in histograms). In case of normal distribution parametric statistics were used. Data from two independent groups was compared using a Student's t-test; data from three or more groups of observations was compared using one-way analysis of variance (ANOVA) with post-hoc t-test comparing subgroups if a main effect was observed. Non-parametric data from two independent groups was assessed using the Mann-Whitney U-test. Three or more groups of observations were compared

using the Kruskal-Wallis test followed by post-hoc Dunn's Multiple Comparison test if the Kruskal-Wallis test was significant.

Different frequencies of variables were analysed using Fisher's exact test. All data was analysed using commercially available software wit statistical significance levels set to $p<0.05$.

CHAPTER 3.

A HEK293 cell model for α-synuclein Parkinson's disease

3.1. Introduction

3.1.1. Clinical features of Parkinson's disease (PD)

Parkinson's disease (PD) is the second most common neurodegenerative disease with an estimated prevalence of 1 to 2% in the population over 65 years of age (de Rijk et al., 2000). PD most commonly manifests between the 5th and the 7th decade with bradykinesia, tremor, rigidity and abnormal postural reflexes. The diagnosis of PD is made on clinical grounds; other clinical signs may indicate other causes of parkinsonism, e.g. frequent falls backwards and supranuclear gaze palsy would suggest progressive supranuclear palsy. However, post mortem neuropathological examination showed that clinical diagnosis is not always able to correctly identify sporadic PD (Hughes et al., 1992a; Hughes et al., 1992b). Thus, the neuropathological examination remains the gold standard for the diagnosis of parkinsonian syndromes.

3.1.2. Pathological features of PD

PD is characterised pathologically by the degeneration of the pars compacta of the substantia nigra, the locus coeruleus and substantia innominata. Within the substantia nigra, the greatest loss of neurones tends to be observed in the ventrolateral tier, followed by the medial ventral tier and dorsal tier (Fearnley and Lees, 1991). The pattern of neuronal cell loss within the substantia nigra is relatively specific for PD and differs from that observed in other parkinsonian syndromes such as striatonigral degeneration or supranuclear palsy. At the time of onset of symptoms, a large proportion (50-70%) of dopaminergic neurones in the substantia nigra pars compacta have already been lost resulting in reduced dopamine

synthesis and release from the striatal nerve terminals (Lang and Lozano, 1998a). Subsequently, the loss of dopamine in the putamen is most prominent in the dorsal and intermediate subdivisions of the putamen, which might underlie some of the symptoms of PD, i.e. akinesia and rigidity (Kish et al., 1988).

The formation of Lewy bodies (LBs), and Lewy neurites in surviving dopaminergic neurones is the hallmark pathological finding in PD. Lewy neurites are degenerating ubiquitin positive neuronal processes found in all affected brainstem regions, in particular the dorsal motor nucleus of the vagus nerve (Gai et al., 1995). LBs are intracytoplasmic eosinophilic inclusions composed predominantly of ubiquitin and α-synuclein (Spillantini et al., 1997); however, a number of other proteins have been identified within LBs such as synphilin-1, parkin, neurofilaments, UCH-L1, proteasomal components, heat-shock protein and nitrated α-synuclein (Giasson et al., 2000; Good et al., 1998; Ii et al., 1997; Lowe et al., 1990; Schlossmacher et al., 2002; Shashidharan et al., 2000; Wakabayashi et al., 2000). On electron microscopy, LBs characteristically consist of a dense granular core surrounded by a halo of radiating filaments (Duffy and Tennyson, 1965). LBs are found in the substantia nigra, locus coeruleus, the dorsal motor nucleus of the vagus nerve, as well as the substantia innominata and the intermediolateral cell column of the spinal cord. LBs are not specific for PD and can also be found in brains of patients with Alzheimer's disease and a disorder called cortical LB dementia; in addition, LBs can be incidental findings in postmortem pathological specimens at a greater frequency than PD (Gibb and Lees, 1988).

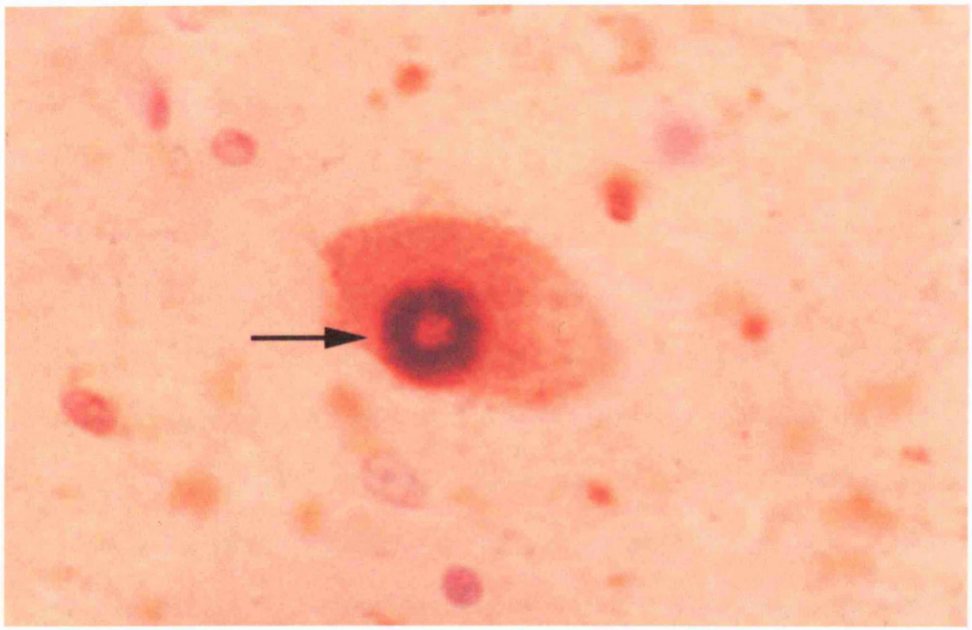

Figure 3.1. Lewy body stained with α-synuclein. A section of substantia nigra of a patient with PD shows a dopaminergic neurone that contains a LB. Immunohistochemistry reveals that the LB stains intensely with an antibody to α-synuclein (dark brown, arrow). This image was downloaded from www.feany-lab.bwh.harvard.edu/link2/.

3.1.3. Pathogenetic mechanisms in PD

Several recent advances have increased our understanding of the pathogenesis of PD. A significant genetic element in the aetiology of PD, in at least a proportion of patients, is suggested by results from twin studies, case control studies and the identification of mutations in several genes in familial PD. In addition, environmental toxins have been associated with parkinsonism including carbon monoxide, manganese and, most importantly, 1-methyl-4-phenyl-1,2,3,6 tetrahydropyridine (MPTP). The clinical and pathological syndromes associated with both the familial PD cases and those caused by environmental agents are remarkably similar; they all cause parkinsonism and give rise to relative selective loss of dopaminergic neurones with, apart from parkin PD, the formation of LBs. This lends support to the hypothesis that PD is a heterogenous disease likely to be caused by more than one specific aetiological factor. The pharmacological replacement, of dopamine by L-Dopa or dopamine agonists, as well as other treatments such as deep brain stimulation, can relieve PD symptoms but do not stop disease progression (Lang and Lozano, 1998b).

3.1.4. Environmental toxins and PD

Epidemiological evidence suggests that toxins are involved in the pathogenesis of PD. Anecdotal reports describe parkinsonism with carbon monoxide (Gordon, 1965; Grinker, 1926; Klawans et al., 1982), manganese (Couper, 1837; Huang et al., 1993; Mena, 1979) and MPTP (Davis et al., 1979; Langston and Ballard, 1983) exposure. One study suggested that prolonged occupational exposure to a combination of either iron and lead, or iron and copper increased the risk for PD (Gorell et al., 1998). Pesticide exposure, e.g. in well water, may be another risk factor for PD, in particular with prolonged exposure (Gorell et al., 1998; Liou et al., 1997; Petrovitch et al., 2002; Seidler et al., 1996; Semchuk et al., 1992). Specific

pesticides including paraquat, organochlorine and carbamate derivatives were identified in some studies (Liou et al., 1997; Seidler et al., 1996; Semchuk et al., 1992). An interaction between paraquat, or rotenone, and α-synuclein, a major component of LBs in PD, has been reported (see section 3.1.8.5.2) possibly linking these environmental agents to a possible genetic factor.

Other environmental agents have been shown to have a neuroprotective effect and hence reduce the risk of PD. These may include caffeine (Ascherio et al., 2001; Ross et al., 2000) and cigarette smoking (Hernan et al., 2001). The amount of cigarette smoking was recently found to inversely correlate with the age of onset of PD in both monozygotic (MZ) and dizygotic (DZ) twins (Tanner et al., 2002). The correlation was stronger in MZ twins despite a high concordance for smoking. Thus, cigarette smoking might be one of the additional factors that are relevant modulators of disease onset in PD.

3.1.5. Evidence for mitochondrial involvement in PD

Research into mitochondrial involvement in the pathogenesis of PD began with the discovery that the metabolite of MPTP, MPP+, inhibited complex I of the mitochondrial respiratory chain (Mizuno et al., 1987; Nicklas et al., 1985; Ramsay et al., 1986). A Parkinsonian syndrome with bradykinesia and rigidity and a good response to L-dopa was first described in drug abusers after exposure to MPTP (Langston and Ballard, 1983). MPTP was also shown to induce Parkinsonism (tremor, rigidity, akinesia and postural instability) in other primates (Langston et al., 1984). A link to PD pathology was observed in squirrel monkeys where prolonged MPTP application in older animals led to loss of dopaminergic neurones and eosinophilic inclusions in a very similar distribution to the pathology of PD (Forno et al., 1986).

Complex I deficiency was first identified in the substantia nigra of post

mortem PD brain (Janetzky et al., 1994; Schapira et al., 1990a; Schapira et al., 1989). The defect appeared to be restricted both to complex I and the substantia nigra with other brain areas such as striatum (caudate and putamen), cortex, cerebellum, globus pallidum, tegmentum and substantia innominata showing normal mitochondrial respiratory chain activity (Cooper et al., 1995; Gu et al., 1998b; Janetzky et al., 1994; Mann et al., 1994; Mann et al., 1992; Schapira et al., 1990b). In multiple system atrophy, a disorder with parkinsonism and degeneration of neurones in substantia nigra, no mitochondrial respiratory chain defect was found (Gu et al., 1997) and there was no complex I abnormality in Lewy body rich cingulate cortex of diffuse Lewy body brains (Gu et al., 1998b). This suggests that the complex I defect is specific to PD and selective for the substantia nigra, but not related to the formation of Lewy bodies and not seen merely when the substantia nigra degenerates, e.g in multiple system atrophy. However, other reports described reduced immunoreactivity for α-ketoglutarate, an enzyme of the citric acid cycle, in substantia nigra of PD patients (Mizuno et al., 1994).

Mitochondrial respiratory chain activity has also been assessed in other PD tissues (Table 3.1.). In skeletal muscle, both reduced (Bindoff et al., 1989; Blin et al., 1994; Cardellach et al., 1993; Nakagawa-Hattori et al., 1992; Shoffner et al., 1991) and normal complex I activity have been reported (Anderson et al., 1993; DiDonato et al., 1993; Mann et al., 1992; Reichmann et al., 1994). Mitochondrial respiratory chain analysis in platelets showed more consistent results, in particular, when isolated platelet mitochondria are used, with a complex I defect either alone or together with a milder defect in other complexes (Benecke et al., 1993; Haas et al., 1995; Krige et al., 1992). In platelets, the severity of the complex I defect has varied between studies from 16-55% deficiency. In lymphoblasts, complex I activity was reported to be either reduced (Barroso et al., 1993) or normal (Martin et al., 1996; Yoshino et al., 1992). One group studied mitochondrial respiratory chain activities in

PD fibroblasts and found a significant decrease in the oxidative decarboxylation of (1-^{14}C) pyruvate but not (1,4-^{14}C) succinate suggesting a differential impairment of complex I but not complex II/III (Mytilineou et al., 1994).

It is unclear whether the discrepancy of results reflects methodological differences or whether they could be explained by heterogeneity of the PD patients in terms of the presence of a mitochondrial defect. Tissue homogenates are most commonly used to assess mitochondrial respiratory chain activity in post mortem brain because mitochondria cannot easily be isolated. However, assays for mitochondrial respiratory chain function are most sensitive in purified mitochondria. This was demonstrated in platelets where homogenate analysis was normal (Mann et al., 1992) whereas isolated mitochondria were abnormal (Krige et al., 1992). Hence, using tissue homogenates may fail to recognise more subtle defects in other areas of the PD brain apart from substantia nigra, where the defect may be more severe.

Taken together, there seems to be consistent evidence for a complex I defect but not for abnormalities in other mitochondrial respiratory chain complexes in PD. The defect was found most consistently in substantia nigra and platelets whereas the results in other tissues were variable. Why the complex I defect should be restricted to platelets and substantia nigra and not affect other brain regions is not clear. In addtion, not all PD patients have an identifiable complex I defect. This might indicate that a complex I defect is relevant only to a subset of PD patients.

Tissue	Reference	MRC defect
Substantia nigra	(Schapira et al., 1989)	Complex I
	(Schapira et al., 1990a)	Complex I
	(Janetzky et al., 1994)	Complex I
	(Mann et al., 1992)	Complex I
	(Mann et al., 1994)	Complex I
	(Mizuno et al., 1994)	Reduced α-ketoglutarate immunoreactivity
Striatum	(Cooper et al., 1995)	No defect
Cortex, cerebellum, globus pallidus, tegmentum,	(Mann et al., 1992)	No defect
Substantia innominata, cingulate cortex	(Gu et al., 1998b)	No defect
Muscle	(Bindoff et al., 1989)	Complex I
	(Blin et al., 1994)	Complex I
	(Cardellach et al., 1993)	Complex I
	(Nakagawa-Hattori et al., 1992)	Complex I
	(Shoffner et al., 1991)	Complex I
	(Anderson et al., 1993)	No defect
	(DiDonato et al., 1993)	No defect
	(Mann et al., 1992)	No defect
	(Reichmann et al., 1994)	No defect
Platelets	(Haas et al., 1995)	Complex I
	(Krige et al., 1992)	Complex I
	(Benecke et al., 1993)	Complex I
Lymphoblasts	(Barroso et al., 1993)	Complex I
	(Martin et al., 1996)	No defect
	(Yoshino et al., 1992)	No defect
Fibroblasts	(Mytilineou et al., 1994)	Complex I

Table 3.1. Mitochondrial respiratory chain activity in PD tissues. Defects in mitochondrial respiratory chain complexes other than complex I have not been reported.

3.1.5.1. Causes of mitochondrial involvement in PD

What causes the complex I defect in at least a subset of patients with PD remains unclear. Primary causes might include abnormalities in the genes, both nuclear and mitochondrial that encode the subunits of mitochondrial respiratory chain complexes. However, a complex I defect may also be secondary, e.g. caused by a mitochondrial toxin such as MPTP or rotenone.

3.1.5.1.1. Mitochondrial DNA (mtDNA)

As dicussed in the general introduction, mitochondria contain their own DNA (mtDNA), which encodes transfer RNAs, ribosomal RNA and some of the subunits of the mitochondrial respiratory chain complexes (see section1.1.1). The following section examines the evidence to support the involvement of mtDNA in PD.

Cybrid models

In order to examine the role of mtDNA cell cybrid systems were first introduced by King and Attardi (King and Attardi, 1989). They combine nuclear DNA from cells rendered mtDNA-less (ρ^0 cells) by the addition of ethidium bromide or dideoxycytosine with mtDNA from enucleated cells, most conveniently platelets, which carry no nuclear DNA. The system allows the investigation of the structural and functional consequences of mutated mtDNA without the influence of the original nucleus. Hence, if mtDNA were important for the phenotype of the original cells, one would expect a defect to be transmitted to and persist in the cybrids. Alternatively, one would expect that a nuclear abnormality, giving rise to a defect in mitochondrial respiratory chain activity, would be corrected by the nucleus of the host cell in the cybrids.

Swerdlow and colleagues generated cybrids from platelets of unselected PD patients, or controls, and ρ^0 neuroblastoma cells. After 5-6 weeks in the PD cybrids

a 20% decrease of complex I activity was observed, and PD cybrids were more sensitive to MPP+ toxicity than controls (Swerdlow et al., 1996). Similar results were reported when platelets from PD patients with a platelet complex I defect were fused with ρ^0 cells (A549 lung-derived) (Gu et al., 1998a). The PD cybrids had a specific complex I defect (mean 25% decrease in activity) which, similar to the Swerdlow et al study, implied that the PD patient's mtDNA caused this deficiency (Gu et al., 1998a). In addition, a correlation of platelet complex I activity and cybrid complex I activity discriminated even more clearly between the PD patients and controls. This suggested that in this group of idiopathic PD patients pre-selected by their low platelet complex I activity, the mitochondrial respiratory chain defect was determined by the mtDNA derived from their platelets.

In these studies no mtDNA mutations have yet been reported and it remains unclear whether mitochondrial changes in PD result from inherited mutations in the genes coding for mitochondrial respiratory chain proteins or whether mitochondrial function is compromised as a consequence of sporadic somatic mutations.

MtDNA studies

Mitochondria contain 2-10 molecules of their own DNA, mitochondrial DNA (mtDNA, see section 1.1.1). Over 100 mtDNA mutations have been associated with human diseases (Zeviani and Carelli, 2003)(www.mitomap.org). The exclusive maternal inheritance of mtDNA is reflected in a proportion of cases where the disease is passed through the maternal line. While maternal inheritance of a disease will implicate a mtDNA mutation, the majority of patients with mitochondrial mutations may have no such family history (Petty et al., 1986). MtDNA deletions, the most common mtDNA mutation, present as sporadic cases; for example, 40% of patients with Leber's hereditary optic neuropathy (LHON) and the A-G 11778 mtDNA mutation have no family history.

Several studies have sequenced mtDNA in unselected PD patients. In many, no mutation has been identified, whilst in others sequence changes of uncertain significance have been described (Kosel et al., 1998; Mayr-Wohlfart et al., 1997). A meta-analysis of candidate genes in PD suggested a significant risk association for the A4336G mutation of $tRNA^{Glu}$ with PD (Tan et al., 2000). However, this analysis was unable to take account of another study published subsequently, which showed no association of this mutation with PD (Simon et al., 2000).

How can the apparently selective complex I defect in PD be reconciled with these findings? The detection of a heteroplasmic mutation by sequence analysis may be dependent upon the mutant load. Hence, with a mutant load of no more than 5-20% it may be impossible to pick up a change in mtDNA. In addition, it is possible that the mutant load in the substantia nigra is higher than in blood, which has been used in most studies. It is also conceivable that the mitochondrial defect observed in PD tissue is associated with abnormalities of nuclear encoded mitochondrial proteins or is the result of exposure to environmental toxins (see next sections). However, as discussed in the previous section the cybrid data indicated that at least in a proportion of PD patients the mitochondrial defect was mediated through mtDNA. Thus maybe subgroups of PD patients differ in the primary cause (mtDNA, nuclear DNA, toxin) but not in the downstream consequence, i.e. mitochondrial dysfunction.

3.1.5.1.2. Nuclear genes

As dicussed in the general introduction (see section 1.1.1) the majority of the subunits of the complexes of the mitochondrial respiratory chain are encoded by nuclear DNA. Patients with neurodegenerative diseases have been described with mutations in nuclear genes encoding mitochondrial respiratory chain subunits. A single base change in the flavoprotein of succinate dehydrogenase (complex II)

(Bourgeron et al., 1995) and in nuclear-encoded complex I genes (Loeffen et al., 1998; Triepels et al., 1999) gave rise to Leigh's syndrome and another mutation in the 18kD subunit of complex I was associated with encephalomyopathy (van den Heuvel et al., 1998). In three siblings leukodystrophy and myoclonic epilepsy developed with a mutation in the NADH binding site encoding nuclear complex I gene (Schuelke et al., 1999). Inheritance was autosomal recessive in all these patients and they were found to be either homozygous or compound heterozygous for the respective gene defect. Recently, the first nuclear-encoded mitochondrial protein, PTEN induced kinase (PINK1, see section 3.1.8.4.) was implicated in PD (Valente et al., 2004). While PINK1 is not part of complex I of the mitochondrial respiratory chain the discovery of PINK1 mutations in families with PD provided the first link between a nuclear encoded mitochondrial protein and PD.

3.1.5.1.3. Mitochondrial toxins

Epidemiological evidence suggested that environmental toxins, such as rotenone (Liou et al., 1997), could be a risk factor for PD (see section 3.1.4). Two of the toxins, MPTP and rotenone, are known to inhibit complex I of the mitochondrial respiratory chain. In fact, as discussed above, it was the discovery of the association of MPTP exposure and the development of parkinsonism, and the subsequent identification of MPP+, the active metabolite of MPTP, as a mitochondrial toxin that led to research into the involvement of mitochondria in PD. While there is no evidence to suggest widespread MPTP exposure rotenone is used as an insecticide and fish poison. It is therefore possible that for example rural populations are exposed to rotenone and could thus be at greater risk to toxin-mediated complex I inhibition and subsequent damage to the substantia nigra. However, the half-life of rotenone in solution is short so that in lakes rotenone may only be present for a few days (Hisata, 2002). Recently, in Guadaloupe atypical parkinsonism (sharing clinical

and pathological similarities with progressive supranuclear palsy) was linked to the consumption of medicinal preparations made from the tropical plant family *Annonacea* (Caparros-Lefebvre and Elbaz, 1999). These plants contain Annonaceae acetogenins, which are lipophilic inhibitors of complex I of the mitochondrial respiratory chain (Cave et al., 1997). MPTP, rotenone and other toxins have been used to generate models of PD (see next section).

3.1.6. Toxin models of PD

The main neurotoxins used to generate toxin models of PD include 6-hydroxydopamine (6-OHDA), MPTP, rotenone and paraquat. It seems that all these toxins generate reactive oxygen species. Only MPTP has been associated with parkinsonism in humans; the MPTP model is therefore the most widely studied toxin model of PD.

6-OHDA toxin models

Models using 6-OHDA have been the first to investigate substantia nigra dopaminergic cell death (Ungerstedt, 1968). 6-OHDA cannot cross the blood brain barrier and therefore needs to be injected stereotactically into the midbrain of animals. 6-OHDA induces relatively selective loss of dopaminergic neurones because it is taken up preferentially by dopamine and monoamine transporters (Luthman et al., 1989). In the cytosol of these neurones 6-OHDA then accumulates and generates oxidative stress and quinones that can damage other molecules. Dopaminergic neurone loss accompanied by an increase in protein bound dopamine oxidation products was ameliorated by concomitant injection of antioxidants (glutathione and ascorbic acid) supporting the hypothesis that 6-OHDA caused neuronal cell death by generating oxidative stress (Hastings et al., 1996). Animals injected with 6-OHDA have a quantifiable motor deficit, but characteristic LBs have

not been observed. This model has been particularly useful for pharmacological screening but does not replicate many key features of PD.

MPTP models

Parkinsonism was induced in a group of drug addicts that used drugs contaminated with MPTP (Langston and Ballard, 1983). MPTP is converted to N-methyl-4-phenylpyridinium (MPP+) within glial cells by monoamine oxidase (preferentially MAO-B (Singer et al., 1986), which is actively taken up by monoamine transporters in the membranes of dopaminergic neurones. Within cells MPP+ enters mitochondria and selectively binds to and inhibits NADH CoQ_{10} reductase (complex I), which leads to an inhibition of ATP synthesis and the generation of free radicals (Krueger et al., 1990; Ramsay and Singer, 1986). MPTP has been used for the development of mouse and primate models of PD (Bloem et al., 1990). In non-human primates, MPTP caused tremor, rigidity, akinesia and postural instability, which were all successfully treated with L-Dopa and dopamine agonists. In the non-human primate brains dopaminergic neurones were selectively lost in brain areas similar to idiopathic PD, including the substantia nigra. However, MPTP-induced subacute or acute onset parkinsonism lacked the typical EM features of LBs (Forno et al., 1988). The MPTP model represents the best-characterised model of PD and fulfils many of the criteria for a good model of the disease with the exception of LB formation. However, it remains unknown whether chronic administration of MPTP may induce the formation of LBs. An in depth discussion of the MPTP model, has been published elsewhere (Beal, 2001).

Rotenone

Rotenone belongs to the family of the rotenoids, which are natural cytotoxic compounds extracted from tropical plants. Rotenone is the most potent member and

is used widely as an insecticide and fish poison. Rotenone is a highly lipophilic molecule (Talpade et al., 2000) that therefore readily enters all cells where it binds to mitochondrial respiratory chain complex I.

As discussed above (section 3.1.4.) epidemiological evidence suggests that the exposure to pesticides may be a risk factor for PD. Rats chronically infused intravenously with rotenone developed hypokinesia, postural instability, gait unsteadiness and paw tremor, and this correlated with the degree of degeneration of dopaminergic nigro-striatal neurones (Betarbet et al., 2000). On light microscopy these neurones exhibited cytoplasmic inclusions immunoreactive for α-synuclein and ubiquitin, which ultrastructurally contained fibrils similar to those in LBs. However, there was a somewhat variable response of the animals to rotenone with only 12 out of 25 rats developing lesions in the dopaminergic neurones of the substantia nigra.

Since rotenone enters all cells the selective loss of dopaminergic neurones in the rat model by Betarbet and colleagues suggested that dopaminergic neurones were particularly sensitive to complex I inhibition. However, acute rotenone intoxication was reported to spare dopaminergic neurones (Ferrante et al., 1997), and in rats chronically infused with rotenone significant reductions in the numbers of DARPP-32-positive, cholinergic and NADPH diaphorase-positive neurones was described (Hoglinger et al., 2003). These findings indicate a more widespread toxicity of rotenone and query the concept of selective toxicity of rotenone to dopaminergic neurones.

Paraquat

As discussed above (section 3.1.4.) exposure to the herbicide paraquat (N,N'-dimethyl-4-4'biperidinium) may increase the risk for PD (Liou et al., 1997). Paraquat has a structure similar to MPP+; paraquat does not easily cross the blood brain

barrier (Shimizu et al., 2001) and it is not known what determines its distribution in the brain (Widdowson et al., 1996a; Widdowson et al., 1996b). Paraquat is a known intracellular generator of superoxide, which is promoted by the mitochondrial NAD(P)H -quinone oxidoreductase (Shimada et al., 1998) and can lead to damage to the cell and in particular to mitochondria (Hirai et al., 1992). Systemic administration of paraquat to mice led to degeneration of dopaminergic neurones in the substantia nigra and the formation of α-synuclein containing inclusions (Manning-Bog et al., 2002). This suggests that models using paraquat may be useful tools with which to explore the interaction of an environmental risk factor for PD and α-synuclein.

3.1.7. Secondary features of PD

The following section covers the evidence for oxidative stress, excitotoxicity and proteolytic stress in PD. These features of PD may be secondary to the primary underlying pathology and might contribute to or be influenced by mitochondrial respiratory chain defects as discussed in the previous section. However, this is only one example of the links that exist between each of these features. Ultimately, they all seem to contribute to the pathological events that result in the death of dopaminergic neurones in the substantia nigra (Figure 3.2). It is not clear what initiates the pathological cascade leading on to dopaminergic neurone loss in the substantia nigra and hence can be regarded as a primary event with subsequent involvement of other pathways. For example while it is clear that oxidative stress plays a role in these events it remains unclear whether oxidative stress is the result or the cause of mitochondrial dysfunction, or might be linked to dopamine metabolism. Further, the cell type specific contribution to these processes in the substantia nigra remains a matter of debate. Evidence is emerging to suggest involvement of glial cells (astrocytes, oligodendrocytes, microglia) in the

pathophysiology of PD. Several studies reported that there was a substantial degree of gliosis, and in particular microglia activation, in PD brains (Banati et al., 1998; Forno et al., 1992; McGeer et al., 1988; Mirza et al., 2000). Astrocytes contribute to dopamine metabolism in that they contain monoamine oxidases A and B as well as catechol-*O*-methyl transferase; in addition they contain glutathione peroxidase and in both ways might protect dopaminergic neurones from ROS (Hirsch et al., 1999). In addition, microglia, but not dopaminergic neurones, in PD were shown to have iNOS (Hunot et al., 1996) and could therefore be an important source of reactive nitrogen species, in particular the membrane permeable $NO^{\bullet}$, resulting in nitration within dopaminergic neurones. However, it remains unclear whether the involvement of glial cells is a primary event, or a contributing but not causally related feature.

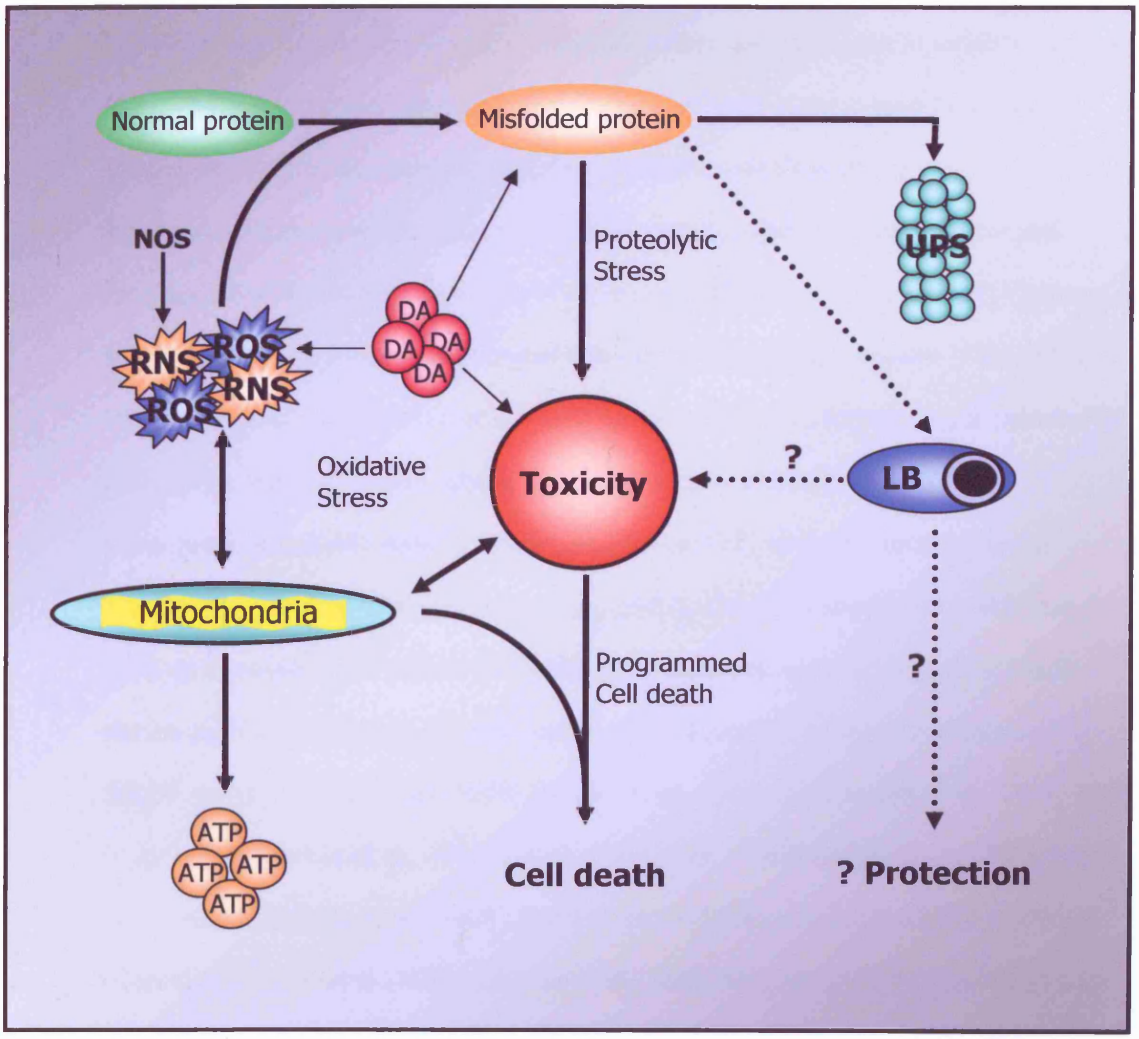

Figure 3.2. Possible common pathomechanisms in PD I. There is good evidence for mitochondrial dysfunction, oxidative stress, protein misfolding, and the involvement of the UPS with proteolytic stress in PD. All these pathways seem to be interconnected. It remains unknown which is the first step in the pathogenetic cascade that leads to cell death (presumably by programmed cell death) and whether events taking place in glial cells are as important as those within dopaminergic neurones in the substantia nigra. DA: dopamine. ATP: adenosin triphosphate. UPS: ubiquitin-proteasome system. ROS: reactive oxygen species. RNS: reactive nitrogen species. NOS: nitric oxide synthase. LB: Lewy body.

3.1.7.1. Evidence for oxidative stress in PD

The basic mechanisms underlying oxidative stress are discussed in detail in chapter 1 (section 1.1.3.). Compromised anti-oxidant defences or increased free radical generation may tip the balance towards increased oxidative stress (Figure 3.2.). Postmortem homogenate analysis of PD substantia nigra consistently revealed increased iron levels (Dexter et al., 1989; Earle, 1968; Hirsch et al., 1991; Olanow, 1992; Sofic et al., 1988) and decreased levels of reduced glutathione (Perry et al., 1982; Sian et al., 1994; Sofic et al., 1992). Iron is known to function as a chelator for H_2O_2 in the Fenton reaction giving hydroxyl radicals; it also interacts with superoxide, which can reduce Fe(III) and oxidise Fe^{2+}, and can accelerate the Fenton reaction (Halliwell and Gutteridge, 1999). Thus increased iron levels can indicate increased free radical production. Others have reported less consistent results regarding GSH, glutathione peroxidase, catalase, increased mitochondrial GSSG levels (Ambani et al., 1975; Damier et al., 1993; Johannsen et al., 1991; Kish et al., 1985; Marttila et al., 1988b; Radunovic et al., 1997; Saggu et al., 1989; Sian et al., 1994; Yoritaka et al., 1997; Yoshida et al., 1994), or abnormalities of ferritin (Cabrera-Valdivia et al., 1994; Connor et al., 1995; Dexter et al., 1990; Jellinger et al., 1990; Kuiper et al., 1994; Logroscino et al., 1997; Mann et al., 1994; Riederer et al., 1989). In PD substantia nigra increased oxidative damage has been reported to lipids (lipid peroxidation) (Dexter et al., 1994), increased levels of 4-hydroxynonenal (also in cerebrospinal fluid) (Picklo et al., 1999; Yoritaka et al., 1996), DNA (rise in 8-OHdG in mitochondria and total DNA) (Alam et al., 1997b; Sanchez-Ramos et al., 1994; Shimura-Miura et al., 1999) and protein carbonyl production (Alam et al., 1997a; Floor and Wetzel, 1998). In addition, increased immunoreactivity has been reported for nitrotyrosine in Lewy bodies in PD substantia nigra (Giasson et al., 2000; Good et al., 1998).

Taken together, these studies provide evidence for oxidative stress in PD

substantia nigra, which has led to oxidative damage to lipids, DNA and proteins. Since these studies were performed on post-mortem tissue of patients with long-standing PD, and in all likelihood including patients who had been on L-dopa therapy, they likely represent a snapshot of end-stage PD substantia nigra. Thus the time course and interrelationship to other processes in PD pathophysiology remain unclear (Figure 3.2.).

However, dispite the evidence in support of oxidative stress treatment of patients with MOA B inhibitors, e.g. deprenyl, or with antioxidants, e.g. tocopherol (vitamin E), has not demonstrated neuroprotection or an effect on the progression of disability in early Parkinson's disease (The Parkinson's Disease Study Group, 1993), although deprenyl can delay the requirement of additional symptomatic therapy by 9-12 months. Since it is not entirely clear whether antioxidants reach the target cells these negative results do not necessarily mean that antioxidants per se are not suitable forms of treatment.

3.1.7.2. Dopamine

The relatively selective loss of dopaminergic neurones in the substantia nigra suggests that dopamine itself might be relevant in the pathogenesis of PD. Substantia nigra neurones, but also cells in other organs such as the adrenal gland, synthesise DA using tyrosine hydroxylase (TH). Vesicular monoamine transporters (VMAT) then actively transport dopamine into specialised monoaminergic storage vesicles within dopaminergic cells. Neuronal cells predominantly express VMAT-2 whereas non-neuronal cells predominantly express VMAT-1. Substantia nigra neurones are known to be TH positive, synthesizing dopamine, and express dopamine uptake transporter (DAT) in pre-synaptic terminals to facilitate re-uptake of extracellular dopamine (Reith et al., 1997). Dopaminergic substantia nigra neurones have their cell bodies in the substantia nigra and their neurites extend

mainly into the striatum where dopamine is released from the nerve terminals. Dopaminergic neurones are not the only cells in the brain that can take up and metabolise dopamine. Glial cells, particularly astrocytes, contain DAT and monoamine oxidases.

Dopamine metabolism includes the enzymatic deamination by monoamine oxidases (MAO-A and MAO-B) to 3,4-dihydroxyphenylacetaldehyde (DOPAL). This can generate H_2O_2 (Sandri et al., 1990) and oxidised glutathione (Werner and Cohen, 1991). DOPAL can be oxidised to 3,4-dihydroxyphenylacetic acid (DOPAC) by DOPAL dehydrogenase or reduced to 3,4-dihydroxyphenylethanol (DOPET) by DOPAL reductase (Figure 3.3). In addition, dopamine can spontaneously undergo auto-oxidation to form catechol-quinones, which themselves can act as oxidants by forming toxic hydroxyl radicals, or they can react as electrophiles and bind to and inhibit sulfhydryl groups within the cell (Graham, 1978; Shen et al., 1997; Terland et al., 1997).

In PD brain, dopamine turnover was found to be increased (Hornykiewicz and Kish, 1987), and 6-OHDA was shown to be toxic after injection into rat striatum (Hastings et al., 1996, see section 3.1.6.). In rat striatal primary cell culture (McLaughlin et al., 1998) and rat foetal mesencephalic cells (Michel and Hefti, 1990; Tanaka et al., 1991) dopamine also led to cell death. Astrocytes were also found to take up and metabolise dopamine (Langeveld et al., 1995; Liesi et al., 1981); in SH-SY5Y cells, co-culturing with astrocytes protected against the toxic effects of 6-OHDA (Yu and Zuo, 1997) suggesting that astrocytes may be able to protect dopaminergic neurones from oxidative stress generated via dopamine metabolism. Evidence to support the hypothesis of oxidative damage from dopamine metabolism comes from the attenuation of dopamine toxicity by antioxidants and free radical scavengers (ascorbic acid, N-acetyl cysteine, cysteine glutathione, harmalol, harmaline) in PC-12 cells (Lee et al., 2000) and primary striatal cell culture

(McLaughlin et al., 1998; Soto-Otero et al., 2000). In addition, exposure of isolated intact mitochondria to dopamine and its metabolites, e.g. dopamine-quinone, led to impaired mitochondrial respiratory chain function and mitochondrial swelling suggestive of opening of the mitochondrial transition pore (MTP) (Berman and Hastings, 1999; Cohen et al., 1997; Kim et al., 1999) thus providing a possible link between dopamine toxicity and mechanisms involved in apoptosis (see section 1.1.2.2). This was attenuated by inhibition of MAO-A and MAO-B, or the addition of catalase suggesting the involvement of free radical generation, and cyclosporin A that can stabilise the MTP (Berman and Hastings, 1999; Cohen et al., 1997). A link of dopamine to mitochondrial respiratory function is not consistent. While one study reported that in mitochondria isolated from rat brain dopamine inhibited complex I activity (Ben-Shachar et al., 1995) others have not established a direct influence of dopamine on mitochondrial function (Morikawa et al., 1996).

An unresolved question is whether L-dopa given as a treatment to PD patients may contribute to the processes leading to neuronal cell death. In healthy humans (Quinn et al., 1986; Rajput et al., 1997), rodents (Perry et al., 1984) or primates (Lyras et al., 2002) chronic administration of L-dopa does not seem to give rise to increased levels of oxidative stress or damage the substantia nigra. However, the effects of L-dopa within substantia nigra in PD patients may be different, and the magnitude of the effect could in fact depend on how many dopaminergic neurones have already been lost. This hypothesis could be addressed using functional imaging studies, such as those that have been used in twin studies (Piccini et al., 1999).

3.1.7.3. Proteolytic stress

Impairment of UPS function may be an important contributor to the pathogenesis of PD (McNaught et al., 2001) (Figure 3.2.). In dopaminergic neurones in the

substantia nigra in PD α-subunits of the 20S proteasome were reported to be differentially lost compared with β-subunits, (McNaught et al., 2002a); this may have consequences for proteasomal function since the proteolytic activity was decreased by about 40% (McNaught and Jenner, 2001). The specific absence in substantia nigra, compared with relatively unaffected areas in PD, of aggresomes, sites of high proteolytic activity that safeguard the nucleus and other cell organelles form toxic proteins (Kopito, 2000) may provide indirect evidence for impaired proteasomal function in dopaminergic neurones in the substantia nigra (Johnston et al., 1998; McNaught and Jenner, 2001; Wigley et al., 1999). As a consequence this could mean that dopaminergic neurones are selectively exposed to increased levels of toxic proteins while areas able to form aggresomes are relatively spared. The observation that the most abundant proteinaceous components of LBs, α-synuclein and oxidised proteins such as nitrotyrosine, do not seem to require ubiquitination for their degradation within the 20S proteasome (Bennett et al., 1999; Davies, 2001; Spillantini et al., 1998; Stefanis et al., 2001; Tofaris et al., 2001) suggests that it is not a failure of ubiquitination but of the 20S proteasome that leads to their accumulation. This hypothesis would be consistent with a report indicating a marked increase in polyubiquitinated proteins within the substantia nigra of patients with sporadic PD (McNaught et al., 2002b).

What causes abnormal 20S proteasomal function in sporadic PD remains unknown. Environmental proteasomal inhibitors (e.g. polyphenols) have been described (Nam et al., 2001), and protesomal function may also be sensitive to oxidative stress (Bulteau et al., 2001). Finally, since a number of the processes of the UPS require ATP a compromise of mitochondrial function might have secondary effects on proteasomal function. Indeed, in rats rotenone mediated complex I inhibition was associated with the formation of LB-like inclusion (Betarbet et al., 2000), and in COS-7 cells normal mitochondrial function was necessary to prevent

and remove α-synuclein aggregates (Lee et al., 2002a). Thus it is likely that in PD proteosomal pathology has to be viewed as one of many other factors that interact in the pathophysiology of PD (Figure 3.2).

3.1.7.4. Evidence for programmed cell death in PD

As discussed in the previous sections, there is good evidence for mitochondrial respiratory chain dysfunction, oxidative stress and free radical mediated damage to lipids, DNA and proteins in PD substantia nigra. These processes may ultimately lead to the initiation of programmed cell death (Figure 3.2, and section 1.1.2.2). Signs of apoptosis have been detected in dopaminergic neurones of the substantia nigra in normal aging (Anglade et al., 1997). In PD, postmortem brain analysis revealed nuclear condensation, chromatin fragmentation and the formation of apoptotic bodies, which indicate programmed cell death (Mochizuki et al., 1996; Tatton et al., 1998; Tompkins et al., 1997). However, concerns have been raised towards some of the techniques used to detect apoptosis, in particular terminal deoxynucleotidyl transferase-mediated deoxyuridine triphosphate nick-end labelling (TUNEL), which was shown to be susceptible to artefacts in the examination of postmortem brain tissue (Tatton et al., 1998). Using this technique conflicting results were reported with evidence showing apoptosis in some studies (Tatton et al., 1998; Anglade et al., 1997; Mochizuki et al., 1996) while other studies reported data that did not support the concept of apoptosis specifically in PD dopaminergic neurones (Banati et al., 1998; Kingsbury et al., 1998; Kosel et al., 1997). In support of apoptois, other studies have reported a rise of BAX, an apoptosis inducing protein (see section 1.1.2.2), in substantia nigra neurones (Hartmann et al., 2001a; Tatton, 2000). In addition, Fas, FADD (Ferrer et al., 2000; Hartmann et al., 2002; Mogi et al., 1996) and caspase 8 (Hartmann et al., 2001b) were also implicated in neuronal cell death in PD substantia nigra. This raises the issue that cell death signals in PD

dopaminergic neurones may not only originate from within the cell (oxidative stress, mitochondrial dysfunction) but that extracellular death signals (?originating from glial cells) could also contribute to triggering programmed cell death in dopaminergic neurones (see section 1.1.2.2).

Data from experimental models supports the involvement of programmed cell death in PD. The substantia nigra of MPTP treated mice showed evidence of apoptotic nuclear changes (Tatton and Kish, 1997); in liver and brain mitochondria, MPP+ opened the MTP and led to cytochrome c release (Cassarino et al., 1999). In neuronal cell culture, MPP+ was shown to up-regulate NF-κB (Cassarino et al., 2000). NF-κB is known, when activated, to translocate from its cytoplasmic location to the nucleus where it binds to DNA and can induced apoptosis (Thanos and Maniatis, 1995). Evidence for activated NF-κB was found in dopaminergic neurones of PD patients (Hunot et al., 1997), and activated NF-κB also protected neuronal cells in culture from apoptosis induced by $FeSO_4$ or amyloid beta peptide mediated oxidative stress (Mattson et al., 1997). Interestingly, pramipexole, a dopamine agonist, inhibited MTP opening in response to MPP+ and attenuated the levels of free radicals in neuronal cells, rats and isolated mitochondria (Cassarino et al., 1998). Caspase inhibitors improved survival of dopaminergic neurones transplanted into the substantia nigra of lesioned animals, and levels of prostate apoptosis response-4 protein (Par-4), an important proapoptotic protein in neurones, are elevated in midbrain dopaminergic neurones of MPTP treated monkeys and mice (Duan et al., 1999a; Duan et al., 1999b). These authors demonstrated that inhibition of Par-4 synthesis by antisense oligonucleotide treatment prevents apoptosis in cultured dopaminergic cells. Furthermore, dopamine induced apoptosis in PC-12 cells and cyanide enhanced DA toxicity (Jones et al., 2000). Thus, it is likely that the pathogenetic factors involved in PD nigral cell death may cause cell dysfunction as well as lower the neurones' threshold to apoptosis.

Taken together the available evidence supports a role of apoptotic cell death in PD neuronal loss. It seems that some of the controversies that arose may have been caused by the susceptibility to artefact in postmortem brain tissue of one particular technique to detect apoptosis, the TUNEL technique (Tatton et al., 2003).

3.1.8. The genetics of PD

Evidence for a genetic contribution to the pathogenesis comes from epidemiological and twin studies. PD was found to be more common among relatives of index cases compared to matched controls in several case control studies (De Michele et al., 1996; Marder et al., 1996; Payami et al., 1994; Sveinbjornsdottir et al., 2000; Vieregge and Heberlein, 1995). It appears that the risk of a given relative to have PD increases depending upon how many members of the family are already affected. From all studies combined it was estimated that the relative risk in first-degree relatives of individuals with PD is in the range of 2-3 times that of the general population (Gasser, 1998). This is in keeping with a multifactorial aetiology of PD that entails an inheritable component in a subset of families (Lazzarini et al., 1994).

In addition, mutations in four different genes - α-synuclein on chromosome 4q21/PARK1 (Polymeropoulos et al., 1997), and 4q/PARK4 (Kruger et al., 1998), parkin on 6q25-27/PARK2 (Kitada et al., 1998), DJ-1 on 1p36/PARK7 (Bonifati et al., 2002; van Duijn et al., 2001), and PINK1/PARK6 on 1p35-p36 (Valente et al., 2004) have been described in familial PD (HUGO, for a review see Foltynie et al., 2002 and Gwinn-Hardy and Farrer, 2002) (Table 3.2.). There is also evidence implicating mutations in ubiquitin carboxyhydrolase -L1 (UCH-L1) in the pathogenesis of PD (4p14/PARK5, (Leroy et al., 1998). In addition, PD-related genes have been linked to five further loci, 2p13/PARK3 (Gasser et al., 1998), 4p15/PARK4 (Farrer et al., 1999), 12p11/PARK8 (Funayama et al., 2002), 1p36/PARK9 (Kufor-Rakeb syndrome; Hampshire et al., 2001), and 1p32/PARK10

(Hicks et al., 2002). Other genes associated with parkinsonism include tau (fronto-temporal dementia with parkinsonism, FTDP17) (Clark et al., 1998), and the X-linked recessive syndrome of parkinsonism and dystonia (Lubag)(Xp13)(Wilhelmsen et al., 1991).

The discoveries of mutations in genes that are associated with PD have offered the chance to gain new insight into the pathogenesis of this disease. As the function of the proteins encoded by these genes is unravelled (see next section) their relevance to the pathological cascade in PD becomes clearer (Figure 3.4). However, this has added another level of complexity to the various inter relationships between the pathological processes involved in PD (Figure 3.4).

Gene	Mode of inheritance	Locus	Chromoso-mal location	Reference
α-synuclein	Autosomal dominant	Park 1	4q21-q23	(Polymeropoulos et al., 1997)
Parkin	Autosomal recessive	Park 2	6q21.2-27	(Kitada et al., 1998)
Unknown	Autosomal dominant	Park 3	2p13	(Gasser et al., 1998)
α-synuclein	Autosomal dominant	Park 4	4q	(Kruger et al., 1998)
UCH-L1	Autosomal dominant	Park 5	4p14	(Leroy et al., 1998)
PINK 1	Autosomal recessive	Park 6	1p35-	(Valente et al., 2004)
DJ-1	Autosomal recessive	Park 7	1p36	(Bonifati et al., 2002)
Unknown	Autosomal dominant	Park 8	12p11q13.1	(Funayama et al., 2002)
Unknown	Autosomal recessive	Park 9	1p36	(Hampshire et al., 2001)
Unknown	Late onset susceptibility gene	Park 10	1p32	(Hicks et al., 2002)
NR4A2	Susceptibility gene	NA	2q22-23	(Le et al., 2003)
Synphilin 1	Susceptibility gene	NA	5q23.1-23.3	(Marx et al., 2003)
Tau	Susceptibility gene	NA	17q21	(Martin et al., 2001)
Unknown	X-linked recessive (Lubag)	NA	Xp13	(Wilhelmsen et al., 1991)

Table 3.2. Genes and chromosomal loci linked to familial PD or implicated in the pathogenesis of PD. NA: not assigned.

3.1.8.1. Twin studies

Since monozygotic twins (MZ) have identical DNA whereas dizygotic twins (DZ) only have 50% DNA in common, an increased concordance rate of a disease in MZ twins as opposed to DZ twins argues for a genetic aetiology of that disease given that environment is either random or more controlled for in twins. In PD, five studies compared the concordance rate in MZ pairs with that in DZ pairs (Marsden, 1987; Marttila et al., 1988a; Tanner et al., 1999; Vieregge et al., 1992; Ward et al., 1983). Taking the results of these studies together, 21 of 162 MZ pairs (13%) showed concordance compared with 16 of 147 DZ pairs (16%). These results would suggest that there is no significant difference in the MZ/DZ concordance ratio (1.2/1.0) and hence they do not support the notion of a genetic contribution in PD. However, it needs to be born in mind that the diagnosis of PD rests on clinical assessment alone. This is not always accurate and cannot predict the onset of PD in a given individual. The onset of PD differed substantially between the MZ co-twins (Golbe, 1999) and it is therefore conceivable that individuals that were to develop PD later in life were missed. A large study on 161 twin pairs that on clinical grounds alone were diagnosed with PD found increased concordance in monozygotic twins in those who developed the disease before the age of 50 years, but no increase in those who manifested at a later age (Tanner et al., 1999). In another twin study employing both clinical assessment and a sensitive and specific marker to identify surviving nigrostriatal dopaminergic neurones, ^{18}fluoro-dopa positron emission tomography, also demonstrated increased concordance amongst identical twins (Piccini et al., 1999). In that study, 18 twin pairs, 10 MZ and 8 DZ, where 1 twin was affected with PD and the other healthy, were scanned twice with an interval of 4 years. In all 10 MZ pairs, but only 2 DZ pairs, ^{18}fluoro-dopa uptake declined substantially between scans indicating a concordance of 72% in MZ pairs and 18% in DZ pairs. This concordance provides evidence to support the notion that genetic factors play a role

in PD; however, since the concordance was not 100% it seems that these genetic factors did not exclusively determine whether an individual developed PD. Thus other non-genetic factors, e.g. environmental toxins, might also have a substantial role in the pathogenesis of PD.

3.1.8.2. Identification of Parkin mutations in autosomal recessive PD

Loss of function mutations (deletions and point mutations) in the parkin gene are associated with autosomal recessive juvenile PD (ARJPD) (Kitada et al., 1998; Shimura et al., 1999). Recently, a case control study revealed an association of a single nucleotide polymorphism (258 T/G) in the parkin promoter with late-onset idiopathic PD (West et al., 2002) suggesting that the parkin gene may also be important in the pathogenesis of idiopathic PD. Clinically, parkin-associated ARJPD resembles idiopathic PD but can also be associated with dystonia and marked L-Dopa induced dyskinesias. While there is a severe loss of dopaminergic neurones in the substantia nigra pars compacta and the locus coeruleus reminiscent of idiopathic PD, with the exception of one reported case (Farrer et al., 2001), LBs have not been observed. However, the true incidence of LB pathology in ARJPD may only be revealed after more parkin-positive patients have undergone post-mortem analysis.

Parkin itself is a 465 amino acid ubiquitin protein ligase (E3) that plays a role in the transfer of ubiquitin to proteins destined for degradation in the ubiquitin-proteasome-system (UPS) (Shimura et al., 2000). E3-ligases specifically target those proteins by facilitating ubiquitination (see section 1.1.6). Thus a loss of parkin function could result in the loss of the specificity of this process; however, it is not understood if alternative mechanisms can compensate for the loss of parkin.

Recently, two parkin knock-out mouse models have been published (Goldberg et al., 2003; Itier et al., 2003). In both models mice were viable, fertile and

had only subtle behavioural abnormalities. Gross pathology was normal and in particular there was no loss of dopaminergic neurones. However, extracellular DA levels in the striatum were increased and medium sized striatal spiny neurones were less excitable with electrical stimulation than controls in the study by Goldberg and colleagues, and Itier and colleagues reported that their parkin deficient animals showed increased dopamine metabolism. Greene and colleagues reported on a parkin knock-out model in drosophila (Greene et al., 2003). Parkin knock-out did not affect viability of flies and brain morphology was normal including tyrosine hydroxylase staining. This is in accord with the findings in the mouse knock-out models. In contrast to the mouse models parkin deficient flies exhibited pathology in muscle and male germ line associated with mitochondrial structural abnormalities (swelling and disintegration of cristae).

Data from the studies of Goldberg and colleagues and Itier and colleagues suggest that parkin may have a role in the functional regulation of dopamine release from the substantia nigra into the striatum whereas a loss of parkin does not seem to be associated with a loss of dopaminergic neurones. The role of parkin in other tissues remains to be elucidated. Constitutive over-expression of mutant parkin in NT2 and SK-N-MC neuronal cells was associated with increased levels of oxidative stress when compared to over-expression of wild-type parkin (Hyun et al., 2002). This was independent of whether or not the mutant parkin retained enzyme activity. It needs to be shown if this is due to specific interference of the mutant parkin protein with UPS function, e.g. abnormal ubiquitin protein ligase activity with subsequent accumulation of mutated or damaged proteins that cannot be ubiquitinated, or a non-specific consequence of abundant expression of a mutant protein in these cells.

3.1.8.3. Ubiquitin carboxyhydrolase -L1 (UCH-L1)

Two siblings from a German pedigree with autosomal dominantly inherited PD with incomplete penetrance carried mutations (I93M) in the ubiquitin carboxyhydrolase - L1 (UCH-L1, PARK 5) gene (Leroy et al., 1998). This resulted in reduced but not completely absent activity of the hydrolase. A polymorphism (S18Y) of the UCH-L1 gene has been described to protect against PD (Levecque et al., 2001; Maraganore et al., 1999; Satoh and Kuroda, 2001). The neuropathological changes caused by the UCH-L1 mutation in humans remain unknown. UCH-L1 belongs to the protein family of ubiquitin C-terminal hydrolases, which hydrolyses the bond between ubiquitin and its substrate in order to recycle ubiquitin. Interestingly though, a second enzymatic function, dimerisation dependent ubiquitin ligase activity, has been described (Liu et al., 2002). The mutation of UCH-L1 seems to confer a loss of ligase activity and may thus promote parkinsonism whereas the polymorphism increases ligase activity and could therefore protect against parkinsonism (Liu et al., 2002). Neurodegeneration associated with the loss of UCH-L1 and UCH-L3 in the gracile axonal dystrophy mice further suggests that these proteins may be particularly important for neuronal function. However, these mice did not develop parkinsonism (Kurihara et al., 2001).

3.1.8.4. Other genes

Mutations in the DJ-1 gene (PARK 7) were recently identified in families with autosomal recessive, early onset PD (Bonifati et al., 2002). The function of DJ-1 is unknown. However, there is evidence to suggest that DJ-1 may be important for the regulation and monitoring of oxidative stress response since it was shown that the intracellular generation of free radicals led to an increase in and oxidation of DJ-1 (Mitsumoto and Nakagawa, 2001; Mitsumoto et al., 2001).

Parkinsonism is a feature of patients with autosomal dominant frontotemporal dementia-parkinsonism (FTDP) associated with tau mutations on chromosome 17 (Hutton et al., 1998). This suggests that tau might also play a role in the pathogenesis of PD. This is consistent with tau immunoreactivity observed in a subset of LBs, i.e. those in the brainstem, of patients with PD (Arima et al., 1999), and also genetic linkage to the tau gene with clinically diagnosed idiopathic PD (Farrer et al., 2002; Gilman et al., 1998; Marks et al., 2001) and an association of 3 out of 5 examined single nucleotide polymorphisms in the tau gene (SNP 3, SNP 9i, SNP 11) with idiopathic PD in 1056 subjects (426 affected) from 235 families (Martin et al., 2001). Tau and α-synuclein were both found within inclusions in the brain of two members of the Contoursi kindred with the G209A α-synuclein mutation and parkinsonism (Duda et al., 2002; Giasson et al., 2003) and may interact in the events leading to aggregation (Giasson et al., 2003). This may be linked to the role of tau in microtubule-based transport of aggregates (Kopito, 2000). However, no association between the tau locus and 157 pathologically confirmed sporadic PD cases has been reported in another study (de Silva et al., 2002), which suggests that any association may be weak, or that the clinical diagnosis of PD may not have been correct in all the original association studies.

Recently, two mutations (G to A transition in exon 4 nucleotide 11185, and G to A transition in nucleotide 15600, in NT_004610) in a gene encoding a putative mitochondrial protein called PTEN-induced kinase (PINK 1, PARK 6) have been identified in three consanguineous families with rare autosomal recessive early onset PD from Italy and Spain (Valente et al., 2004). Immunocytochemically, PINK 1 localised to mitochondria in transfected COS-7 cells and Western blot of mitochondrial enriched fractions confirmed mitochondrial localisation. Expression of wild-type or G309D mutant PINK 1 in SH-SY5Y cells had no effect on mitochondrial membrane potential but cells overexpressing the wild-type form were protected from

the effects of the proteosomal inhibitor MG-132 on mitochondrial membrane potential and apoptosis (Valente et al., 2004). This is the first nuclear-encoded mitochondrial protein that has firmly been associated with PD.

3.1.8.5. Identification of α-synuclein mutations in autosomal dominant PD

In a large Italian-Greek-American PD pedigree (the Contursi kindred, a pedigree with 592 members of which 60 were affected), PD was observed with highly penetrant autosomal dominant inheritance (Polymeropoulos et al., 1997). The clinical picture was very similar to PD apart from tremor being infrequent; patients had on average an earlier onset (46±13 years) of the disease and a more rapid progression to death with a mean survival of about 10 years (Golbe et al., 1990; Polymeropoulos et al., 1996) and pathological features similar to those of typical PD. In this kindred, Polymeropoulos and collegues identified a G209A substitution in the α-synuclein gene, leading to the substitution of alanine to threonine at position 53 (A53T) in the α-synuclein protein (Polymeropoulos et al., 1997). A second mutation in the α-synuclein gene (G88C; causing an alanine to proline (A30P) substitution in the α-synuclein protein) was identified in a German pedigree with early-onset PD (Kruger et al., 1998). Recently, genetic analysis in another family with young onset autosomal dominant PD revealed a triplication of the α-synuclein locus. This suggests that not only can mutations in the α-synuclein gene cause PD but also that the over-expression of the wild-type form alone may by associated with PD (Singleton et al., 2003). However, the number of PD patients in whom such genetic abnormalities in the α-synuclein gene underlie their disease is small (<10%). The analysis of the α-synuclein gene in two case series of patients with sporadic PD (Vaughan et al., 1998a; Warner and Schapira, 1998) or familial PD (Vaughan et al.,

1998b) did not reveal any abnormalities suggesting that for the vast majority of PD patients mutations in the α-synuclein are not relevant.

3.1.8.5.1. α-synuclein

The 19kD (140 amino acid) protein α-synuclein belongs to the synuclein family of proteins (Lavedan, 1998). Synucleins are abundant in the brain; α-synuclein, β-synuclein and γ-synuclein are similar in amino acid length (127-140), share 55-62% of amino acid sequences and have a similar domain organisation (Lavedan, 1998). α-synuclein was first sequenced in the electric ray (*Torpedo californica*) (Maroteaux et al., 1988). The function of α-synuclein is incompletely understood. The protein contains 11 imperfect amino acid repeats with the consensus sequence of KTKEGV. A hydrophobic amino acid sequence in the centre of α-synuclein is essential for filament assembly (Giasson et al., 2001), while it can bind to lipid membranes through its the amino-terminal repeats (Eliezer et al., 2001; Jensen et al., 1998; Jo et al., 2000; McLean et al., 2000; Perrin et al., 2000).

3.1.8.5.2. α-synuclein and fibrillogenesis

Synucleins in their native state are unfolded proteins with minimal secondary structure (Jakes et al., 1994; Weinreb et al., 1996). When α-synuclein binds to lipid membranes it changes its structure to assume a α-helix conformation (Davidson et al., 1998; Eliezer et al., 2001; Jo et al., 2000; Perrin et al., 2000). *In vitro*, both the full-length and the carboxy-terminated form of α-synuclein can assemble into filaments resembling those seen in humans; the PD associated G209A mutation was consistently shown to facilitate fibril formation possibly leading to the generation of seeds that enhance further fibril formation in a nucleation-dependent process (Biere et al., 2000; Conway et al., 1998; Conway et al., 2000a; Conway et al.,

2000b; Crowther et al., 1998; El-Agnaf et al., 1998; Giasson et al., 2001; Giasson et al., 1999; Narhi et al., 1999; Serpell et al., 2000; Wood et al., 1999). However, results regarding the effects of the G88C α-synuclein mutation are not consistent; promotion of fibrillogenesis (Narhi et al., 1999), no change (Serpell et al., 2000) or inhibition of fibril formation (Conway et al., 2000b) has been reported. Fibillogenesis may not only be facilitated by α-synuclein mutations. *In vitro* work showed that paraquat and rotenone, an inhibitor of complex I of the mitochondrial respiratory chain, promoted α-synuclein fibrillogenesis (Uversky et al., 2001). Interestingly, the same group also found that metals and pesticides had a synergistic effect on α-synuclein fibril formation (Uversky et al., 2002).

3.1.8.5.3. Tissue and subcellular distribution of α-synuclein

By immunohistochemistry and ultrastructural anlysis α-synuclein was found in nerve terminals close to synaptic vesicles (Clayton and George, 1999). α-synuclein has been shown to bind to lipid membranes through its amino-terminal repeats (Eliezer et al., 2001; Jensen et al., 1998; Jo et al., 2000; McLean et al., 2000; Perrin et al., 2000). Subcellular fractionation analysis in human temporal cortex and immunostaining in neocortical and limbic regions confirmed that α-synuclein is expressed in synaptic vesicles (Irizarry et al., 1996). α-synuclein was shown to inhibit phospholipase D2, which localises to the plasma membrane where it could be involved in signal-induced cytoskeletal regulation and exocytosis; this might indicate that α-synuclein contributes to the regulation of vesicular transport (Jenco et al., 1998) within axons (Jensen et al., 1998) or regulation of the size of the vesicular pool (Murphy et al., 2000). Recently, transient transfection of wild-type, G88C or G209A mutant α-synuclein into primary cortical rat neurones revealed that axonal

transport was slower with both mutant α-synuclein forms when compared to cells transfected with the wild-type form (Saha et al., 2004).

α-synuclein expression was also described in rat substantia nigra pars compacta (Kholodilov et al., 1999) suggesting an association with dopaminergic structures, and, as discussed in the next section there is evidence to suggest that the absence of α-synuclein has a bearing on the regulation of dopamine release (Masliah et al., 2000) further linking α-synuclein with the vesicular catecholamine-storing compartment (Figure 3.3).

3.1.8.5.4. Role of α-synuclein in dopamine metabolism

The mechanisms of dopamine synthesis, storage, release and re-uptake have been described in section 3.1.7.2. α-synuclein may be important for dopamine homoeostasis because there is evidence to suggest it is involved in the regulation of dopamine synthesis, dopamine uptake and vesicular storage of dopamine (Figure 3.3). Immunoprecipitation and immunoelectronmicroscopy in brain homogenates and dopaminergic cells revealed an association of α-synuclein with tyrosine hydroxylase (Perez et al., 2002). In a cell free system recombinant α-synuclein inhibited tyrosine hydroxylase activity, which may indicate a regulatory role for α-synuclein in dopamine synthesis (Perez et al., 2002). There are also suggestions that there may be an interaction between α-synuclein and the dopamine uptake transporter (DAT); however, the data are not consistent since they either showed an increase in DAT activity with α-synuclein expression (Lee et al., 2001a), an inhibition of DAT function (Wersinger and Sidhu, 2003) or no change of DAT acitivity in a α-synuclein knock-out mouse model indicating that α-synuclein may not be essential for DAT function (Dauer et al., 2002).

3.1.8.5.5. Consequences of altered dopamine metabolism

As discussed above the metabolism of dopamine can contribute to oxidative stress (see section 3.1.7.2.). Increased levels of oxidative stress generated from dopamine oxidation may be relevant to the formation of α-synuclein aggregates (Figures 3.2 and 3.3). It has been reported that mutated (G209A) α-synuclein expression promoted the formation of α-synuclein oligomers or protofibrils, a non-fibrillar precursor of the fibrils found in LBs (Conway et al., 2001). The same group revealed that dopamine-quinones derived from oxidation of dopamine and L-Dopa stabilised the protofibrils whereas antioxidants enhanced fibril formation. This could indicate that enhanced dopamine oxidation or diminished cellular antioxidant defences or/and increased α-synuclein expression may lead to the formation of presumably toxic protofibrils.

Taken together there is evidence for a close link of α-synuclein and dopamine (Figure 3.3). This seems to be an important factor that might contribute to the relative selective loss of dopaminergic neurones in PD. The co-occurrence of α-synuclein and dopamine might not only promote aggregate formation but also may contribute to the generation of oxidative stress with respect to the potentially important role of α-synuclein for dopamine compartmentalisation within and release from catecholamine-storing vesicles (Figure 3.3). In addition, the regulation of dopamine synthesis may involve α-synuclein (Figure 3.3.).

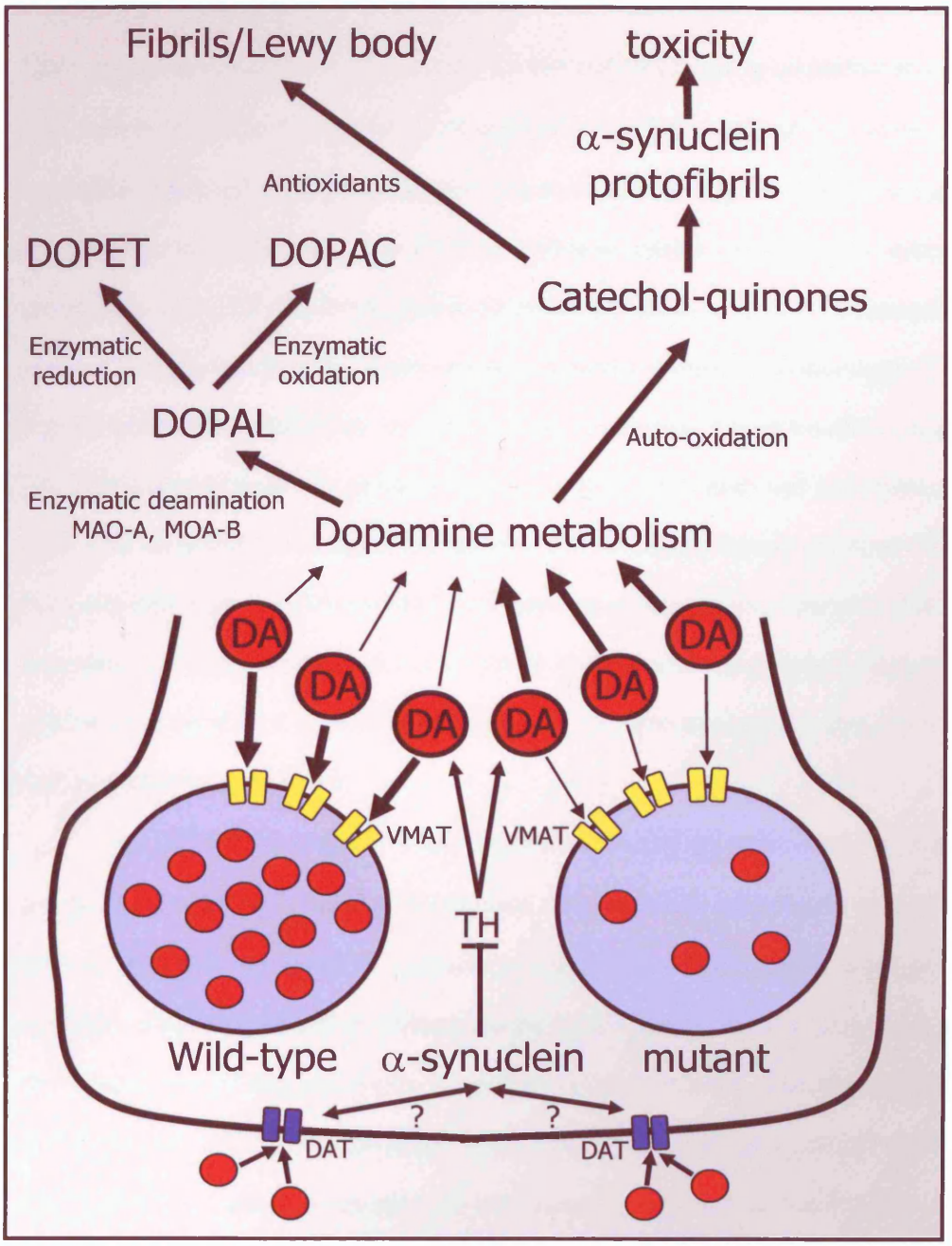

Figure 3.3. Interaction of α-synuclein and dopamine (DA). α-synuclein down-regulates tyrosine hydroxylase (TH) expression and could interact with the dopamine uptake transporter (DAT) regulating DA uptake. α-synuclein may contribute to the regulation of vesicular dopamine handling. Mutations in α-synuclein could decrease vesicular dopamine uptake through the vesicular monoamine transporter (VMAT) leading to increased cytoplasmic DA concentrations. DA undergoes enzymatic deamination by monoamine oxidases (MAO, in astrocytes) to form3,4-dihydroxyphenylacetal-Dehyde (DOPAL), which can be oxidised to 3,4-dihydroxyphenylacetic acid (DOPAC) by DOPAL dehydrogenase or reduced to 3,4-dihydroxyphenylethanol (DOPET) by DOPAL reductase. DA can also auto-oxidise resulting in catechol-quinones, which may stabilise potentially toxic α-synuclein proto-fibrils. Antioxidants enhance the transformation of protofibrils into inert fibrils found in Lewy bodies.

3.1.8.5.6. α-synuclein knock-out models

The study of α-synuclein knock-out models can contribute to the understanding of α-synuclein function (for the principles of knock-out models see chapter 1, section). α-synuclein knock-out mice did not exhibit any obvious pathological features when compared to wild-type mice, their development was normal and they were fertile (Abeliovich et al., 2000). Histological examination revealed a normal complement of tyrosine hydroxylase positive dopaminergic neurones in the substantia nigra without any morphological differences when compared to wild-type dopaminergic neurones. The distribution of vesicular proteins was indistinguishable from wild-type mice, and there was no difference in dopamine release and re-uptake. Knock-out mice differed from wild-type mice with respect to their dopamine content in the striatum (18% reduction), an attenuated locomotor response to amphetamine-induced dopamine release, and increased dopamine release in response to two consecutive electrical stimuli in striatal brain slices.

In a different α-synuclein knock-out mouse model animals were also viable and fertile (Dauer et al., 2002). The absence of α-synuclein was shown to protect animals from MPTP and MPP+ induced degeneration and loss of dopaminergic neurones (Dauer et al., 2002). Similar results were obtained in the knock-out mice by Schlüter and colleagues. Again, mice were viable and fertile, and were resistant to the toxic effects of MPTP (Schluter et al., 2003). Cabin and colleagues reported that in their α-synuclein knockout mice the population of vesicles that form the reserve pool (those vesicles that have not docked to the cell membranes) was diminished compared to control mice (Cabin et al., 2002). In electrical stimulation experiments in hippocampal slices of these mice, both the depletion of reserve pool vesicles and the substitution of docked vesicles by reserve pool vesicles observed in normal control mice were impaired in the α-synuclein knockout mice (Cabin et al., 2002).

These data suggest that α-synuclein is not essential for either mouse brain development or intact dopaminergic neuronal function. However α-synuclein may play a role in the generation of certain vesicular subpopulations (reserve pool) in the synapse and the regulation of dopamine release from the vesicular pre-synaptic population where it may exert activity-dependent inhibitory control over dopamine neurotransmission (Abeliovich et al., 2000). In addition, data from these models indicated the possibility of a link between α-synuclein expression and the ability of MPP+ to cause cell death via inhibition of complex I of the mitochondrial respiratory chain.

3.1.8.5.7. Transgenic mouse models of wild-type α-synuclein over-expression

Five different transgenic models of wild-type α-synuclein over-expression have been published. These models used different promoters, and showed variable phenotypes and pathological changes. However, none of the models were able to demonstrate selective toxicity of α-synuclein to dopaminergic neurones. This limits the power of the models considerably.

Transgenic mice expressed wild-type human α-synuclein driven by the platelet derived growth factor-ß (Masliah et al., 2000). Clinical assessement showed deficits in the rotarod performance of one-year-old animals with high α-synuclein expression. Pathologically, animals developed nuclear and cytoplasmic intraneuronal inclusions in the neocortex, the hippocampus, the olfactory bulb and the substantia nigra (Masliah et al., 2000). These inclusions were immunoreactive to human α-synuclein and ubiquitin, and EM revealed electron dense deposits associated with endoplasmic reticulum and the nucleus. In older mice with more prolonged α-synuclein expression, cytoplasmic inclusions contained fine granular material which was ultrastructurally immuno-positive for α-synuclein, but lacked

fibrillar aggregates typical of LBs. Tyrosine hydroxylase expression was reduced in the substantia nigra of transgenic animals, and the number of tyrosine hydroxylase-positive nerve terminals in the striatum was reduced in animals with high α-synuclein expression. However, there was no loss of tyrosine hydroxylase-positive dopaminergic neurones in the substantia nigra. In this model, some features of PD were reproduced (α-synuclein and ubiquitin positive inclusions, and locomotor impairment) whereas others were lacking (including no loss of substantia nigra dopaminergic neurones, no formation of fibrils, as described in section 3.1.8.5.2, which are one of the key morphological features of LBs and atypical nuclear localisation of some of the inclusions).

Transgenic mice expressing wild-type α-synuclein under the control of Thy-1 promoter exhibited prominent locomotor abnormalities as assessed by the rotarod test as early as 3 weeks of age (van der Putten et al., 2000). The Thy-1 promoter is expressed in spinal cord, brainstem, cerebellum and telencephalon but not in dopaminergic neurones of the substantia nigra. Thus, there was no pathology in dopaminergic neurones of the substantia nigra. In contrast, corresponding to the expression of the Thy-1 promoter pathological changes were observed in motor neurones in the spinal cord, brainstem, cerebellum and telencephalon. Some of these neurones showed cytoplasmic α-synuclein and ubiquitin immunoreactivity similar to LBs, however, no filaments were observed on EM. Hence, this model does not reproduce the selective loss of dopaminergic substantia nigra neurones, but mimics the extra-nigral pathology of dementia with Lewy bodies and Lewy neurites. In addition, as the pathological changes involved motor neurones in the spinal cord - a feature which is not seen in PD - this may have contributed to the abnormal motor performance of these transgenic mice.

In two models the prion promoter was used to regulate α-synuclein expression (Giasson et al., 2002; Lee et al., 2002b). This promoter is expressed in

most neurones including those in the substantia nigra. In both models wild-type overexpression did not cause any overt behavioural or pathological changes; Giasson and co-workers describe that all mice with the wild-type α-synuclein transgene were healthy up to 28 months of age. Matsuoka and colleagues used the tyrosine hydroxylase promoter to drive the α-synuclein transgene (Matsuoka et al., 2001). This led to accumulation of α-synuclein within dopaminergic cell bodies but, in mice up to one year of age, not to the formation of inclusions or any quantitative differences in dopaminergic neurone numbers or dopamine content between transgenic animals and controls, and there were no histopathological abnormalities (Matsuoka et al., 2001).

Taken together the over-expression of human wild-type α-synuclein in mice did not give consistent results. Only two models (those by Abeliovich and colleagues and by van der Putten and colleagues) had a phenotype with deficits in motor performance; animals in the other three transgenic mouse models did not show any phenotype. While the model reported by Abeliovich and colleagues demonstrated the formation of α-synuclein and ubiquitin positive inclusions in the substantia nigra and a possible role of α-synuclein in dopamine homoeostasis the other models did not show any abnormalities of dopaminergic neurones in the substantia nigra. The reasons for the discrepant results in these models remain unclear. One possible explanation may be the type of promotor chosen, which differed in the models. This determines the site and level of expression of the transgene and may explain why for example in the model by van der Putten and colleagues α-synuclein may not have been expressed in dopaminergic neurones in the substantia nigra.

3.1.8.5.8. Transgenic mouse models of mutant α-synuclein over-expression

Mice overexpressing G209A α-synuclein under the control of the prion promoter remained healthy until 7 months of age (Giasson et al., 2002). At 8 months, mice

started to neglect their grooming behaviour, lost weight and exhibited decreased ambulation. Resistance to passive movement of the limbs and "freezing" of the hind limbs was noted, and these mice developed weakness. The mice rapidly deteriorated and had to be sacrificed within 10-21 days after onset of symptoms. Histologically, no changes were observed before 6 months of age. Between 8 and 16 months, mutant G209A transgenic mice showed inclusions immunoreactive for the native and the nitrated form of α-synuclein in the spinal cord, brainstem, cerebellum and the thalamus while tyrosine hydroxylase-positive substantia nigra neurones were not involved. α-synuclein immunoreactive cytoplasmic inclusions in the spinal cord contained 10-16nm fibrils ultrastructurally (ubiquitin immunostaining was present in only 10-25%). Mutant G209A transgenic mice also showed evidence of axonal degeneration in the spinal cord and an axonal neuropathy. However, no pathological changes were observed in the dopaminergic neurones of the substantia nigra and the phenotype may at least to some degree be caused by the pronounced pathological involvement of the spinal cord and peripheral nerves. It is currently not known whether these animals will develop a neurological phenotype at a greater age.

In another transgenic mouse model mutant α-synuclein was over-expressed under the control of the prion promoter (Lee et al., 2002b). G209A but not G88C mutant α-synuclein was associated with a rapidly progressive phenotype including reduced posturing and movement, leading to paralysis and death. Pathological accumulations of α-synuclein and ubiquitin were shown in neuronal cell bodies in brainstem, midbrain, cerebellum and spinal cord before clinical symptoms developed. However, there was no loss of striatal dopamine, and no qualitative changes of tyrosine hydroxylase or dopamine-uptake transporter expression were observed.

In conclusion, in some of these transgenic mouse models, whether over-expressing the wild-type or mutant form of the protein, α-synuclein expression led to neurodegeneration that involved the dopaminergic system. However, selective loss of dopaminergic neurones has not been observed. Hence, these transgenic mice may actually model synucleinopathies, a group of neurodegenerative disorders where α-synuclein pathology is a common theme, rather than PD (Goedert, 2001). Reasons for the variability of the phenotype of these transgenic α-synuclein mice include the type of promoter chosen, which directly influences where the transgene is expressed. In one model at least, pathology was observed in the substantia nigra, although the promoter was not expressed in dopaminergic neurones in the substantia nigra (van der Putten et al., 2000), whereas in another model with a tyrosine hydroxylase promoter the animals remained healthy and no pathological changes were noted (Matsuoka et al., 2001). Variable expression of the transgene, different mouse genetic backgrounds and the integration site may also contribute to the differences observed between the models.

3.1.8.5.9. Other animal models of α-synuclein PD

Transgenic Drosophila models of PD expressing human wild-type, G209A or G88C mutant α-synuclein were generated using a bipartite expression system where the transcriptional activation of the transgene depends on the yeast protein GAL-4 (Feany and Bender, 2000). Flies with a transgene downstream of a GAL-4 responsive element were crossbred with flies expressing the yeast activator in a tissue- and cell-type specific pattern. Overall, the nervous system developed normally in the transgenic flies with central nervous system transgene activation. However, there was clear age-dependant loss of specific tyrosine hydroxylase positive dorso-medial dopaminergic neurones in flies over-expressing either wild-type or the mutant forms of α-synuclein. Other dopaminergic neuronal subsets,

cortical and serotoninergic neurones were spared. Thus, the anatomical specificity of dopaminergic neurodegeneration in this model resembled idiopathic PD. α-synuclein immunostaining revealed cytoplasmic aggregates similar to LBs ultrastructurally. However, α-synuclein aggregates and degenerative changes also developed in the flies with retinal activation only of α-synuclein expression suggesting that the effect of α-synuclein overexpression was not specific to dopaminergic neurones. While the locomotor behaviour of young transgenic flies did not differ from control flies, their climbing ability was lost prematurely. Thus, this model captured all the essential features of PD with age-dependant selective dopaminergic loss, development of LBs and a neurological phenotype with motor impairment (for a more detailed review of transgenic Drosophila models of neurodegenerative diseases see Muqit and Feany, 2002).

Over-expression of α-synuclein has been selectively induced unilaterally in the substantia nigra of adult rats by targeted injection of an adenovirus vector containing either wild-type, G209A (Kirik et al., 2002) or G88C (Klein et al., 2002) mutant α-synuclein under the control of the chicken ß-actin promoter. Both wild-type and G209A mutant α-synuclein expressing rats developed dystrophic neurites; and cytoplasmic α-synuclein, but not ubiquitin, immunoreactive inclusions (Kirik et al., 2002) or accumulation (Klein et al., 2002) were observed histologically. These changes were accompanied by a loss of 30-80% (Kirik et al., 2002) or 53% (Klein et al., 2002) of the nigral dopaminergic neurones with an associated reduction in striatal dopamine and tyrosine hydroxylase levels. However, despite substantial dopamine loss, motor behaviour was only marginally affected (Kirik et al., 2002) or not affected at all (Klein et al., 2002) in all the treated animals at all time points.

In summary, targeted α-synuclein over-expression in the nigro-striatal system using viral vectors reproduced some of the features of PD. However, these models did not reliably develop a movement disorder, and whilst selective

histological changes within the substantia nigra dopaminergic neurones were observed, unlike in human PD the α-synuclein immunoreactive inclusions were ubiquitin negative, and no EM data was presented to assess whether or not they contained fibrils.

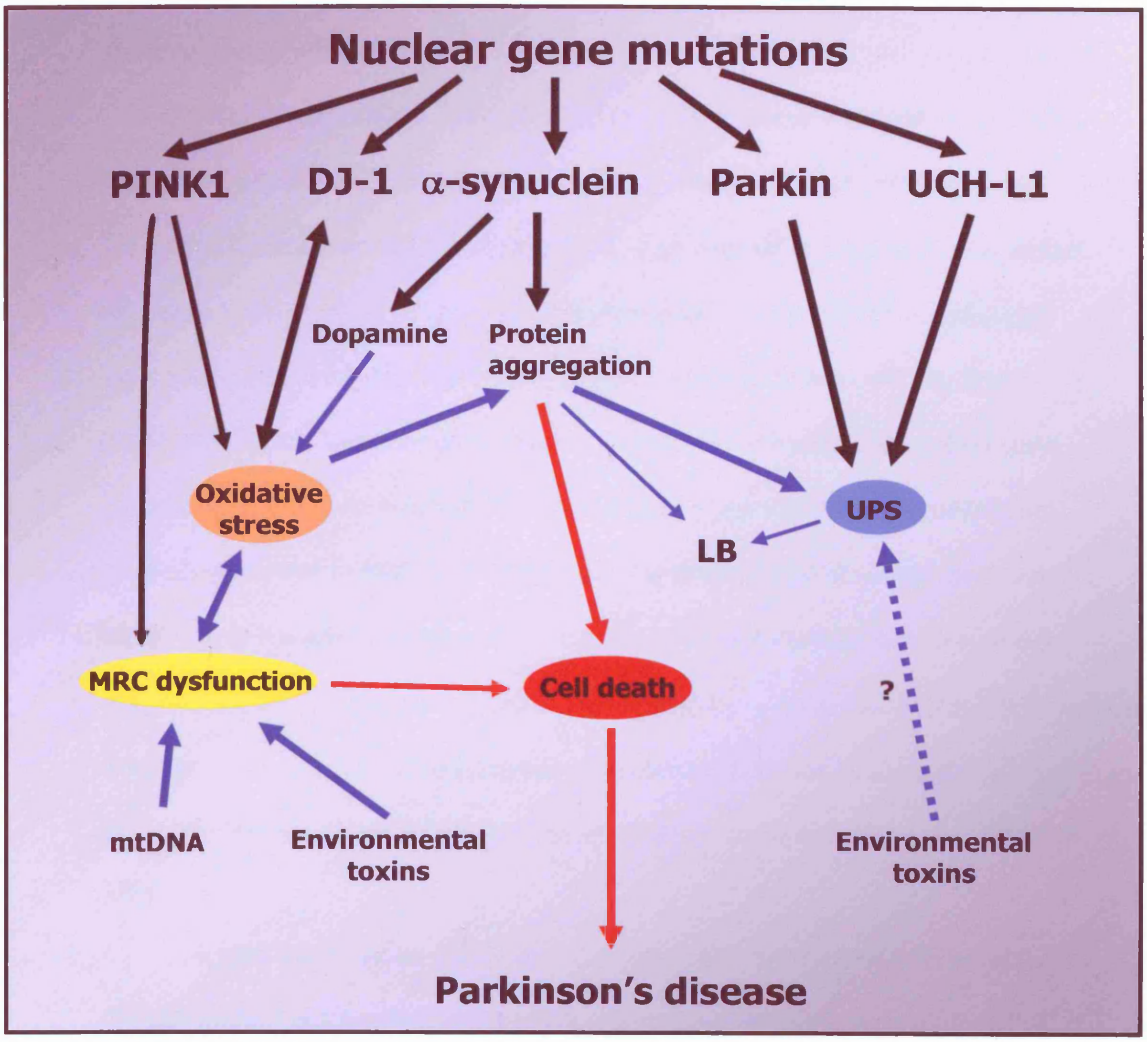

Figure 3.4. Possible common pathomechanisms in PD II. Mutations in five genes are known to cause familial PD. These genes encode α-synuclein, DJ-1, parkin, ubiquitin carboxyhydrolase L1 (UCH-L1) and PINK-1. Mutations in these genes, or altered expression, but also environmental toxins, are likely to contribute to the pathogenesis of PD. Common pathways include mitochondrial dysfunction, oxidative stress, protein misfolding and the UPS. α-synuclein is present in the cytosol and is also associated with vesicles. It interacts with dopamine compartmentalisation and forms adducts with dopamine which can promote its aggregation and can cause oxidative stress. Parkin UCH-L1 contribute to the function of the ubiquitin-proteasome system (UPS). Abnormal UPS function may increase the levels of toxic proteins increasing oxidative stress and aggregate formation including Lewy bodies (LB). This may enhance cell death or cell survival. DJ-1 protects against oxidative stress. PINK-1 encodes for a mitochondrial protein kinase. Environmental toxins such as rotenone or paraquat can interfere with mitochondrial function leading to oxidative stress which can promote e.g. α-synuclein aggregation. Cytosolic dopamine can be oxidised causing oxidative stress and potentially compromising mitochondrial function. Black arrows indicate primary causative genetic links, blue arrows indicated presumably secondary consequences of either genetic or environmental primary effects. MRC: mitochondrial respiratory chain.

3.2. Rationale to study inducible wild-type and G209A mutant α-synuclein expression in HEK293 cells

The generation of a stable, inducible cell culture model of wild-type and G209A mutant α-synuclein PD will allow the study of the structural, biochemical and functional consequences of increased wild-type and G209A mutant α-synuclein expression as a model of sporadic and autosomal dominant PD. α-synuclein appears to play a central role in PD; it is the main component of LBs, the histopathological hallmark of sporadic PD, and two different α-synuclein gene mutations give rise to autosomal dominant PD with a clinical and pathological phenotype similar to that of sporadic PD. The precise role of α-synuclein is not clear, nor is the effect of the various mutations on α-synuclein function or the significance of α-synuclein in LBs. In PD caused by α-synuclein mutations it remains unclear whether the pathomechanisms are similar to those of sporadic PD and may include oxidative stress, mitochondrial respiratory chain defects or the formation of LBs.

It was the purpose of this thesis to generate cell models with wild-type or G209A mutant α-synuclein expression under the control of ponasterone A in HEK293 cells. These models were used to study the subcellular localisation of wild-type or G209A mutant α-synuclein to examine whether expression of either protein was associated with particular organelles such as mitochondria or the Golgi network, or the formation of aggregates. The models were further used to examine the effect of wild-type or G209A mutant α-synuclein expression on mitochondrial respiratory function and the sensitivity to the complex I inhibitor rotenone given the evidence that suggests an involvement of a complex I defect in sporadic PD. Finally, the models were used to test whether the expression of wild-type or G209A mutant α-synuclein was associated with the generation of oxidative stress or increased the

vulnerability to toxins that generate oxidative stress such as paraquat and dopamine because of the evidence suggesting that increased levels of oxidative stress may contribute to cell death in sporadic PD.

3.3. Results

3.3.1. Characterisation of dopaminergic properties in HEK293, SH-SY5Y neuroblastoma and hNT2 teratocarcinoma cells

HEK293, SH-SY5Y neuroblastoma (undifferentiated and differentiated for 14 days) and hNT2 teratocarcinoma (undifferentiated) cells were characterised regarding their dopaminergic properties using immunocytochemistry (see section 2.5.2) and Western blotting (see section 2.6.5.) with antibodies against tyrosine hydroxylase (TH), VMAT 1 and 2, dopamine uptake transporter (DAT).

Immunocytochemistry revealed that all cell lines had cytoplasmic immunoreactivity with the tyrosine hydroxylase (TH) antibody (Figure 3.5A, D, G, J). However, after SH-SY5Y differentiation for 14 days not all cells expressed neurofilament so that not all cells were differentiated (Figure 3.5J), and not all cells expressing neurofilament were immunoreactive for TH (Figure 3.5J). Staining with the VMAT-1 antibody was positive in the cytoplasm of all cell lines and in cell processes of both non-differentiated and differentiated SH-SY5Y cells (Figure 3.5B, E, H, K). Staining with the VMAT-2 antibody showed some cytoplasmic immunoreactivity in hNT2 (Figure 3.5F) and SH-SY5Y cells (Figure 3.5I) with enhancement of staining intensity in differentiated SH-SY5Y cells (Figure 3.5L). HEK293 cells exhibited no VMAT-2 staining (Figure 3.5C). All the cell lines were negative for staining with an antibody to the dopamine uptake transporter (DAT, data not shown). Controls for each antibody and cell line (omission of the primary antibody) showed no immunostaining. Western blot analysis failed to reveal any specific band of the predicted size (data not shown).

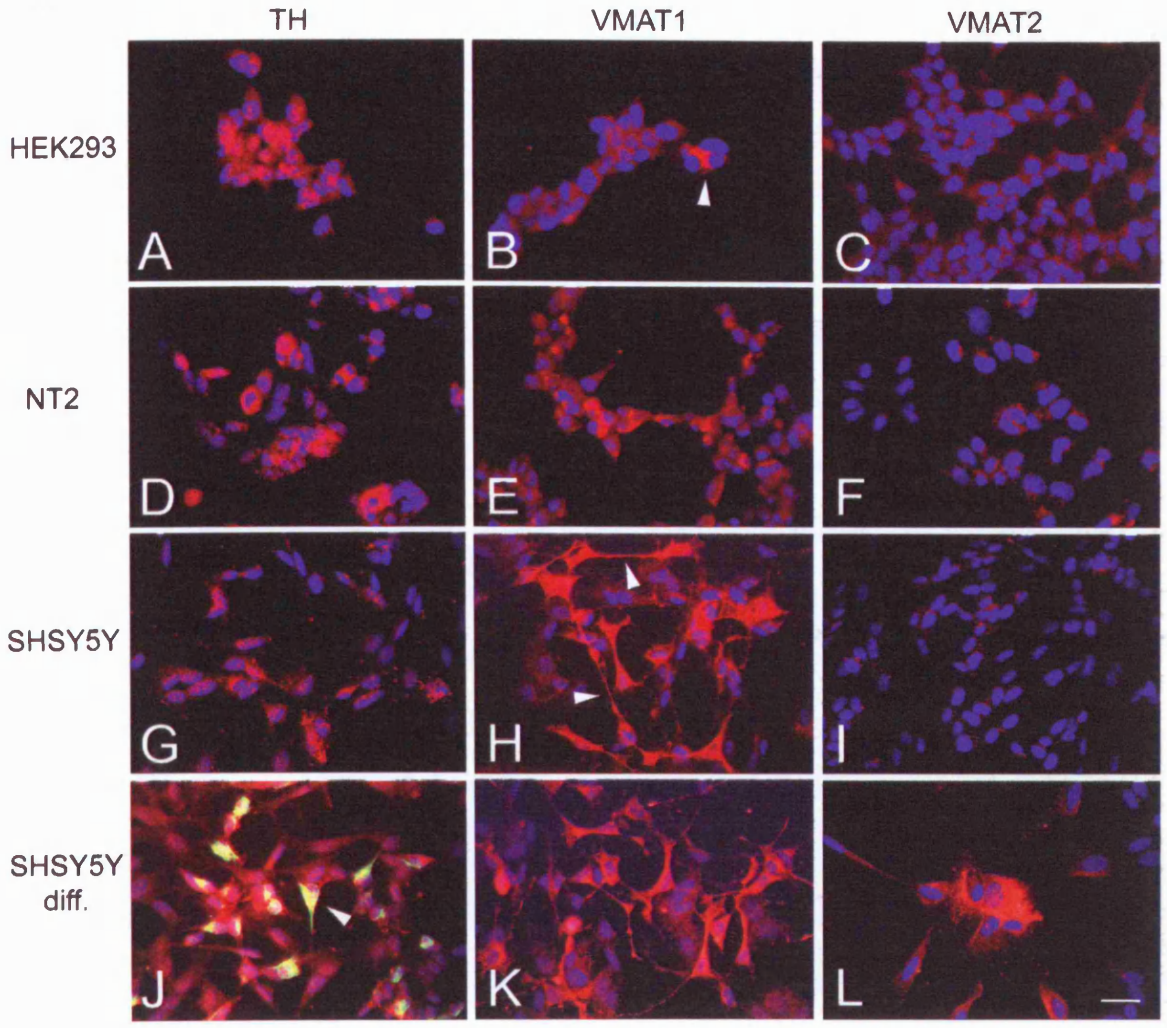

Figure 3.5: Immunocytochemistry. All cell lines stained positive for tyrosine hydroxylase (**A,D,G,J**). Expression was cytoplasmic, in particular in differentiated SHSY5Y (arrow heads indicate co-localisation with neurofilament antibody, yellow in **J**). Staining with the VMAT-1 antibody was positive in the cytoplasm of all cell lines (**B,E,H,K**, arrow head in **B**) and in cell processes of both non-differentiated and differentiated SHSY5Y cells (arrow heads in **H**). Staining with the VMAT-2 antibody showed some cytoplasmic staining in hNT2 (**F**) and SHSY5Y cells with enhancement in differentiated SHSY5Y cells (**I** and **L**). There was no VMAT-2 staining in the HEK293 cells (**C**). Scale bar=20μm.

3.3.2. Generation of vectors

This work was performed in collaboration with Dr. Sarah Tabrizi (Department of Clinical Neurosciences, Royal Free and University College London Medical School). RNA was extracted from lymphoblasts of an affected male patient of the Contoursi kindred with the G209A α-synuclein mutation and controls lymphoblasts containing wild-type α-synuclein. Using RT-PCR, cDNA was generated from the isolated RNA. The resultant cDNA was immediately used to amplify total α-synuclein cDNA by PCR using the nested primers. This total α-synuclein cDNA PCR product served as the template for PCR amplification of the α-synuclein open reading frame using the forward and revers primers as described (see section 2.4.2.). A haemagglutinine (HA) epitope was cloned in at the 3' end to serve as a reporter gene. This allowed tagging of the expressed protein.

Both G209A mutant and wild-type α-synuclein-HA amplified fragments were restricted with *Kpn*-I and *Bcl*-I and cloned into the *Kpn*-I and *BamH* I sites of the pIND vector. The ligation products were then propagated through E.coli and then individual clones screened by PCR amplification for the presence of α-synuclein insert. Colonies containing the α-synuclein insert were picked off, and the pIND plasmid was isolated from the E.coli and sequenced. Eight α-synuclein constructs of each wild-type and G209A mutant α-synuclein were sequenced and found to have the correct orientation and sequences.

This yielded two vectors for transfection: pIND containing wild-type α-synuclein with a haemagglutinine tag (pIND. α-syn-HA) and pIND containing G209A mutant α-synuclein with a haemagglutinine tag (pIND. α-syn/G209A-HA).

3.3.3. Analysis of the Ecdysone Mammalian system in neuronal cell lines

SH-SY5Y cells and hNT2 cells were transfected with the pVgRxR plasmid and cells selected with Zeocin (for methods see section 2.4.3.). Resistant lines were cloned and transfected with either the pIND plasmid alone, the pIND.α-synuclein-HA plasmid or the pIND.G209Aα-synuclein-HA plasmid, which confers resistance to G418. G418 resistant SH-SY5Y and hNT2 cultures were cloned (see section 2.4.4.) indicating the successful transfection with both plasmids. In each cell line, a mixed pIND0 cell line, 10 wild-type α-synuclein and 10 G209A mutant α-synuclein clones were then screened by immunocytochemistry for expression of α-synuclein or haemagglutinin. There was low-level immunostaining of α-synuclein without ponasterone A induction (Figure 3.6A). None of the clones showed any α-synuclein (Figure 3.6B) or haemagglutinin (Figure 3.6D) expression upon induction with ponasterone A while positive controls (transfected ECR293 cell lines, see next section) showed clear α-synuclein or haemagglutinine immunostaining (Figure 3.7).

In order to test whether the cell cultures contained the pIND.α-synuclein construct DNA was extracted (see section 2.4.5.) from a clone resistant to Zeocin and G418 transfected with the empty pIND plasmid (hNT2.pIND0) and a clone resistant to Zeocin and G418 transfected with pIND containing G209A mutant α-synuclein cDNA (hNT2. pIND.α-syn/G209A). Using PCR (see section 2.4.8.), the multiple cloning site of the pIND0 plasmid was amplified and separated on an agarose gel. This revealed that there was no insert in the pIND0 culture (Figure 3.6C). In contrast, a band at about 700bp was found in the hNT2 culture with the pIND.α-syn/G209A insert (Figure 3.6C). This indicated that neuronal cell lines had successfully been transfected with the pIND. α-synuclein-HA plasmid and thus acquired resistance to both Zeocin and G418 antibiotics. However, ponasterone A failed to induce the Ecdysone system to express α-synuclein/HA. This suggests that

in the neuronal lines one of the two plasmids was non-functional or, alternatively, that there might have been an alteration within the cDNA containing multiple cloning site within pIND0, e.g. a shift of the open reading frame or a change in the position of the ATG stop codon. Since identical plasmid and cDNA stocks were successfully used to transfect HEK293 cells (see next section) a problem inherent to the cell lines may be more likely. This would be consistent with the failure of other researchers within the Department of Clinical Neurosciences to induce expression after transient transfections of many other lines (Dr M Cleeter, Dr JM Cooper, personal communication).

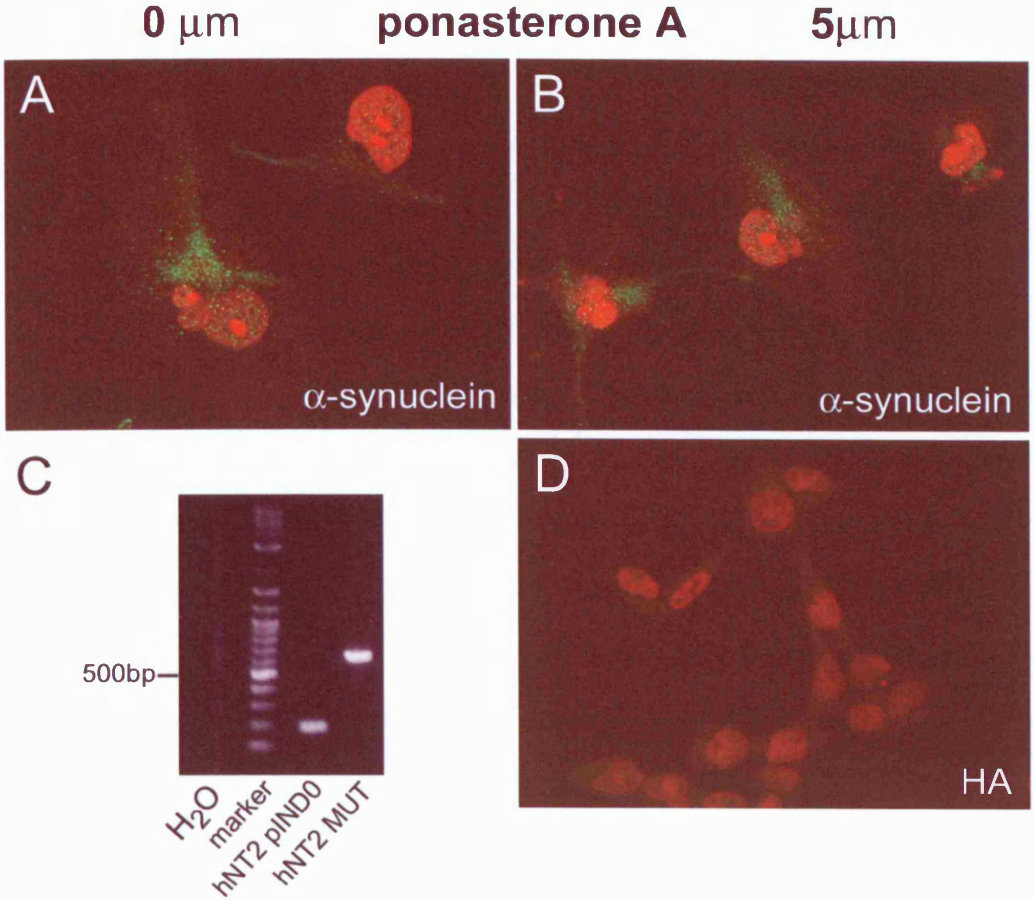

Figure 3.6. Assessment of hNT2 cells after transfection with pVgRxR and pIND. Endogenous α-synuclein expression is shown in **A**. Upon induction with ponasterone A (5μM for 48 hours) there was no change in α-synuclein staining (**B**), and staining for haemagglutinine (HA) was negative (**D**). PCR amplification of the multiple cloning site of pIND revealed a band of about 700bp (**C**) in cells transfected with α-synuclein cDNA (hNT2 MUT) indicating that these cells contained the pIND.α-syn/HA plasmid.

3.3.4. Expression of α-synuclein cDNA in EcR293 cells

Immunocytochemistry

The EcR293 cell line that contained a functional pVgRxR plasmid (Invitrogen) was transfected with pIND0, pIND.α-synuclein-HA or pIND.G209Aα-synuclein-HA, as described (see section 2.4.3.). Cells were selected for resistance to G418. A dose was chosen that killed all untransfected cells within 10 days. This dose was established in collaboration with Dr S Tabrizi, Department of Clinical Neurosciences, RFH+UCL Medical School. Resistant colonies from each transfection were selected after 2-3 weeks and individual clones isolated through ring cloning (see section 2.4.4.). A total of three clonal cultures transfected with wild-type α-synuclein (WTsyn 1-3), 3 clonal cultures transfected with G209A mutant α-synuclein (MUTsyn 1-3) with >70% of cells expressing α-synuclein/HA after ponasterone A induction, and a mixed culture transfected with pIND without insert (pIND0) were isolated (section 2.4.4.).

These cells were immunostained with antibodies to HA (for detection of the HA tag) or α-synuclein (see section 2.5.1.). In the absence of ponasterone A, there was very weak, if any, staining with the α-synuclein antibody, and no staining with the HA antibody (data not shown), in the pIND0 (Figure 3.7A), WTsyn (Figure 3.7C) or MUTsyn (Figure 3.7E) transfected cells. This suggests that the background expression of WTsyn and pIND.α-syn/G209A cells is the result of endogenous α-synuclein and not due to leakage of the introduced gene constructs. Induction with 5μM ponasterone A for 48 hours did not result in α-synuclein or HA immunostaining in the pIND0 cell culture (Figure 3.7B); in WTsyn (Figure 3.7D) or MUTsyn cell lines (Figure 3.7F) ponasterone A led to the expression of extranuclear α-synuclein. Staining was diffuse (Figure 3.7D and F) but in a subset of cells aggregate-like staining of WTsyn (Figure 3.7G) or MUTsyn (Figure 3.7H) was observed.

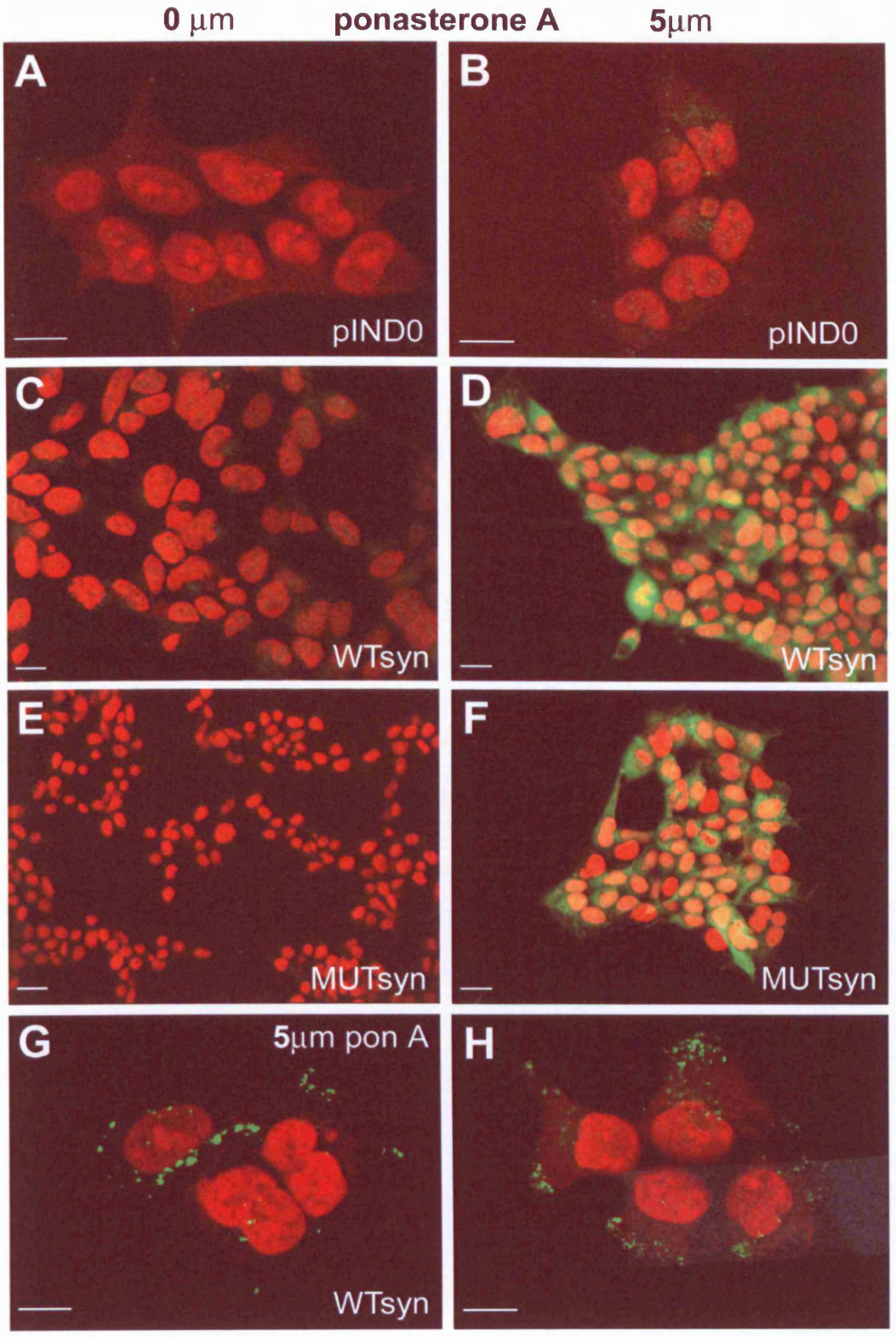

Figure 3.7. Expression of α-synuclein cDNA in in EcR293 cells. Staining after induction with 5μM ponasterone A for 48 hours in cells transfected with pIND0 (**A** and **B**), pIND.α-syn/HA (WTsyn **C** and **D**) or pIND.α-synG209A/HA (MUTsyn **E** and **F**). There was no immunostaining without induction (**A**, **C** and **E**), or with ponasterone A induction in pIND0 (**B**). In pIND.α-syn/HA cells (**D**), or pIND.α-synG209A/HA cells (**F**) ponasterone A induced expression of α-synuclein outside the nucleus (red staining). Staining was diffuse (**D** and **F**) but in a subset of cells aggregate-like staining was observed for both wild-type (**G**) and G209A mutant α–synclein (**H**). Scale bar = 10μm, except E (=20μm).

In ponasterone A induced WTsyn (Figure 3.8A, C and E) and MUTsyn cell lines (Figure 3.8B, D and F) α-synuclein immunostaining co-localised with HA immunoreactivity (Figure 3.8E for WTsyn, F for MUTsyn) indicating expression of the transfected cDNA.

Induction of α-synuclein/HA expression with different concentrations of ponasterone A revealed that the number of cells expressing α-synuclein, but not the intensity of α-synuclein staining, increased from with increasing concentrations of ponasterone A (data not shown). Assessment of α-synuclein expression over time (24, 48, 72, 96 hours) revealed no difference in the staining intensity or the number of expressing cells (data not shown). Because cells grew over-confluent after 96 hours in culture longer expression of α-synuclein was not possible without harvesting and splitting cells.

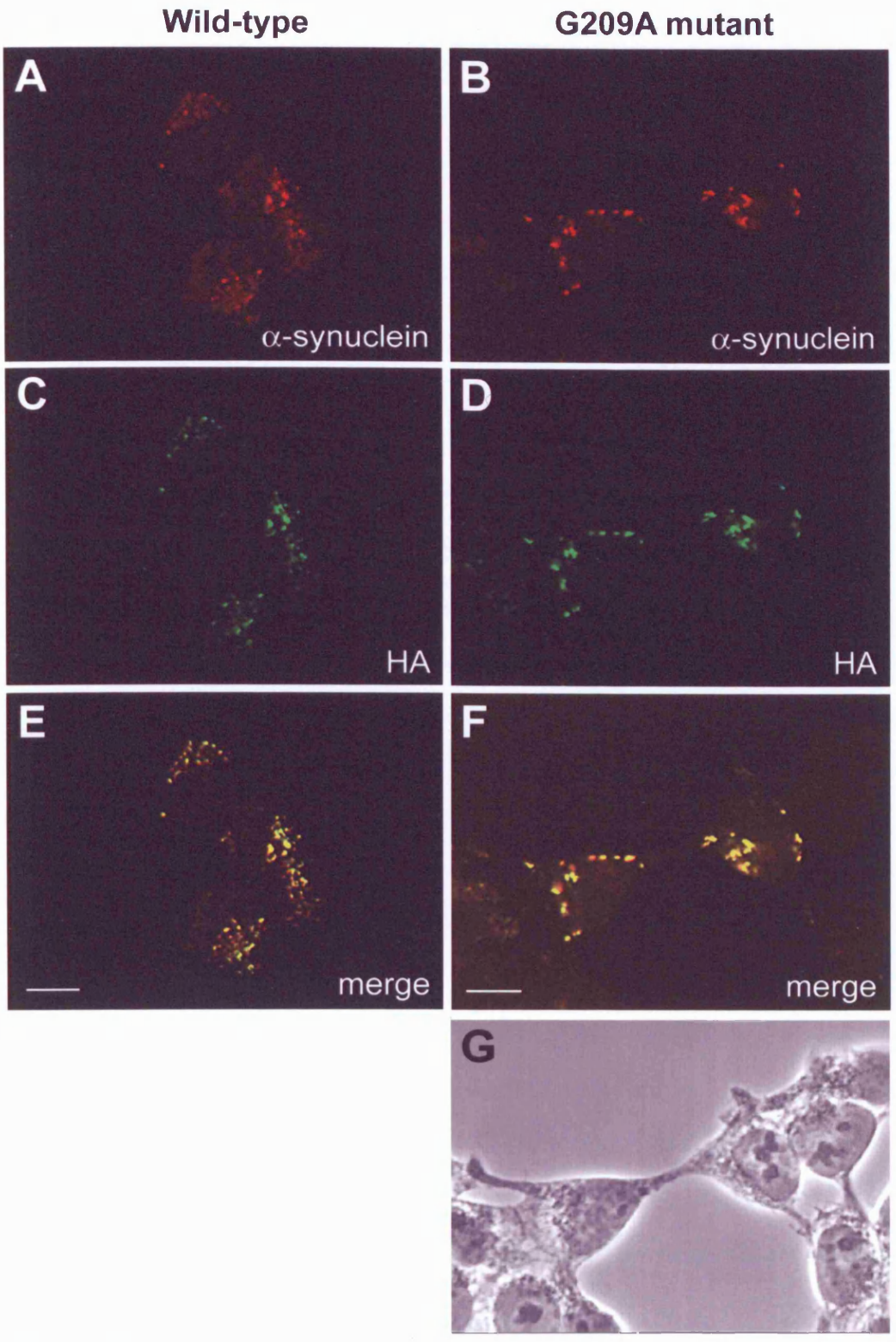

Figure 3.8. Immunocytochemical localisation of α-synuclein and HA in HEK 293 derived cell lines after induction with 5μM pon A for 48 hours. Double labelling showes that wild-type α-synuclein (red in **A**) or G209A mutant α-synuclein (red in **B**) co-localised with HA (green in **C** and **D**) as indicated on merged images (yellow in **E** and **F**). **G.** Phase contrast to B, D and F. Scale bar = 10μm.

Western blots

Levels of protein expression were assessed by Western blot using a mouse monoclonal antibody against α-synuclein or rat monoclonal antibody against haemagglutinin (for methods see section 2.6.5.). In the absence of ponasterone A induction, with either antibody there was no significant staining at 20kD, the size of the band expected from the molecular weight of α-synuclein, in either the pIND0 or any of the WTsyn or MUTsyn clones (Figure 3.9A and B). Following ponasterone A (5μM for 48h) induction, a band of about 20kD was stained in the three WTsyn and the three MUTsyn clones with both the α-synuclein antibody (Figure 3.9A) or the HA antibody (Figure 3.9B) while there was no band in the ponasterone A induced pIND0 cells. Levels of α-synuclein/HA expression in all cell cultures containing the α-synuclein pIND constructs were similar at 5μM ponasterone A. The level of α-synuclein expression (wild-type or mutant) was proportional to the concentration of ponasterone A used with the inducible cell lines (Figure 3.9C). Thus the production of α-synuclein protein by these cell lines was tightly controlled by ponasterone A.

3.3.5. DNA sequencing

The α-synuclein cDNA was sequenced in the three WTsyn and MUTsyn clones. The inserted α-synuclein cDNA was amplified by PCR using primers to the plasmid multiple cloning site and separated on agarose gels to confirm the size of the product (for methods see sections 2.4.5., 2.4.8. and 2.4.11.). The sequence was determined commercially at MWG (MWG, Germany). This documented that the three WTsyn EcR 293 clones contained the wild-type α-synuclein insert (Figure 3.10), and the MUTsyn EcR293 cell lines contained the mutant G209A α-synuclein insert (Figure 3.10, and appendix).

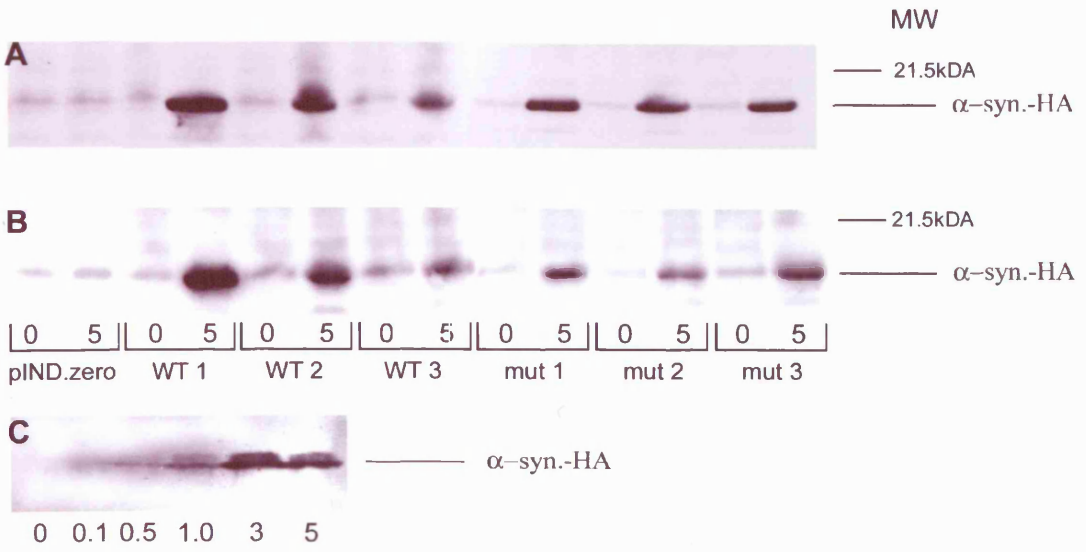

Figure 3.9. Western blot showing α-synuclein and HA expression following ponasterone A induction. **A.** pIND.α-synuclein-HA expression induced by pon A in three cell lines each of wild-type α–syn and mut α-syn and pIND.0 is tested with a α-synuclein antibody. **B.** pIND. α-synuclein-HA expression induced by pon A in three cell lines each of wild-type α-syn and mut α-syn and pIND.0 tested with a HA antibody. **C.** Increasing concentrations of ponasterone A (0.1, 0.5, 1.0, 3.0 and 5μm) resulted in greater expression of the mutant protein. Similar results were obtained with the wild-type pIND.α-syn cell lines (data not shown).

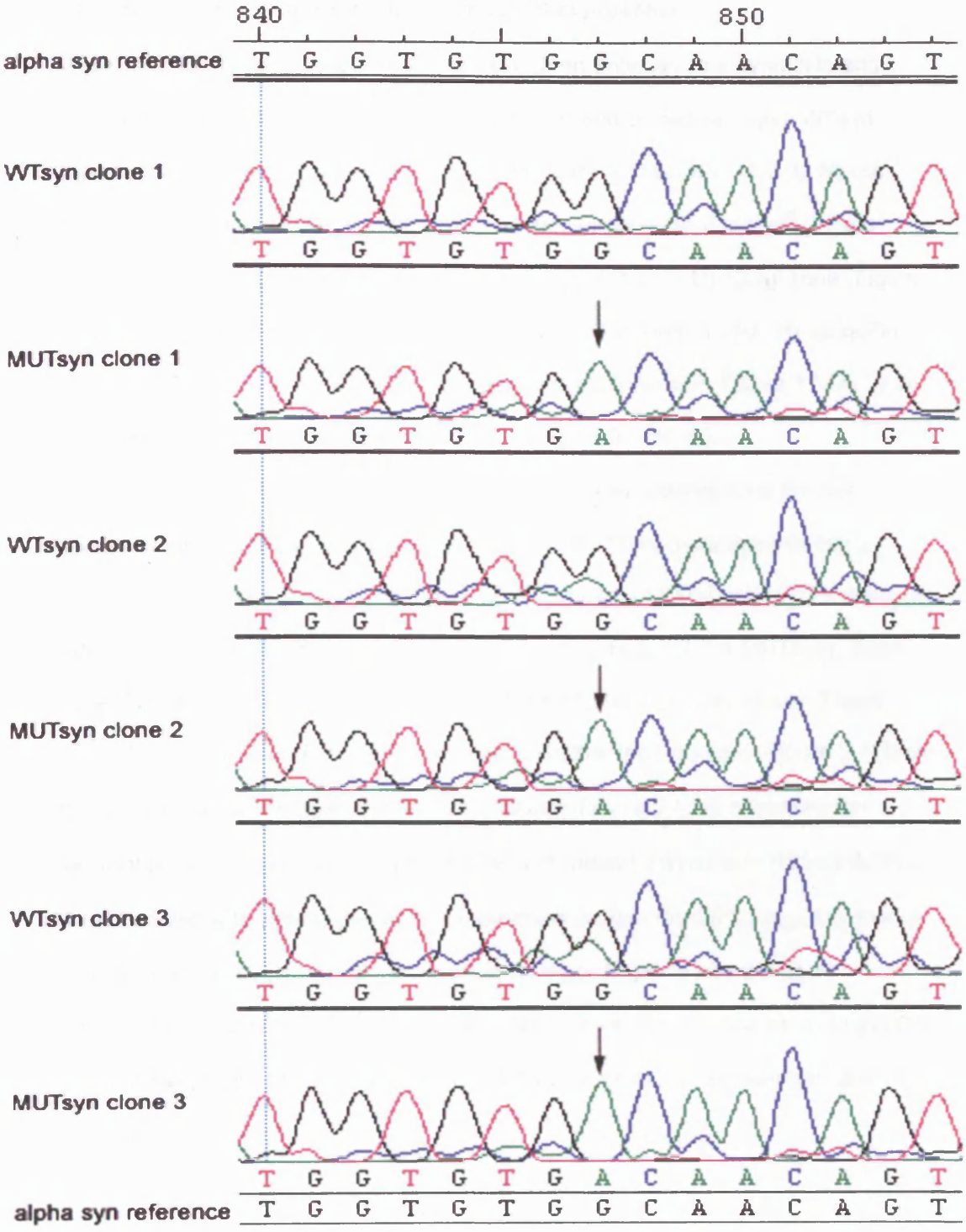

Figure 3.10. Sequence section of the α-synuclein gene. A sequence section is shown that contains the G209A α-synuclein mutation in 3 MUTsyn clones and wild-type genotype in the 3 WTsyn cell lines. For the complete sequences see appendix 3.

3.3.6. Subcellular localisation of α-synuclein expression

WTsyn and MUTsyn cell lines were stained with an antibody to α-synuclein and propidium iodide to label the nucleus (Figure 3.7B and D, respectively). WTsyn (Figure 3.11A, C, E, G, I, K, M) and MUTsyn (Figure 3.11B, D, F, H, J, L, N) cell cultures were stained with an antibody to α-synuclein and MitoTracker® (Figure 3.11A, B), COI cytochrome c oxidase subunit (Figure 3.11C, D), Golgi zone (Figure 3.11E, F), lysosomal associated membrane protein-1 (Figure 3.11G, H), ubiquitin (Figure 3.11I, J), vesicle associated membrane protein (VAMP, Figure 3.11K, L) or vesicular monoamine transporter-1 (VMAT-1, Figure 3.11M, N).

There was no co-localisation of α-synuclein with markers for the cell nucleus (Figure 3.7B for WTsyn, Figure 3.7D for MUTsyn), mitochondria using MitoTracker® (Figure 3.11A for WTsyn, Figure 3.11B for MUTsyn) or COI subunit of cytochrome c oxidase (Figure 3.11C for WTsyn, Figure 3.11D for MUTsyn), Golgi zone (Figure 3.11E for WTsyn, Figure 3.11F for MUTsyn), or lysosomes (Figure 3.11G for WTsyn, Figure 3.11H for MUTsyn). Neither the wild-type (Figure 3.11I) nor mutant α-synuclein deposits stained for ubiquitin (Figure 3.11J). However, co-localisation of both wild-type (Figure 3.11K) and mutant α-synuclein (Figure 3.11L) was observed with vesicle associated membrane protein (VAMP), indicating that α-synuclein was associated with intracellular vesicles. Staining for vesicular monoamine transporter (VMAT 1) showed that a proportion of vesicles were positive for both this protein and wild-type (Figure 3.11M) or mutant α-synuclein (Figure 3.11N).

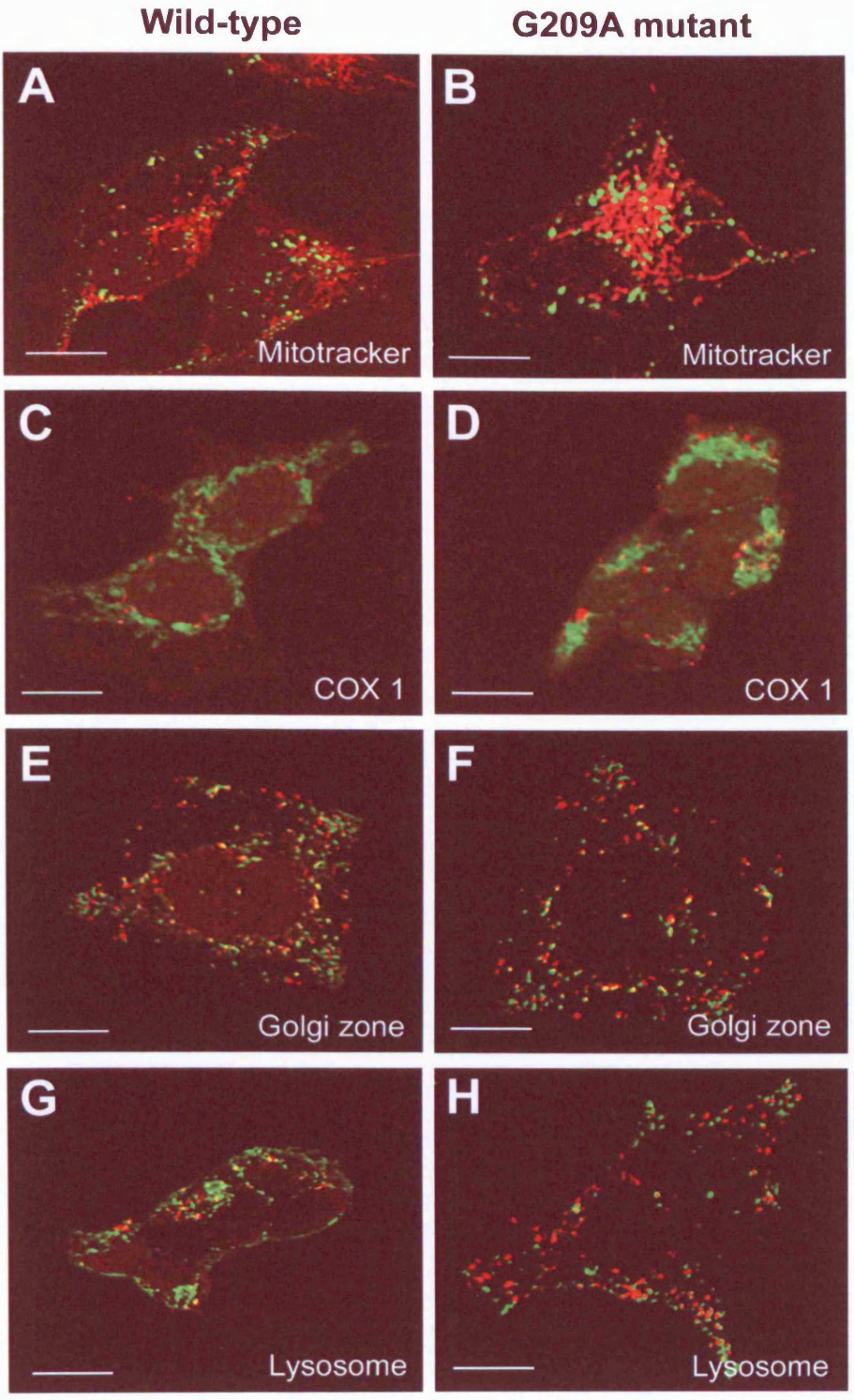

Figure 3.11. Subcellular localisation of α-synuclein in HEK 293 derived cell lines. Immunocytochemistry of cells expressing wild-type or mutant G209A α-synuclein. Co-staining of α-synuclein (green fluorescence) with MitoTracker (red fluorescence) showed that wild-type or mutant α-synuclein were not localised in mitochondria (**A** and **B**). This was confirmed with COI subunit stain of cytochrome oxidase (**C** and **D**, COX 1, green; α-synuclein in red). Dual staining with green fluorescence for the Golgi network (**E** and **F**) and lysosomes (**G** and **H**) showed separate l ocalisation for wild-type (**E** and **G**) and mutant (**F** and **H**) α-synuclein (red fluorescence). Scale bar equals 10μm.

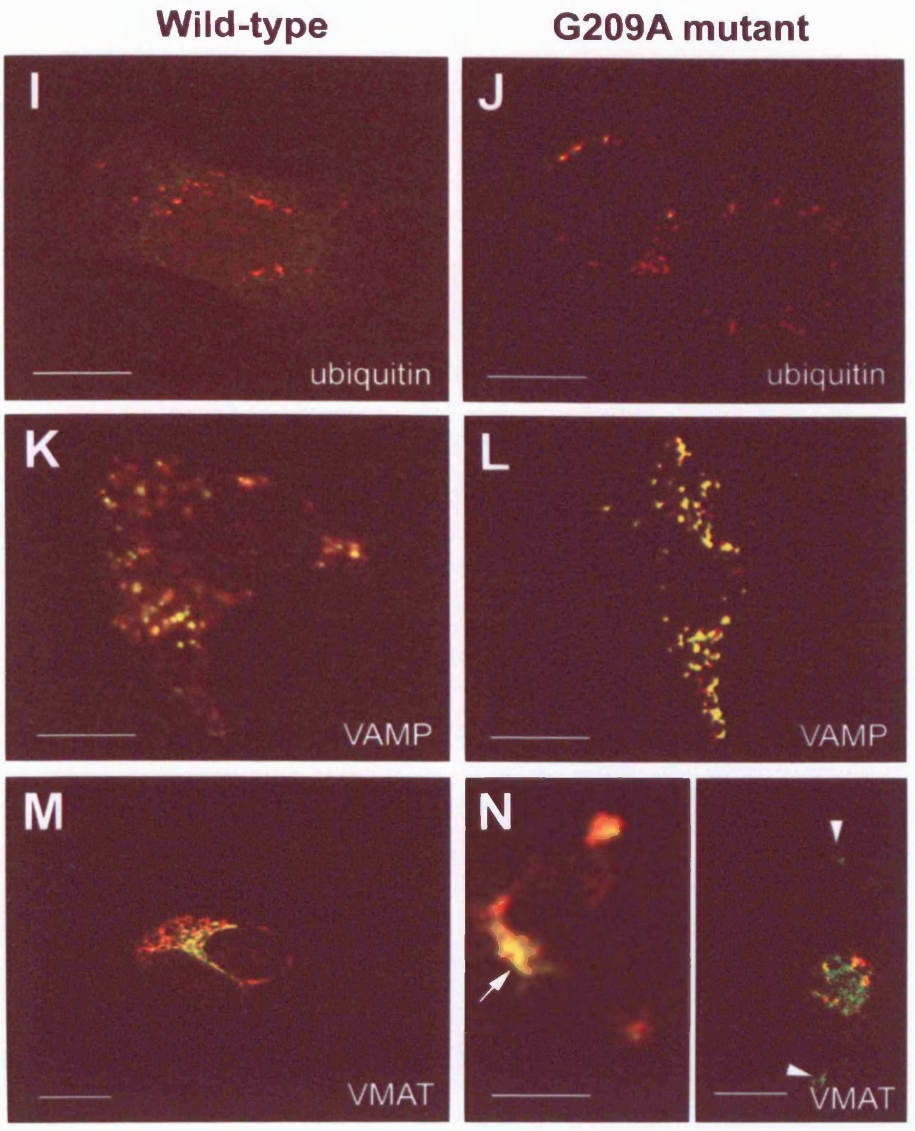

Figure 3.11, continued. Dual labeling studies indicated that wild-type α-synuclein (**I**) or mutant α-synuclein (**J**) (red fluorescence) did not stain for ubiquitin (green in **I** and **J**). Both wild-type (red in **K**) and mutant α-synuclein (red in **L**) co-localised with VAMP (green) as shown by the merged fluorescence (yellow in **K** and **L**), they also stained with VMAT-1 (wild-type in **M** and mutant in **N**, arrow) although this was not exclusive to the distribution of either of the vesicle stains (arrow heads in **N**). VAMP: vesicular associated membrane protein; VMAT: vesicular monoamine transporter.
Scale bar equals 10μm.

3.3.7. Cell viability

Cell viability experiments addressed the questions whether wild-type α-synuclein or G209A mutant α-synuclein alone lead to increased cell death or whether their expression enhanced the vulnerability to dopamine or rotenone.

Cell viability was not significantly affected by ponasterone A induction of wild-type or G209A mutant α-synuclein expression for 48 hours as shown both by LDH assay (Figure 3.12A; for methods see section 2.9.1.) or flow cytometry (Figure 3.12B; for methods see section 2.9.2.) (Kruskal-Wallis test, see section 2.12.).

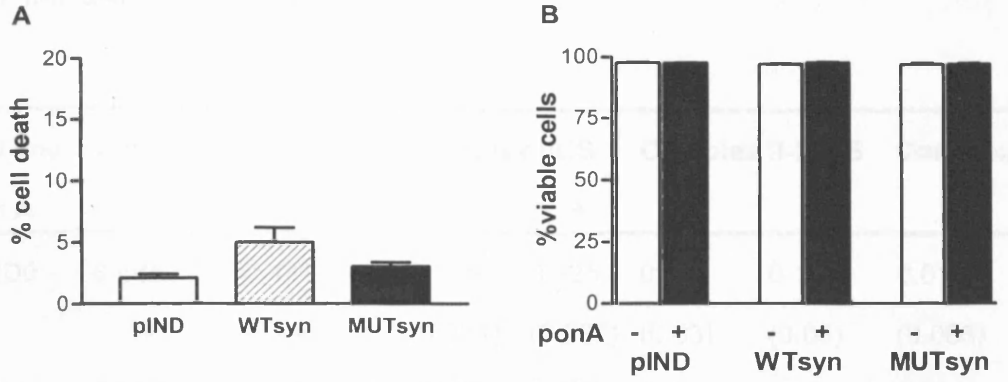

Figure 3.12. Cell viability with α-synuclein expression after 48 hours 5μM ponasterone alone. **A.** LDH assays revealed that less than 10% of cells died with α-synuclein expression (wild-type or G209A mutant) or ponasterone A treatment alone. **B.** Propidium iodide staining followed by flow cytometry confirmed that there was very little cell death with or without ponasterone A induction.

3.3.8. Mitochondrial function

3.3.8.1. Mitochondrial Respiratory Chain activities

Mitochondrial citrate synthase activities and the complex I, II/III and IV citrate synthase ratios were measured in pIND0, WTsyn and MUTsyn cells in the absence of ponasterone A and compared to those activities after induction with ponasterone A (5μM) for 48h (for methods see section 2.7.2.). Ponasterone A caused a slight, but not significant, decrease in the CS activity and complex I, II/III and IV CS ratios in the pIND0 cells (Table 3.3.). Ponasterone A induction of WTsyn or MUTsyn had no significant effect upon the CS activities or CS ratios for mitochondrial complexes I, II-III and IV (Table 3.3.).

Cell line	Citrate synthase (CS)		Complex I/CS		Complex II-III/CS		Complex IV/CS	
pon A	-	+	-	+	-	+	-	+
PIND0	0.486	0.437	0.135	0.125	0.19	0.18	0.011	0.010
	(0.092)	(0.043)	(0.034)	(0.037)	(0.03)	(0.03)	(0.003)	(0.003)
WTsyn	0.619	0.636	0.124	0.123	0.19	0.19	0.011	0.011
	(0.102)	(0.128)	(0.028)	(0.029)	(0.04)	(0.04)	(0.001)	(0.001)
MUTsyn	0.850	0.860	0.080	0.074	0.16	0.16	0.010	0.009
	(0.150)	(0.227)	(0.015)	(0.014)	(0.03)	(0.04)	(0.001)	(0.001)

Table 3.3. Effect of ponasterone A induction on (mitochondrial respiratory chain/citrate synthase) ratios. Ponasterone A induction of wild-type or mutant α-synuclein expression or ponasterone A treatment alone had no significant effect on mitochondrial respiratory chain/citrate synthase ratios when compared to non-induced cells (Kruskal-Wallis test, see section 2.12.). Values are expressed as mean (± SEM), n=4, (except n=3 for WTsyn and MUTsyn Complex IV). Citrate synthase (CS) is expressed as the specific activity, nmol/min/mg protein.

3.3.8.2. Mitochondrial membrane potential

To optimise the selectivity of the lipophylic dye $DiOC_{6(3)}$ (3,3'-dihexyloacarbocyanine, Molecular Probes) for mitochondrial localisation HEK293 pIND0 cells, grown on coverslips, were incubated with either 5, 25 or 50nM $DiOC_{6(3)}$ for 20 minutes, washed and mounted in PBS. To confirm mitochondrial co-localisation of $DiOC_{6(3)}$, cells on coverslips were stained first with the mitochondrial dye MitoTracker® (3 μM CMXRos-H_2, Molecular Probes) and thereafter with $DiOC_{6(3)}$, washed and mounted in PBS (for methods see section 2.8.3.1.).

Using fluorescence microscopy $DiOC_{6(3)}$ staining of HEK293 cells was not detectable at 5nM (Figure 3.13A) and was weak at 25nM (Figure 3.13B). Clear mitochondrial networks could be seen with 50nM $DiOC_{6(3)}$ (Figure 3.13C). Co-staining with the mitochondrial marker MitoTracker® revealed $DiOC_{6(3)}$ staining that co-localised with the mitochondria on confocal microscopy (Figure 3.13D). To test the specificity of the $DiOC_{6(3)}$ stain for mitochondrial membrane depolarisation, cells were treated with the ionophore CCCP (100μM, m-chlorophenylhydrazone) for 30 minutes. On microscopy, $DiOC_{6(3)}$ staining was abolished from the majority of cells after treatment with CCCP (100μM) to depolarise mitochondria (Figure 3.13G), which correlated with approximately 75% decrease in the median $DiOC_{6(3)}$ fluorescence signal when analysed by flow cytometry (Figure 3.14).

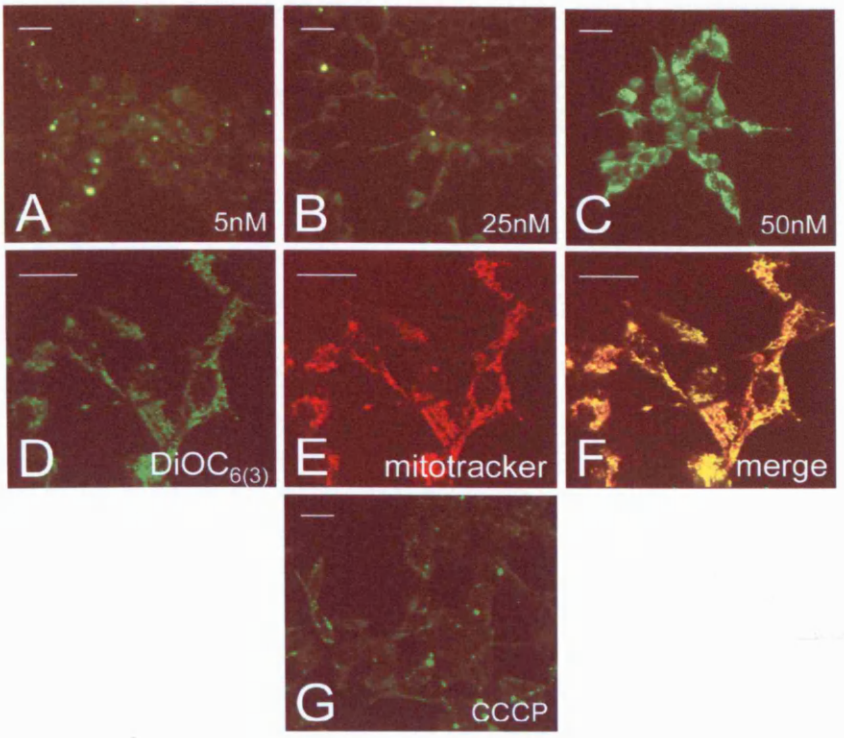

Figure 3.13. $DiOC_{6(3)}$ staining. No or minimal staining with 5 (A) or 25nM (B) $DiOC_{6(3)}$. Mitochondrial networks are clearly visible with 50nM $DiOC_{6(3)}$ (C,D) and co-staining with 3μM mitotracker (E) reveals co-localisation with $DiOC_{6(3)}$ (F). $DiOC_{6(3)}$ staining is abolished when cells are pre-treated with 100μM CCCP (G). Scale bar = 20μm.

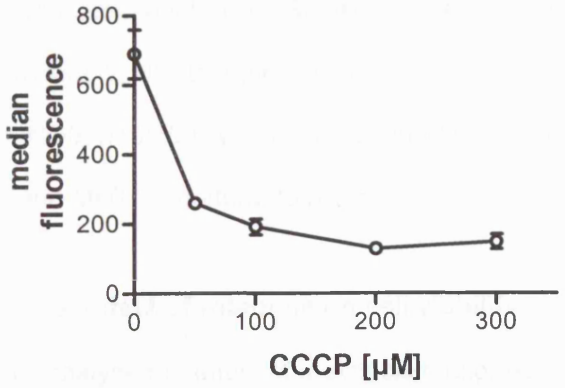

Figure 3.14. The effect of CCCP on mitochondrial membrane potential using flow cytometry and staining with 50nM $DiOC_{6(3)}$ Increasing concentrations of CCCP caused a reduction of 50nM $DiOC_{6(3)}$ median fluorescence intensity of HEK293 pIND0 cells. Values are expressed as mean ±SEM, n=3.

To determine the effect of α-synuclein expression on mitochondrial membrane potential, cells were grown in the presence and absence of 5µM ponasterone A, stained for $DiOC_{6(3)}$ (50nM) and analysed by flow cytometry (for methods see section 2.8.3.). The median fluorescence for $DiOC_{6(3)}$ was not significantly affected by ponasterone A in pIND0, WTsyn cells or MUTsyn cells (Figure 3.15).

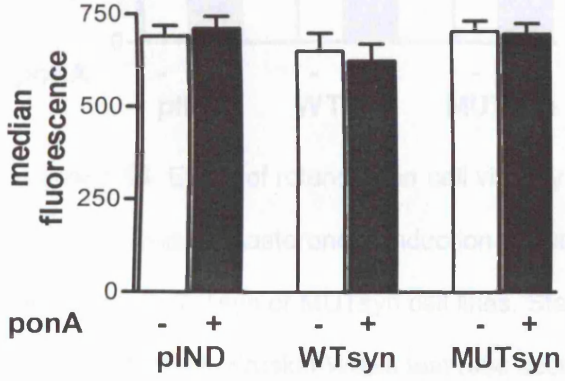

Figure 3.15. Effect of wild-type and mutant α-synuclein expression upon mitochondrial membrane potential. Ponasterone A (48 hours, 5µM) induction of wild-

type or mutant α-synuclein expression did not significantly affect $DiOC_{6(3)}$ median fluorescence intensity. Statistical analyses compared open versus solid bars, Kruskal-Wallis test (see section 2.12.). Values are expressed as mean ±SEM; pIND0, n=6; WTsyn, n=6 for each WT1-3 culture, total n=18; and MUTsyn, n=6 for each MUT1-3 culture, total n=18.

3.3.9. Effect of rotenone on cell viability

To analyse the effect of α-synuclein expression on rotenone toxicity the pIND0, WTsyn and MUTsyn cell lines were exposed to 50nM rotenone for 36 hours following 48h incubation with 5μM ponasterone A or DMSO. In PC12 cells, this concentration of rotenone inhibits about 50% of complex I activity after 3 hours of exposure (Hartley et al., 1994). Rotenone caused a significant increase in cell death compared with no rotenone treatment; however, α-synuclein expression, either wild-type or G209A mutant, did not significantly affect levels of cell death (Figure 3.16).

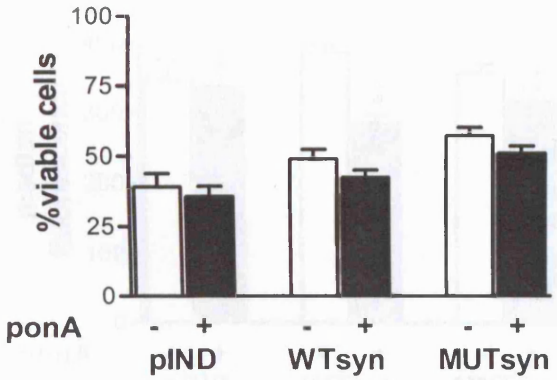

Figure 3.16. Effect of rotenone on cell viability using flow cytometry and propidium iodide staining. Ponasterone A induction did not influence the percentage of viable cells in pIND, WTsyn or MUTsyn cell lines. Statistical analysis compared open versus solid bars, Kruskal-Wallis test (see section 2.12). Values are expressed as means ±SEM; pIND0, n=6; WTsyn, n=6 for each WT1-3 culture, total n=18; and MUTsyn, n=6 for each MUT1-3 culture, total n=18.

3.3.10. Effect of rotenone on mitochondrial membrane potential

The effect of α-synuclein on mitochondrial membrane potential was analysed after pIND0, WTsyn and MUTsyn cell lines were incubated for 48h with 5μM ponasterone A or DMSO followed by exposure to 50nM rotenone for 36 hours (for methods see section 2.8.3.1.). $DiOC_{6(3)}$ staining intensity after rotenone exposure was compared to and expressed as a proportion of $DiOC_{6(3)}$ staining intensity in untreated cells of the respective cell line. In pIND0 cells rotenone caused a 52.2± 9.5% decrease in $DiOC_{6(3)}$ staining, which was very similar after ponasterone A induction (50± 8%, Figure 3.17). However, WTsyn expression enhanced the rotenone induced mitochondrial depolarisation from 41± 2.6% decrease in the absence to 54± 3.8% in the presence of ponasterone A respectively (p=0.001, Figure 3.17), A similar but smaller change was observed with G209A mutant α-synuclein expression (49± 3.9% decrease in fluorescence enhanced to 54± 5.7% decrease in the presence of ponasterone A, p=0.05, Figure 3.17).

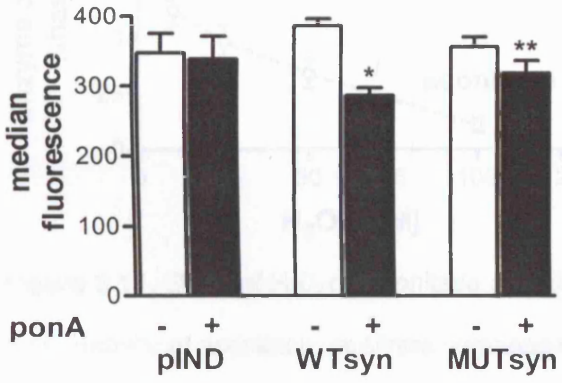

Figure 3.17. Effect of wild-type or mutant α-synuclein expression upon mitochondrial membrane potential and rotenone toxicity. Ponasterone A (48 hours, 5μM) induction of wild-type or mutant α-synuclein expression exacerbated the reduction of $DiOC_{6(3)}$ median fluorescence intensity in response to 50nM rotenone. Statistical analyses (see section 2.12.) compared open versus solid bars, Kruskal-Wallis test, p=0.006. Post-hoc Dunn's Multiple Comparison Test revealed a

significant difference in WTsyn comparing before and after ponA *: p= 0.001; in MUTsyn this comparison almost reached statistical significance **: p=0.05. Values are expressed as mean ±SEM, pIND0, n=6; WTsyn, n=6 for each WT1-3 culture, total n=18; and MUTsyn, n=6 for each MUT1-3 culture, total n=18.

3.3.11. Oxidative stress

3.3.11.1. Effect of α-synuclein expression alone on levels of oxidative stress

Aconitase is an enzyme present in the mitochondrial matrix and also in the cytoplasm. Aconitase activity decreased following incubation with increasing concentrations of H_2O_2 whereas there was little change in citrate synthase activity (Figure 3.18). This confirmed that aconitase activity was a sensitive marker of oxidative stress (for methods see section 2.7.4.).

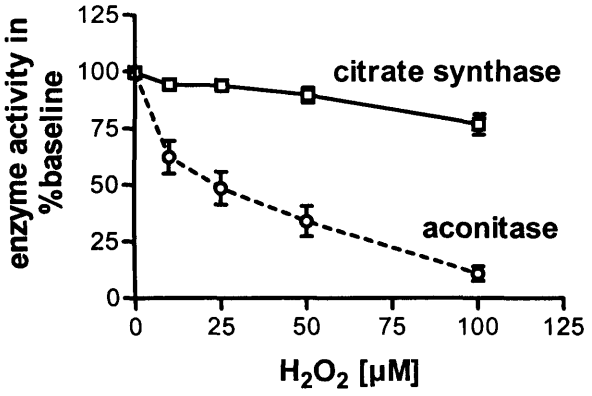

Figure 3.18. Effect of H_2O_2 on aconitase and citrate synthase activity in HEK293 cells. Activity of aconitase, or citrate synthase respectively, was assayed before the addition of H_2O_2 (10, 25, 50 and 100µM) in each sample (baseline). H_2O_2 was then added, the sample incubated for 5 minutes and the assay continued for a further 45 minutes. In each sample, the enzyme activity after H_2O_2 incubation was expressed in % of the respective baseline enzyme activity. There was little effect of H_2O_2 on citrate synthase activity whereas aconitase activity decreased with increasing concentrations of H_2O_2. Data is expressed as means of n=3, error bars are SDs.

Ponasterone A induction (5μM for 48 hours) had no significant effect upon aconitase activity in pIND0 cells (Figure 3.19). The results were similar in cells expressing wild-type α-synuclein or G209A mutant α-synuclein (Figure 3.19) implying that α-synuclein expression alone in these cells did not cause increased oxidative stress.

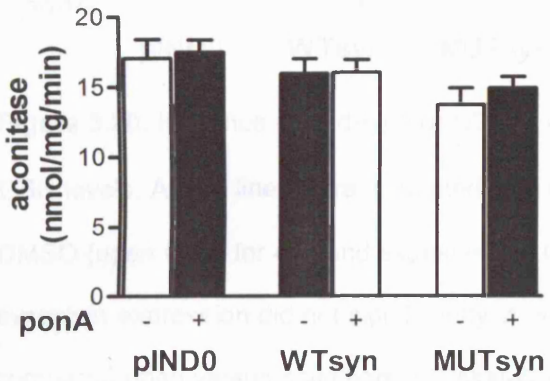

Figure 3.19. Influence of α-synuclein expression upon aconitase activity. All cell lines were incubated with ponasterone A (5μM, solid bars) or DMSO (open bars) for 48h and assessed for aconitase activity. Wild-type and mutant α-synuclein expression did not significantly affect aconitase activity. Statistical analysis compared open versus solid bars, Kruskal-Wallis test (see section 2.12.). Values are expressed as mean ± SEM; pIND0 n = 7, WTsyn and MUTsyn n=12.

Ponasterone A induction (5μM for 48 hours) had no significant effect on GSH levels in pIND0 cells (Figure 3.20; for methods see section 2.10.). In cells expressing wild-type or G209A mutant α-synuclein the results were similar to those in the pIND0 cells. This is consistent with the results obtained in the aconitase assays and suggests that the expression of either form of α-synuclein did not cause oxidative stress in these cells.

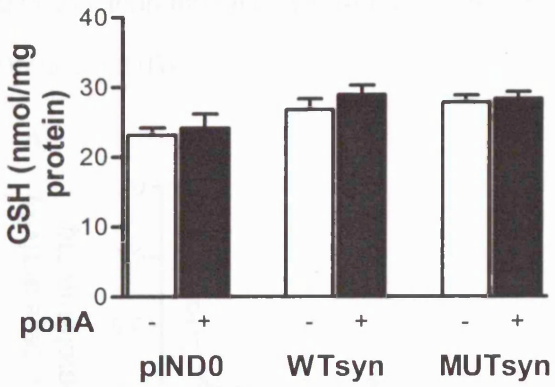

Figure 3.20. Influence of wild-type or G209A mutant α-synuclein expression upon GSH levels. All cell lines were incubated with ponasterone A (5μM, solid bars) or DMSO (open bars) for 48h and assessed for GSH levels. Wild-type and mutant α-synuclein expression did not significantly affect GSH levels. Statistical analysis compared open versus solid bars, Kruskal-Wallis test (see section 2.12.). Values are expressed as mean ± SEM; n=4.

3.3.11.2. Effect of α-synuclein upon vulnerability to oxidative stress

HEK293 cell cultures were exposed to the free radical generator paraquat. Incubation of HEK293 pIND0 cells with increasing concentrations of paraquat (0-500μM) over 24 hours had no discernible effect upon cell death or cell proliferation on microscopical evaluation. Consistent with increasing free radical generation it caused a dose dependent decrease in aconitase activity (Figure 3.21A). At a paraquat concentration of 75μM, aconitase activity was decreased by approximately 60%, and this was the concentration chosen for further experiments.

Incubation of pIND0 cells with ponasterone A (5μM) had no significant effect upon the paraquat-induced inhibition of aconitase activity (Figure 3.21B). However, in both WTsyn and the MUTsyn cell lines, ponasterone A induced α-synuclein expression partially protected the aconitase activity from paraquat (75μM) induced inactivation. The protection was greater in the WTsyn (40% increase in activity, p=

0.0001), than the MUTsyn expressing cell lines (25% increase in activity, $p<0.05$) (Figure 3.21B).

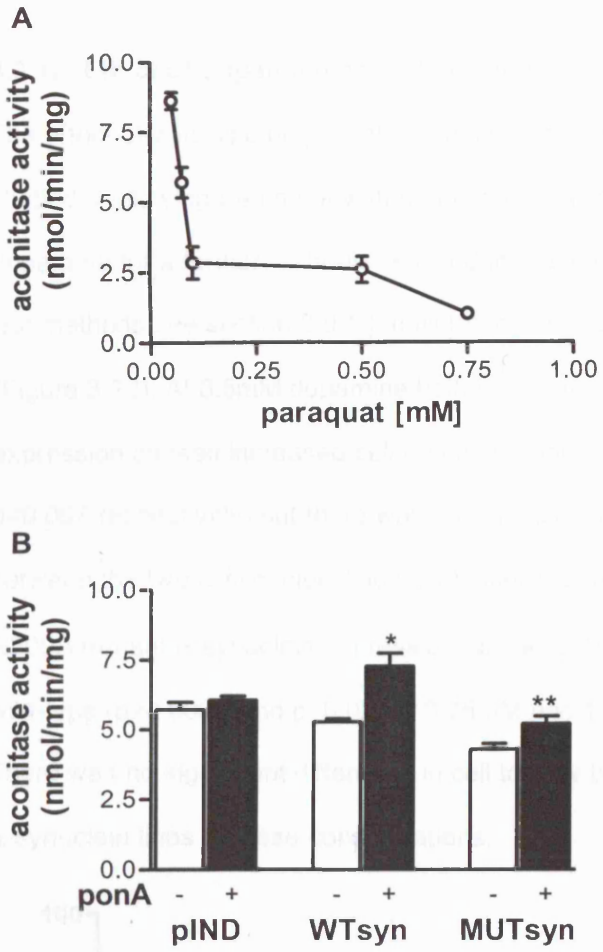

Figure 3.21. Effect of paraquat exposure on aconitase activity. **A.** Effect of exposure to increasing concentrations of paraquat for 24 h upon aconitase activity in pIND0 cells. Values are expressed as mean ± SEM (n=3). **B.** Effect of 5μM ponasterone A induction for 48h upon paraquat (0.075mM for 24h) induced aconitase inactivation in pIND0, WTsyn and MUTsyn cell lines. Wild-type and mutant α-synuclein expression partially protected aconitase activity from inactivation by paraquat (statistical analyses (see section 2.12.) compared open versus solid bars, Kruskal-Wallis test

p< 0.0001; post-hoc Dunn's Multiple Comparisons test *p=0.001; **p<0.05). Values are expressed as mean ±SEM, pIND0 (n=4), WTsyn and MUTsyn (n=9).

3.3.12. Effect of dopamine on cell viability

The effect of wild-type or mutant α-synuclein expression on dopamine toxicity was studied. Following treatment with ponasterone A (5μM) for 48 hours the addition of dopamine for a further 48 hours resulted in a dose dependent increase in cell death (for methods see section 2.9.1.) in all three cell lines, pIND0, WTsyn and MUTsyn (Figure 3.22). At 0.5mM dopamine both wild-type and G209A mutant α-synuclein expression caused increased cell death compared to pIND-zero lines (p=0.05 and p=0.007 respectively) but there was no significant difference in susceptibility between the two α-synuclein lines. At higher concentrations of dopamine, however, G209A mutant α-synuclein expression caused significantly greater cell death than wild-type (p=0.0003 and p=0.02 for 0.75mM and 1mM dopamine respectively). There was no significant difference in cell toxicity between pIND-zero and wild-type α-synuclein lines at these concentrations.

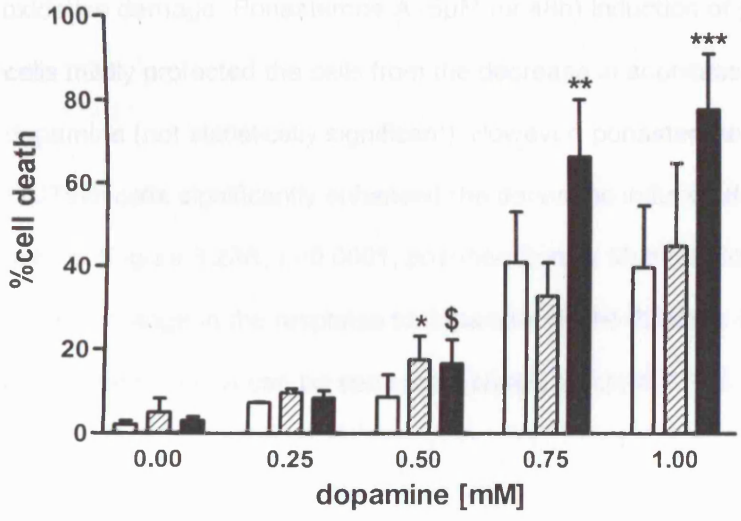

Figure 3.22. Effect of dopamine at increasing concentrations on cell death (determined using LDH assays, for methods see section 2.9.1.). Cell lines were

induced with 5μM ponasterone A for 48 hours and then treated with dopamine at the stated doses for a further 48 hours. Increasing concentrations of dopamine caused cell death in all cell lines (Kruskal-Wallis test, $p<0.001$, see section 2.12.). Dunn's post-hoc Multiple Comparison test revealed that at 0.5mM dopamine there was significantly more cell death in wild-type α-synuclein expressing cells (hatched bars, *p=0.05) and G209 mutant α-synuclein expressing cells (filled bars, $^{\$}p=0.007$) compared with pIND0 cells (open bars). At 0.75 and 1.0mM dopamine there was significantly more cell death in the MUTsyn cell line than in either the pIND0 or WTsyn lines (**p=0.0003 and ***p=0.02 respectively). Values are means ± SEM, n=5.

3.3.13. Effect of alpha-synuclein on oxidative stress caused by dopamine

Aconitase activity was determined to identify whether oxidative stress contributed to these increased levels of cell death due to dopamine. Without ponasterone A induction, exposure to dopamine (0.5mM) for 24h caused a significant decrease in aconitase activity in pIND0, WTsyn and MUTsyn (20.4%, 29.3% and 21.5% decrease respectively, $p<0.0001$, Kruskal-Wallis test, Figure 3.23A), consistent with oxidative damage. Ponasterone A (5μM for 48h) induction of pIND0 and WTsyn cells mildly protected the cells from the decrease in aconitase activity induced by dopamine (not statistically significant). However, ponasterone A induction of MUTsyn cells significantly enhanced the dopamine induced decrease in aconitase activity (Figure 3.23A, $p=0.0001$, post-hoc Dunn's Multiple Comparison test). The relative change in the response to dopamine by the different cell lines after induction with ponasterone A can be seen more clearly in figure 3.23B.

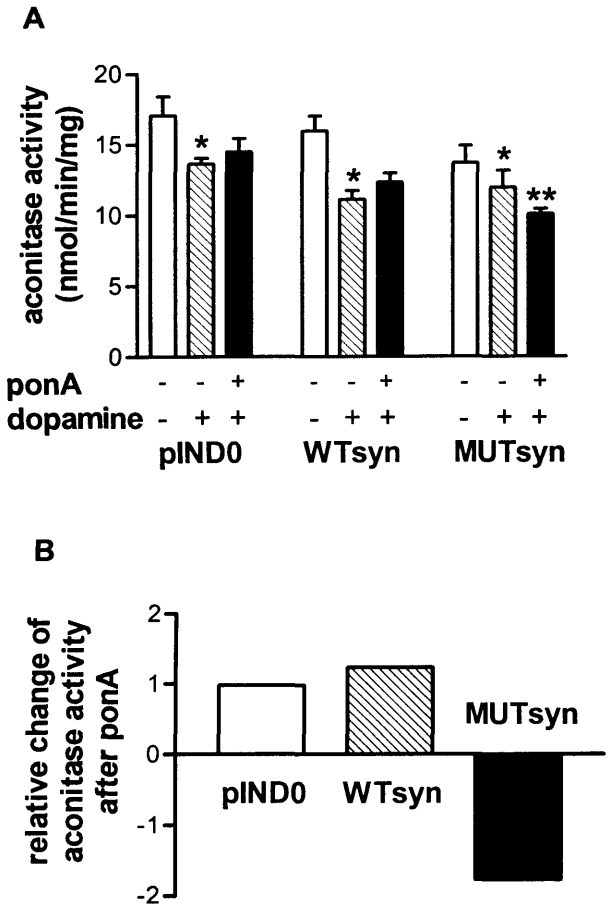

Figure 3.23. Influence of dopamine upon oxidative damage. **A.** In pIND0, WTsyn and MUTsyn HEK293 cell lines, aconitase activity was determined under normal growth conditions (open bars), and following exposure to dopamine alone (0.5mM, hatched bars) or dopamine exposure after ponasterone A (5μM) induction (solid bars). Dopamine caused significant aconitase inactivation (open bars versus hatched bars, * $p<0.0001$, Kruskal-Wallis test, see section 2.12.). Mutant α-synuclein expression enhanced dopamine induced aconitase inactivation (solid bar versus hatched bar, **$p=0.0001$, post-hoc Dunn's Multiple Comparison test). Values are expressed as mean ± SEM, n=6, 12 and 12 for pIND0, WTsyn and MUTsyn. **B.** From the data in A, in pIND0, WTsyn and MUTsyn cells, aconitase activities in the presence of dopamine (0.5mM) were subtracted from aconitase activities determined in the presence of dopamine (0.5mM) following ponasterone A (5μM for

48h) induction showing the change in aconitase activity more clearly.

3.3.14. Effect of dopamine compartmentalisation on dopamine induced oxidative stress

Preincubation with the vesicular monoamine transporter inhibitor reserpine (500nM) was used to investigate whether the increased oxidative damage was consistent with an abnormality of the vesicular uptake of dopamine in MUTsyn cells exposed to dopamine. Reserpine had no effect upon aconitase activity on its own (data not shown); however, the dopamine-induced inactivation of aconitase activity was significantly enhanced in the pIND0 (52.3% greater inhibition, $p<0.001$) cells following reserpine pre-treatment (Figure 3.24). This is consistent with reserpine inducing increased cytoplasmic dopamine concentrations resulting in increased free radical damage in pIND0. However, in the MUTsyn expressing cells the inhibition in aconitase activity was only enhanced by 20.6% ($p<0.05$) relative to the inhibition seen in the absence of reserpine (Figure 3.24). This diminished effect of reserpine in MUTsyn expressing cells is consistent with the suggestion that MUTsyn is acting in a similar way to reserpine.

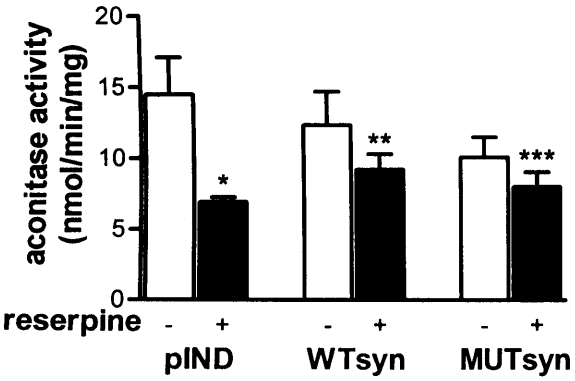

Figure 3.24. Dopamine compartmentalisation and aconitase activity. Influence of reserpine pre-treatment upon dopamine (0.5mM) induced aconitase inactivation in ponasterone A induced cells (open versus solid bars, $p<0.0001$, Kruskal-Wallis test,

see section 2.12.). Post-hoc analysis (Dunn's Multiple Comparison Test) shows that reserpine lead to significant aconitase inactivation in pIND0 cells (*p<0.001), and WTsyn cells (**p<0.01) while in MUTsyn cells the difference was less significant (**p<0.05). Values are expressed as means ± SD (n=4 for pIND0, n=12 for WTsyn and MUTsyn cells respectively).

3.3.15. Effect of α-synuclein on dopamine uptake

Catecholamine fluorescence (for methods see section 2.5.5.) revealed punctate cytoplasmic staining (Figure 3.25A) which increased in intensity following exposure to 0.5mM dopamine for 24 hours (Figure 3.25B).

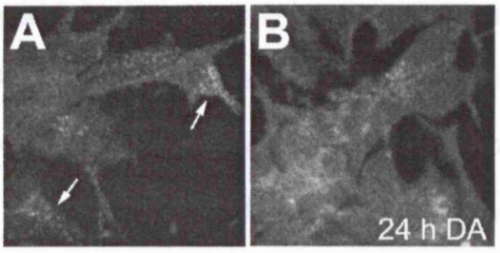

Figure 3.25. Catecholamine stain in HEK293 cells. Glyoxylic acid catecholamine fluorescence in normal HEK293 cells (A) and cells exposed to 0.5mM dopamine for 24 hours (B).

The uptake of radioactively labelled dopamine was investigated in collaboration with Dr K Messmer and Dr P Korlipara, Department of Clinical Neurosciences, RFH and University College London School of Medicine (for methods see section 2.11.). This showed that there was a time dependant uptake of ^{3}H-dopamine in HEK293 cells (Figure 3.26).

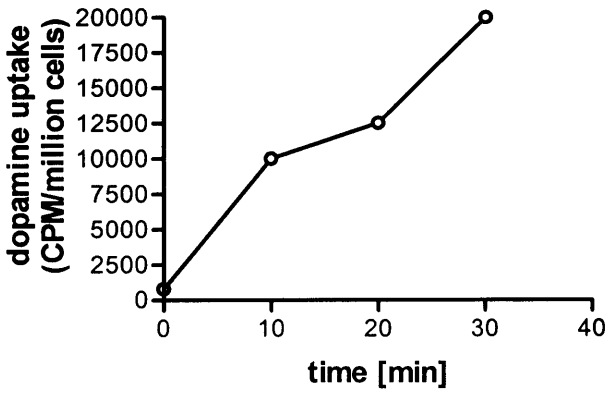

Figure 3.26. ^{3}H dopamine uptake in HEK293 cells. Uptake analysis of ^{3}H dopamine demonstrated a time dependent increase in cellular accumulation of ^{3}H dopamine.

The effect of wild-type or G209A mutant α-synuclein expression on ^{3}H dopamine uptake was examined in collaboration with Dr JM Cooper, Department of Clinical Neurosciences, RFH+UCL Medical School. Following induction with 5μM ponasterone A for 48 hours the mean ^{3}H dopamine uptake in wild-type or G209A mutant α-synuclein expressing cells was not statistically different compared with the respective values in the absence of ponasterone A (Figure 3.27). Ponasterone A had no influence on ^{3}H dopamine uptake in pIND0 cells (Figure 3.27).

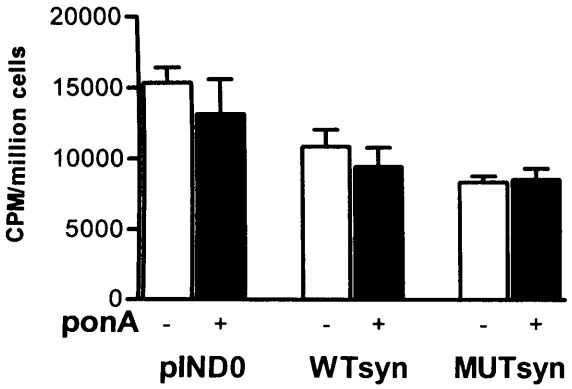

Figure 3.27. Expression of α-synuclein on ^{3}H dopamine uptake in HEK293 cells. The influence of ponasterone A induction upon ^{3}H dopamine uptake in pIND0, WTsyn and MUTsyn cells after 30 minutes. There was no significant effect of either

wild-type or G209A mutant α-synuclein on ^{3}H dopamine uptake (open versus solid bars, Kruskal-Wallis test, see section 2.12.). Values are expressed as mean ±SEM, n=4.

3.4. Discussion

3.4.1. Dopaminergic properties of neuronal (SH-SY5Y and hNT2) and EcR293 cells

Parkinson's disease (PD) is characterised by the selective loss of neurones of the nigro-striatal dopaminergic system, which suggests that pathogenetic events relating to the dopamine (DA) system are relevant for PD pathogenesis. Thus, the cell line used for the establishment of the cell culture model should ideally have properties similar to those of the substantia nigra.

Substantia nigra neurones, but also cells in other organs such as the adrenal gland, synthesise DA using tyrosine hydroxylase (TH). Vesicular monoamine transporters (VMAT) then actively transport dopamine into specialised monoaminergic storage vesicles. Neuronal cells predominantly express VMAT-2 whereas non-neuronal cells predominantly express VMAT-1. Substantia nigra neurones are known to be TH positive, synthesizing dopamine, and express DAT in pre-synaptic terminals to facilitate re-uptake of extracellular dopamine (Reith et al., 1997). PD was found to coincide with a loss of DAT and VMAT-2 positive cells in the substantia nigra indicating the presence of VMAT-2 positive storage vesicles (Harrington et al., 1996; Hirsch et al., 1988; Lehericy et al., 1994). Thus, key features of substantia nigra neurones are the facility to synthesise, store and release dopamine using TH and VMAT-2 positive vesicles, respectively, as well as the capacity for re-uptake of released dopamine through DAT.

In the first part of this work, the dopaminergic properties of the neuronal cell lines NT2 and SH-SY5Y (differentiated and undifferentiated), and human embryonic kidney cells (HEK293), were characterised using immunocytochemistry and Western blot. In light of the key features of substantia nigra neurones cell lines were characterised using antibodies against TH, VMAT-1 and 2, and DAT. Although the antibodies used for Western blot analysis did not give bands of the expected sizes, the antibodies were suitable for immunocytochemistry.

HNT2 neuroblastoma cells immunoreacted with antibodies against tyrosine hydroxylase and VMAT-1 and 2 suggesting they can synthesise and store catecholamines. However, no immunostaining was observed with the DAT antibody. This is consistent with a previous report showing tyrosine hydroxylase expression in hNT2 cells immunocytochemically (Zigova et al., 1999); interestingly, in that study tyrosine hydroxylase expression was upregulated in hNT2 cells following treatment with lithium. A mixture of VMAT-1 and 2 expression in hNT2 cells may indicate that these cells had a mixed peripheral (VMAT-1) and central nervous system (VMAT-2) phenotype. HNT2 cells were only assessed in the undifferentiated state. It is possible that following full differentiation into post-mitotic neurones they might adopt a more central nervous system phenotype with respect to VMAT expression.

SH-SH5Y neuroblastoma cells in the undifferentiated state also immunostained for tyrosine hydroxylase, VMAT-1 and VMAT-2 suggesting that, similar to hNT2 cells, they were capable of catecholamine synthesis and storage. These results are consistent with TH enzyme activity measurements in SH-SY5Y cells (Ross et al., 1983), immonoblotting in SH-SY5Y cells (Chen et al., 1998), as well as immunocytochemical evidence for tyrosine hydroxylase expression in SH-SY5Y (Presgraves et al., 2004). Similar to hNT2 cells, in SH-SY5Y cells a mixture of VMAT-1 and VMAT-2 expression could indicate that these cells had properties of both peripheral neurones and central nervous system neurones. However, SH-

SY5Y cells did not have immunostaining with the DAT antibody. This is in accord with absent DAT gene expression reported in a previous study in SH-SY5Y cells (Lode et al., 1995).

Differentiated SH-SY5Y cells resembled undifferentiated SH-SY5Y cells. Tyrosine hydroxylase staining was observed in both differentiated (neurofilament positive) and undifferentiated cells. This may indicate that qualitatively the expression of tyrosine hydroxylase expression did not depend on cell differentiation so that the staining pattern was similar in differentiated and undifferentiated cells. With immunocytochemistry it was not possible to assess whether quantitatively tyrosine hydroxylase expression changes depending on the state of differentiation. Differentiated SH-SY5Y cells did not express DAT. However, SH-SY5Y cells were shown to take up ^{3}H-dopamine suggesting that dopamine enters these cells by different mechanisms (P Korlipara, personal communication). This is in agreement with the presence of the noradrenaline-uptake transporter, which also transports dopamine (Pacholczyk et al., 1991).

Immunocytochemically, HEK293 cells expressed TH indicating they are able to synthesise dopamine, and VMAT-1 indicating that they can store catecholamines. In addition, HEK293 cells were able to take up ^{3}H-dopamine but did not have immunostaining for DAT. These results are consistent with reports showing that proximal tubules in the kidney can synthesize dopamine (Goldstein et al., 1972), and it is well-established hat dopamine has a substantial influence on renal function, e.g. sodium excretion (Hussain and Lokhandwala, 1998). HEK293 cells were described to synthesise and store dopamine (Eshleman et al., 1997). Previous studies have also shown that HEK293 cells accumulated dopamine and MPP^{+} (Grundemann et al., 1998; Okada et al., 1998), and were sensitive to dopamine (Luo and Roth, 2000). While HEK293 cells do not express the dopamine or noradrenalin transporters (DAT or NAT, Burton et al., 1998), it has been shown that other

transporters transport dopamine including the organic cation transporter (Grundemann et al., 1998). This is in accord with reports that relatively high concentrations of DA were needed to have a toxic effect on HEK293 cells (Okada et al., 1998) as well as relative resistance to MPP+ in HEK293 cells (Storch et al., 1999) with enhancement of DA or MPP+ toxicity after transfection of DAT (Wersinger and Sidhu, 2003).

Taken together these results indicate that HEK293, SH-SY5Y and hNT2 cells had dopaminergic features. While HEK293 cells expressed the phenotype of peripheral dopaminergic cells, SH-SY5Y and hNT2 cells exhibited a mixture of peripheral/central nervous system characteristics. This mirrored the properties of substantia nigra neurons apart from the expression of DAT. Thus, SH-SY5Y cells are possibly superior to the other cell lines as they are neuronal, can be differentiated easily and have been shown to express the noradrenaline-uptake transporter, which also transports dopamine (Pacholczyk et al., 1991). Since hNT2 cells are also neuronal and can be differentiated, hNT2 and SH-SY5Y cell lines might be the most suitable cell lines of these three cell lines for the generation of cell culture models for Parkinson's disease.

However, while HEK293 cells are not dopaminergic neurones, they expressed tyrosine hydroxylase, VMAT1 positive vesicles and catecholamines, and showed dopamine uptake. There is evidence to suggest that HEK293 cells may have originated form a neuronal lineage within kidney epithelium (Graham et al., 1977; Shaw et al., 2002). HEK293 cells were derived originally by transformation with adenovirus DNA, a virus that is highly neurotropic. There is evidence showing that HEK293 cells have neuronal properties (http://www.mbi.ufl.edu/~shaw/293.html); e.g., immunohistochemistry and immunoblotting revealed positive staining for neurofilaments, an intermediate

filament of neurones (Shaw et al., 2002). This indicates that HEK293 cells are a suitable model for α-synuclein over expression.

3.4.2. The stable and inducible HEK293 cell model for α-synuclein PD

The model described in this thesis chapter is a stable and inducible model for wild-type or G209A mutant α-synuclein expression in HEK293 cells. It utilised the Ecdysone-Inducible Mammalian Expression System, which has been described in detail in section 2.4.1.. Mammalian cells are not normally responsive to the inducing agent ponasterone A, an analogue of the insect hormone ecdysone, and do not contain the ecdysone receptor. Therefore, basal levels of transcription are very low or absent altogether. Disadvantages of this system include the amount of time needed to generate a cell model de novo since it requires the successive transfection of two plasmids (pVgRxR and pIND) and screening and isolation of clones that are expressing as has been the case in the neuronal cell lines described in this thesis chapter. Furthermore, while the SH-SY5Y or hNT-2 cell lines would have been suitable cell lines to establish a α-synuclein cell culture model using the Ecdysone-Inducible Mammalian Expression System was not successful in these cells. This problem was overcome to some degree in that Invitrogen offers a cell line (EcR293) of HEK293 cells successfully transfected with pVgRxR plasmid.

α-synuclein immunocytochemistry and Western blot documented that there were only very low endogenous levels of α-synuclein in the pIND.α-syn or pIND.α-syn/G209A transfected cells in the absence of ponasterone A (Fig. 1A) and likewise no or only weak expression in the pIND.zero cells. The detection of the HA tag distinguished between endogenous α-synuclein and ponasterone A induced expression of the α-synuclein constructs. In the absence of ponasterone A there was no HA signal indicating that the background expression of pIND.α-syn and

pIND.α-syn/G209A cells reflected endogenous α-synuclein expression and was not due to leakage of the introduced gene constructs.

The level of α-synuclein expression (wild-type or G209A mutant) was proportional to the concentration of ponasterone A used with the inducible cell lines. Thus the production of α-synuclein protein by these cell lines was tightly controlled by ponasterone A. Levels of α-synuclein expression from the constructs were higher at all concentrations of ponasterone A compared with expression levels of endogenous α-synuclein. This indicated that any effects of α-synuclein expression from following ponasterone A induction were most likely due to construct expression alone and less likely caused by an interaction between endogenous and ponasterone A induced α-synuclein. Immunocytochemical analysis suggested that the increase in α-synuclein/HA levels on Western blot may be due to a greater number of cells expressing with increasing concentrations of ponasterone A while the intensity of staining in individual expressing cells was similar irrespective of ponasterone A concentration. This could indicate that there was a threshold for expression in each individual cell and that variation of the ponasterone A concentration above this threshold, once the cell had been 'switched on', resulted in similar levels of expression.

Taken together, the HEK293 α-synuclein model described in this thesis chapter has a number of advantages. Expression of wild-type or G209A mutant α-synuclein was stable and inducible with good control over the levels of protein expressed and no expression in the absence of the inducing agent ponasterone A. In addition, in contrast to constitutive cell models this inducible model made it possible to assess the effect of α-synuclein expression against the same cellular background in the absence of expression. This helped to remove the inherent cell-to-cell variability, which can make interpretation difficult in constitutive models. In

addition, models with constitutive expression can lead to a selection of cell populations that have adapted to the expressed protein, a problem that does not occur with this inducible model. A weakness of the model is the cell line HEK293 in that it is not a neuronal dopaminergic cell line. However, the cell line exhibited features similar to those of dopaminergic neurones in the substantia nigra; the cells were able to express tyrosine hydroxylase indicating catecholamine production, they expressed VMAT-1 as evidence for the presence of catecholamine storage vesicles, and there was clear evidence of dopamine uptake. Hence HEK293 cells are a suitable cell line with which to investigate PD, a disease that relatively selectively affects dopaminergic neurones. A drawback of the cell line is that HEK293 cells cannot be differentiated into post-mitotic neurones. Thus aspects of PD that pertain to e.g. neurites cannot be easily addressed with this model. In addition, experiments addressing long-term consequences of α-synuclein expression are difficult because the cells continue to divide so that one cannot assess the consequences of prolonged exposure to the expressed protein in individual cells.

3.4.3. Subcellular localisation of wild-type and G209A mutant α-synuclein

There is evidence to suggest that α-synuclein is localised in nerve terminals near synaptic vesicles (see section 3.1.9.5.3.). Immunocytochemistry in HEK293 cells expressing either wild-type or G209A mutant α-synuclein showed co-localisation of α-synuclein with vesicle associated membrane protein (VAMP). This indicated that the localisation of α-synuclein in these cell models was similar to that observed in human cortex (Irizarry et al., 1996) and in primary rat hippocampal neurones (Murphy et al., 2000). Staining with an antibody to vesicle associated membrane transporter (VMAT) a marker for catecholaminergic vesicles revealed partial co-localisation with wild-type or G209A mutant α-synuclein in the HEK293 cells. This suggested that at least some of the α-synuclein might be associated with these

vesicles, and it also indicates that in the HEK293 model there was no difference between wild-type and G209A mutant α-synuclein.

The role of α-synuclein for synaptic vesicles in nerve terminals is not clear. Studies in α-synuclein knock-out mice indicated that α-synuclein is not essential for neuronal function but that its function might be more subtle, e.g. in regulating vesicle function and transmitter release including dopamine (Abeliovich et al., 2000; Lotharius and Brundin, 2002), the regulation of vesicular transport (Jenco et al., 1998) within axons (Jensen et al., 1998; Saha et al., 2004) or the size of the vesicular pool (Murphy et al., 2000).

There was no association of α-synuclein with other organelles such as mitochondria, lysosomes, Golgi-network or the nucleus. This was in accord with the association of α-synuclein with vesicles as discussed above and did not indicate that α-synuclein was involved directly with other organelles. Immunocytochemistry revealed two different types (aggregate-like and diffuse) of staining for both wild-type or G209A mutant α-synuclein and neither form of α-synuclein co-localised with ubiquitin. Why there were different α-synuclein staining patterns was not clear. It is possible that the aggregate-like staining reflected the presence of α-synuclein in the vesicular population rather than true Lewy-body like aggregates. This would be in keeping with the absence of ubiquitination. In other cell culture models (non-differentiated SH-SY5Y (Lee et al., 2004), HEK293 (Tanaka et al., 2004), or PC-12 cells (Stefanis et al., 2001) wild-type α-synuclein over-expression did not always lead to aggregate formation or impairment of the UPS (for a summary of different cell culture models and results see appendix 2). However, 'aggregate-like' immunostaining was found in mouse hypothalamic GT1-7 cells (Hsu et al., 2000) and wild-type α-synuclein over-expression promoted inclusion formation in BE-M17 neuroblastoma cells (Ostrerova-Golts et al., 2000), COS-7 (monkey kidney) cells

and differentiated SH-SY5Y cells (Lee et al., 2004). Over-expression of either mutant form of α-synuclein enhanced inclusion formation in In SH-SY5Y neuroblastoma cells (Ostrerova-Golts et al., 2000), or was associated with impaired function of the UPS and apoptosis in PC-12 cells (Stefanis et al., 2001; Tanaka et al., 2001). The differences between the cell culture models could be due to the different cell lines used, or the expression systems (see appendix 2). In particular the level of protein expression may be much higher with constitutive expression compared with the inducible Ecdysone System. This may be relevant to the functional capacity of the UPS, so that some UPS impairment could be non-specific.

3.4.4. α-synuclein expression in HEK-293 cells had no effect on mitochondrial function

The data presented in this thesis chapter and in other *in vitro* models examined the relationship of wild-type or mutant α-synuclein over-expression. Over-expression of wild-type α-synuclein was associated with PD in a family with α-synuclein gene triplication (Singleton et al., 2003). However, in sporadic PD mitochondrial dysfunction, in particular complex I, may precede α-synuclein accumulation and aggregation (Kowall et al., 2000; Manning-Bog et al., 2002; Sherer et al., 2002; Sherer et al., 2003)(see appendix 2). It is not known if in patients with α-synuclein mutations mitochondrial respiratory chain function is affected.

There was no evidence that wild-type or G209A mutant α-synuclein expression affected mitochondrial function as measured by either respiratory chain enzyme activities in isolated mitochondria or mitochondrial membrane potential in live cells. This is in agreement with the observations in PC-12 cells where mitochondrial membrane potential was unaffected by the expression of either wild-type or G88C mutant α-synuclein (Tanaka et al., 2001). It conflicts with a report of decreased MTT activity in murine hypothalamic cells constitutively over-expressing

wild-type α-synuclein (Hsu et al., 2000)(see appendix 2). However, MTT activity has been reported to be relatively non-specific, and in the absence of confirmatory data, a less reliable marker of respiratory chain activity (Berridge and Tan, 1993). The data suggest that expression of either wild-type or mutant α-synuclein does not interfere directly with mitochondrial function. This is in accord with the immunocytochemical data showing no direct association between α-synuclein and mitochondria at the cellular level (Tabrizi et al., 2000a). However, it is not possible to exclude mitochondrial dysfunction induced by α-synuclein over prolonged periods of time, or as a secondary or cell specific effect. The HEK293 cells did exhibit dopaminergic characteristics, but the analysis of post-mitotic cells, which resemble dopaminergic neurones more closely, would help address these questions.

There is strong evidence for a role of a complex I defect in PD (see section 3.1.5.). This is supported by the observation that α-synuclein knock-out mice were resistant to the selective complex I inhibitor MPTP (Dauer et al., 2002), and by the recent identification of a mutation in a putative mitochondrial protein called PTEN-induced kinase (PINK 1) in a family with PD (Valente et al., 2004). Thus it is conceivable that a complex I defect is responsible for the generation of oxidative stress, which subsequently leads to α-synuclein aggregation and the loss of dopaminergic neurones. However, it is not likely that wild-type or mutant α-synuclein cause a defect of the mitochondrial respiratory chain.

3.4.5. α-synuclein expression in HEK-293 cells enhanced the mitochondrial sensitivity to Rotenone

Rotenone, a selective inhibitor of complex I of the mitochondrial respiratory chain, has been implicated as an environmental toxin that could be relevant to the pathogenesis of PD (see section 3.1.5.3.), and it has been used to generate animal models of PD (see section 3.1.6.). Short-term rotenone exposure induced a

decrease in mitochondrial membrane potential, as predicted for a respiratory chain inhibitor. This was potentiated by wild-type α-synuclein expression and, to a lesser degree by mutant α-synuclein expression suggesting that both enhance the sensitivity of the mitochondrial membrane potential to inhibition of the respiratory chain. While this did not significantly induce cell death over the short term, it might lead to decreased viability with prolonged exposure as previously reported (Lehmensiek et al., 2002)(see appendix 2). Although the data obtained with cell models can only be extrapolated with caution to the situation in the natural disease state, these data emphasise the power of inducible models in that this model revealed relatively small differences in sensitivity to rotenone of α-synuclein expressing cells.

The results suggest that increased wild type or mutant α-synuclein expression promoted the sensitisation of dopaminergic neurones to exogenous mitochondrial toxins such as rotenone which may have led to cell damage and death. This raises the question of how α-synuclein enhanced the rotenone dependent decrease in mitochondrial membrane potential and why expression of the wild-type protein rendered these cells more vulnerable than the mutant protein. Immunocytochemical analysis did not provide evidence that α-synuclein is associated with complex I, and therefore the influence of α-synuclein upon the rotenone induced decrease in mitochondrial membrane potential is likely to be indirect. Rotenone is known to increase oxidative stress, α-synuclein aggregation and apoptosis (Sherer et al., 2002)(see appendix 2). Therefore it is possible that the increased expression of wild type and to a lesser degree mutant α-synuclein potentiated these effects leading to a greater fall in mitochondrial membrane potential. In support of this suggestion the absence of α-synuclein in knockout mice resulted in a decrease in MPP+ induced cell death (Dauer et al., 2002). This

suggests that expression of α-synuclein was necessary so that this selective complex I inhibitor could become toxic indicating an interaction of α-synuclein and MPP+.

These findings lend support to the hypothesis that mitochondrial dysfunction and α-synuclein toxicity are reciprocal. Previous observations suggested that respiratory chain dysfunction leads to α-synuclein accumulation and aggregation (Kowall et al., 2000; Manning-Bog et al., 2002; Sherer et al., 2002; Sherer et al., 2003), and we have demonstrated that α-synuclein expression, both wild-type and G209A mutant, potentiated the toxicity of respiratory chain inhibitors. This latter effect was more pronounced with wild type α-synuclein expression and may be a contributory factor in sporadic PD, whereas abnormal dopamine handling may be more important for mutant α-synuclein pathology.

3.4.6. Effect of α-synuclein expression alone on oxidative stress

Considerable evidence suggests the involvement of free radicals in the pathogenesis of PD (Olanow and Tatton, 1999). Oxidative stress may promote α-synuclein aggregation and oxidative damage to α-synuclein (Giasson et al., 2000; Ischiropoulos and Beckman, 2003). It remains unknown, however, how exactly free radicals are involved and whether free radical generation is a feature of the familial forms of the disease. In the inducible cell models used in this thesis chapter, wild-type or mutant G209A α-synuclein expression did not affect GSH levels or aconitase activity, two reliable markers of oxidative stress (Gardner et al., 1994; Hausladen and Fridovich, 1994; Patel et al., 1996). This is in accord with over-expression of wild-type α-synuclein in stably transfected SH-SY5Y neuroblastoma cells, which had no effect on aconitase activity (Kalivendi et al., 2004) or the exposure to H_2O_2 (Kanda et al., 2000), and it protected SK-NM-C neuronal cells against the effects of

serum deprivation or H_2O_2 (Lee et al., 2001c). The results differ from those in mouse hypothalamic GT1-7 cells constitutively over-expressing wild-type α-synuclein where increased oxidative stress was indicated by qualitatively enhanced oxidation of 2',7'-dichlorofluorescein and increased glutathione levels (Hsu et al., 2000)(see appendix 2). It is not known whether these differences reflect cell specific differences or indeed differences in protein expression levels. With constitutive expression protein expression levels tend to be generally higher, and cells are exposed to the expressed protein for longer periods than in the inducible model reported in this thesis chapter.

If using increased wild-type or mutant α-synuclein expression as a model of idiopathic PD then the lack of oxidative stress contrasts with what is found in patients with idiopathic PD (see section 3.1.7.1.). This therefore suggests that increased α-synuclein expression alone did not cause oxidative stress. The data from the α-synuclein HEK293 cell culture model presented in this thesis chapter would therefore predict that in the family with α-synuclein over-expression as a result of genomic triplication of the α-synuclein gene (Singleton et al., 2003) oxidative stress is not a primary event in the pathogenesis.

3.4.7. α-synuclein expression protected against paraquat toxicity

α-synuclein expression did not increase oxidative stress. However, α-synuclein could increase the susceptibility to free radicals. Evidence from epidemiological studies suggests that environmental toxins such as pesticides could be involved in the pathogenesis of PD (see section 3.1.4.). Paraquat (1,1'-dimethyl-4,4'-5 bipyridinium) is a common herbicide and rotenone is a widely used insecticide and fish poison. The systemic administration of rotenone or paraquat to rodents was associated with the development of α-synuclein aggregation (Betarbet et al., 2000; Manning-Bog et al., 2002).

In normal HEK293 cells paraquat incubation caused a dose dependant decrease in aconitase activity. This was consistent with paraquat induced oxidative stress within cells where it generates superoxide promoted by the mitochondrial NAD(P)H -quinone oxidoreductase (Shimada et al., 1998). This can lead to damage to the cell and in particular the mitochondria (Hirai et al., 1992). In the α-synuclein HEK293 cell model expression of wild-type α-synuclein partially protected the aconitase activity from inhibition by paraquat generated superoxide production. This indicates that this increase of antioxidant protection may be a consequence of wild-type α-synuclein expression. It is possible that α-synuclein itself has antioxidant properties; alternatively it may have induced the cell to increase its own antioxidant defences. This is in accord with elevated GSH levels reported with wild-type α-synuclein expression (Hsu et al., 2000)(see appendix 2). Elevated GSH levels were not seen in the HEK293 α-synuclein model. However, this does not exclude changes in other antioxidants. The protective effect of α-synuclein expression against paraquat induced oxidative stress was also observed with mutant α-synuclein expression. However, compared to wild-type α-synuclein it was less pronounced. This implies that G209A mutant α-synuclein either had an impaired antioxidant role or did not induce the cellular defences as much as the wild-type form. A loss of anti-oxidant action of α-synuclein conferred by the G209A mutation is in agreement with other studies using SH-SY5Y neuroblastoma cells; cells constitutively over-expressing mutant α-synuclein were more vulnerable to free radical damage induced by H_2O_2 (Kanda et al., 2000) or menadione (Ko et al., 2000)(see appendix 2).

3.4.8. α-synuclein expression in HEK-293 cells increased dopamine mediated toxicity

In HEK293 cells dopamine clearly caused cell death at concentrations above 0.25mM. At concentrations of ≥0.5mM the expression of G209A mutant α-synuclein enhanced dopamine mediated cell death compared to no expression or the expression of wild-type α-synuclein. Dopamine induced cell death has been confirmed in a number of systems (Alexander et al., 1997; Lai and Yu, 1997; Ziv et al., 1994), and increased susceptibility of α-synuclein, both wild-type and G88C or G209A mutant, expressing SH-SY5Y cells has also been reported (Junn and Mouradian, 2002). The concentrations of dopamine used in these experiments are similar to those reported in the cell bodies of dopaminergic neurones (Jonsson, 1971). At present the mechanisms by which G209A mutant α-synuclein increases dopamine toxicity are not known. α-synuclein is highly expressed in human brain presynaptic terminals (Irizarry et al., 1996), in rat substantia nigra pars compacta (Kholodilov et al., 1999) and is also a major component in the Lewy bodies of dopamine containing neurones in PD brains (Spillantini et al., 1997). Thus α-synuclein is expressed at sites of high dopamine content and it may function to modulate dopamine release (Abeliovich et al., 2000).

It was also clear that dopamine caused oxidative stress in HEK293 cells, and this was exacerbated by the expression of G209A mutant α-synuclein but unchanged by wild-type α-synuclein expression. Consequently the increase in cell death following dopamine exposure in mutant α-synuclein expressing cells may be explained by an increase in free radical damage presumably via dopamine metabolism. Dopamine is unstable and is readily oxidised to the dopamine quinone and generates superoxide and hydrogen peroxide. Dopamine can also co-valently modify free cysteine, cysteine in glutathione and cysteinyl residues in protein

(LaVoie and Hastings, 1999). Sulphydryl groups on cysteines are often associated with active sites on proteins and thus their modification could alter function irreversibly. Interestingly, the formation of S-cysteinyl dopamine is associated with the loss of monoaminergic striatal terminals in dopamine-induced toxicity (Hastings et al., 1996). Thus dopamine toxicity may be mediated via increased reactive oxygen species generation and by direct protein modification. It is not likely that the enhanced sensitivity is due to a greater vulnerability of G209A mutant α-synuclein expressing cells to the free radicals per se because G209A mutant α-synuclein partially protected the cells from the oxidative stress induced by paraquat. Hence, it is possible that mutant α-synuclein expression itself may cause the cells to generate more free radicals in the presence of dopamine.

α-synuclein may influence the uptake of dopamine. If a mutation of α-synuclein increased the uptake of dopamine this could elevate the cytoplasmic concentration of dopamine. However, no change in uptake of ^{3}H-dopamine was observed in the HEK293 α-synuclein cell model irrespective of whether the cells expressed wild-type of G209A mutant α-synuclein. Hence, any effect of the G209A mutation on dopamine uptake is not a likely explanation for the increased levels of dopamine induced oxidative stress that was observed in this model.

Mutant α-synuclein may lead to a decrease in dopaminergic vesicles as reported in a model of α-synuclein down regulation (Murphy et al., 2000). Alternatively mutant α-synuclein may prevent the normal compartmentalisation of dopamine into vesicles, thus elevating cytoplasmic dopamine concentrations. In the HEK293 α-synuclein cell model immunocytochemical analysis revealed co-localisation of α-synuclein, both wild-type and G209A mutant, with a marker for vesicles, and at least partial co-localisation with VMAT-1, a marker for catecholaminergic vesicles. This provides evidence for a spatial relationship of α-

synuclein with the catecholaminergic vesicular compartment. The toxicity of dopamine may be increased by failure of dopamine compartmentalisation within vesicles (Figure 3.3). The damaging effects of dopamine would therefore be enhanced if mutant α-synuclein interfered with the function of the vesicular monoamine transporter, thereby increasing intra-cytoplasmic dopamine concentrations and the potential for cell damage sufficient to cause cell death. The use of reserpine mimicked a situation in which the vesicular uptake of dopamine was inhibited (Parti et al., 1987). Consistent with the dopamine-induced changes in the mutant α-synuclein expressing cells, reserpine enhanced the dopamine induced decrease in aconitase activity. Consistent with a report in human mesencephalic cells (Lotharius and Brundin, 2002) this data lend further support to the hypothesis that α-synuclein is involved in the regulation of vesicular dopamine handling. A defect of dopamine compartmentalisation may increase cytoplasmic dopamine concentrations resulting in the gradual accumulation of superoxide radicals and auto-oxidation products (Lotharius and Brundin, 2002). This may promote α-synuclein aggregation and Lewy body formation leading to a slow but progressive loss of striatal terminals and nigral neurones. The over-expression of wild-type α-synuclein might lead to a similar effect, but over a longer period — such as seen in the human wild-type α-synuclein transgenic mice described above (Masliah et al., 2000).

Free radicals generated from dopamine metabolism in dopaminergic neurones may specifically contribute to α-synuclein aggregation and Lewy body formation and help to explain their relative selective loss in PD (Giasson et al., 2000; Paxinou et al., 2001). Indeed there is recent evidence that dopamine may influence α-synuclein toxicity by forming oxidative adducts with α-synuclein preventing the conversion of the toxic protofibrils to inert fibrils which are found in Lewy bodies (Conway et al., 2001). In addition, accumulation of soluble α-synuclein protein

complexes has been shown to result in apoptosis mediated by free radicals selectively in cultured human dopaminergic neurones (Xu et al., 2002). Further evidence linking α-synuclein and dopamine was revealed by the interaction of α-synuclein expression and tyrosine hydroxylase activity which may indicate a regulatory role of α-synuclein in dopamine synthesis (Perez et al., 2002). The data in the HEK293 α-synuclein models add to the accumulating evidence for an interaction between α-synuclein and dopamine, which may be important in the pathophysiology underlying the relatively selective neuronal death seen in Parkinson's disease.

3.5. Conclusion

Models were established in human embryonic kidney cells with inducible expression of increased wild-type α-synuclein expression (to model sporadic PD) and increased mutant G209A α-synuclein to model a familial form of Parkinson's disease. Both wild-type and mutant α-synuclein were localised to vesicles, some of which were catecholaminergic. Over-expression of wild-type or mutant (G209A) α-synuclein alone did not reduce cell viability, cause oxidative stress or impair mitochondrial function. However, mutant α-synuclein expression enhanced the susceptibility to dopamine toxicity causing increased oxidative stress and cell death. This effect was similar to that of reserpine, an inhibitor of vesicular monoamine uptake, in controls. These results suggest that in these cell models α-synuclein did not directly cause oxidative stress or mitochondrial respiratory chain dysfunction. However, the data indicated that α-synuclein may increase the susceptibility of HEK293 cells to rotenone induced mitochondrial complex I inhibition (wild-type α-synuclein) and may play a role in dopamine compartmentalisation. Loss of function conferred by the G209A mutation could therefore increase cytoplasmic dopamine concentrations with

subsequent cell damage or death. These models might be useful to investigate the mechanisms underlying these effects in more detail, and they may also be suitable to study the effect of treatment aimed at protecting against rotenone or dopamine mediated toxicity.

CHAPTER 4.

Myoblast and myotube cell culture model for Huntington's disease

4.1. Introduction

In 1872, George Huntington first described in detail the disease that bears his name. He recognised the most important clinical features of Huntington's disease, namely behavioural abnormalities, cognitive decline and movement disorder. In addition, he recognised that the disease was transmitted in a dominant pattern within affected families. The disease has an estimated prevalence in North America and Europe of 4-10 in 100,000 (Folstein, 1989).

4.1.1. Clinical features of Huntingtons's disease

Huntington's disease (HD) is clinically characterised by chorea, ataxia, psychiatric abnormalities and dementia. The disease usually manifests during the forth or fifth decade of life. The mean survival is 15 to 20 years; HD is inevitably fatal and there is no effective treatment.

Patients may present first with behavioural changes, most commonly alterations of character, before they develop a movement disorder and cognitive function deteriorates. However, they may also develop primarily a movement disorder that precedes the psychiatric/cognitive disorder. Symptoms can appear as early as 4 years of age (Farrer and Conneally, 1987; van Dijk et al., 1986) or as late as 60 or 70 years of age (Folstein, 1989). The movement disorder characteristically consists of choreoathetosis, but ataxia, tics and akinetic rigid syndromes are well recognised, in particularly in young onset cases (e.g. Westphal variant). Death often results from dysphagia; patients may subsequently develop aspiration pneumonia, they may suffocate, and suicide is also not infrequent (Harper, 1991).

In addition to the many signs and symptoms indicative of a brain disorder the vast majority of HD patients suffers from marked muscle wasting and weight loss in the course of the disease despite adequate dietary intake (Farrer and Conneally, 1985; Morales et al., 1989; Sanberg et al., 1981). While dysphagia may contribute to weight loss a catabolic state as a consequence of increased energy expenditure could also be a contributing factor (Pratley et al., 2000). However, in the same study total free-living energy expenditure was not different to controls; patients with HD may engage in less voluntary physical activity thus balancing the increase in energy expenditure because of the movement disorder (Pratley et al., 2000).

4.1.2. Pathology of Huntington's disease

Macroscopically, the characteristic neuropathological findings in HD comprise atrophy of the head of the caudate nucleus and the putamen bilaterally. Cell loss of deeper layers can be observed in additional brain areas including frontal and temporal cortex, thalamus, globus pallidus and cerebellum (de la Monte et al., 1988; Hedreen et al., 1991; Vonsattel et al., 1985). Microscopically, the striatal medium spiny neurones are most affected (Reiner et al., 1988). These cells make up the vast majority of striatal cells and receive inputs from cortex and thalamus, and substantia nigra (Albin et al., 1989). All striatal medium spiny neurones employ the inhibitory transmitter GABA but two different populations can be differentiated by their receptor status. One population projecting to globus pallidus predominantly has substance P, dynorphin and dopamine D_1 receptors while the other projects to the substantia nigra and mainly has enkephalin and dopamine D_2 receptors (Albin et al., 1989). Nuclear and cytoplasmic aggregates are also a typical pathological feature of HD (DiFiglia et al., 1997) (see section 4.1.8.2.1.).

4.1.3. Huntingtin expression and localisation

Huntingtin is a large protein with 3144 amino acids. The polyQ domain begins at amino acid 18 and is followed by a 2 prolin repeat domain. The normal function of huntingtin remains unclear. Huntingtin does not show any major homology with other known proteins, which might have provided some insight into its function. The study of huntingtin gene homologues in mouse, rat and pufferfish indicate that this gene is highly conserved through evolution (Sharp and Ross, 1996) suggesting that it has an important cellular function. Huntingtin contains HEAT (huntingtin elongation factor 3) repeats, which consist of multipe repeats of sequences of about 40 amino acids (Takano and Gusella, 2002). HEATs are found in proteins that are relevant for intracellular transport and chromosomal segregation (Neuwald and Hirano, 2000).

Northern blot analysis of gene expression and in situ hybridisation revealed that huntingtin is widely expressed throughout the brain and non-neuronal tissues with particularly high levels of expression in testes, ovaries, and lung (The Huntington's Disease Collaborative Research Group, 1993; Strong et al., 1993). There is evidence from immunohistochemical studies that huntingtin predominantly localises to the cytoplasm of both neuronal and non-neuronal tissue (Hoogeveen et al., 1993; Trottier et al., 1995a). In HD patients, expression was observed primarily in nerve fibres and their varicosities but also in some cell bodies (Trottier et al., 1995a). In normal brain, huntingtin was immunolocalised to the cytoplasm of neuronal somata, dendrites and axons (DiFiglia et al., 1995) whereas mutant huntingtin was found in neuronal perikarya and proximal nerve processes but not nerve endings (Gourfinkel-An et al., 1997). More specifically, huntingtin was described in vesicle enriched fractions (DiFiglia et al., 1995) with an association to cytoplasmic granules, which resembled multivesicular bodies that were thought to be involved in protein transport and degradation in HD cortical and striatal neurones (Sapp et al., 1997). It was further noted that huntingtin could be associated with

microtubules, which may indicate that huntingtin plays a role in vesicle trafficking (Aronin et al., 1999). In support of this notion mutant and normal huntingtin were found to be associated with clathrin-coated vesicles in the Golgi network, the cytoplasm and the plasma membrane (Velier et al., 1998), and N-terminal fragments of mutant huntingtin interfered with synaptic vesicle glutamate uptake in synaptic vesicles isolated from a full-length mutant huntingtin mouse model (Li et al., 2000a). Thus huntingtin is a widely distributed protein, which may serve a variety of functions (Figure 4.1.).

4.1.4. Huntingtin-interacting proteins

In order to understand the normal function of huntingtin several studies have used the yeast two-hybrid technique or other biochemical techniques to identifiy proteins that interact with HD. This revealed multiple proteins involved in gene transcription, intracellular trafficking and vesicle function (for a review see Li and Li, 2004). Many of these proteins bind to the N-terminal region of huntingtin, and the length of the polyQ repeat can modify the affinity of huntingtin to the interacting proteins. This indicates that the N-terminal section of huntingtin might be particularly relevant in this process, and abnormal polyQ expansions could thus alter cell function (Figure 4.1.).

The interaction of huntingtin with other proteins has been documented in the nucleus and in the cytoplasm (Figure 4.1.). In the nucleus, the formation of nuclear huntingtin aggregates or aggregation foci may impair the function of, or interfere in another way with, nuclear proteins. These proteins include a number of nuclear transcription factors that might be sequestered into aggregates (for a review see Sugars and Rubinsztein, 2003). The most extensively studied pathways are those involving cAMP response element (CRE) and specificity protein-1 (Sp1). The CRE pathway has been found to be involved in neuronal survival (Lonze et al., 2002) and

is therefore of particular interest. For a more extensive discussion of transcriptional abnormalities and references see Sugars and Rubinsztein (Sugars and Rubinsztein, 2003). Problems inherent to microarray analysis, the technique employed to identify changes in gene transcription need to be considered, including reproducibility limited by cost, and importantly, the correlation of altered gene expression to the disease process. In other words, the question is whether altered expression of a gene is important in the pathology of HD, and if so, if it is a primary event or secondary to something else.

In addition to the interaction of huntingtin with nuclear transcription factors an interaction with cytoplasmic proteins has been described, e.g. HAP1 (huntingtin-associated protein 1) and HIP1 (huntingtin-interacting protein 1). Both proteins are highly expressed in neurones and have been associated with microtubule-dependent transport (Engelender et al., 1997; Li et al., 1998b), endocytosis (Li et al., 2002) and neuronal survival (Marcora et al., 2003) (Figure 4.1.).

4.1.5. Huntingtin processing

In vitro evidence indicates that full-length huntingtin contains several protease cleavage sites within the first 550 amino acids including caspase 3, calpain and an aspartatic protease (Gafni and Ellerby, 2002; Kim et al., 2001; Wellington et al., 1998). How full-length huntingtin is cleaved into fragments in humans is not fully understood. Caspase cleaving sites have been identified in huntingtin, atrophin, and the androgen receptor, and mutant huntingtin was found to be cleaved most effectively at amino acid 513 resulting in truncated N-terminal fragments that contain the polyQ expansion (Wellington et al., 1998). Beause of its small size the N-terminal huntingtin fragements are thought to diffuse passively into the nucleus (Figure 4.1.).

4.1.6. Genetics of HD and other CAG repeat disorders

HD is an autosomal dominant disorder caused by an expanded CAG repeat of the huntingtin gene on the short arm of chromosome 4 (The Huntington's Disease Collaborative Research Group, 1993; Strong et al., 1993); 35 or fewer CAG repeats do not cause the disease whereas patients with 40 or more repeats will always develop HD. Individuals with 35-39 repeats are at increased risk of developing HD.

In HD, instability of the CAG repeat and an increase in repeat length is more likely when the HD gene is inherited from an affected father (MacDonald et al., 1993). This is often associated with earlier age of onset in these children, a phenomenon called "anticipation", which is most marked with paternal inheritance of the HD gene (Harper and Newcombe, 1992). CAG repeat number has been used as an approximate measure for disease severity (Becher et al., 1998). In addition, longer CAG repeat length often is associated with earlier onset (Gusella et al., 1997). However, this association is not reliable enough to allow prediction of the age of onset from genetic testing in a clinically unaffected individual. This indicates that, while there is a substantial contribution of CAG size to age of onset and phenotype, other factors, either genetic or environmental, might also be relevant.

HD is one of 9 inherited neurodegenerative diseases caused by an increased CAG repeat length (Table 4.1). These diseases include dentatorubral pallidolysian atrophy (DRPLA) (Koide et al., 1994; Nagafuchi et al., 1994), spinal and bulbar muscular atrophy (SBMA, Kennedy's disease) (La Spada et al., 1991) and the spinocerebellar ataxias (SCA) 1 (Banfi et al., 1994; Orr et al., 1993), 2 (Imbert et al., 1996; Pulst et al., 1996), 3 (Kawaguchi et al., 1994), 6 (Zhuchenko et al., 1997), 7 (David et al., 1997) and 17 (Nakamura et al., 2001). CAG repeat disorders share a number of features; except for SBMA they all are autosomal dominant, onset of symptoms is in midlife, all progress towards a fatal outcome, all disorders cause degeneration and neuronal cell death in both hemispheres in a symmetric way, they

show genetic anticipation and the size of the CAG expansion correlates with disease severity and age of onset (for a review see Ross, 2002). In many of these CAG repeat disorders neuronal intranuclear inclusions have been described, which contain the protein encoded by the abnormal gene and ubiquitin.

Disorder	Mode of inheritance	Locus	Protein	Normal CAG repeats	Mutant CAG repeats
HD	Dominant	4p	Huntingtin	11-34	37-120
DRPLA	dominant	12p	Atrophin 1	7-25	49-85
SBMA	X-linked		Androgen receptor	11-33	40-62
SCA1	Dominant	6p	Ataxin 1	25-36	41-81
SCA2	Dominant	12q	Ataxin 2	17-29	36-52
SCA3	Dominant	14q	Ataxin 3	13-36	62-82
SCA6	Dominant	19p	Ataxin 6	4-16	21-27
SCA7	Dominant	3p	Ataxin 7	7-17	38-130
SCA17	Dominant	6q27	TATA binding protein	29-42	47-55

Table 4.1. Neurological CAG repeat disorders. HD: Huntington's disease. DRPLA: dentatorubropallidolysian atrophy. SBMA: spinobulbar muscular atrophy. SCA1,2,3,6,7,17: spinocerebellar atrophy types 1,2,3,6,7,17.

4.1.7. The R6/2 and other mouse models of HD

The R6/2 HD mouse model

The identification of the gene mutation causing HD enabled the generation of mouse models of the disease. The first such model was the R6/2 mouse (Mangiarini et al.,

1996). The R6/2 mouse is transgenic for exon 1 of the human HD gene with ~145 CAG repeats under the control of the human HD promoter (Davies et al., 1997; Mangiarini et al., 1996). The transgene is expressed ubiquitously at both the mRNA and protein level including brain and skeletal muscle. Initially the mice develop normally; at the age of about 8 weeks they exhibit a progressive neurological phenotype with features very similar to HD. Mice have a complex movement disorder including choreiform movements, stereotypical movements, tremor, and they have seizures (Mangiarini et al., 1996). From about week 6 they start to loose weight, a feature also observed in HD. The disease progresses rapidly and mice usually die at about 14 weeks of age. Pathologically, brains of transgenic mice weigh less than control brains but appear grossly normal. Histologically, even before the onset of symptoms neuronal intranuclear inclusions containing the expanded polyQ repeat and ubiquitin are present in cortex at 3.5 weeks and striatum at 4.5 weeks (Davies et al., 1997).

In the R6/2 transgenic mouse model of HD, nuclear ubiquitinated huntingtin aggregates were described in cardiac and skeletal muscle, kidney, liver, adrenal glands and pancreas (Sathasivam et al., 1999). In muscle, the occurrence of inclusions correlated with the onset of muscle atrophy. Further histochemical analysis of muscle sections from animals with end stage disease revealed a reduction in muscle fibre diameters compared with control littermates but no evidence to suggest an underlying myopathic or neuropathic process (Sathasivam et al., 1999). In the R6/2 mouse the formation of nuclear ubiquitinated huntingtin inclusions suggests that muscle cells express and modify the human transgene in a similar way to neurones.

Other HD mouse models

Other R6 lines also contain exon 1 of the human HD gene under the control of the

human HD promoter sequences but with different CAG repeat lengths; the R6/1 line has 115 and the R6/5 line has 128-156 repeats. The phenotype is similar to that of the R6/2 line, however, with a later onset than the R6/2 (4-5 months in R6/1 hemizygotes, 9 months in homozygous R6/5). Schilling and colleagues developed mouse lines with a longer N-terminal fragment (171 aminoacids compared to 91 aminoacids in the R6 lines) and 18, 44 or 82 CAG repeats under the control of the prion protein promoter (Schilling et al., 1999). Lines with 82 CAG repeats developed a progressive neurological phenotype similar to the R6 lines, and life span was shorter. Laforet and colleagues designed lines with a N-terminal fragment encoding for 1000 aminoacids containing either 18, 46 or 100 CAG repeats (Laforet et al., 2001). Lines with 18 CAG repeats were indistinguishable from normal controls while lines with 46 or 100 CAG repeats developed a neurological phenotype during their life span characterised by impairment in either clasping, gait, general activity or rotarod performance (Laforet et al., 2001).

Other mouse models express the mutant form of the whole human huntingtin gene. The first such mouse lines were established by Reddy et al with 16, 48 or 89 CAG repeats under the control of the CMV promoter (Reddy et al., 1998). Lines with 48 CAG repeats that were expressing higher levels of the transgene than the endogenous gene and those with 89 CAG repeats showed a progressive neurological phenotype with hyperactivity and a movement disorder (Reddy et al., 1998). In another model full-length human huntingtin was introduced within a human yeast artificial chromosome (YAC). Mouse lines contained 18, 46 or 72 CAG repeats; only lines with 72 CAG repeats developed a mild neurological phenotype characterised by mild dark-phase hyperkinesias whereas the line with 46 CAG repeats was no different to the line with 18 CAG repeats (Hodgson et al., 1999). Another approach to generating mouse models targets the mouse huntingtin gene directly either replacing the exon 1 sequence with a CAG repeat length that is

pathogenic in humans (Lin et al., 2001; Shelbourne et al., 1999) or generating a hybrid gene in which the human exon 1 containing expanded CAG repeats replaces the mouse exon 1 (Levine et al., 1999; Wheeler et al., 2000). These "knock-in" mice express between 50 and 150 CAG repeats; however, only one line with 150 CAG repeats developed a clear progressive neurological phenotype (Lin et al., 2001). Comparing the mouse models to date reveals the difficulties to model a disease with onset in mid-life in an animal with a much shorter life span than humans. The R6/2 model accelerates the manifestation of the disease in two ways: it uses very long CAG repeat lengths that in humans are associated with a young onset of the disease; and it uses N-terminal fragments of human huntingtin which may bypass the initial step of the pathophysiology (see section 4.1.5.) and lead to an earlier onset of the disease. On the other hand, this may also be associated with a phenotype and pathological changes that are different from the human disease. A model expressing the full-length mouse huntingtin gene manipulated using the "knock-in" approach is theoretically more likely to be a faithful model of HD; however, this approach seems so far less reliable in generating a mouse with an early onset of the phenotype.

4.1.8. Pathogenic mechanisms in HD

4.1.8.1. Genetic gain of function

Several lines of evidence suggest that the mutation in the huntingtin gene confers a toxic gain of function. Targeted disruption of the homologous mouse gene, either of exon 5 (Nasir et al., 1995), exon 4 (Duyao et al., 1995) or the promoter region (Zeitlin et al., 1995) revealed that mouse embryos with targeted disruption of both genes (nullizygous) were developmentally retarded and died in utero. This suggests that huntingtin is important for normal development. Heterozygous mice carrying one disrupted and one normal allele appeared normal (Nasir et al., 1995). However,

abnormalities were detected on specific tests of cognition and motor function similar to those animals with lesions in the striatum. This might indicate that huntingtin is particularly important for basal ganglia development (Nasir et al., 1995). The mutation does not inhibit transcription or translation since mutant huntingtin can be detected on Western blots of protein extracted from brain and peripheral tissue (Trottier et al., 1995a). This indicated that there is no loss of the protein or mRNA that could lead to subsequent cell dysfunction. Patients homozygous and heterozygous for the mutant huntingtin gene have an almost identical phenotype suggesting that the normal allele is not important (Wexler et al., 1987). It is therefore likely that the abnormal allele is responsible for a novel CAG-length-dependent feature leading to cell dysfunction and death of specific neuronal subpopulations. The gene product, mutant huntingtin with an expansion of polyglutamine repeats (polyQ), might in itself have toxic properties leading to impairment of important neuronal function such as ATP production, or it may interfere with the function of other specific proteins, e.g. transcription factors, thus indirectly affecting neuronal function (Figure 4.1.).

On the other hand, huntingtin was also shown to enhance the production of neurotrophic factors such as brain derived neurotrophic factor suggesting that it might also have a neuroprotective function (Cattaneo et al., 2001). In particular, it was shown that wild-type huntingtin inhibits apoptosis at the level of procaspase 9 (Rigamonti et al., 2001). These authors demonstrated that huntingtin had no effect on cytochrome c release following proapoptotic insults but inhibited activation of procaspase 9 (Rigamonti et al., 2001). These downstream consequences for normal huntingtin function may be related to the interaction of mutant huntingtin with wild-type huntingtin, which can be sequestered into aggregates that had been seeded by mutant N-terminal fragments (Busch et al., 2003). Thus, a mutation in huntingtin may not only lead to a toxic gain of function but also to a loss of function.

4.1.8.2. Formation and toxicity of polyQ aggregates

4.1.8.2.1. PolyQ aggregate formation

Analysing the structure of polyglutamine peptides Perutz demonstrated that polyglutamines are able to form β-pleated sheets. These sheets in turn can link together to form a polar zipper structure, which gains in stability with longer polyglutamine repeat length (Perutz, 1995; Perutz et al., 1994). In support of this concept, in vitro studies with recombinant N-terminal huntingtin fragments revealed aggregate formation with polyQ size in the pathological range (51-122) but not in the normal range (20 and 30 repeats) (Scherzinger et al., 1997). Electron microscopy showed that aggregates had a fibrillar structure similar to β-amyloid (Scherzinger et al., 1997). In addition, Scherzinger et al demonstrated that the formation of these aggregates critically depended upon protein concentration and incubation time; in a self-initiated process aggregate formation depended upon the formation of a nucleus that serves as a seed for aggregate propagation (Lansbury, 1997; Scherzinger et al., 1997).

PolyQ aggregates were subsequently described *in vivo*. Nuclear and extranuclear (in neuronal processes and axonal terminals) huntingtin aggregates have been found in brains of HD patients and R6/2 HD transgenic mice (Davies et al., 1997; DiFiglia et al., 1997; Gutekunst et al., 1999; Li et al., 1999; Schilling et al., 1999). In addition, a number of studies provided evidence that the number of aggregates formed correlated with the severity of the disease phenotype. In the cortex of HD patients the number of aggregates correlated with CAG repeat number, which has been used as an approximate measure for disease severity (Becher et al., 1998). In R6/2 HD transgenic mice the formation of neuronal intranuclear huntingtin aggregates preceded clinical manifestation of a movement disorder (Davies et al., 1997); aggregate formation was also found to be associated with cell death in HEK293 and neuroblastoma cell culture models of HD (Cooper et al., 1998;

Martindale et al., 1998), and the association of aggregate formation and neuronal loss was observed in other CAG repeat disorders (Ellerby et al., 1999; Paulson et al., 1997; Sato et al., 1999).

Toxic fibrillar aggregates can form from non-pathogenic polyQ repeat lenghts (Perutz et al., 1994; Scherzinger et al., 1999; Yang et al., 2002). *In vitro* the initiation of aggregate formation was found to depend upon a critical concentration of polyQ containing aggregate precursor and was associated with a lag time (Chen et al., 2002). Thus, it is conceivable that it is the polyQ size that determines the likelihood that aggregates form within an individuals' lifespan, and, hence, whether the individual will have the disease (pathological polyQ size) or not (non-pathological polyQ size). In addition, other factors influencing the concentration of huntingtin, and the length of time that huntingtin is free in the cytoplasm, and thus prone to aggregation, might also contribute to aggregate formation.

4.1.8.2.2. Huntingtin aggregates: full-length versus N-terminal fragment

In HD patients nuclear and cytoplasmic aggregates were shown to contain only N-terminal fragments (DiFiglia et al., 1997). A number of HD models, both cell culture and animal, have indicated that truncated polyQ fragments may be more toxic than the full-length protein (Davies et al., 1997; Hackam et al., 1998; Hodgson et al., 1999; Reddy et al., 1998; Schilling et al., 1999). The R6/2 HD mouse model contains a very short N-terminal huntingtin fragment (exon 1) causing a marked disease phenotype and neuropathological changes (see section 4.1.7.). This contrasts to a transgenic mouse with full-length huntingtin transgene where animals had a later onset of symptoms and survived longer (Reddy et al., 1998) and the more diffuse cytoplasmic huntingtin staining in normal human brain (DiFiglia et al., 1995; DiFiglia et al., 1997; Sharp et al., 1995). It would thus appear that indeed N-terminal huntingtin fragments are of paramount importance to the formation of

aggregates, possibly by forming a seed with subsequent nucleation-dependent aggregate formation as discussed above.

The hypthesis of N-terminal fragments as central to the generation of aggregates in HD would imply that mutated huntingtin was more readily cleaved than wild-type huntingtin. The results of a recent study that examined huntingtin protein from patients with HD, transgenic HD mice and cell culture models of HD questioned this view (Dyer and McMurray, 2001). This study revealed that *in vitro* mutant huntingtin was more resistant to proteolysis than wild-type. In addition, N-terminal cleavage products were found to result from cleavage of normal huntingtin, and not the mutant form, but were then sequestered by mutant huntingtin (Dyer and McMurray, 2001). These results indicated that the consequences of mutant huntingtin expression may extend beyond those known to be caused by expression of N-terminal fragments alone.

4.1.8.2.3. Huntingtin aggregates: nuclear versus cytoplasmic toxicity

Nuclear polyQ aggregates represent a typical pathological feature of HD that is observed both in the nucleus and in the cytoplasm, and in particular in neurites and axonal terminals. It is not clear whether the nuclear or the cytoplasmic localisation of aggregates is more relevant to HD pathogenesis.

Recent cell culture studies have re-examined the issue of polyQ aggregate toxicity (Chen et al., 2001; Chen and Wetzel, 2001; Yang et al., 2002). In these studies, polyQ peptides (either Q20 or Q40) were constructed with two lysine residues to confer solubility and a fluorescence tag at the N-terminus to enable visualisation. *In vitro*, both polypeptides could be induced to form fibrillar aggregates after cold shock and at high concentrations. These aggregates were readily taken up by cultured cells in which they were localised in the cytoplasm. In order to examine the relevance of localisation of aggregates the polyQ peptides were fitted

with a nuclear localisation signal. Aggregates from these modified polyQ peptides passed the nuclear membrane and entered the nucleus. Irrespective of the original polyQ repeat length, aggregates caused substantial cell death when directed to the nucleus but were not toxic when present in the cytoplasm. Control experiments using preformed aggregates from bacterial cold-shock protein showed that aggregates also entered the nucleus but were not toxic. These experiments illustrate that polyQ aggregates are toxic within the nucleus, regardless of whether they formed from normal polyQ or pathogenic polyQ repeat length, but that the polyQ sequence is not required for entry into the nucleus.

As discussed in section 4.1.8.2.1., in addition to nuclear aggregates there is convincing evidence for huntingtin aggregates in neuronal processes and axonal terminals. In HD brains neuropil aggregates were more common than nuclear aggregates and were abundantly present before the onset of symptoms (Gutekunst et al., 1999). It is possible that neuropil aggregates precede dystrophic neurites, which are both observed as the disease progresses (DiFiglia et al., 1997). Neuropil aggregates correlated with disease severity in R6/2 transgenic mice (Li et al., 1999) and full-length huntingtin expression in mice resulted in neuropil aggregates and axonal degeneration in early stages of disease (Li et al., 2001). Aggregate formation in neurites and neuropil could lead to pathological interactions with cytoplasmic huntingtin-interacting proteins (see section 4.1.4., Figure 4.1.) as these could become sequestered within polyQ aggregates. These interacting proteins, e.g. HIP1 or HAP1, are involved in endocytosis, vescle trafficking and recycling, as well as microtubule-dependent transport and neuronal survival (Engelender et al., 1997; Li et al., 1998b; Li et al., 2002; Marcora et al., 2003). These functions may be compromised as an indirect consequence of cytoplasmic inclusion formation possibly leading to impaired synaptic function including neurotransmitter release

(Figure 4.1.). This may cause e.g. excitotoxicity due to abnormal glutamate homoeostasis (Cepeda et al., 2001; Li et al., 2003).

4.1.8.2.4. Huntingtin aggregates: unresolved issues

Taken together there is now good evidence to suggest that aggregates are indeed toxic and that there is a close link between aggregate formation and pathogenesis. On the other hand, in cultured striatal neurones transfected with mutant full-length huntingtin, cytoplasmic aggregate formation was inversely related to cell death casting doubt upon a causal role for huntingtin aggregate formation in the pathogenesis of HD (Saudou et al., 1998). This raises the question whether aggregate formation always has to be toxic or whether it can be protective.

It remains unclear whether aggregate formation *in vivo* is initiated by the generation of N-terminal fragments of mutant huntingtin since there is evidence to suggest that mutant huntingtin may actually be more resistant to cleavage. Alternatively, the N-terminal fragment from normal huntingtin proteolysis could sequester full-length mutant huntingtin. Huntingtin aggregates form in the nucleus and the cytoplasm (Figure 4.1.). There is evidence indicating that both these aggregate localisations have downstream consequences presumable via the interaction with transcription factors or synaptic proteins respectively. It is not clear whether nuclear or cytoplasmic aggregates cause more neuronal damage, or whether neurones degenerate as a consequence of a mixture of both (Figure 4.1.).

There are several more unresolved issues regarding aggregate formation. One relates to the size the inclusions have to reach in order to be toxic, i.e. whether they have to be visible by light microscopy or not. Recent studies have described polyQ protofibrils as possible precursors of mature fibrils (Poirier et al., 2002) and, using a novel technique, huntingtin aggregates that were not detected using light microscopy were found within numerous so called aggregation foci in post mortem

HD brains but not in control brains (Osmond et al., 2002). Another important question is whether aggregates have to form in the neurones that are most susceptible to cell death, i.e. in the striatum. In HD brains more aggregates have been described in the cerebral cortex than in the striatum (DiFiglia et al., 1997; Gutekunst et al., 1999). If aggregates caused the cells in which they form to die one would expect more cell death in the cerebral cortex than in the striatum. It is possible that aggregates distinct from those detected by immunohistochemistry play a greater role (as discussed above) or that synaptic dysfunction leads to functional consequences downstream of the affected neurone (Figure 4.1.).

4.1.8.2.5. The effect of aggregate prevention

As discussed above there is evidence to suggest that the formation of huntingtin aggregates is toxic and is correlated to disease progression. Thus treatment to prevent aggregate formation or enhance aggregate removal could be beneficial in HD. In *in vitro* models several studies investigated whether such treatment had an effect on the disease phenotype. Treatment of R6/2 HD transgenic mice with caspase-1 inhibitors reduced aggregate formation, and this was associated with improvements in the disease phenotype (Chen et al., 2000; Ona et al., 1999); other treatments, all of which reduced aggregate load and improved the phenotype, consisted of switching-off the mutant huntingtin transgene in mice expressing a tetracyclin regulatable mutant huntingtin fragment (Yamamoto et al., 2000), inhibition of aggregate formation with Congo red in a HD mouse model (Sanchez et al., 2003), or the expression of anti-aggregation peptides in a *Drosophila* model of polyQ disease (Kazantsev et al., 2002). These results indicated that prevention of aggregate formation or removal of existing aggregates can improve the phenotype in transgenic animal models of HD, which suggests that these aggregates were toxic. However, it is not known whether similar treatment of patients with HD would

have such an effect. There may be important species differences, and, in addition, some of the mouse models contained human N-terminal huntingtin fragments rather than the full-length mutant huntingtin that is present in humans. Dispite these reservations the results in these animal models are encouraging for the quest to find treatment for patients with HD.

4.1.8.2.6. Extraneuronal aggregate formation

The presence of huntingtin aggregates in non-neuronal tissues has not been systematically investigated in patients with HD. In SBMA, another CAG repeat disorder intranuclear aggregates of androgen receptor protein were observed in skin, heart, testis and kidney but not in spleen, liver or muscle (Li et al., 1998a). In the R6/2 transgenic mouse model of HD, nuclear inclusions were described in cardiac and skeletal muscle, kidney, liver, adrenal glands and pancreas (Sathasivam et al., 1999). In muscle, the occurrence of inclusions correlated with the onset of muscle atrophy. Further histochemical analysis of muscle sections from animals with end stage disease revealed a reduction in muscle fibre diameters compared with control littermates but no evidence to suggest an underlying myopathic or neuropathic process (Sathasivam et al., 1999). In the R6/2 mouse these findings indicate that in tissues other than brain that express the human transgene the critical concentrations of polyQ for aggregate formation are present. In addition, what seems to be important for causing neurones to die, namely nuclear localisation of huntingtin fragment aggregates, is also observed within extraneuronal tissues, in particular muscle. Since the CAG size in the R6/2 mouse exceeds that of even juvenile onset human HD cases it remains unknown whether the findings in the mouse model will be reproduced in human HD patients.

4.1.9. Programmed cell death

In HD transgenic mouse models, both the R6/2 (Mangiarini et al., 1996) and full-length huntingtin models (Reddy et al., 1998), neuronal cell death was found to involve apoptotic pathways. The caspase family of proteases (cysteine-dependent, aspartate-specific proteases) play a major role in the execution of apoptosis (Alnemri et al., 1996; Hengartner, 2000). A number of studies provide evidence for an involvement of caspases in HD. Transcriptional caspase-1 gene up-regulation was described early in the HD disease process (Ona et al., 1999); this may be the result of nuclear translocation of N-terminal fragments of mutant huntingtin (Li et al., 2000b). There is evidence to suggest that later on this could be followed by increased transcription of the caspase-3 gene with subsequent activation of the caspase-3 protein (Chen et al., 2000). Huntingtin itself was found to be a substrate of caspase-1 and caspase-3 (Goldberg et al., 1996; Wellington et al., 1998) with subsequent huntingtin cleavage and the generation of huntingtin fragments (Ona et al., 1999) (Figure 4.1.). Since huntingtin fragments enter the nucleus this may in turn maintain up-regulation of caspase-1 and caspase-3 activation but may also deplete the available huntingtin (Chen et al., 2000; Ona et al., 1999; Rigamonti et al., 2000; Rigamonti et al., 2001; Zuccato et al., 2001) with a subsequent loss of huntingtin function.

Several findings in mouse models of HD have been reproduced in human HD brains. In striatum of HD patients activation of caspases 1, 3, 8 and 9 as well as the release of cytochrome c from mitochondria has also been documented (Kiechle et al., 2002; Ona et al., 1999; Sanchez et al., 1999) (Figure 4.1.).

4.1.10. Mitochondrial involvement and impairment of energy metabolism

Evidence for mitochondrial involvement in HD comes from post mortem, in vivo and in vitro studies (Figure 4.1.). A defect in mitochondrial respiratory chain complex II

and III was found in putamen and caudate with an additional complex IV defect in putamen in HD brains (Browne et al., 1997; Gu et al., 1996; Mann et al., 1990; Tabrizi et al., 1999). Further support for the hypothesis that complex II and III of the mitochondrial respiratory chain might be selectively affected came from animal models of HD using complex II inhibitors 3-nitropropionic acid or malonate (Beal et al., 1993; Brouillet and Hantraye, 1995; Brouillet et al., 1995). In addition, striatal cells derived from a knock-in mouse model of HD were found to be more vulnerable to 3-nitropropionic acid than the selective complex I inhibitor rotenone (Ruan et al., 2004). In the same study some evidence suggested that mitochondria's calcium handling might be compromised in accord with data from HD patient lymphoblasts (Panov et al., 2002). Furthermore, there were indications for impaired cerebral energy metabolism (Koroshetz et al., 1997), and elevated lactate levels correlating with CAG repeat length were reported in HD occipital cortex and striatum (Jenkins et al., 1998).

A few studies examined respiratory chain function in extraneuronal tissues. In HD muscle, a decrease in complex I activity was found in the biopsies of three patient (Arenas et al., 1998) whereas mitochondrial respiratory chain activities were normal in HD platelets (Gu et al., 1996) and fibroblasts (Tabrizi et al., 1999). HD lymphoblasts showed increased sensitivity of mitochondrial membrane depolarisation and MTP-opening to cyanide, a complex IV inhibitor, and the apoptosis inducing agent staurosporine (Sawa et al., 1999). This indicates that the underlying disease mechanism in HD may render mitochondria more vulnerable to exogenous mitochondrial toxins. Taken together these results suggest that in extraneuronal tissues there is less complex II or III deficiency compared to the brain but rather a reduction, or increased sensitivity to toxins, of complex I or IV. Interestingly, 31P magnetic resonance spectroscopy revealed a reduced ratio of phosphocreatine to inorganic phosphate in symptomatic HD patients both at rest

and in the recovery period after exercise (Lodi et al., 2000). This suggests that mitochondrial respiratory chain dysfunction at a molecular level may be mirrored by the deficit in *in vivo* mitochondrial oxidative metabolism as shown by Lodi and colleagues (Lodi et al., 2000).

4.1.11. Oxidative stress and excitotoxicity

HD brains and HD models have been investigated for evidence of oxidative stress and excitotoxicity. In HD patients oxidative damage was found in mtDNA in human HD parietal but not frontal cortex or cerebellum (Polidori et al., 1999) (Figure 4.1.); however, another study failed to document oxidative damage to lipids, proteins or DNA in caudate, putamen and frontal cortex in 10 HD patients (Alam et al., 2000). Most of the evidence to support the involvement of oxidative stress in HD comes form HD models. Increased lipid peroxidation was observed in striatum of the R6/1 huntingtin transgenic mice with 116 CAG repeats (Perez-Severiano et al., 2000). Isolated striatal and cortical synaptosomes of rat brains treated with the complex II inhibitor 3-nitropropionic acid (3-NP) showed decreased oxidative damage with free radical scavengers suggesting that 3-NP caused striatal degeneration involved oxidative stress (La Fontaine et al., 2000).

There is also evidence for increased nitration in HD mouse models suggestive of excitotoxicity (Tabrizi et al., 2000b). Huntingtin was found to interact with a protein called postsynaptic density protein 95 (PSD-95) that modulates the arrangement and the activity of postsynaptic receptors. Mutant huntingtin interacted less with PSD-95; this enhanced the sensitivity of NMDA and kainate receptors, which may promote receptor activity and could cause excitotoxic damage as a consequence (Sun et al., 2001) (Figure 4.1.). An NMDA receptor antagonist and over-expression of normal huntingtin ameliorated this (Sun et al., 2001). This hypothesis is supported by *in vitro* findings in HEK293 cells transfected with both

mutant huntingtin and NMDA receptors that were more susceptible to NMDA exposure than controls (Zeron et al., 2001), and electrophysiological studies in HD mouse models, which revealed altered synaptic activity and an increase in NMDA glutamate receptor activity (Cepeda et al., 2001; Zeron et al., 2002). Within neurites mutant huntingtin might interfere with glutamate uptake into vesicles thus increasing cytoplasmic glutamate levels and the risk to incur excitotoxic damage (Li et al., 2000a; Li et al., 2003) (Figure 4.1.).

Figure 4.1. Possible relationship of disease mechanisms in HD. Much of how the pieces of the pathogenetic puzzle fit together in HD remains speculative. Normal huntingtin seems to be predominantly cytoplasmic possibly associated with the cytoskeleton, and vesicle transport and function. It is likely subject to processing in the cytoplasm leading to the generation of huntingtin fragments. Extended CAG repeat sequences translate into a mutant protein with excessive polyQ repeats that render huntingtin or in particular its N-terminal fragments more prone to the assumption of a β-pleated sheet structure, and subsequent aggregate formation. Aggregate formation can take place in the cytoplasm or in the nucleus. In the cytoplasm this may lead to a toxic gain of function either through the full-length protein or the N-terminal fragment including the activation of the caspase cascade, interference with mitochondrial function and excitotoxicity, or depletion of functional normal huntingtin. Within the nucleus, mutant huntingtin and aggregates very likely interfere with gene transcription thus exerting a deleterious effect on neurones, and possibly other extreneuronal tissues. This may affect cell function, e.g. of cells harbouring aggregates in the cerebral cortex. This may lead to abnormal stimulation of striatal cells, possibly involving excitotoxicity, or to a decrease in the delivery of trophic factors with subsequent damage to striatal cells.

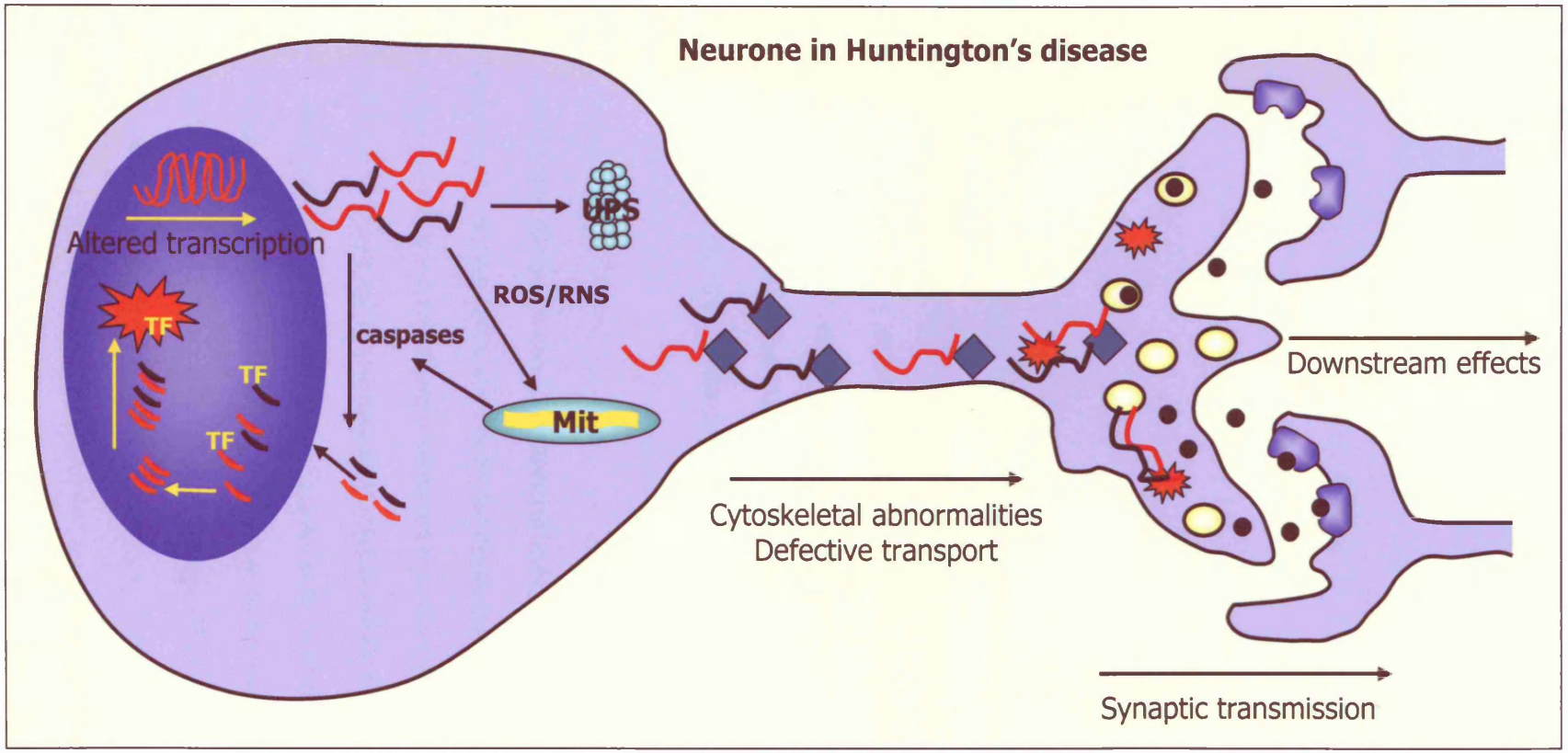
Neurone in Huntington's disease
Altered transcription
TF
TF
TF
UPS
ROS/RNS
caspases
Mit
Cytoskeletal abnormalities
Defective transport
Downstream effects
Synaptic transmission
Neurotransmitter
Normal huntingtin
Mutant huntingtin
polyQ
Vesicle
Aggregate
Interacting protein
Receptor
TF: transcription factor
Mit: mitochondria
ROS/RNS: reactive oxygen/nitrogen species

4.2. Rationale and aim

Ubiquitinated huntigtin inclusions are a common feature in HD and R6/2 transgenic mouse cells. The formation of huntingtin aggregates has been suggested to play an important pathological role but the factors that influence huntingtin aggregate formation in postmitotic cells is not understood. Huntingtin aggregates have been observed in skeletal muscle of the R6/2 transgenic mouse model it was hypothesised that huntingtin inclusion formation may be a feature of myoblast cultures from these animals. Furthermore, differentiation into postmitotic myotubes may serve as a useful postmitotic model to investigate the biochemical mechanisms downstream of mutant huntingtin expression, which influence huntingtin inclusion body formation.

It was the aim of this work to establish myoblast cultures from R6/2 and littermate control mice and to differentiate them into myotubes. The R6/2 transgenic mouse model was used as a model of N-terminal huntingtin expression to study inclusion formation in myoblasts and differentiated myotubes. This study further investigated which factors might modify inclusion formation, and it examined downstream consequences of N-terminal huntingtin over-expression and inclusion formation.

4.3. Results

4.3.1. Analysis of R6/2 myoblast cultures

Myoblast cultures were freshly established from 12-week-old R6/2 mice and littermate controls as described (see section 2.2.4.). Myoblasts were plated onto glass coverslips coated with laminin; in preliminary experiments to optimise culture conditions laminin coating was found to facilitate myoblast growth better than gelatin (2% (v/v in PBS) or collagen (data not shown). After one week in culture cells reached about 60% confluency, and after around 10 days the cultures were over-confluent. Therefore, after 1 week in culture growth medium was replaced by differentiation medium to induce myotube formation. Myotubes were detected using morphological criteria (multinucleated syncithium as the result of myoblast fusion). This was confirmed by staining the cultures with an antibody against desmin, the intermediate filament specific of muscle cells (Figure 4.2A, C, E, G, I, J).

4.3.2. Myoblast and myotube culture

Within the first week in growth medium (data not shown) and after one week in differentiation medium, double labelling indicated that desmin positive cells (myoblasts and myotubes) from both control (Figure 4.2A) and R6/2 (Figure 4.2C) cultures immunostained intensely for huntingtin (Figure 4.2B and D respectively), while huntingtin immunoreactivity was very weak in desmin negative cells (Figure 4.2B and D). However, because the anti huntingtin antibody recognised both mouse and human huntingtin it was not possible to distinguish between the truncated human and the normal mouse huntingtin in the R6/2 cultures. The intensity of huntingtin staining in the myotubes diminished with increasing time post fusion, so that after 4 weeks in differentiation medium, huntingtin immunoreactivity was similar in desmin positive and desmin negative cells (Figure 4.2E, F and Figure 4.2G, H for control and R6/2 respectively).

Qualitatively it was clear that in all cultures established there were consistently more myotubes in the R6/2 cultures (Figure 4.2J) than the controls (Figure 4.2I). Semi-quantitative assessment of the cultures after 1 week in differentiation medium confirmed that the number of desmin positive cells (myoblasts and myotubes) in the R6/2 cultures was consistently greater than in the control cultures (Mann-Whitney U-test, $p<0.0001$; Figure 4.3A). However, the total number of cells in each culture did not differ significantly between control and R6/2 cultures (Figure 4.3B). In addition, desmin positive cells in the R6/2 cultures contained significantly more nuclei compared to control cultures (Mann-Whitney U-test, $p=0.0011$; Figure 4.3C).

Cytoplasmic inclusions positive for ubiquitin (Figure 4.2K) and huntingtin (Figure 4.2L) were observed in R6/2 but not control cultures (Figure 4.2M and N) after 3 weeks in differentiation medium, but only in non-myotube cells. Qualitatively, the incidence of these cytoplasmic inclusions was relatively static between 3 and 6 weeks following differentiation.

After 6 weeks in differentiation medium dual labelling revealed nuclear inclusions immunoreactive for ubiquitin (Figure 4.2O) and huntingtin (Figure 4.2P) in less than 10% ofR6/2 myotubes as assessed semi-quantitatively (mean 7.8; range 6.7-8%), but not control myotubes (Figure 4.2M, N). However, nuclear inclusions were not observed in all the nuclei within a positive myotube (Figure 4.2O). Nuclear inclusions staining positively for both huntingtin and ubiquitin were also occasionally observed in groups of desmin negative cells in R6/2 cultures (Figure 4.2Q, 1R), and occasionally multiple nuclear inclusions were present in a single nucleus (Figure 4.2S, T). Occasionally vacuoles were observed in desmin negative cells, which grew in larger clusters (Figure 4.2U) and showed intense extra nuclear huntingtin immunoreactivity (Figure 4.2V).

When the cultures were grown in serum free medium, after 6 weeks virtually all the myotubes and all their nuclei showed huntingtin (Figure 4.2W) and ubiquitin (Figure 4.2X) positive nuclear aggregates as assessed semi-quantitatively (mean 92; range 89-96%). In addition, the number of non-myotube cells harbouring nuclear inclusions was increased (Figure 4.2W). However, cytoplasmic inclusions were less frequent (Figure 4.2W).

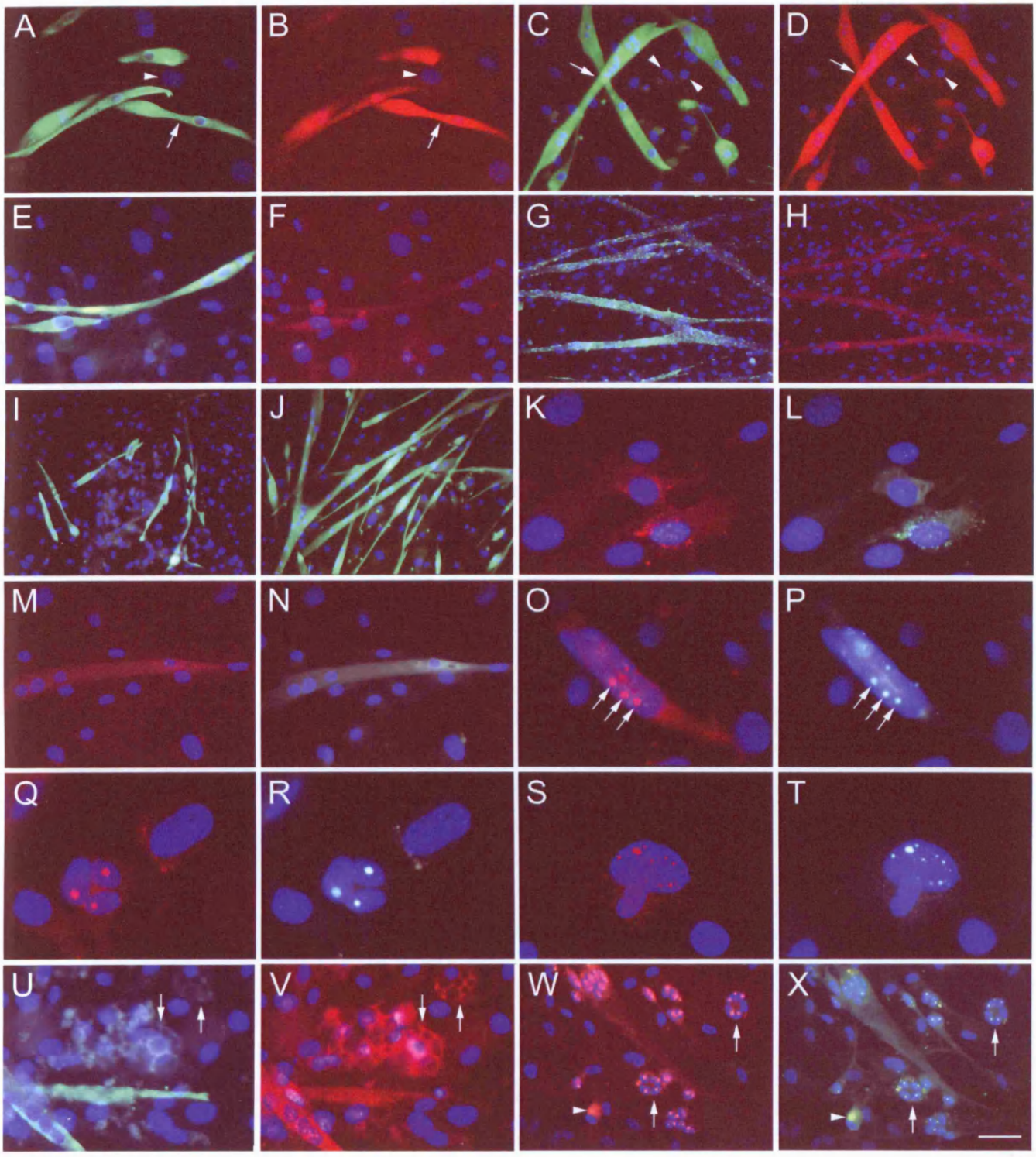
A
B
C
D
E
F
G
H
I
J
K
L
M
N
O
P
Q
R
S
T
U
V
W
X

Figure 4.2. Immunocytochemistry of myoblasts and myotubes of R6/2 mouse and control muscle cultures. Myoblast differentiation and inclusion body formation in control (A, B, E, F, I, M, N) and R6/2 (C, D, G, H, J, K, L, O - X) myoblast cultures. Cultures were immunostained for desmin (A, C, E, G, I, J, U, green staining), huntingtin (B, D, F, H, K, M, O, Q, S, V, W, red staining) or ubiquitin (L, N, P, R, T, X, green staining). Nuclei were stained with DAPI (blue). Cultures were grown in differentiation medium (A -V) or serum free medium (W, X) for 1 week (A, D, I, J), 4 weeks (E-H, U, V) or 6 weeks (K-T, W, X).

After 1 week of culture in differentiation medium, myoblasts and myotubes in both control and R6/2 cultures stained positively for desmin (green staining, A and C respectively, arrows) and strongly for huntingtin (red staining, B and D respectively, arrow). There was no detectable huntingtin staining in desmin negative cells (A-D, arrow heads). However after 4 weeks in culture huntingtin immunoreactivity diminished markedly in both control (F) and R6/2 cultures (H), while desmin immunoreactivity remained very clear (E and G). The number of desmin positive myoblasts and myotubes was qualitatively greater in R6/2 (J) than the control (I) cultures.

In R6/2 cultures cytoplasmic inclusions immunoreacted with huntingtin (K) and ubiquitin (L) following 3 weeks in differentiation medium. No cytoplasmic or nuclear inclusions were observed at any time in controls (M and N). After 6 weeks of culture, R6/2 myotubes showed single nuclear inclusions positive for huntingtin (O, pink, arrow) and ubiquitin (P, white, arrow). After 6 weeks in culture occasional, groups of non-myotube cells exhibited single nuclear inclusions with huntingtin (Q) and ubiquitin (R) cross-reactivity. Some individual non-myotube cells exhibited multiple nuclear inclusions positive for huntingtin (S) and ubiquitin (T). After 2 weeks of culture, clusters of desmin negative cells (U, arrows) showed cytoplasmic vacuoles and stained intensely for huntingtin (V, arrows).

Culture in serum-free medium enhanced the formation of huntingtin (W) and ubiquitin (X) positive nuclear inclusions in both myotubes and non-myotube groups of cells (W and X arrows). Cytoplasmic huntingtin (W, arrow head) and ubiquitin (X, arrow head) positive inclusions were infrequently present. Scale bar: 20 μm in A-F, M, N, U-X; 50μm in G-J and 10μm in K, L and O-T.

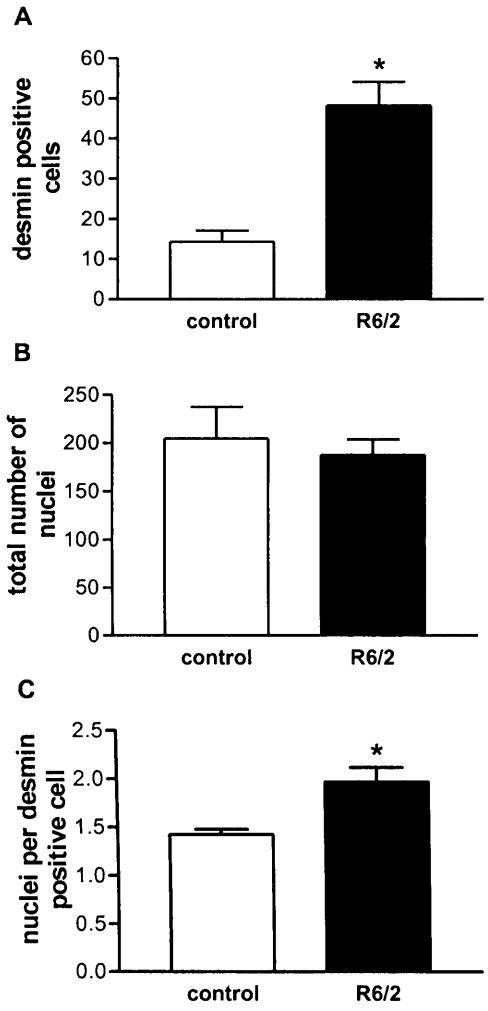

Figure 4.3. Semi-quantitative analysis of control and R6/2 myoblast cultures. Cells were immunostained for desmin and co stained with the nuclear dye DAPI to determine cell numbers after 2 weeks of culture in differentiation medium. **A.** The number of desmin positive cells was greater in R6/2 cultures than in controls (solid

bar versus open bar, *p<0.0001, Mann-Whitney U test, see section 2.12.). **B.** Comparison of the total number of nuclei revealed no statistical difference between controls (open bars) and R6/2 cultures (solid bars). **C.** The number of nuclei per myotube / myoblast was increased in the R6/2 (solid bars) muscle cultures in comparison with the control cultures (open bars) (solid versus open bar, *p=0.0011, Mann-Whitney U test). Values are expressed as means ±SEM. N=4 representative areas were evaluated on a cover-slip in each of n=3 control and n=3 R6/2 myoblast cultures.

4.4. Discussion

4.4.1. Huntingtin immunostaining

In both control and R6/2 mouse muscle cultures high levels of huntingtin immunoreactivity were apparent in the first weeks after the addition of differentiation medium. Only a proportion of cells immunoreacted with the huntingtin antibody; these cells were predominantly multi-nucleated myotubes but the occasional myoblast could be identified. It was not possible to distinguish between the mouse and human protein using immunocytochemical staining; however, the intensity of huntingtin staining in individual cells and the localisation of huntingtin immunoreactivity to the cytoplasm was similar in the control and R6/2 cultures. While this suggests that protein levels in those cells expressing the mutant human transgene, i.e. R6/2 cultures, were similar to the control cells that expressed the mouse huntingtin gene alone this does not allow a comparison of gene expression levels or a quantitative comparison of huntingtin protein levels. In order to draw these comparisons mRNA studies, and Western blot respectively, would have been useful. However, this was not possible in these cultures since they did not contain a homogenous population of cells that all immunoreacted with the huntingtin antibody. Thus the results of any such analysis would have been derived from a sample with a

mixture of different cells of which only a proportion would have stained huntingtin positive. This would have made these results very difficult to interprete.

4.4.2. Huntingtin and myotube differentiation

In both the cell cultures form the R6/2 transgenic mice and the control cultures huntingtin immunoreactivity was observed in cells that also stained with a desmin antibody. The intermediate filament desmin is expressed in conjunction with muscle-specific gene products, such as myogenin and myoD (Weintraub, 1993), and serves as an indicator for the maturity of cells growing in the myoblast cultures (Bennett et al., 1979). Concomitant desmin expression indicated that huntingtin was specifically expressed in differentiating myoblasts and myotubes. Further support for the association of huntingtin with myoblast differentiation was derived from the differential intensity of huntingtin immunostaining over time. Immunostaining for huntingtin was very intense within the first two weeks of culture and thereafter decreased in intensity. Thus more huntingtin protein was likely present within myoblast and myotubes at the time of differentiation after which levels declined. This might indicate that huntingtin plays a role in the differentiation process of muscle. In accord with a possible role of huntingtin in differentiation huntingtin has been shown to be important for haematopoiesis (Metzler et al., 2000), and knock-out of the huntingtin gene in mice was found to be lethal in utero (Zeitlin et al., 1995). This suggests huntingtin may have a more general role in cell maturation. However, how precisely huntingtin regulates differentiation, and whether there are differences between cell types, remains unknown.

At the level of the individual cell the association of huntingtin staining with desmin immunoreactivity did not differ between cell cultures derived from the R6/2 mice or those from control mice, and the time course of the intensity of huntingtin staining was similar. However, the number of desmin positive myotubes was

consistently greater in the R6/2 cultures compared to the control cultures. Since the R6/2 derived myoblast cultures differed from the controls in the expression of the human N-terminal huntingtin transgene this suggests that increased expression of the N-terminal human huntingtin transgene may have promoted myoblast differentiation. It is likely that mutant huntingtin associated promotion of myotube differentiation was due to a gain of function and not to a loss of normal huntingtin function. This is supported by a report showing that targeted inactivation of huntingtin in forebrain and testis of mice resulted in neurodegeneration of this brain area and sterility (Dragatsis et al., 2000). However, it is not clear whether this effect was due to the expanded CAG repeats in the N-terminal human huntingtin transgene or due to the expression of the human transgene per se irrespective of the mutation. This question could have been addressed in myoblast cultures from control mice containing the wild-type human N-terminal huntingtin transgene; however, since such animals were not available this was not possible in the context of this thesis.

The function of huntingtin remains incompletely understood. Huntingtin is expressed ubiquitously in both the central nervous system and peripheral tissues (Trottier et al., 1995b) suggesting it has a general housekeeping role. In human and rat brains huntingtin has been associated with neuronal vesicles, and has been suggested to be involved in endocytosis, vesicle trafficking and microtubules as well as the regulation of transcriptional activity (DiFiglia et al., 1995; Gutekunst et al., 1995; Sharp et al., 1995; Velier et al., 1998). Huntingtin undergoes proteolysis, which generates N-terminal fragments that presumably can diffuse freely into the nucleus (see section 4.1.5.). Huntingtin has also been shown to interact with numerous proteins including proteins involved in gene transcription, intracellular trafficking and vesicle function (for a review see Li and Li, 2004). The N-terminal

region of huntingtin seems to bind many of these proteins, and the length of the polyQ repeat can modify the affinity of huntingtin to the interacting proteins.

It is not known if this includes proteins that are relevant for myoblast differentiation. Abnormal polyQ repeat length in R6/2 derived myoblast cultures may have altered the affinity of huntingtin to its interacting proteins including myoblast differentiation proteins thus facilitating myotube differentiation. However, since the control myoblast cultures expressed full-length normal mouse huntingtin it is not clear whether the enhancement of myotube formation in the R6/2 mouse myoblast cultures was due to the extended polyQ size or the fact that N-terminal huntingtin fragments were over-expressed. N-terminal fragments can freely diffuse into the nucleus whereas full-length huntingtin remains in the cytoplasm. If the effect of N-terminal huntingtin fragments on myotube differentiation was mediated by interactions in the nucleus this could explain the observation that full-length mutant huntingtin presumably in the cytoplasm disrupted cellular signalling mediated by epithelial growth factor and nerve growth factor receptors in PC-12 cells thus blocking neuronal differentiation (Song et al., 2002). In support of this hypothesis mutant huntingtin was found to be more resistant to proteolysis, which would mean that less N-terminal fragments are generated (Dyer and McMurray, 2001). How this relates to R6/2 transgenic mice and the loss of muscle bulk in these animals remains unclear.

4.4.3. Inclusion formation

In HD patients, striatal medium spinal neurones degenerate relatively selectively, and both patient and HD transgenic mice brains exhibit nuclear and cytoplasmic polyQ aggregates (Davies et al., 1997; DiFiglia et al., 1997; Gutekunst et al., 1999; Li et al., 1999; Schilling et al., 1999). There is evidence to suggest that these polyQ inclusions are toxic (see section 4.1.8.2.) but a number of issues regarding their

localisation (nuclear versus cytoplasmic), their composition (N-terminal fragments versus full-length huntingtin) and their impact on neuronal function remain unresolved (see section 4.1.8.2.4.). In HD, it is not known whether PolyQ aggregates form in extraneuronal tissues. In SBMA, an X-linked CAG repeat disorder, androgen receptor aggregates were observed in skin, heart, testis and kidney but not in spleen, liver or muscle (Li et al., 1998a). However, muscle atrophy is commonly observed in patients and HD transgenic mice, in particular in the later stages of the disease (Sathasivam et al., 1999). Muscle from R6/2 transgenic mice expressing the N-terminus of the human HD gene with more than 150 CAG repeats exhibited huntingtin intranuclear inclusions similar to those found in HD and R6/2 brain tissue (Sathasivam et al., 1999). The role that these inclusions play in muscle remains unclear.

The presence of polyQ aggregates in muscle of R6/2 mice suggested that R6/2 myoblast cultures could be useful to study the role of huntingtin inclusions in postmitotic cells. The R6/2 transgenic mice model over-expression of human N-terminal huntingtin with large CAG repeat size (~145 repeats). This is a good model of HD in that it reproduces important pathological features of the human disease, in particular the formation of nuclear huntingtin inclusions, and a progressive neurological phenotyp including a movement disorder with early onset (Davies et al., 1997; Mangiarini et al., 1996). A limitation of the model is that issues regarding the differential involvement of N-terminal fragments and full-length huntingtin cannot be easily addressed. In addition, there is no control mouse model available that expresses the wild-type human N-terminal transgene. This means that it is not possible to distinguish effects of over-expression of the mutation in the transgene form those due to over-expression of N-terminal fragments alone.

In R6/2 muscle cultures the presence of ubiquitin positive huntingtin aggregates was identified in a proportion of myotubes 6 weeks after differentiation

but inclusions were absent in other cells present in the culture. Interestingly, this time course corresponded with the appearance of nuclear inclusions in brain and muscle of R6/2 mice (Davies et al., 1997; Sathasivam et al., 1999). The absence of nuclear inclusions in other cells present in the culture corresponds with the absence of inclusions in skin in the mouse model (Sathasivam et al., 1999). This suggests that pathogenetic events in R6/2 myotubes parallel those in fully differentiated R6/2 mouse muscle and neuronal cells. Why nuclear inclusions formed only in myotubes is not clear. Myotubes differed from non-myotube cells in their level of huntingtin immunoreactivity suggesting that the formation of inclusions could be due to the relative higher concentration of mutant huntingtin in myotubes. This is in accord with concentration dependent initiation of aggregate formation *in vitro* (Chen et al., 2002). It is possible that in myotubes, but not in non-myotubes, the concentration of polyQ containing aggregate precursor exceeded the critical concentration needed to form aggregates (Chen et al., 2002).

Extra-nuclear ubiquitinated huntingtin aggregates were observed 3 weeks after the addition of differentiation medium, but only in desmin-negative cells. At earlier stages, similar looking cells exhibited large vacuoles. While vacuoles have been observed in fibroblast cultures from R6/2 mice (Sathasivam et al., 2001), no evidence of huntingtin inclusion formation was detected. It is possible that inclusions may have formed in the R6/2 fibroblasts with prolonged culture. In contrast to myotubes no nuclear inclusions were observed in those cells that contained cytoplasmic inclusions. In HD brains both nuclear and cytoplasmic inclusions occur (DiFiglia et al., 1997), and there is also support for synaptic dysfunction due to cytoplasmic aggregates (Cepeda et al., 2001; Li et al., 2000a; Zeron et al., 2001; Zeron et al., 2002). The vacuoles that were observed in non-myotube cells, and in fibroblasts, could therefore be a consequence of cell dysfunction due to cytoplasmic

inclusion formation. It is possible that the disappearance of cells with vacuoles over time was due to the death of these cells. However, this remains speculative.

In the R6/2 myblast cultures cell death was not quantitatively assessed. Nonetheless, on microscopy there was no overt loss of cells over the 6 weeks of culture. *In vitro* evidence indicated that nuclear polyQ aggregates are toxic (Chen et al., 2001; Chen and Wetzel, 2001; Yang et al., 2002), so that a loss of cells containing inclusions could have been expected. The molecular mechanisms underlying HD pathogenesis are not completely understood. The presence of nuclear and cytoplasmic accumulation of mutant N-terminal huntingtin fragments is universally acknowledged, however, their role in disease pathogenesis remains controversial (Gutekunst et al., 1999; Li et al., 2000a; Wellington et al., 2000). There is considerable evidence suggesting huntingtin aggregate formation plays a direct role in the induction of cell dysfunction and death (as discussed in detail in the introduction to this chapter). However, *in vitro* evidence in cultured striatal neurones showed that while the translocation of N-terminal fragments to the nucleus induced apoptosis the degree of apoptosis depended on the ability of the cells to form nuclear inclusions suggesting that inclusion formation may also have a protective role (Saudou et al., 1998). In addition, full-length mutant huntingtin appears to be more resistant to proteolysis and was found to sequester N-terminal cleavage fragments from normal huntingtin within aggregates (Dyer and McMurray, 2001). In the R6/2 transgenic HD mouse huntingtin positive inclusions formed in neuronal nuclei and the neuropil in some brain areas before the age of 4 weeks (Davies et al., 1997; Li et al., 1999). This is observed prior to neuronal death, which is not apparent under 14 weeks of age and limited to selected brain areas (Turmaine et al., 2000) suggesting a causal relationship between inclusion formation and neuronal death in this model.

4.4.4. Serum deprivation enhanced inclusion formation

The modulation of aggregate formation can be promising as a treatment for patients with HD. Several studies in animal models of HD have shown that treatment consisting of caspase 1 inhibition (Chen et al., 2000; Ona et al., 1999), Congo-red (Sanchez et al., 2003), anti-aggregation peptides (Kazantsev et al., 2002), or by switching-off the mutant huntingtin gene (Yamamoto et al., 2000) can reduce aggregate formation and improve the phenotype of these animals. In addition, in cells transfected with expanded polyQ, huntingtin antibodies against the N-terminus of huntingtin have been shown to reduce aggregate formation (Lecerf et al., 2001), while aggregates were more frequent following inhibition of the proteasome (Jana et al., 2001; Wyttenbach et al., 2000).

Aggregate formation in R6/2 muscle cultures increased in response to stress inflicted by 6 weeks of serum deprivation. This is in agreement with the observation that serum deprivation increased aggregate formation in rat striatal cells (Wellington et al., 2000). It is possible that serum contains factors that protect against inclusion body formation or enhance their degradation, or that lack of serum induces pathways that lead to enhanced huntingtin transport into the nucleus and aggregation. Serum deprivation has been used as a model to induce apoptosis (Navas et al., 2002; Rukenstein et al., 1991), and mitochondrial membrane permeabilisation and oxidative stress have been reported as a consequence of serum deprivation *in vitro* (Colombaioni et al., 2002a; Colombaioni et al., 2002b; Joza et al., 2001; Navas et al., 2002; Pandey et al., 2003). Thus the stress conferred by serum deprivation may have increased the formation of huntingtin aggregates in the R6/2 myotubes. However, an increase in proteasome protease activity was also reported following serum deprivation in hepatocytes (Pandey et al., 2003). This is difficult to reconcile with the increase in aggregate formation observed in the R6/2 myotubes and rat striatal cells (Wellington et al., 2000) since with an increase in

proteasome activity more effective clearance of aggregates would be expected. However, it is possible that similar to cultured striatal neurones (Saudou et al., 1998) the formation of aggregates may have been protective to the R6/2 myotubes. This would be in agreement with the absence of gross cell death over the 6 weeks of serum deprivation.

4.5. Conclusion

In this thesis chapter it was demonstrated that R6/2 myotubes can be used as a non-neuronal post-mitotic cell culture model exhibiting nuclear huntingtin inclusions very similar to those observed in R6/2 HD mouse brains. The number of inclusions was influenced by environmental conditions suggesting that this model could be useful to study the pathophysiology of huntingtin aggregate formation and could serve as a tool to examine treatment strategies designed to influence aggregate formation.

CHAPTER 5.

PRNP codon 129 polymorphism in sporadic inclusion body myositis muscle (sIBM)

5.1. Introduction

5.1.2. Clinical and histopathological characteristics of sIBM

Sporadic inclusion body myositis (sIBM) is the most common muscle disorder affecting patients 50 years and older (Griggs et al., 1995). Patients suffer from atrophic usually painless but insidiously progressing weakness afflicting mainly proximal and distal muscles of arms and legs. The diagnosis of sIBM is made on muscle biopsy. Histologically, sIBM is characterised by endomysial inflammation with non-necrotic muscle fibres being invaded by mononuclear lymphocytes and by vacuoles lined with granular material (rimmed vacuoles) (Griggs et al., 1995). Amyloid deposits can be identified with Congo red staining using polarised light or fluorescence (Figure 5.1D). Electron microscopy demonstrates intranuclear or cytoplasmic amyloid-like fibrills with a diameter of 6-10nm or paired helical tubulofilaments with 15-21nm diameter. Immunocytochemical techniques reveal that the inflammatory cells are mainly macrophages and $CD8^+$ cytotoxic/suppressor T-cells (Figure 5.1B). In addition, invaded and non-invaded muscle fibres express class 1 major histocompatibility complex (MHC-1) antigens on their surface.

Hereditary inclusion body myopathy differs from sIBM in that there is no inflammation on muscle biopsy and clinically the disease spares the quadriceps muscle (Argov and Yarom, 1984; Sadeh et al., 1993). Inclusion body myopathy is inherited as an autosomal recessive disorder with linkage analysis suggesting that it may be the same entity as Nonoka distal myopathy, a disorder linked to chromosome 9 (Argov et al., 1997; Ikeuchi et al., 1997).

5.1.3. Pathogenesis of sIBM

The pathogenesis of sIBM remains unknown. The prominent inflammatory changes with invasion of non-necrotic muscle fibres by lymphocytes suggest that sIBM might be a primary inflammatory muscle disease similar to polymyositis. This is in accord with a quantitative analysis showing that fibres invaded by inflammatory cells were more frequent than those with amyloid deposits or rimmed vacuoles (Pruitt et al., 1996). However, immunosuppressive treatment, including immunoglobulins, does not lead to significant clinical improvement (Amato et al., 1994; Barohn et al., 1995; Dalakas et al., 1997). It has been reported that CK levels drop following immunosupression for up to 24 months, and compared to pre-treatment the post treatment muscle biopsies showed fewer inflammatory changes. However, the number of vacuolated fibres and fibres with amyloid deposits increased (Barohn et al., 1995). This would be in keeping with the hypothesis that sIBM is a primary degenerative disease with secondary inflammatory changes. In support of this hypothesis accumulation of proteins characteristic for Alzheimer's disease has been reported within vacuolated muscle fibres. These proteins include β-amyloid, C- and N-terminal epitopes of β-amyloid precursor protein, apolipoprotein E, α1-antichymotrypsin, ubiquitin, hyperphosphorylated tau, neurofilament heavy chain, α-synuclein and prion protein (Askanas et al., 1993a; Askanas et al., 1993b; Askanas et al., 2000; Askanas et al., 1994a; Askanas et al., 1994b; Griggs et al., 1995; Mendell et al., 1991). Increased levels of mRNA for the acetylcholine receptor, β-amyloid precursor protein and PrP have also been reported (Griggs et al., 1995; Sarkozi et al., 1994; Sarkozi et al., 1993). This may suggest that the deposits of these proteins are linked to their increased transcription. However, it is not clear whether any of these changes are primary or secondary to another, as yet unknown, pathological event.

While the pathogenesis of sIBM remains elusive, increased transcription and accumulation of ß-amyloid possibly facilitated by factors related to ageing might be an important early event in sIBM pathogenesis (Askanas and Engel, 2001). The remarkable similarities between the pathological changes observed in sIBM and Alzheimer´s disease give rise to the hypothesis that abnormal protein folding plays an important part at least in the mechanisms downstream of the (unknown) causative factor(s). Thus, the accumulation of numerous proteins including the PrP and ubiquitin in inclusions in sIBM might link this disease to neurodegenerative diseases where protein folding and aggregation seem to be at the forefront of the pathogenetic process (Sherman and Goldberg, 2001).

5.1.4. The prion protein

The *PRNP*, a housekeeping gene with 3 exons on chromosome 20, encodes the PrP^c with highest expression levels observed in neurones (Oesch et al., 1985). Initially, the PrP^c is synthesised as a 253-aminoacid polypeptide. Soon after translation begins the first 22 aminoacids (signal peptide) are cleaved. A C-terminal glycosylphosphatidylinositol anchor, added in the post-translational processing, facilitates glycolipid linkage to cell membranes. PrP^c contains 2 N-linked glycosylation sites and a naturally occurring polymorphism at codon 129.

PrP^c is a cell surface glycoprotein of unknown function (Prusiner, 2001). PrP^c, a glycosylphosphatidylinositol-anchored cell surface glycoprotein, is mainly expressed in the central nervous system, but is also, to a lower extent, produced in lymphocytes (Cashman et al., 1990) and stromal cells of lymphoid organs such as tonsil, spleen and gut associated lymphoid tissue (Kitamoto et al., 1991), and muscle where it was found at the neuromuscular junction (Gohel). PrP^c has been linked to neuronal copper metabolism (Brown et al., 1997) and synaptic transmission (Collinge et al., 1994).

5.1.5. Transmissible spongiform encephalopathies

In the transmissible prion diseases, or transmissible spongiform encephalopathies (TSE), a misfolded conformation of PrP^{c}, a detergent-insoluble and proteinase K resistant isoform of the prion protein, termed PrP^{sc}, results in the conversion of normal PrP^{c} encoded by the host into the insoluble and aggregate-prone PrP^{sc}. PrP^{c} and PrP^{sc} do not differ in their primary aminoacid sequences; the conformational change from a high α helix and a low β sheet content of PrP^{c} to a relatively high β sheet content in PrP^{sc} (>30%) has been linked to low solubility of PrP^{sc} and its propensity to from fibrils and amyloid (Pan et al., 1993). In cell free systems it was shown that once PrP^{sc} has formed it can serve as a template to promote the conversion of PrP^{c} to PrP^{sc} (Kocisko et al., 1994).

The mechanisms leading from the conversion of PrP^{c} to PrP^{sc} on to neurodegeneration are incompletely understood. Studies in mice showed that mouse neurones that were not expressing PrP^{c} were well and immune to the toxicity of PrP^{sc} accumulation and deposition (Brandner et al., 1996; Bueler et al., 1993; Bueler et al., 1992). This suggests that an interaction between the transmitted PrP^{sc} and the normal host PrP^{c} is necessary to cause disease.

The most common human form of TSE is Creutzfeld-Jacob disease (CJD). Patients with sporadic CJD commonly present with a rapidly progressive dementia, myoclonus and cerebellar ataxia. The majority of patients die within one year of disease onset. Iatrogenic forms of CJD have been observed in patients following neurosurgery, corneal grafts, dura mater implantation, treatment with human cadaveric pituitary growth hormone and gonadotrophins, and direct infection with stereotactic electroencephalogram electrodes. Up until 2000, world-wide a total of 267 patients with iatrogenic CJD have been reported (Brown et al., 2000).

Another form of TSE was observed in the Fore linguistic group in Papua New Guinea in the context of ritualistic cannibalism, termed Kuru (Gajdusek, 1977;

Gajdusek and Zigas, 1957; Zigas and Gajdusek, 1957). In 1996, the first case of new variant CJD was reported (Will et al., 1996). The clinical presentation differs from sporadic CJD in that patients are much younger (median age at death 29 years) and often initially suffer from psychiatric symptoms including anxiety, withdrawal or insomnia weeks or months before cognition becomes impaired and abnormal movements occur (Spencer et al., 2002). A link with the agent causing bovine spongiform encephalopathy (BSE) was established on epidemiological, biochemical and histological grounds suggesting that the human disease is caused by the prion responsible for BSE (Aguzzi, 1996; Aguzzi and Weissmann, 1996; Bruce et al., 1997; Hill et al., 1997a).

5.1.6. Genetic prion diseases

Mutations of *PRNP* have been associated with hereditary prion neurodegenerative diseases. Three main forms of autosomal dominantly inherited prion disease are distinguished: familial CJD, Gerstmann-Sträussler-Scheinker syndrome and fatal familial insomnia. Gerstmann- Sträussler-Scheinker syndrome differs from CJD in it's clinical presentation; most commonly patients have the P102L (where Proline is substituted at position 102 by Lysine) *PRNP* mutation, which leads to slowly progressive cerebellar ataxia and cognitive decline (Hsiao et al., 1989). However, other phenotypes have been described associated with various other *PRNP* mutations (Collins et al., 2004).

5.1.7. *PRNP* codon 129 polymorphisms

A polymorphism occurs naturally at codon 129 of *PRNP*, which can encode for methionine or valine leading to methionine/valine (M/V), methionine/methionine (M/M) or valine/valine (V/V) genotypes. Normal populations across the world differ markedly with respect to the frequencies of *PRNP* codon 129 alleles (Tables 5.1 and

2). However, within Western Europe several studies documented very similar frequencies (Table 5.1); about 50% are homozygous (40% M/M and 10% V/V) and 50% are heterozygous (Table 5.1).

Western European controls	**M/M (%)**	**V/V (%)**	**M/V (%)**
(Owen et al., 1990), n=106	39 (36)	13 (12.3)	54 (50)
(Schulz-Schaeffer et al., 1996), n=74	31 (41)	10 (13)	33 (44)
(Deslys et al., 1994), n=69	25 (36)	7 (10)	37 (53)
(Laplanche et al., 1994), n=92	38 (41)	9 (9)	45 (48)
(Lampe et al., 1999), n=57	23 (40)	5 (8)	29 (50)
(Zimmermann et al., 1999), n=300	129 (43)	25 (8.3)	146 (48.7)
Pooled, n=698	**285 (40.8)**	**69 (9.9)**	**344 (49.3)**

Table 5.1. Frequency distribution of *PRNP* codon 129 polymorphisms in the normal population in Western Europe.

Other control populations	**M/M**	**V/V**	**M/V**
Papua New Guinea controls (Cervenakova et al., 1998)	32%	24%	43%
Japanese controls (Doh-ura et al., 1991)	92%	0%	8%

Table 5.2. Frequency distribution of *PRNP* codon 129 polymorphisms in non-European control populations.

Homozygosity for methionine or valine at codon 129 of the *PRNP* was suggested to be a predisposing factor in the iatrogenic and sporadic cases of CJD (Collinge et al., 1991; Palmer et al., 1991). In contrast to the normal population in Western Europe close to 90% of sporadic CJD patients (Brown et al., 2000; Windl et al., 1996), between 80 and 90% of iatrogenic CJD cases (Brown et al., 1994; Brown

et al., 2000; Johnson and Gibbs, 1998) and 100% of cases with new variant CJD (Spencer et al., 2002; Will et al., 1996), Andrews http://www.cjd.ed.ac.uk/vcjdq.htm) are homozygous (Table 5.3).

In the iatrogenic CJD cases, those associated with dura mater implants were predominantly methionine homozygotes (Brown et al., 2000), whereas in those cases associated with growth hormone treatment the main increase in homozygosity frequency seems to stem from cases homozygous for valine (Brown et al., 2000) (Table 5.3). Why there appears to be a differential increase in homozygosity frequencies for either methionine or valine in iatrogenic CJD remains unclear. Methionine homozygosity predominates in sporadic CJD and in new variant CJD (Table 5.3). Taken together this suggests that homozygosity at *PRNP* codon 129 increases the risk for these forms of CJD while heterozygosity seems to reduce this risk. This is consistent with studies in the Fore people of Papua New Guinea; methionine homozygosity seems to be a relevant susceptibility factor in Kuru where it is associated with a shorter incubation period, shorter duration of illness and younger age at onset of the disease (Cervenakova et al., 1998; Lee et al., 2001b). Since the ritualistic consumption of brains has been abandoned the number of cases of Kuru has decreased. However, Kuru is still observed in older patients suggesting a longer incubation period. Contemporary Fore survivors are predominantly heterozygous for *PRNP* codon 129 polymorphism (Mead et al., 2003). This is consistent with the hypothesis that codon 129 heterozygosity protects from Kuru, which in turn may have led to selection of a heterozygous codon 129 genotype in the Fore people (Mead et al., 2003). In new variant CJD all of 143 definite or probable cases (with 137 deaths) reported to date (http://www.cjd.ed.ac.uk/figures/htm) were homozygous for methionine suggesting that methionine homozygotes were particularly susceptible to transmission of BSE. In agreement with human data, in mice expressing human codon 129 encoding for

methionine the inoculation with BSE and new variant CJD prions induced a neuropathological and molecular phenotype similar to human new variant CJD (Asante et al., 2002). It remains unknown whether heterozygotes will develop new variant CJD after longer incubation periods; thus although UK surveillance data (Andrews http://www.cjd.ed.ac.uk/vcjdq.htm) and assumptions based on modelling data (d'Aignaux et al., 2001; Valleron et al., 2001) indicate that new variant CJD may have peaked already it remains uncertain whether the future will see a second wave of cases amongst heterozygotes.

How codon 129 homozygosity increases the vulnerability to CJD is not understood. Since the host PrP^{c} needs to interact with the PrP^{sc} it is possible that the aminoacid composition encoded by *PRNP* codon 129 plays an important, albeit currently unknown, role in the cellular events following PrP^{sc} infection. *In vitro* studies suggest that methionine at codon 129 may be more susceptible to a conformational switch from α helix to β sheet than valine (Petchanikow et al., 2001). Codon 129 status may also influence post translational changes in PrP^{c}. In sporadic CJD patients, *PRNP* codon 129 status was shown to correlate with different types of PrP^{sc}, as differentiated on Western blot after limited proteinase K digestion by fragments with different molecular mass and intensity, which reflect un- mono- and di-glycosylated forms (Collinge et al., 1996; Wadsworth et al., 1999). It is not known how *PRNP* codon 129 polymorphisms translate into the link that has been observed to disease duration and neuropathological characteristics in CJD (Hauw et al., 2000; Hill et al., 2003; Parchi et al., 1997; Parchi et al., 1999; Parchi et al., 2000).

Prion disease groups	M/M	V/V	M/V
Historical Fore people with Kuru (Cervenakova et al., 1998; Lee et al., 2001b)	53%	20%	27%
Historical Fore survivors (males 20 years and younger) (Cervenakova et al., 1998; Lee et al., 2001b)	0%	35%	65%
Contemporary Fore survivors (women 50 years and older) (Mead et al., 2003)	na	na	77%
Classic sporadic CJD (Windl et al., 1996), n=58	83%	9%	9%
Classic sporadic CJD (Brown et al., 2000), n=832	71%	16%	13%
New variant CJD (Spencer et al., 2002; Will et al., 1996), http://www.cjd.ed.ac.uk/figures/htm), n=143	100%	0%	0%
Iatrogenic CJD combined (Brown et al., 2000), n=128	57%	23%	20%
Iatrogenic (growth hormone) CJD (Brown et al., 2000), n=82	48%	32%	21%
Iatrogenic (dura mater) (Brown et al., 2000), n=43	74%	7%	19%

Table 5.3. Frequency distribution of the *PRNP* codon 129 polymorphisms in Kuru, sporadic CJD, new variant CJD and iatrogenic CJD. Na: not available.

5.1.8. Extraneuronal PrP^{sc}

The pathological form of the prion protein, PrP^{sc}, has, quite like PrP^{c}, been found mainly in the central nervous system. However, the examination of other tissues of patients with sporadic CJD has revealed PrP^{sc} in other tissues that express PrP^{c}, including a substantial proportion of muscle samples (Glatzel et al., 2003), and in patients with new variant CJD tonsil biopsy can be used as a diagnostic test (Hill et al., 1999; Hill et al., 1997b). Following the inoculation of scrapie strains adapted to hamster and mice PrP^{sc} propagation was shown in muscle albeit at only about 5-10% of brain levels (Bosque et al., 2002; Thomzig et al., 2003).

5.1.9. Prion protein and sIBM

The prion protein is one of the proteins described within vacuolated muscle fibres of sIBM muscle biopsies. There is evidence for increased transcription of *PRNP* from mRNA and increased expression of the prion protein from immunohistochemistry studies (Askanas et al., 1993b; Sarkozi et al., 1994). These studies did not differentiate between PrP^{c} and PrP^{sc}.

Mice transgenic for wild-type *PRNP* developed spongiform degeneration of the brains but also demyelination of peripheral nerves and a necrotising myopathy (Westaway et al., 1994). Similar to sIBM occasional ragged-red fibres were observed but contrary to the characteristic inflammatory changes in muscle biopsies of sIBM the muscle of transgenic mice did not show any lymphocytic infiltration, and no PrP^{sc} was detected (Westaway et al., 1994). The results of this study indicate that over-expression of wild-type *PRNP* might be toxic to muscle; however, at least in mice the muscle histology differed from sIBM.

Apart from one case report an association of sIBM and CJD has not been reported. This single patient was recently reported with both sporadic CJD and a muscle disorder with many pathological features indicative of sIBM (Kovacs et al., 2004). In this patient muscle disease preceded the onset of neurological symptoms by about ten years. The patient presented with dysphasia as the first symptom to indicate a disease afflicting the central nervous system and he survived for more than three years thereafter. Thus, clinically a number of unusual features were present in addition to typical symptoms and signs, and pathological changes, of sporadic CJD. The authors showed PrP^{sc} present in both brain and muscle with levels in muscle reaching about 30% of those in brain (Kovacs et al., 2004). However, in another study the normal PrP^{c} but not the prion disease isoform PrP^{sc} was detected in sIBM muscle (Zanusso et al., 2001).

The potential connection between PrP and sIBM led Lampe and colleagues to study the frequency of methionine homozygosity of codon 129 of *PRNP* in sIBM (Lampe et al., 1999). They studied the PRNP codon 129 polymorphism in 22 Western European patients with a clinical and histological diagnosis of sIBM and 57 controls without neurological disease (Table 5.4). This showed that 14 patients were M/M homozygous (64%), 7 (32%) were M/V heterozygous and 1 patient was V/V homozygous (5%). Analysis of frequency distribution compared to the results of their own control group did not reveal a significant difference; however, a comparison with pooled data from normal controls in 3 Western European countries showed that the M/M polymorphism was more common in their patients (p=0.023).

	M/M (%)	**V/V (%)**	**M/V (%)**
sIBM, n=22	14 (63)	1 (4)	7 (31)
Controls, n=57	23 (40)	5 (8)	29 (50)
Pooled controls, n=398	156 (39)	44 (11)	198 (50)

Table 5.4. Results of the study by Lampe and colleagues.

5.2. Rational and aim

There is good evidence to suggest that sIBM is a degenerative disorder with many pathological similarities to degenerative brain disorders, in particular Alzheimer's disease. It is not clear how to view the involvement of the prion protein in the pathogenesis of sIBM. There is clear evidence that expression of PrP^{c} is increased in muscle of patients with sIBM, and PrP^{c}, in particular in vacuolated muscle fibres in sIBM. Patients with CJD contain PrP^{sc} in muscle and mice transgenic for PrP^{sc} developed not only a spongiform encephalopathy but also a necrotising myopathy with some similarities to sIBM histologically. Since homozygosity for either methionine or valine at the naturally occurring polymorphism at *PRNP* codon 129 is

associated with an increased susceptibility to sporadic, iatrogenic and new variant CJD a previous study examined the *PRNP* codon 129 polymorphism in sIBM patients (Lampe et al., 1999). Lampe and colleagues suggested that homozygosity for methionine was more common in patients with sIBM; however, the number of sIBM patients in their study was small (22). Therefore, it was the aim of this study to examine the *PRNP* codon 129 polymorphism in a larger number of patients with sIBM to identify if the relationship persists.

5.3. Results

5.3.1. Patients

The DNA of a muscle biopsy specimen was analysed in muscle from 41 white Western European patients (14 women, median age 62 years, range 49-74). All patients were given a diagnosis of sIBM on the basis of clinical and histopathological characteristics according to the published criteria (Griggs et al., 1995).

5.3.2. Histology

All biopsies showed morphological changes characteristic for sIBM. On Haematoxylin and Eosin (H+E) stains, muscle biopsies showed a mixture of inflammatory changes with non-necrotic muscle fibres invaded by mononuclear lymphocytes (Figure 5.1A, arrows); immunostaining with antibodies to CD8+ revealed that the majority of lymphocytes were cytotoxic T-cells (red staining in Figure 5.1B). On H+E stains and Gomori trichrome stains biopsies had numerous vacuoles rimmed by basophilic (on H+E, Figure 5.1A, arrow heads), or fuscinophilic (on Gomori trichrome, Figure 5.1C, arrows) granular material, "rimmed vacuoles". On Congo red stained sections congophilic material suggests the presence of amyloid (Congo red stain, red fluorescence, Figure 5.1D). The morphological features of all biopsies were similar.

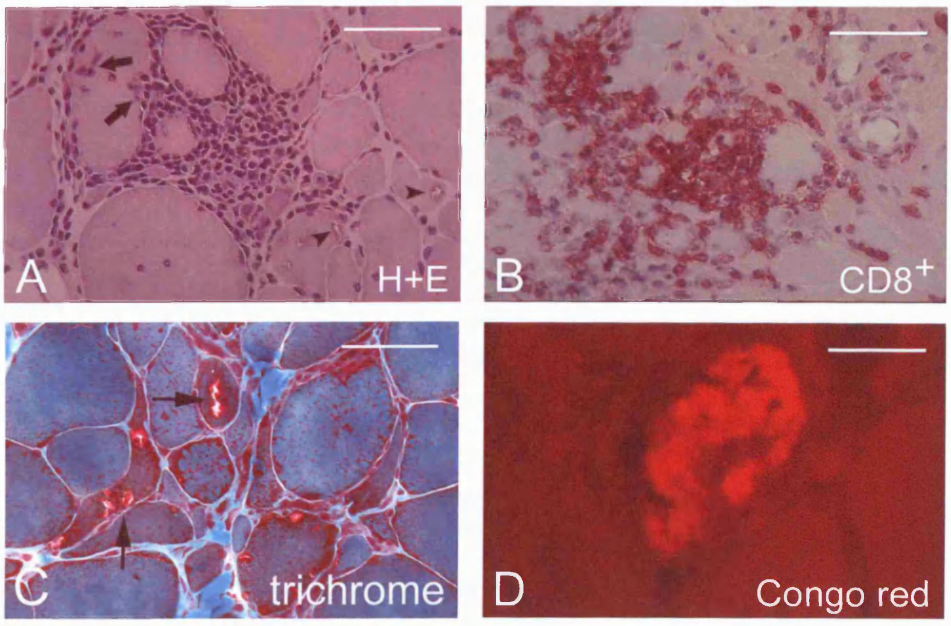

Figure 5.1. Histology of sporadic inclusion body myositis. **A.** H+E stain showing endomysial infiltration of lymphocytes with invaded non-necrotic muscle fibre (arrows). Some fibres also contain small "rimmed vacuoles (arrow heads). **B.** Immunohistochemistry with an antibody to CD8+ (red stain) indicated that a large proportion of the inflammatory cells are cytotoxic T-lymphocytes. **C.** Gomori trichrome stain shows numerous "rimmed vacuole" (arrows). **D.** Congo red stained section under fluorescent light indicates the presence of amyloid. Scale bar in A-C=50μm, in D=25μm.

5.3.3. *PRNP* codon 129 polymorphism

PCR amplification of *PRNP* gene resulted in a 755bp band on agarose gel electrophoresis. The restriction enzyme *NsP*I cuts at codon 129 when it encodes methionine and also at codon 155. Thus in case of a methionine allele *NsP*I digests the 755bp PCR product into three bands of 352, 328 and 75bp (schematic drawing in Figure 5.2). In case of a valine allele, *NsP*I digestion results in the 352bp band and a 427bp band (Figure 5.2). *Mae*II cuts at codon 203 and at codon 129 when it encodes valine. Thus the 755bp *PRNP* PCR product will be digested into three DNA fragments (350, 220, 185 bp) in case of a valine and into two bands (185 and 570bp) in case of a methionine allele at codon 129. Thus, *Mae*II restriction digestion in an individual with heterozygosity yields 4 bands (185, 220, 350 and 570bp, M/V in Figure 5.2), methionine homozygosity results in the three DNA fragments of the methionine allele (185, 220 and 350bp, M/M in Figure 5.2) and valine homozygosity gives 2 bands of the valine allele (185 and 570bp, V/V in Figure 5.2).

Restriction digests using *NsP*I did not yield consistent results with most samples not being cut (left lane of each pair in Figure 5.3). Thus the results with *NsP*I were not deemed reliable. The samples were therefore interpreted using *Mae*II alone (Table 5.5). 41 patients muscle samples were analysed; the results of 17 are shown in Figure 5.3. 21 were homozygous for methionine (51.2 %, M/M in a representative gel run after restriction digest of *PRNP* gene PCR product shown in Figure 5.3) and one patient for valine (2.4 %; V/V in Figures 5.2 and 5.3); 19 patients were heterozygous (46.4 %; M/V in Figure 5.2 and 5.3).

	M/M (%)	**V/V (%)**	**M/V (%)**
sIBM, n=41	21 (51.2)	1 (2.4)	19 (46.4)
Pooled controls, n=698	285 (40.8)	69 (9.9)	344 (49.3)

Table 5.5. Frequency distribution of *PRNP* codon 129 polymorphism in sIBM patients.

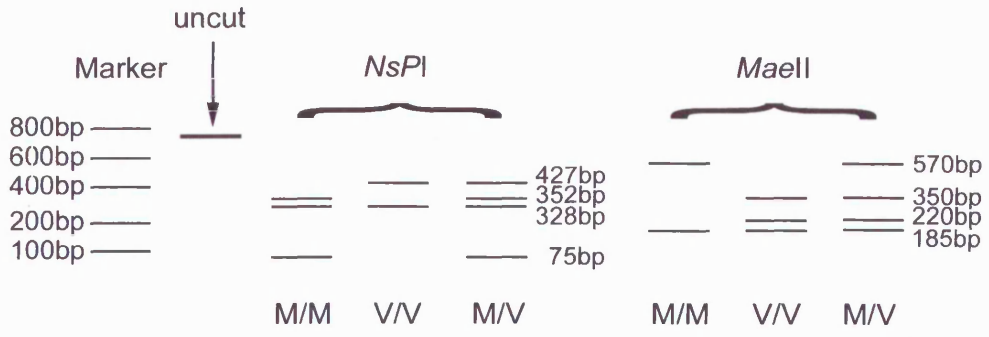

Figure 5.2. Schematic drawing of the restriction fragment length following digestion of the 755bp PRNP open reading frame PCR product with the restriction endonucleases NsPI or MaeII. M/M: methionine homozygous. V/V: valine homozygous. M/V: heterozygous.

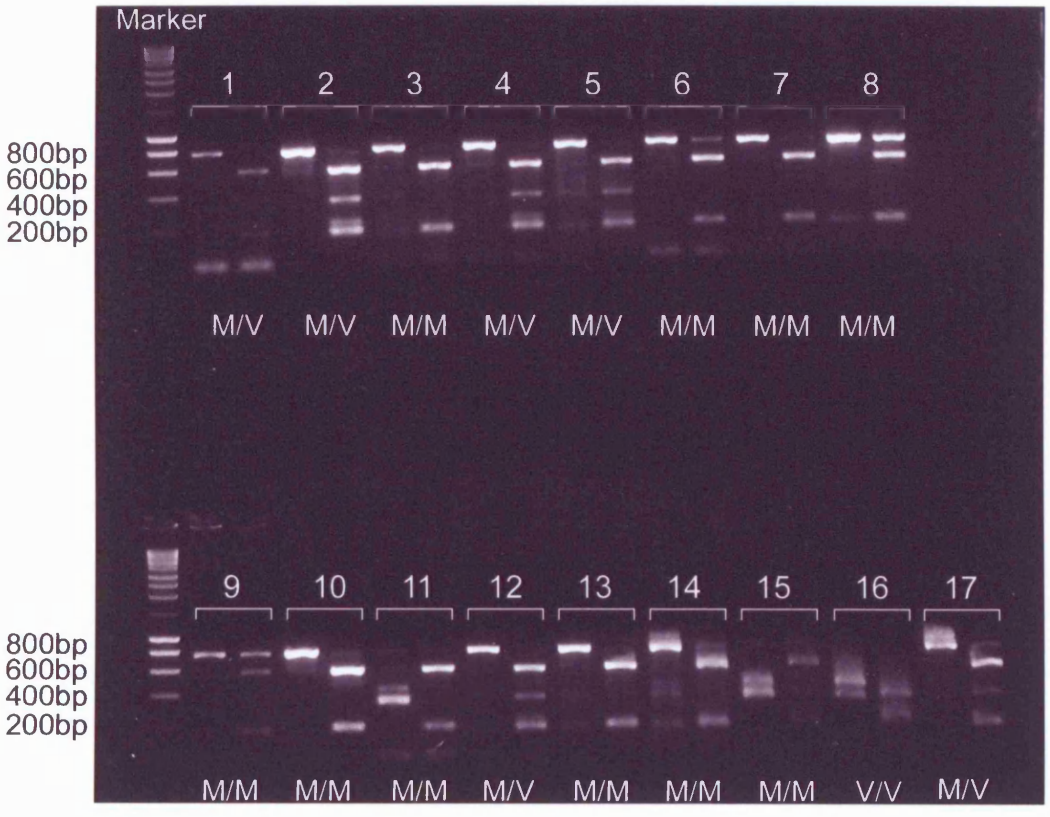

Figure 5.3. Restriction digest of *PRNP* PCR product. 2% agarose gel showing two lanes for eachsample for a total of 17 samples. On the left of each pair, unsuccessful NsPI digestion of PCR amplification of the PRNP results in the 755bp PRNP band while the right lane shows examples for Methionine/Valine (M/V), Methionine/ Methionine (M/M) and Valine/Valine (V/V) phenotypes after digestion of the PCR product with the restriction endonclease MaeII. M/M: methionine homozygous. V/V: valine homozygous. M/V: heterozygous. The numbers 1-17 each represent one sIBM patient.

These results were compared with those from 6 studies in Western European countries (Table 5.5). When combined these studies demonstrated that 40.8 % of individuals had the Met/Met and 9.9% had the Val/Val phenotypes whereas 49.3 % were heterozygous (Table 5.5). The statistical analysis addressed the question whether in sIBM patients homozygosity, i.e. M/M or V/V, was more common than heterozygosity compared with published results from 6 studies in Western European countries (Table 5.5). To this end Fisher's exact test was used, which compares frequencies of homozygosity, or heterozygosity in patients with, or without, sIBM in a 2 X 2 frequency table. The two-sided p value was 0.2497 considered not significant (Odds ratio 1.419, 95%CI 0.785-2.832).

We went on to repeat this analysis combining our data with the data of Lampe and colleagues, and with data from 16 more patients reported by Lampe and co-workers (Lampe et al., 2001), Table 5.6). Comparing frequencies of homozygosity with heterozygosity revealed no statistically significant difference between patients with sIBM and controls (Fisher's exact test, p=0.2353, Odds ratio 1.355, 95%CI 0.8456-2.17 using the approximation of Woolf). When comparing the frequencies of M/M homozygotes with M/V heterozygotes there was a trend towards a higher frequency in the sIBM group (Fisher's exact test, p=0.0869, Odds ratio 1.536, 95%CI 0.984-2.488).

Study (sIBM)	**M/M (%)**	**V/V (%)**	**M/V (%)**
Pooled controls, n=698	285 (40.8)	69 (9.9)	344 (49.3)
This study, n=41	21 (51.2)	1 (2.4)	19 (46.4)
(Lampe et al., 1999), n=22	14 (63)	1 (4)	7 (31)
(Lampe et al., 2001), n=16	7 (43.8%)	2 (12.5%)	7 (43.8%
Pooled, n=79	42 (53.2)	4 (5.1)	33 (41.8)

Table 5.6. Frequency distribution of *PRNP* codon 129 polymorphism in patients with sporadic inclusion body myositis.

5.4. Discussion

It was the aim of this study to re-examine the relationship between the *PRNP* codon 129 polymorphism and sIBM. A previous study reported in 22 patients that the M/M polymorphism was more frequent in sIBM than in Western European controls (Lampe et al., 1999). The results presented in this thesis did not demonstrate a significant difference in homozygosity of codon 129 of the *PRNP* between patients with sIBM and the combined results of several studies in normal control subjects from Western European countries.

This discrepancy could have been caused by different frequencies of the *PRNP* codon 129 polymorphism in the control populations used in the respective studies. However, the genotype distribution of the *PRNP* codon 129 polymorphism is relatively consistent comparing the different studies in Western European controls. Between 44 and 53% of individuals were M/V heterozygous and between 46 and 54% were homozygous (Table 5.1). This contrasts to studies in other populations such as the Japanese or the Fore people in Papua New Guinea (Table 5.2). Therefore, differences in *PRNP* codon 129 polymorphism frequencies between the controls cannot explain the different results.

In the present study 41 patients were examined for the *PRNP* codon 129 polymorphism compared with the 22 patients in the previous study (Lampe et al., 1999). Thus, the smaller number of patients in the Lampe et al study may have led to a chance selection of patients with methionine homozygosity. To assess an even larger number patients we performed a meta-analysis on the pooled data of both studies, and data on a further 16 sIBM patients reported by Lampe and colleagues (Lampe et al., 2001). The results indicated that the M/M polymorphism compared with heterozygosity was not significantly more frequent in sIBM patients. However, there was a trend towards higher M/M frequency in sIBM patients.

This type of analysis (comparing M/M with M/V) does not take the V/V homozygous cases into account. Studies in transmissible spongiform encephalopathies indicated that homozygosity in general, i.e. either M/M or V/V, is more frequent (Table 5.3). We therefore compared frequencies of homozygosity with heterozygosity in our meta-analysis. This did not reveal any significant differences between the patients with sIBM and controls. Therefore, the results presented here suggest that sIBM is not linked to homozygosity of the *PRNP* codon 129 polymorphism. It is possible that the accumulation of PrP^c in sIBM muscle is a non-specific event. This notion would be in accord with a recent report that showed increased expression of PrP^c in other inflammatory muscle diseases (polymyositis and dermatomyositis) and neurogenic muscle atrophy (Zanusso et al., 2001).

This does not exclude the possibility that the prion protein plays a role in sIBM. However, so far there is no evidence that the insoluble form of PrP, PrP^{sc}, occurs in sIBM, and the results presented in this thesis chapter do not support the notion that a potential susceptibility factor for transmissible prion diseases, codon 129 homozygosity, is more common in patients with sIBM. In light of the small number of patients evaluated and the recent observation of both CJD and sIBM in the same patient (Kovacs et al., 2004), more research is warranted to investigate this issue in more detail.

6. Future work

Parkinson's disease

Dispite the advances that have been made in understanding Parkinson's disease several important issues regarding the pathophysiology remain incompletely understood and need to be the subject of future work. It is still not clear why there is selective dopaminergic cell death in PD and why it takes decades, even in the young onset genetic forms of parkinsonism, for the disease to develop. In sporadic PD, future work needs to clarify the relationship between the various pathways that have been identified in PD (e.g. mitochondrial involvement, UPS) and how these pathways are influenced by and linked to genetic factors to try and differentiate the primary event that initiates the disease process from effects further downstream. Unless at least some of these fundamental issues regarding the cause of dopaminergic cell death in PD are better understood treatment of PD will likely remain symptomatic, and it will be difficult to identify pre-symptomatic patients and to develop markers of disease progression. The knowledge about pathways that contribute to PD can, however, provide the basis for potential treatment strategies once the disease has manifested itself. For instance, it has become clear that the UPS is involved in the disease process. Modification of the UPS may be one way to try and stop disease progression.

Powerful animal models are the key to progress in a number of these areas. Toxin models such as the MPTP model have provided valuable insight into PD, and the identification of several genes that cause familial forms of PD has enabled the generation of genetic disease models. These models documented that α-synuclein over-expression can cause a variety of neuropathological changes. However, none of the genetic mouse models to date has been able to recapitulate the most striking pathological feature of the human disease, i.e. selective degeneration of

dopaminergic neurones. A major challenge will therefore remain the generation of a genetic animal model that does show selective dopaminergic cell death.

Huntington's disease

Unlike in PD, the genetic basis for HD has been identified and the genetic test for the HD gene can be used for pre-symptomatic testing. This is an important pre-requesite in order to identify patients at risk to develop HD; these are the patients that would benefit most from any treatment that could be designed to prevent neuronal degeneration. However, it is not known how the disease develops in a given patient with positive predictive testing. This means that it remains unclear when the expression of mutant huntingtin begins to affect neuronal function and when neurones start to degenerate. Thus future work needs to identify biomarkers of disease activity, which would also be invaluable for treatment trials.

A number of suitable animal models have been generated since the HD gene has been found. These models have provided valuable insight into the consequences of the expression of the extended polyQ size in the huntingtin protein. One of the most prominent features in these models was the development of inclusions that contain the N-terminus of huntingtin with polyQ. There is good evidence to suggest that these inclusions are toxic and treatment aimed at preventing or reversing inclusion formation improved the phenotype in transgenic animals. Thus similar trials in human HD patients could be promising. However, future work needs to increase our understanding of the normal function of huntingtin and of the complex interactions of mutant huntingtin with wild-type huntingtin and the whole array of huntingtin-interacting proteins. This could form the basis for the identification of genes and drugs that could restore normal huntingtin function or alter toxicity of mutant huntingtin. Such modifiers of huntingtin function or toxicity could also identify novel treatments for HD patients.

References

Abeliovich A, Schmitz Y, Farinas I, Choi-Lundberg D, Ho WH, Castillo PE, et al. Mice lacking alpha-synuclein display functional deficits in the nigrostriatal dopamine system. Neuron 2000; 25: 239-52.

Aguzzi A. Between cows and monkeys. Nature 1996; 381: 734.

Aguzzi A, Weissmann C. Spongiform encephalopathies: a suspicious signature. Nature 1996; 383: 666-7.

Alam ZI, Daniel SE, Lees AJ, Marsden DC, Jenner P, Halliwell B. A generalised increase in protein carbonyls in the brain in Parkinson's but not incidental Lewy body disease. J Neurochem 1997a; 69: 1326-9.

Alam ZI, Halliwell B, Jenner P. No evidence for increased oxidative damage to lipids, proteins, or DNA in Huntington's disease. J Neurochem 2000; 75: 840-6.

Alam ZI, Jenner A, Daniel SE, Lees AJ, Cairns N, Marsden CD, et al. Oxidative DNA damage in the parkinsonian brain: an apparent selective increase in 8-hydroxyguanine levels in substantia nigra. J Neurochem 1997b; 69: 1196-203.

Albin RL, Young AB, Penney JB. The functional anatomy of basal ganglia disorders. Trends Neurosci 1989; 12: 366-75.

Alexander T, Sortwell CE, Sladek CD, Roth RH, Steece-Collier K. Comparison of neurotoxicity following repeated administration of l-dopa, d-dopa and dopamine to embryonic mesencephalic dopamine neurons in cultures derived from Fisher 344 and Sprague-Dawley donors. Cell Transplant 1997; 6: 309-15.

Alnemri ES, Livingston DJ, Nicholson DW, Salvesen G, Thornberry NA, Wong WW, et al. Human ICE/CED-3 protease nomenclature. Cell 1996; 87: 171.

Amato AA, Barohn RJ, Jackson CE, Pappert EJ, Sahenk Z, Kissel JT. Inclusion body myositis: treatment with intravenous immunoglobulin. Neurology 1994; 44: 1516-8.

Ambani LM, Van Woert MH, Murphy S. Brain peroxidase and catalase in Parkinson disease. Arch Neurol 1975; 32: 114-8.

Anderson JJ, Bravi D, Ferrari R, Davis TL, Baronti F, Chase TN, et al. No evidence for altered muscle mitochondrial function in Parkinson's disease. J Neurol Neurosurg Psychiatry 1993; 56: 477-80.

Anglade P, Vyas S, Hirsch EC, Agid Y. Apoptosis in dopaminergic neurons of the human substantia nigra during normal aging. Histol Histopathol 1997; 12: 603-10.

Arenas J, Campos Y, Ribacoba R, Martin MA, Rubio JC, Ablanedo P, et al. Complex I defect in muscle from patients with Huntington's disease. Ann Neurol 1998; 43: 397-400.

Argov Z, Tiram E, Eisenberg I, Sadeh M, Seidman CE, Seidman JG, et al. Various types of hereditary inclusion body myopathies map to chromosome 9p1-q1. Ann Neurol 1997; 41: 548-51.

Argov Z, Yarom R. "Rimmed vacuole myopathy" sparing the quadriceps. A unique disorder in Iranian Jews. J Neurol Sci 1984; 64: 33-43.

Arima K, Hirai S, Sunohara N, Aoto K, Izumiyama Y, Ueda K, et al. Cellular co-localization of phosphorylated tau- and NACP/alpha- synuclein-epitopes in lewy bodies in sporadic Parkinson's disease and in dementia with Lewy bodies. Brain Res 1999; 843: 53-61.

Aronin N, Kim M, Laforet G, DiFiglia M. Are there multiple pathways in the pathogenesis of Huntington's disease? Philos Trans R Soc Lond B Biol Sci 1999; 354: 995-1003.

Asante EA, Linehan JM, Desbruslais M, Joiner S, Gowland I, Wood AL, et al. BSE prions propagate as either variant CJD-like or sporadic CJD-like prion strains in transgenic mice expressing human prion protein. Embo J 2002; 21: 6358-66.

Ascherio A, Zhang SM, Hernan MA, Kawachi I, Colditz GA, Speizer FE, et al. Prospective study of caffeine consumption and risk of Parkinson's disease in men and women. Ann Neurol 2001; 50: 56-63.

Askanas V, Alvarez RB, Engel WK. beta-Amyloid precursor epitopes in muscle fibers of inclusion body myositis. Ann Neurol 1993a; 34: 551-60.

Askanas V, Bilak M, Engel WK, Alvarez RB, Tome F, Leclerc A. Prion protein is abnormally accumulated in inclusion-body myositis. Neuroreport 1993b; 5: 25-8.

Askanas V, Engel WK. Inclusion-body myositis: newest concepts of pathogenesis and relation to aging and Alzheimer disease. J Neuropathol Exp Neurol 2001; 60: 1-14.

Askanas V, Engel WK, Alvarez RB, McFerrin J, Broccolini A. Novel immunolocalization of alpha-synuclein in human muscle of inclusion-body myositis, regenerating and necrotic muscle fibers, and at neuromuscular junctions. J Neuropathol Exp Neurol 2000; 59: 592-8.

Askanas V, Engel WK, Bilak M, Alvarez RB, Selkoe DJ. Twisted tubulofilaments of inclusion body myositis muscle resemble paired helical filaments of Alzheimer brain and contain hyperphosphorylated tau. Am J Pathol 1994a; 144: 177-87.

Askanas V, Mirabella M, Engel WK, Alvarez RB, Weisgraber KH. Apolipoprotein E immunoreactive deposits in inclusion-body muscle diseases. Lancet 1994b; 343: 364-5.

Banati RB, Daniel SE, Blunt SB. Glial pathology but absence of apoptotic nigral neurons in long-standing Parkinson's disease. Mov Disord 1998; 13: 221-7.

Banfi S, Servadio A, Chung MY, Kwiatkowski TJ, Jr., McCall AE, Duvick LA, et al. Identification and characterization of the gene causing type 1 spinocerebellar ataxia. Nat Genet 1994; 7: 513-20.

Barohn RJ, Amato AA, Sahenk Z, Kissel JT, Mendell JR. Inclusion body myositis: explanation for poor response to immunosuppressive therapy. Neurology 1995; 45: 1302-4.

Barroso N, Campos Y, Huertas R, Esteban J, Molina JA, Alonso A, et al. Respiratory chain enzyme activities in lymphocytes from untreated patients with Parkinson disease. Clin Chem 1993; 39: 667-9.

Beal MF. Experimental models of Parkinson's disease. Nat Rev Neurosci 2001; 2: 325-34.

Beal MF, Brouillet E, Jenkins BG, Ferrante RJ, Kowall NW, Miller JM, et al. Neurochemical and histologic characterization of striatal excitotoxic lesions produced by the mitochondrial toxin 3-nitropropionic acid. J Neurosci 1993; 13: 4181-92.

Becher MW, Kotzuk JA, Sharp AH, Davies SW, Bates GP, Price DL, et al. Intranuclear neuronal inclusions in Huntington's disease and dentatorubral and pallidoluysian atrophy: correlation between the density of inclusions and IT15 CAG triplet repeat length. Neurobiol Dis 1998; 4: 387-97.

Benecke R, Strumper P, Weiss H. Electron transfer complexes I and IV of platelets are abnormal in Parkinson's disease but normal in Parkinson-plus syndromes. Brain 1993; 116: 1451-63.

Bennett DA, Beckett LA, Murray AM, Shannon KM, Goetz CG, Pilgrim DM, et al. Prevalence of parkinsonian signs and associated mortality in a community population of older people. N Engl J Med 1996; 334: 71-6.

Bennett GS, Fellini SA, Toyama Y, Holtzer H. Redistribution of intermediate filament subunits during skeletal myogenesis and maturation in vitro. J Cell Biol 1979; 82: 577-84.

Bennett MC, Bishop JF, Leng Y, Chock PB, Chase TN, Mouradian MM. Degradation of alpha-synuclein by proteasome. J Biol Chem 1999; 274: 33855-8.

Ben-Shachar D, Zuk R, Glinka Y. Dopamine neurotoxicity: inhibition of mitochondrial respiration. J Neurochem 1995; 64: 718-23.

Berman SB, Hastings TG. Dopamine oxidation alters mitochondrial respiration and induces permeability transition in brain mitochondria: implications for Parkinson's disease. J Neurochem 1999; 73: 1127-37.

Berridge MV, Tan AS. Characterization of the cellular reduction of 3-(4,5-dimethylthiazol-2-yl)-2,5-diphenyltetrazolium bromide (MTT): subcellular localization, substrate dependence, and involvement of mitochondrial electron transport in MTT reduction. Arch Biochem Biophys 1993; 303: 474-82.

Betarbet R, Sherer TB, MacKenzie G, Garcia-Osuna M, Panov AV, Greenamyre JT. Chronic systemic pesticide exposure reproduces features of Parkinson's disease. Nat Neurosci 2000; 3: 1301-6.

Biere AL, Wood SJ, Wypych J, Steavenson S, Jiang Y, Anafi D, et al. Parkinson's disease-associated alpha-synuclein is more fibrillogenic than beta- and gamma-synuclein and cannot cross-seed its homologs. J Biol Chem 2000; 275: 34574-9.

Bindoff LA, Birch-Machin M, Cartlidge NE, Parker WD, Jr., Turnbull DM. Mitochondrial function in Parkinson's disease. Lancet 1989; 2: 49.

Blin O, Desnuelle C, Rascol O, Borg M, Peyro Saint Paul H, Azulay JP, et al. Mitochondrial respiratory failure in skeletal muscle from patients with Parkinson's disease and multiple system atrophy. J Neurol Sci 1994; 125: 95-101.

Bloem BR, Irwin I, Buruma OJ, Haan J, Roos RA, Tetrud JW, et al. The MPTP model: versatile contributions to the treatment of idiopathic Parkinson's disease. J Neurol Sci 1990; 97: 273-93.

Bonifati V, Rizzu P, Van Baren MJ, Schaap O, Breedveld GJ, Krieger E, et al. Mutations in the DJ-1 Gene Associated with Autosomal Recessive Early- Onset Parkinsonism. Science 2002; 21: 21.

Bosque PJ, Ryou C, Telling G, Peretz D, Legname G, DeArmond SJ, et al. Prions in skeletal muscle. Proc Natl Acad Sci U S A 2002; 99: 3812-7.

Bourgeron T, Rustin P, Chretien D, Birch-Machin M, Bourgeois M, Viegas-Pequignot E, et al. Mutation of a nuclear succinate dehydrogenase gene results in mitochondrial respiratory chain deficiency. Nat Genet 1995; 11: 144-9.

Boveris A, Chance B. The mitochondrial generation of hydrogen peroxide. General properties and effect of hyperbaric oxygen. Biochem J 1973; 134: 707-16.

Brandner S, Isenmann S, Raeber A, Fischer M, Sailer A, Kobayashi Y, et al. Normal host prion protein necessary for scrapie-induced neurotoxicity. Nature 1996; 379: 339-43.

Brouillet E, Hantraye P. Effects of chronic MPTP and 3-nitropropionic acid in nonhuman primates. Curr Opin Neurol 1995; 8: 469-73.

Brouillet E, Hantraye P, Ferrante RJ, Dolan R, Leroy-Willig A, Kowall NW, et al. Chronic mitochondrial energy impairment produces selective striatal degeneration and abnormal choreiform movements in primates. Proc Natl Acad Sci U S A 1995; 92: 7105-9.

Brown DR, Qin K, Herms JW, Madlung A, Manson J, Strome R, et al. The cellular prion protein binds copper in vivo. Nature 1997; 390: 684-7.

Brown P, Gibbs CJ, Jr., Rodgers-Johnson P, Asher DM, Sulima MP, Bacote A, et al. Human spongiform encephalopathy: the National Institutes of Health series of 300 cases of experimentally transmitted disease. Ann Neurol 1994; 35: 513-29.

Brown P, Preece M, Brandel JP, Sato T, McShane L, Zerr I, et al. Iatrogenic Creutzfeldt-Jakob disease at the millennium. Neurology 2000; 55: 1075-81.

Browne SE, Bowling AC, MacGarvey U, Baik MJ, Berger SC, Muqit MM, et al. Oxidative damage and metabolic dysfunction in Huntington's disease: selective vulnerability of the basal ganglia. Ann Neurol 1997; 41: 646-53.

Bruce ME, Will RG, Ironside JW, McConnell I, Drummond D, Suttie A, et al. Transmissions to mice indicate that 'new variant' CJD is caused by the BSE agent. Nature 1997; 389: 498-501.

Bueler H, Aguzzi A, Sailer A, Greiner RA, Autenried P, Aguet M, et al. Mice devoid of PrP are resistant to scrapie. Cell 1993; 73: 1339-47.

Bueler H, Fischer M, Lang Y, Bluethmann H, Lipp HP, DeArmond SJ, et al. Normal development and behaviour of mice lacking the neuronal cell-surface PrP protein. Nature 1992; 356: 577-82.

Bulteau AL, Lundberg KC, Humphries KM, Sadek HA, Szweda PA, Friguet B, et al. Oxidative modification and inactivation of the proteasome during coronary occlusion/reperfusion. J Biol Chem 2001; 276: 30057-63. Epub 2001 May 25.

Burton LD, Kippenberger AG, Lingen B, Bruss M, Bonisch H, Christie DL. A variant of the bovine noradrenaline transporter reveals the importance of the C-terminal region for correct targeting to the membrane and functional expression. Biochem J 1998; 330: 909-14.

Busch A, Engemann S, Lurz R, Okazawa H, Lehrach H, Wanker EE. Mutant huntingtin promotes the fibrillogenesis of wild-type huntingtin: a potential mechanism for loss of huntingtin function in Huntington's disease. J Biol Chem 2003; 278: 41452-61. Epub 2003 Jul 29.

Cabin DE, Shimazu K, Murphy D, Cole NB, Gottschalk W, McIlwain KL, et al. Synaptic vesicle depletion correlates with attenuated synaptic responses to prolonged repetitive stimulation in mice lacking alpha-synuclein. J Neurosci 2002; 22: 8797-807.

Cabrera-Valdivia F, Jimenez-Jimenez FJ, Molina JA, Fernandez-Calle P, Vazquez A, Canizares-Liebana F, et al. Peripheral iron metabolism in patients with Parkinson's disease. J Neurol Sci 1994; 125: 82-6.

Caparros-Lefebvre D, Elbaz A. Possible relation of atypical parkinsonism in the French West Indies with consumption of tropical plants: a case-control study. Caribbean Parkinsonism Study Group. Lancet 1999; 354: 281-6.

Cardellach F, Marti MJ, Fernandez-Sola J, Marin C, Hoek JB, Tolosa E, et al. Mitochondrial respiratory chain activity in skeletal muscle from patients with Parkinson's disease. Neurology 1993; 43: 2258-62.

Cashman NR, Loertscher R, Nalbantoglu J, Shaw I, Kascsak RJ, Bolton DC, et al. Cellular isoform of the scrapie agent protein participates in lymphocyte activation. Cell 1990; 61: 185-92.

Cassarino DS, Fall CP, Smith TS, Bennett JP, Jr. Pramipexole reduces reactive oxygen species production in vivo and in vitro and inhibits the mitochondrial permeability transition produced by the parkinsonian neurotoxin methylpyridinium ion. J Neurochem 1998; 71: 295-301.

Cassarino DS, Halvorsen EM, Swerdlow RH, Abramova NN, Parker WD, Jr., Sturgill TW, et al. Interaction among mitochondria, mitogen-activated protein kinases, and nuclear factor-kappaB in cellular models of Parkinson's disease. J Neurochem 2000; 74: 1384-92.

Cassarino DS, Parks JK, Parker WD, Jr., Bennett JP, Jr. The parkinsonian neurotoxin MPP+ opens the mitochondrial permeability transition pore and releases cytochrome c in isolated mitochondria via an oxidative mechanism. Biochim Biophys Acta 1999; 1453: 49-62.

Cattaneo E, Rigamonti D, Goffredo D, Zuccato C, Squitieri F, Sipione S. Loss of normal huntingtin function: new developments in Huntington's disease research. Trends Neurosci 2001; 24: 182-8.

Cave A, Figadere B, Laurens A, Cortes D. Acetogenins from Annonaceae. In: Herz W, Kirby GW, Moore RE and al. e, editors. Progress in the chemistry of organic natural products. New York: Springer, 1997: 88-288.

Cepeda C, Ariano MA, Calvert CR, Flores-Hernandez J, Chandler SH, Leavitt BR, et al. NMDA receptor function in mouse models of Huntington disease. J Neurosci Res 2001; 66: 525-39.

Cervenakova L, Goldfarb LG, Garruto R, Lee HS, Gajdusek DC, Brown P. Phenotype-genotype studies in kuru: implications for new variant Creutzfeldt-Jakob disease. Proc Natl Acad Sci U S A 1998; 95: 13239-41.

Chen G, Yuan PX, Jiang YM, Huang LD, Manji HK. Lithium increases tyrosine hydroxylase levels both in vivo and in vitro. J Neurochem 1998; 70: 1768-71.

Chen M, Ona VO, Li M, Ferrante RJ, Fink KB, Zhu S, et al. Minocycline inhibits caspase-1 and caspase-3 expression and delays mortality in a transgenic mouse model of Huntington disease. Nat Med 2000; 6: 797-801.

Chen S, Berthelier V, Yang W, Wetzel R. Polyglutamine aggregation behavior in vitro supports a recruitment mechanism of cytotoxicity. J Mol Biol 2001; 311: 173-82.

Chen S, Ferrone FA, Wetzel R. Huntington's disease age-of-onset linked to polyglutamine aggregation nucleation. Proc Natl Acad Sci U S A 2002; 99: 11884-9. Epub 2002 Aug 19.

Chen S, Wetzel R. Solubilization and disaggregation of polyglutamine peptides. Protein Sci 2001; 10: 887-91.

Chomczynski P, Sacchi N. Single-step method of RNA isolation by acid guanidinium thiocyanate-phenol-chloroform extraction. Anal Biochem 1987; 162: 156-9.

Ciechanover A, Brundin P. The ubiquitin proteasome system in neurodegenerative diseases: sometimes the chicken, sometimes the egg. Neuron 2003; 40: 427-46.

Clark JB, Nicklas WJ. The metabolism of rat brain mitochondria. Preparation and characterization. J Biol Chem 1970; 245: 4724-31.

Clark LN, Poorkaj P, Wszolek Z, Geschwind DH, Nasreddine ZS, Miller B, et al. Pathogenic implications of mutations in the tau gene in pallido-ponto- nigral degeneration and related neurodegenerative disorders linked to chromosome 17. Proc Natl Acad Sci U S A 1998; 95: 13103-7.

Clayton DF, George JM. Synucleins in synaptic plasticity and neurodegenerative disorders. J Neurosci Res 1999; 58: 120-9.

Cohen G, Farooqui R, Kesler N. Parkinson disease: a new link between monoamine oxidase and mitochondrial electron flow. Proc Natl Acad Sci U S A 1997; 94: 4890-4.

Collinge J, Palmer MS, Dryden AJ. Genetic predisposition to iatrogenic Creutzfeldt-Jakob disease. Lancet 1991; 337: 1441-2.

Collinge J, Sidle KC, Meads J, Ironside J, Hill AF. Molecular analysis of prion strain variation and the aetiology of 'new variant' CJD. Nature 1996; 383: 685-90.

Collinge J, Whittington MA, Sidle KC, Smith CJ, Palmer MS, Clarke AR, et al. Prion protein is necessary for normal synaptic function. Nature 1994; 370: 295-7.

Collins SJ, Lawson VA, Masters CL. Transmissible spongiform encephalopathies. Lancet 2004; 363: 51-61.

Colombaioni L, Colombini L, Garcia-Gil M. Role of mitochondria in serum withdrawal-induced apoptosis of immortalized neuronal precursors. Brain Res Dev Brain Res 2002a; 134: 93-102.

Colombaioni L, Frago LM, Varela-Nieto I, Pesi R, Garcia-Gil M. Serum deprivation increases ceramide levels and induces apoptosis in undifferentiated HN9.10e cells. Neurochem Int 2002b; 40: 327-36.

Connor JR, Snyder BS, Arosio P, Loeffler DA, LeWitt P. A quantitative analysis of isoferritins in select regions of aged, parkinsonian, and Alzheimer's diseased brains. J Neurochem 1995; 65: 717-24.

Conway KA, Harper JD, Lansbury PT. Accelerated in vitro fibril formation by a mutant alpha-synuclein linked to early-onset Parkinson disease. Nat Med 1998; 4: 1318-20.

Conway KA, Harper JD, Lansbury PT, Jr. Fibrils formed in vitro from alpha-synuclein and two mutant forms linked to Parkinson's disease are typical amyloid. Biochemistry 2000a; 39: 2552-63.

Conway KA, Lee SJ, Rochet JC, Ding TT, Williamson RE, Lansbury PT, Jr. Acceleration of oligomerization, not fibrillization, is a shared property of both alpha-synuclein mutations linked to early-onset Parkinson's disease: implications for pathogenesis and therapy. Proc Natl Acad Sci U S A 2000b; 97: 571-6.

Conway KA, Rochet JC, Bieganski RM, Lansbury PT, Jr. Kinetic stabilization of the alpha-synuclein protofibril by a dopamine- alpha-synuclein adduct. Science 2001; 294: 1346-9.

Cooper JK, Schilling G, Peters MF, Herring WJ, Sharp AH, Kaminsky Z, et al. Truncated N-terminal fragments of huntingtin with expanded glutamine repeats form nuclear and cytoplasmic aggregates in cell culture. Hum Mol Genet 1998; 7: 783-90.

Cooper JM, Daniel SE, Marsden CD, Schapira AH. L-dihydroxyphenylalanine and complex I deficiency in Parkinson's disease brain. Mov Disord 1995; 10: 295-7.

Coore HG, Denton RM, Martin BR, Randle PJ. Regulation of adipose tissue pyruvate dehydrogenase by insulin and other hormones. Biochem J 1971; 125: 115-27.

Couper J. On the effects of black oxide of manganese when inhaled into the lungs. British Annals of Medicine, Pharmacy, Vital Statistics and General Science 1837; 1: 41-42.

Crowther RA, Jakes R, Spillantini MG, Goedert M. Synthetic filaments assembled from C-terminally truncated alpha- synuclein. FEBS Lett 1998; 436: 309-12.

da Costa CA, Ancolio K, Checler F. Wild-type but not Parkinson's disease-related ala-53 --> Thr mutant alpha -synuclein protects neuronal cells from apoptotic stimuli. J Biol Chem 2000; 275: 24065-9.

d'Aignaux JN, Cousens SN, Smith PG. Predictability of the UK variant Creutzfeldt-Jakob disease epidemic. Science 2001; 294: 1729-31. Epub 2001 Oct 25.

Dalakas MC, Sonies B, Dambrosia J, Sekul E, Cupler E, Sivakumar K. Treatment of inclusion-body myositis with IVIg: a double-blind, placebo-controlled study. Neurology 1997; 48: 712-6.

Damier P, Hirsch EC, Zhang P, Agid Y, Javoy-Agid F. Glutathione peroxidase, glial cells and Parkinson's disease. Neuroscience 1993; 52: 1-6.

Dauer W, Kholodilov N, Vila M, Trillat AC, Goodchild R, Larsen KE, et al. Resistance of alpha -synuclein null mice to the parkinsonian neurotoxin MPTP. Proc Natl Acad Sci U S A 2002; 99: 14524-9. Epub 2002 Oct 10.

David G, Abbas N, Stevanin G, Durr A, Yvert G, Cancel G, et al. Cloning of the SCA7 gene reveals a highly unstable CAG repeat expansion. Nat Genet 1997; 17: 65-70.

Davidson WS, Jonas A, Clayton DF, George JM. Stabilization of alpha-synuclein secondary structure upon binding to synthetic membranes. J Biol Chem 1998; 273: 9443-9.

Davies KJ. Degradation of oxidized proteins by the 20S proteasome. Biochimie 2001; 83: 301-10.

Davies SW, Turmaine M, Cozens BA, DiFiglia M, Sharp AH, Ross CA, et al. Formation of neuronal intranuclear inclusions underlies the neurological dysfunction in mice transgenic for the HD mutation. Cell 1997; 90: 537-48.

Davis GC, Williams AC, Markey SP, Ebert MH, Caine ED, Reichert CM, et al. Chronic Parkinsonism secondary to intravenous injection of meperidine analogues. Psychiatry Res 1979; 1: 249-54.

Dawson VL, Dawson TM, London ED, Bredt DS, Snyder SH. Nitric oxide mediates glutamate neurotoxicity in primary cortical cultures. Proc Natl Acad Sci U S A 1991; 88: 6368-71.

de la Monte SM, Vonsattel JP, Richardson EP, Jr. Morphometric demonstration of atrophic changes in the cerebral cortex, white matter, and neostriatum in Huntington's disease. J Neuropathol Exp Neurol 1988; 47: 516-25.

De Michele G, Filla A, Volpe G, De Marco V, Gogliettino A, Ambrosio G, et al. Environmental and genetic risk factors in Parkinson's disease: a case-control study in southern Italy. Mov Disord 1996; 11: 17-23.

de Rijk MC, Launer LJ, Berger K, Breteler MM, Dartigues JF, Baldereschi M, et al. Prevalence of Parkinson's disease in Europe: A collaborative study of population-based cohorts. Neurologic Diseases in the Elderly Research Group. Neurology 2000; 54: S21-3.

de Silva R, Hardy J, Crook J, Khan N, Graham EA, Morris CM, et al. The tau locus is not significantly associated with pathologically confirmed sporadic Parkinson's disease. Neurosci Lett 2002; 330: 201-3.

Deslys JP, Marce D, Dormont D. Similar genetic susceptibility in iatrogenic and sporadic Creutzfeldt-Jakob disease. J Gen Virol 1994; 75: 23-7.

Dexter DT, Carayon A, Vidailhet M, Ruberg M, Agid F, Agid Y, et al. Decreased ferritin levels in brain in Parkinson's disease. J Neurochem 1990; 55: 16-20.

Dexter DT, Holley AE, Flitter WD, Slater TF, Wells FR, Daniel SE, et al. Increased levels of lipid hydroperoxides in the parkinsonian substantia nigra: an HPLC and ESR study. Mov Disord 1994; 9: 92-7.

Dexter DT, Wells FR, Lees AJ, Agid F, Agid Y, Jenner P, et al. Increased nigral iron content and alterations in other metal ions occurring in brain in Parkinson's disease. J Neurochem 1989; 52: 1830-6.

DiDonato S, Zeviani M, Giovannini P, Savarese N, Rimoldi M, Mariotti C, et al. Respiratory chain and mitochondrial DNA in muscle and brain in Parkinson's disease patients. Neurology 1993; 43: 2262-8.

DiFiglia M, Sapp E, Chase K, Schwarz C, Meloni A, Young C, et al. Huntingtin is a cytoplasmic protein associated with vesicles in human and rat brain neurons. Neuron 1995; 14: 1075-81.

DiFiglia M, Sapp E, Chase KO, Davies SW, Bates GP, Vonsattel JP, et al. Aggregation of huntingtin in neuronal intranuclear inclusions and dystrophic neurites in brain. Science 1997; 277: 1990-3.

Doh-ura K, Kitamoto T, Sakaki Y, Tateishi J. CJD discrepancy. Nature 1991; 353: 801-2.

Dragatsis I, Levine MS, Zeitlin S. Inactivation of Hdh in the brain and testis results in progressive neurodegeneration and sterility in mice. Nat Genet 2000; 26: 300-6.

Duan W, Rangnekar VM, Mattson MP. Prostate apoptosis response-4 production in synaptic compartments following apoptotic and excitotoxic insults: evidence for a pivotal role in mitochondrial dysfunction and neuronal degeneration. J Neurochem 1999a; 72: 2312-22.

Duan W, Zhang Z, Gash DM, Mattson MP. Participation of prostate apoptosis response-4 in degeneration of dopaminergic neurons in models of Parkinson's disease. Ann Neurol 1999b; 46: 587-97.

Dubowitz V. Muscle biopsy: a practical approach. London: Baillere Tindall, 1985.

Duda JE, Giasson BI, Mabon ME, Miller DC, Golbe LI, Lee VM, et al. Concurrence of alpha-synuclein and tau brain pathology in the Contursi kindred. Acta Neuropathol (Berl) 2002; 104: 7-11. Epub 2002 Apr 27.

Duffy PE, Tennyson VM. Phase and electron microscopic observations of Lewy bodies and melanin granules in the substantia nigra and locus coeruleus in Parkinson's disease. J Neuropathol Exp Neurol 1965; 24: 398-414.

Duyao MP, Auerbach AB, Ryan A, Persichetti F, Barnes GT, McNeil SM, et al. Inactivation of the mouse Huntington's disease gene homolog Hdh. Science 1995; 269: 407-10.

Dyer RB, McMurray CT. Mutant protein in Huntington disease is resistant to proteolysis in affected brain. Nat Genet 2001; 29: 270-8.

Earle KM. Studies on Parkinson's disease including x-ray fluorescent spectroscopy of formalin fixed brain tissue. J Neuropathol Exp Neurol 1968; 27: 1-14.

El-Agnaf OM, Jakes R, Curran MD, Wallace A. Effects of the mutations Ala30 to Pro and Ala53 to Thr on the physical and morphological properties of alpha-synuclein protein implicated in Parkinson's disease. FEBS Lett 1998; 440: 67-70.

Eliezer D, Kutluay E, Bussell R, Jr., Browne G. Conformational properties of alpha-synuclein in its free and lipid- associated states. J Mol Biol 2001; 307: 1061-73.

Ellerby LM, Hackam AS, Propp SS, Ellerby HM, Rabizadeh S, Cashman NR, et al. Kennedy's disease: caspase cleavage of the androgen receptor is a crucial event in cytotoxicity. J Neurochem 1999; 72: 185-95.

Emery E, Aldana P, Bunge MB, Puckett W, Srinivasan A, Keane RW, et al. Apoptosis after traumatic human spinal cord injury. J Neurosurg 1998; 89: 911-20.

Enari M, Sakahira H, Yokoyama H, Okawa K, Iwamatsu A, Nagata S. A caspase-activated DNase that degrades DNA during apoptosis, and its inhibitor ICAD. Nature 1998; 391: 43-50.

Engel AG. The muscle biopsy. In: Engel AG and Franzini-Armstrong C, editors. Myology: Basic and clinical. Vol 1. New York: Mc Graw-Hill, Inc., 1994: 822-83.

Engel WK, Cunningham GG. Rapid Examination of Muscle Tissue. An Improved Trichrome Method for Fresh-Frozen Biopsy Sections. Neurology 1963; 13: 919-23.

Engelender S, Kaminsky Z, Guo X, Sharp AH, Amaravi RK, Kleiderlein JJ, et al. Synphilin-1 associates with alpha-synuclein and promotes the formation of cytosolic inclusions. Nat Genet 1999; 22: 110-4.

Engelender S, Sharp AH, Colomer V, Tokito MK, Lanahan A, Worley P, et al. Huntingtin-associated protein 1 (HAP1) interacts with the p150Glued subunit of dynactin. Hum Mol Genet 1997; 6: 2205-12.

Eshleman AJ, Stewart E, Evenson AK, Mason JN, Blakely RD, Janowsky A, et al. Metabolism of catecholamines by catechol-O-methyltransferase in cells expressing recombinant catecholamine transporters. J Neurochem 1997; 69: 1459-66.

Evans DA, Funkenstein HH, Albert MS, Scherr PA, Cook NR, Chown MJ, et al. Prevalence of Alzheimer's disease in a community population of older persons. Higher than previously reported. Jama 1989; 262: 2551-6.

Farrer LA, Conneally PM. A genetic model for age at onset in Huntington disease. Am J Hum Genet 1985; 37: 350-7.

Farrer LA, Conneally PM. Predictability of phenotype in Huntington's disease. Arch Neurol 1987; 44: 109-13.

Farrer M, Chan P, Chen R, Tan L, Lincoln S, Hernandez D, et al. Lewy bodies and parkinsonism in families with parkin mutations. Ann Neurol 2001; 50: 293-300.

Farrer M, Gwinn-Hardy K, Muenter M, DeVrieze FW, Crook R, Perez-Tur J, et al. A chromosome 4p haplotype segregating with Parkinson's disease and postural tremor. Hum Mol Genet 1999; 8: 81-5.

Farrer M, Skipper L, Berg M, Bisceglio G, Hanson M, Hardy J, et al. The tau H1 haplotype is associated with Parkinson's disease in the Norwegian population. Neurosci Lett 2002; 322: 83-6.

Feany MB, Bender WW. A Drosophila model of Parkinson's disease. Nature 2000; 404: 394-8.

Fearnley JM, Lees AJ. Ageing and Parkinson's disease: substantia nigra regional selectivity. Brain 1991; 114: 2283-301.

Ferrante RJ, Schulz JB, Kowall NW, Beal MF. Systemic administration of rotenone produces selective damage in the striatum and globus pallidus, but not in the substantia nigra. Brain Res 1997; 753: 157-62.

Ferrer I, Blanco R, Cutillas B, Ambrosio S. Fas and Fas-L expression in Huntington's disease and Parkinson's disease. Neuropathol Appl Neurobiol 2000; 26: 424-33.

Floor E, Wetzel MG. Increased protein oxidation in human substantia nigra pars compacta in comparison with basal ganglia and prefrontal cortex measured with an improved dinitrophenylhydrazine assay. J Neurochem 1998; 70: 268-75.

Folstein M. Huntington's disease: a disorder of families: The John Hopkins University Press, 1989.

Foltynie T, Sawcer S, Brayne C, Barker RA. The genetic basis of Parkinson's disease. J Neurol Neurosurg Psychiatry 2002; 73: 363-70.

Forno LS, DeLanney LE, Irwin I, Di Monte D, Langston JW. Astrocytes and Parkinson's disease. Prog Brain Res 1992; 94: 429-36.

Forno LS, Langston JW, DeLanney LE, Irwin I. An electron microscopic study of MPTP-induced inclusion bodies in an old monkey. Brain Res 1988; 448: 150-7.

Forno LS, Langston JW, DeLanney LE, Irwin I, Ricaurte GA. Locus ceruleus lesions and eosinophilic inclusions in MPTP-treated monkeys. Ann Neurol 1986; 20: 449-55.

Fridovich I. Superoxide radical and superoxide dismutases. Annu Rev Biochem 1995; 64: 97-112.

Funayama M, Hasegawa K, Kowa H, Saito M, Tsuji S, Obata F. A new locus for Parkinson's disease (PARK8) maps to chromosome 12p11.2- q13.1. Ann Neurol 2002; 51: 296-301.

Gafni J, Ellerby LM. Calpain activation in Huntington's disease. J Neurosci 2002; 22: 4842-9.

Gai WP, Blessing WW, Blumbergs PC. Ubiquitin-positive degenerating neurites in the brainstem in Parkinson's disease. Brain 1995; 118: 1447-59.

Gajdusek DC. Unconventional viruses and the origin and disappearance of kuru. Science 1977; 197: 943-60.

Gajdusek DC, Zigas V. Degenerative disease of the central nervous system in New Guinea; the endemic occurrence of kuru in the native population. N Engl J Med 1957; 257: 974-8.

Gardner PR, Nguyen DD, White CW. Aconitase is a sensitive and critical target of oxygen poisoning in cultured mammalian cells and in rat lungs. Proc Natl Acad Sci U S A 1994; 91: 12248-52.

Gasser T. Genetics of Parkinson's disease. Ann Neurol 1998; 44: S53-7.

Gasser T, Muller-Myhsok B, Wszolek ZK, Oehlmann R, Calne DB, Bonifati V, et al. A susceptibility locus for Parkinson's disease maps to chromosome 2p13. Nat Genet 1998; 18: 262-5.

Giasson BI, Duda JE, Murray IV, Chen Q, Souza JM, Hurtig HI, et al. Oxidative damage linked to neurodegeneration by selective alpha- synuclein nitration in synucleinopathy lesions. Science 2000; 290: 985-9.

Giasson BI, Duda JE, Quinn SM, Zhang B, Trojanowski JQ, Lee VM. Neuronal alpha-Synucleinopathy with Severe Movement Disorder in Mice Expressing A53T Human alpha-Synuclein. Neuron 2002; 34: 521-33.

Giasson BI, Forman MS, Higuchi M, Golbe LI, Graves CL, Kotzbauer PT, et al. Initiation and synergistic fibrillization of tau and alpha-synuclein. Science 2003; 300: 636-40.

Giasson BI, Murray IV, Trojanowski JQ, Lee VM. A hydrophobic stretch of 12 amino acid residues in the middle of alpha- synuclein is essential for filament assembly. J Biol Chem 2001; 276: 2380-6.

Giasson BI, Uryu K, Trojanowski JQ, Lee VM. Mutant and wild type human alpha-synucleins assemble into elongated filaments with distinct morphologies in vitro. J Biol Chem 1999; 274: 7619-22.

Gibb WR, Lees AJ. The relevance of the Lewy body to the pathogenesis of idiopathic Parkinson's disease. J Neurol Neurosurg Psychiatry 1988; 51: 745-52.

Gilman S, Low P, Quinn N, Albanese A, Ben-Shlomo Y, Fowler C, et al. Consensus statement on the diagnosis of multiple system atrophy. American Autonomic Society and American Academy of Neurology. Clin Auton Res 1998; 8: 359-62.

Glatzel M, Abela E, Maissen M, Aguzzi A. Extraneural pathologic prion protein in sporadic Creutzfeldt-Jakob disease. N Engl J Med 2003; 349: 1812-20.

Goedert M. Alpha-synuclein and neurodegenerative diseases. Nat Rev Neurosci 2001; 2: 492-501.

Golbe LI. Positron emission tomography reveals strong genetic influence in Parkinson's disease. Ann Neurol 1999; 45: 557-8.

Golbe LI, Di Iorio G, Bonavita V, Miller DC, Duvoisin RC. A large kindred with autosomal dominant Parkinson's disease. Ann Neurol 1990; 27: 276-82.

Goldberg MS, Fleming SM, Palacino JJ, Cepeda C, Lam HA, Bhatnagar A, et al. Parkin-deficient mice exhibit nigrostriatal deficits but not loss of dopaminergic neurons. J Biol Chem 2003; 278: 43628-35. Epub 2003 Aug 20.

Goldberg YP, Nicholson DW, Rasper DM, Kalchman MA, Koide HB, Graham RK, et al. Cleavage of huntingtin by apopain, a proapoptotic cysteine protease, is modulated by the polyglutamine tract. Nat Genet 1996; 13: 442-9.

Goldstein M, Fuxe K, Hokfelt T. Characterization and tissue localization of catecholamine synthesizing enzymes. Pharmacol Rev 1972; 24: 293-309.

Good PF, Hsu A, Werner P, Perl DP, Olanow CW. Protein nitration in Parkinson's disease. J Neuropathol Exp Neurol 1998; 57: 338-42.

Gordon EB. Carbon-Monoxide Encephalopathy. Br Med J 1965; 5444: 1232.

Gorell JM, Johnson CC, Rybicki BA, Peterson EL, Richardson RJ. The risk of Parkinson's disease with exposure to pesticides, farming, well water, and rural living. Neurology 1998; 50: 1346-50.

Gourfinkel-An I, Cancel G, Trottier Y, Devys D, Tora L, Lutz Y, et al. Differential distribution of the normal and mutated forms of huntingtin in the human brain. Ann Neurol 1997; 42: 712-9.

Graham DG. Oxidative pathways for catecholamines in the genesis of neuromelanin and cytotoxic quinones. Mol Pharmacol 1978; 14: 633-43.

Graham FL, Smiley J, Russell WC, Nairn R. Characteristics of a human cell line transformed by DNA from human adenovirus type 5. J Gen Virol 1977; 36: 59-74.

Green DR, Kroemer G. The pathophysiology of mitochondrial cell death. Science 2004; 305: 626-9.

Greene JC, Whitworth AJ, Kuo I, Andrews LA, Feany MB, Pallanck LJ. Mitochondrial pathology and apoptotic muscle degeneration in Drosophila parkin mutants. Proc Natl Acad Sci U S A 2003; 100: 4078-83. Epub 2003 Mar 17.

Griggs RC, Askanas V, DiMauro S, Engel A, Karpati G, Mendell JR, et al. Inclusion body myositis and myopathies. Ann Neurol 1995; 38: 705-13.

Grinker RR. Parkinsonism following carbon monoxide poisoning. Journal of Nervous and Mental Disorders 1926; 64: 18-28.

Gross A, McDonnell JM, Korsmeyer SJ. BCL-2 family members and the mitochondria in apoptosis. Genes Dev 1999; 13: 1899-911.

Grundemann D, Koster S, Kiefer N, Breidert T, Engelhardt M, Spitzenberger F, et al. Transport of monoamine transmitters by the organic cation transporter type 2, OCT2. J Biol Chem 1998; 273: 30915-20.

Gu M, Cooper JM, Taanman JW, Schapira AH. Mitochondrial DNA transmission of the mitochondrial defect in Parkinson's disease. Ann Neurol 1998a; 44: 177-86.

Gu M, Gash MT, Cooper JM, Wenning GK, Daniel SE, Quinn NP, et al. Mitochondrial respiratory chain function in multiple system atrophy. Mov Disord 1997; 12: 418-22.

Gu M, Gash MT, Mann VM, Javoy-Agid F, Cooper JM, Schapira AH. Mitochondrial defect in Huntington's disease caudate nucleus. Ann Neurol 1996; 39: 385-9.

Gu M, Owen AD, Toffa SE, Cooper JM, Dexter DT, Jenner P, et al. Mitochondrial function, GSH and iron in neurodegeneration and Lewy body diseases. J Neurol Sci 1998b; 158: 24-9.

Gusella JF, Persichetti F, MacDonald ME. The genetic defect causing Huntington's disease: repeated in other contexts? Mol Med 1997; 3: 238-46.

Gutekunst CA, Levey AI, Heilman CJ, Whaley WL, Yi H, Nash NR, et al. Identification and localization of huntingtin in brain and human lymphoblastoid cell lines with anti-fusion protein antibodies. Proc Natl Acad Sci U S A 1995; 92: 8710-4.

Gutekunst CA, Li SH, Yi H, Mulroy JS, Kuemmerle S, Jones R, et al. Nuclear and neuropil aggregates in Huntington's disease: relationship to neuropathology. J Neurosci 1999; 19: 2522-34.

Gutteridge JM, Halliwell B. The measurement and mechanism of lipid peroxidation in biological systems. Trends Biochem Sci 1990; 15: 129-35.

Gwinn-Hardy K, Farrer M. Parkinson's genetics: an embarrassment of riches. Ann Neurol 2002; 51: 7-8.

Haas RH, Nasirian F, Nakano K, Ward D, Pay M, Hill R, et al. Low platelet mitochondrial complex I and complex II/III activity in early untreated Parkinson's disease. Ann Neurol 1995; 37: 714-22.

Hackam AS, Singaraja R, Wellington CL, Metzler M, McCutcheon K, Zhang T, et al. The influence of huntingtin protein size on nuclear localization and cellular toxicity. J Cell Biol 1998; 141: 1097-105.

Halliwell B, Gutteridge GMC. Free radicals in biology and medicine. Oxford: Oxford University Press, 1999.

Hampshire DJ, Roberts E, Crow Y, Bond J, Mubaidin A, Wriekat AL, et al. Kufor-Rakeb syndrome, pallido-pyramidal degeneration with supranuclear upgaze paresis and dementia, maps to 1p36. J Med Genet 2001; 38: 680-2.

Harper P. Huntington's disease. London: WB Saunders, 1991.

Harper PS, Newcombe RG. Age at onset and life table risks in genetic counselling for Huntington's disease. J Med Genet 1992; 29: 239-42.

Harrington KA, Augood SJ, Kingsbury AE, Foster OJ, Emson PC. Dopamine transporter (Dat) and synaptic vesicle amine transporter (VMAT2) gene expression in the substantia nigra of control and Parkinson's disease. Brain Res Mol Brain Res 1996; 36: 157-62.

Hartley A, Stone JM, Heron C, Cooper JM, Schapira AH. Complex I inhibitors induce dose-dependent apoptosis in PC12 cells: relevance to Parkinson's disease. J Neurochem 1994; 63: 1987-90.

Hartmann A, Michel PP, Troadec JD, Mouatt-Prigent A, Faucheux BA, Ruberg M, et al. Is Bax a mitochondrial mediator in apoptotic death of dopaminergic neurons in Parkinson's disease? J Neurochem 2001a; 76: 1785-93.

Hartmann A, Mouatt-Prigent A, Faucheux BA, Agid Y, Hirsch EC. FADD: A link between TNF family receptors and caspases in Parkinson's disease. Neurology 2002; 58: 308-10.

Hartmann A, Troadec JD, Hunot S, Kikly K, Faucheux BA, Mouatt-Prigent A, et al. Caspase-8 is an effector in apoptotic death of dopaminergic neurons in Parkinson's disease, but pathway inhibition results in neuronal necrosis. J Neurosci 2001b; 21: 2247-55.

Hastings TG, Lewis DA, Zigmond MJ. Role of oxidation in the neurotoxic effects of intrastriatal dopamine injections. Proc Natl Acad Sci U S A 1996; 93: 1956-61.

Hausladen A, Fridovich I. Superoxide and peroxynitrite inactivate aconitases, but nitric oxide does not. J Biol Chem 1994; 269: 29405-8.

Hauw JJ, Sazdovitch V, Laplanche JL, Peoc'h K, Kopp N, Kemeny J, et al. Neuropathologic variants of sporadic Creutzfeldt-Jakob disease and codon 129 of PrP gene. Neurology 2000; 54: 1641-6.

Hedreen JC, Peyser CE, Folstein SE, Ross CA. Neuronal loss in layers V and VI of cerebral cortex in Huntington's disease. Neurosci Lett 1991; 133: 257-61.

Hengartner MO. The biochemistry of apoptosis. Nature 2000; 407: 770-6.

Hernan MA, Zhang SM, Rueda-deCastro AM, Colditz GA, Speizer FE, Ascherio A. Cigarette smoking and the incidence of Parkinson's disease in two prospective studies. Ann Neurol 2001; 50: 780-6.

Hicks AA, Petursson H, Jonsson T, Stefansson H, Johannsdottir HS, Sainz J, et al. A susceptibility gene for late-onset idiopathic Parkinson's disease. Ann Neurol 2002; 52: 549-55.

Hill AF, Butterworth RJ, Joiner S, Jackson G, Rossor MN, Thomas DJ, et al. Investigation of variant Creutzfeldt-Jakob disease and other human prion diseases with tonsil biopsy samples. Lancet 1999; 353: 183-9.

Hill AF, Desbruslais M, Joiner S, Sidle KC, Gowland I, Collinge J, et al. The same prion strain causes vCJD and BSE. Nature 1997a; 389: 448-50, 526.

Hill AF, Joiner S, Wadsworth JD, Sidle KC, Bell JE, Budka H, et al. Molecular classification of sporadic Creutzfeldt-Jakob disease. Brain 2003; 126: 1333-46.

Hill AF, Zeidler M, Ironside J, Collinge J. Diagnosis of new variant Creutzfeldt-Jakob disease by tonsil biopsy. Lancet 1997b; 349: 99-100.

Hirai K, Ikeda K, Wang GY. Paraquat damage of rat liver mitochondria by superoxide production depends on extramitochondrial NADH. Toxicology 1992; 72: 1-16.

Hirsch E, Graybiel AM, Agid YA. Melanized dopaminergic neurons are differentially susceptible to degeneration in Parkinson's disease. Nature 1988; 334: 345-8.

Hirsch EC, Brandel JP, Galle P, Javoy-Agid F, Agid Y. Iron and aluminum increase in the substantia nigra of patients with Parkinson's disease: an X-ray microanalysis. J Neurochem 1991; 56: 446-51.

Hirsch EC, Hunot S, Damier P, Brugg B, Faucheux BA, Michel PP, et al. Glial cell participation in the degeneration of dopaminergic neurons in Parkinson's disease. Adv Neurol 1999; 80: 9-18.

Hisata J. Final supplemental environmental impact statement. Lake and stream rehabilitation: rotenone use and health risks. Washington Department of Fish and Wildlife 2002.

Hodgson JG, Agopyan N, Gutekunst CA, Leavitt BR, LePiane F, Singaraja R, et al. A YAC mouse model for Huntington's disease with full-length mutant huntingtin, cytoplasmic toxicity, and selective striatal neurodegeneration. Neuron 1999; 23: 181-92.

Hoglinger GU, Feger J, Prigent A, Michel PP, Parain K, Champy P, et al. Chronic systemic complex I inhibition induces a hypokinetic multisystem degeneration in rats. J Neurochem 2003; 84: 491-502.

Hoogeveen AT, Willemsen R, Meyer N, de Rooij KE, Roos RA, van Ommen GJ, et al. Characterization and localization of the Huntington disease gene product. Hum Mol Genet 1993; 2: 2069-73.

Hornykiewicz O, Kish SJ. Biochemical pathophysiology of Parkinson's disease. Adv Neurol 1987; 45: 19-34.

Hsiao K, Baker HF, Crow TJ, Poulter M, Owen F, Terwilliger JD, et al. Linkage of a prion protein missense variant to Gerstmann-Straussler syndrome. Nature 1989; 338: 342-5.

Hsu LJ, Sagara Y, Arroyo A, Rockenstein E, Sisk A, Mallory M, et al. alpha-synuclein promotes mitochondrial deficit and oxidative stress. Am J Pathol 2000; 157: 401-10.

Huang CC, Lu CS, Chu NS, Hochberg F, Lilienfeld D, Olanow W, et al. Progression after chronic manganese exposure. Neurology 1993; 43: 1479-83.

Hughes AJ, Ben-Shlomo Y, Daniel SE, Lees AJ, Kilford L. What features improve the accuracy of clinical diagnosis in Parkinson's disease: a clinicopathologic study. Neurology 1992a; 42: 1142-6.

Hughes AJ, Daniel SE, Kilford L, Lees AJ. Accuracy of clinical diagnosis of idiopathic Parkinson's disease: a clinico-pathological study of 100 cases. J Neurol Neurosurg Psychiatry 1992b; 55: 181-4.

Hunot S, Boissiere F, Faucheux B, Brugg B, Mouatt-Prigent A, Agid Y, et al. Nitric oxide synthase and neuronal vulnerability in Parkinson's disease. Neuroscience 1996; 72: 355-63.

Hunot S, Brugg B, Ricard D, Michel PP, Muriel MP, Ruberg M, et al. Nuclear translocation of NF-kappaB is increased in dopaminergic neurons of patients with parkinson disease. Proc Natl Acad Sci U S A 1997; 94: 7531-6.

Hussain T, Lokhandwala MF. Renal dopamine receptor function in hypertension. Hypertension 1998; 32: 187-97.

Hutton M, Lendon CL, Rizzu P, Baker M, Froelich S, Houlden H, et al. Association of missense and 5'-splice-site mutations in tau with the inherited dementia FTDP-17. Nature 1998; 393: 702-5.

Hyun DH, Lee M, Hattori N, Kubo S, Mizuno Y, Halliwell B, et al. Effect of wild-type or mutant Parkin on oxidative damage, nitric oxide, antioxidant defenses, and the proteasome. J Biol Chem 2002; 277: 28572-7.

Ii K, Ito H, Tanaka K, Hirano A. Immunocytochemical co-localization of the proteasome in ubiquitinated structures in neurodegenerative diseases and the elderly. J Neuropathol Exp Neurol 1997; 56: 125-31.

Ikeuchi T, Asaka T, Saito M, Tanaka H, Higuchi S, Tanaka K, et al. Gene locus for autosomal recessive distal myopathy with rimmed vacuoles maps to chromosome 9. Ann Neurol 1997; 41: 432-7.

Imbert G, Saudou F, Yvert G, Devys D, Trottier Y, Garnier JM, et al. Cloning of the gene for spinocerebellar ataxia 2 reveals a locus with high sensitivity to expanded CAG/glutamine repeats. Nat Genet 1996; 14: 285-91.

Irizarry MC, Kim TW, McNamara M, Tanzi RE, George JM, Clayton DF, et al. Characterization of the precursor protein of the non-A beta component of senile plaques (NACP) in the human central nervous system. J Neuropathol Exp Neurol 1996; 55: 889-95.

Ischiropoulos H, Beckman JS. Oxidative stress and nitration in neurodegeneration: cause, effect, or association? J Clin Invest 2003; 111: 163-9.

Itier JM, Ibanez P, Mena MA, Abbas N, Cohen-Salmon C, Bohme GA, et al. Parkin gene inactivation alters behaviour and dopamine neurotransmission in the mouse. Hum Mol Genet 2003; 12: 2277-91. Epub 2003 Jul 22.

Jakes R, Spillantini MG, Goedert M. Identification of two distinct synucleins from human brain. FEBS Lett 1994; 345: 27-32.

Jana NR, Zemskov EA, Wang G, Nukina N. Altered proteasomal function due to the expression of polyglutamine- expanded truncated N-terminal huntingtin induces apoptosis by caspase activation through mitochondrial cytochrome c release. Hum Mol Genet 2001; 10: 1049-59.

Janetzky B, Hauck S, Youdim MB, Riederer P, Jellinger K, Pantucek F, et al. Unaltered aconitase activity, but decreased complex I activity in substantia nigra pars compacta of patients with Parkinson's disease. Neurosci Lett 1994; 169: 126-8.

Jellinger K, Paulus W, Grundke-Iqbal I, Riederer P, Youdim MB. Brain iron and ferritin in Parkinson's and Alzheimer's diseases. J Neural Transm Park Dis Dement Sect 1990; 2: 327-40.

Jenco JM, Rawlingson A, Daniels B, Morris AJ. Regulation of phospholipase D2: selective inhibition of mammalian phospholipase D isoenzymes by alpha- and beta-synucleins. Biochemistry 1998; 37: 4901-9.

Jenkins BG, Rosas HD, Chen YC, Makabe T, Myers R, MacDonald M, et al. 1H NMR spectroscopy studies of Huntington's disease: correlations with CAG repeat numbers. Neurology 1998; 50: 1357-65.

Jensen PH, Nielsen MS, Jakes R, Dotti CG, Goedert M. Binding of alpha-synuclein to brain vesicles is abolished by familial Parkinson's disease mutation. J Biol Chem 1998; 273: 26292-4.

Jensen PJ, Alter BJ, O'Malley KL. Alpha-synuclein protects naive but not dbcAMP-treated dopaminergic cell types from 1-methyl-4-phenylpyridinium toxicity. J Neurochem 2003; 86: 196-209.

Jo E, McLaurin J, Yip CM, St George-Hyslop P, Fraser PE. alpha-Synuclein membrane interactions and lipid specificity. J Biol Chem 2000; 275: 34328-34.

Johannsen P, Velander G, Mai J, Thorling EB, Dupont E. Glutathione peroxidase in early and advanced Parkinson's disease. J Neurol Neurosurg Psychiatry 1991; 54: 679-82.

Johnson RT, Gibbs CJ, Jr. Creutzfeldt-Jakob disease and related transmissible spongiform encephalopathies. N Engl J Med 1998; 339: 1994-2004.

Johnston JA, Ward CL, Kopito RR. Aggresomes: a cellular response to misfolded proteins. J Cell Biol 1998; 143: 1883-98.

Jones DC, Gunasekar PG, Borowitz JL, Isom GE. Dopamine-induced apoptosis is mediated by oxidative stress and Is enhanced by cyanide in differentiated PC12 cells. J Neurochem 2000; 74: 2296-304.

Jonsson G. Quantitation of fluorescence of biogenic monoamines. Prog Histochem Cytochem 1971; 2: 299-344.

Joza N, Susin SA, Daugas E, Stanford WL, Cho SK, Li CY, et al. Essential role of the mitochondrial apoptosis-inducing factor in programmed cell death. Nature 2001; 410: 549-54.

Junn E, Mouradian MM. Human alpha-synuclein over-expression increases intracellular reactive oxygen species levels and susceptibility to dopamine. Neurosci Lett 2002; 320: 146-50.

Kalivendi SV, Cunningham S, Kotamraju S, Joseph J, Hillard CJ, Kalyanaraman B. Alpha-synuclein up-regulation and aggregation during MPP+-induced apoptosis in neuroblastoma cells: intermediacy of transferrin receptor iron and hydrogen peroxide. J Biol Chem 2004; 279: 15240-7. Epub 2004 Jan 23.

Kanda S, Bishop JF, Eglitis MA, Yang Y, Mouradian MM. Enhanced vulnerability to oxidative stress by alpha-synuclein mutations and C-terminal truncation. Neuroscience 2000; 97: 279-84.

Katzman R. Alzheimer's disease. N Engl J Med 1986; 314: 964-73.

Kawaguchi Y, Okamoto T, Taniwaki M, Aizawa M, Inoue M, Katayama S, et al. CAG expansions in a novel gene for Machado-Joseph disease at chromosome 14q32.1. Nat Genet 1994; 8: 221-8.

Kawas CH, Katzman R. Epidemiology of dementia and Alzheimer disease. In: Terry RD, Katzman R, Bick KL and Sisodia SS, editors. Alzheimer disease. Philadelphia: Lippincott Williams and Wilkins, 1999: 96-116.

Kazantsev A, Walker HA, Slepko N, Bear JE, Preisinger E, Steffan JS, et al. A bivalent Huntingtin binding peptide suppresses polyglutamine aggregation and pathogenesis in Drosophila. Nat Genet 2002; 30: 367-76.

Kholodilov NG, Neystat M, Oo TF, Lo SE, Larsen KE, Sulzer D, et al. Increased expression of rat synuclein in the substantia nigra pars compacta identified by mRNA differential display in a model of developmental target injury. J Neurochem 1999; 73: 2586-99.

Kiechle T, Dedeoglu A, Kubilus J, Kowall NW, Beal MF, Friedlander RM, et al. Cytochrome C and caspase-9 expression in Huntington's disease. Neuromolecular Med 2002; 1: 183-95.

Kim KJ, Jang YY, Han ES, Lee CS. Modulation of brain mitochondrial membrane permeability and synaptosomal Ca2+ transport by dopamine oxidation. Mol Cell Biochem 1999; 201: 89-98.

Kim YJ, Yi Y, Sapp E, Wang Y, Cuiffo B, Kegel KB, et al. Caspase 3-cleaved N-terminal fragments of wild-type and mutant huntingtin are present in normal and Huntington's disease brains, associate with membranes, and undergo calpain-dependent proteolysis. Proc Natl Acad Sci U S A 2001; 98: 12784-9.

King MP, Attardi G. Human cells lacking mtDNA: repopulation with exogenous mitochondria by complementation. Science 1989; 246: 500-3.

King TE. Preparation of succinate cytochrome c reductase, and the cytochrome b-c1 particle, and reconstitution of cytochrome c reductase. Methods Enzymol 1967; 10: 216-225.

Kingsbury AE, Mardsen CD, Foster OJ. DNA fragmentation in human substantia nigra: apoptosis or perimortem effect? Mov Disord 1998; 13: 877-84.

Kirik D, Rosenblad C, Burger C, Lundberg C, Johansen TE, Muzyczka N, et al. Parkinson-like neurodegeneration induced by targeted overexpression of alpha-synuclein in the nigrostriatal system. J Neurosci 2002; 22: 2780-91.

Kish SJ, Morito C, Hornykiewicz O. Glutathione peroxidase activity in Parkinson's disease brain. Neurosci Lett 1985; 58: 343-6.

Kish SJ, Shannak K, Hornykiewicz O. Uneven pattern of dopamine loss in the striatum of patients with idiopathic Parkinson's disease. Pathophysiologic and clinical implications. N Engl J Med 1988; 318: 876-80.

Kitada T, Asakawa S, Hattori N, Matsumine H, Yamamura Y, Minoshima S, et al. Mutations in the parkin gene cause autosomal recessive juvenile parkinsonism. Nature 1998; 392: 605-8.

Kitamoto T, Muramoto T, Mohri S, Doh-Ura K, Tateishi J. Abnormal isoform of prion protein accumulates in follicular dendritic cells in mice with Creutzfeldt-Jakob disease. J Virol 1991; 65: 6292-5.

Klawans HL, Stein RW, Tanner CM, Goetz CG. A pure parkinsonian syndrome following acute carbon monoxide intoxication. Arch Neurol 1982; 39: 302-4.

Klein RL, King MA, Hamby ME, Meyer EM. Dopaminergic cell loss induced by human A30P alpha-synuclein gene transfer to the rat substantia nigra. Hum Gene Ther 2002; 13: 605-12.

Ko L, Mehta ND, Farrer M, Easson C, Hussey J, Yen S, et al. Sensitization of neuronal cells to oxidative stress with mutated human alpha-synuclein. J Neurochem 2000; 75: 2546-54.

Kocisko DA, Come JH, Priola SA, Chesebro B, Raymond GJ, Lansbury PT, et al. Cell-free formation of protease-resistant prion protein. Nature 1994; 370: 471-4.

Koide R, Ikeuchi T, Onodera O, Tanaka H, Igarashi S, Endo K, et al. Unstable expansion of CAG repeat in hereditary dentatorubral-pallidoluysian atrophy (DRPLA). Nat Genet 1994; 6: 9-13.

Kopito RR. Aggresomes, inclusion bodies and protein aggregation. Trends Cell Biol 2000; 10: 524-30.

Koroshetz WJ, Jenkins BG, Rosen BR, Beal MF. Energy metabolism defects in Huntington's disease and effects of coenzyme Q10. Ann Neurol 1997; 41: 160-5.

Kosel S, Egensperger R, von Eitzen U, Mehraein P, Graeber MB. On the question of apoptosis in the parkinsonian substantia nigra. Acta Neuropathol (Berl) 1997; 93: 105-8.

Kosel S, Grasbon-Frodl EM, Mautsch U, Egensperger R, von Eitzen U, Frishman D, et al. Novel mutations of mitochondrial complex I in pathologically proven Parkinson disease. Neurogenetics 1998; 1: 197-204.

Kovacs GG, Lindeck-Pozza E, Chimelli L, Araujo AQ, Gabbai AA, Strobel T, et al. Creutzfeldt-Jakob disease and inclusion body myositis: abundant disease-associated prion protein in muscle. Ann Neurol 2004; 55: 121-5.

Kowall NW, Hantraye P, Brouillet E, Beal MF, McKee AC, Ferrante RJ. MPTP induces alpha-synuclein aggregation in the substantia nigra of baboons. Neuroreport 2000; 11: 211-3.

Krige D, Carroll MT, Cooper JM, Marsden CD, Schapira AH. Platelet mitochondrial function in Parkinson's disease. The Royal Kings and Queens Parkinson Disease Research Group. Ann Neurol 1992; 32: 782-8.

Krueger MJ, Singer TP, Casida JE, Ramsay RR. Evidence that the blockade of mitochondrial respiration by the neurotoxin 1-methyl-4-phenylpyridinium (MPP+) involves binding at the same site as the respiratory inhibitor, rotenone. Biochem Biophys Res Commun 1990; 169: 123-8.

Kruger R, Kuhn W, Muller T, Woitalla D, Graeber M, Kosel S, et al. Ala30Pro mutation in the gene encoding alpha-synuclein in Parkinson's disease. Nat Genet 1998; 18: 106-8.

Kuiper MA, Mulder C, van Kamp GJ, Scheltens P, Wolters EC. Cerebrospinal fluid ferritin levels of patients with Parkinson's disease, Alzheimer's disease, and multiple system atrophy. J Neural Transm Park Dis Dement Sect 1994; 7: 109-14.

Kurihara LJ, Kikuchi T, Wada K, Tilghman SM. Loss of Uch-L1 and Uch-L3 leads to neurodegeneration, posterior paralysis and dysphagia. Hum Mol Genet 2001; 10: 1963-70.

La Fontaine MA, Geddes JW, Banks A, Butterfield DA. 3-nitropropionic acid induced in vivo protein oxidation in striatal and cortical synaptosomes: insights into Huntington's disease. Brain Res 2000; 858: 356-62.

La Spada AR, Wilson EM, Lubahn DB, Harding AE, Fischbeck KH. Androgen receptor gene mutations in X-linked spinal and bulbar muscular atrophy. Nature 1991; 352: 77-9.

Laforet GA, Sapp E, Chase K, McIntyre C, Boyce FM, Campbell M, et al. Changes in cortical and striatal neurons predict behavioral and electrophysiological abnormalities in a transgenic murine model of Huntington's disease. J Neurosci 2001; 21: 9112-23.

Lai CT, Yu PH. Dopamine- and L-beta-3,4-dihydroxyphenylalanine hydrochloride (L-Dopa)-induced cytotoxicity towards catecholaminergic neuroblastoma SH-SY5Y cells. Effects of oxidative stress and antioxidative factors. Biochem Pharmacol 1997; 53: 363-72.

Lampe J, Gossrau G, Reichmann H, Walter MC, Mendel B, Lochmuller H. Prion codon 129 homozygosity and sporadic inclusion body myositis. Neurology 2001; 57: 368.

Lampe J, Kitzler H, Walter MC, Lochmuller H, Reichmann H. Methionine homozygosity at prion gene codon 129 may predispose to sporadic inclusion-body myositis. Lancet 1999; 353: 465-6.

Lang AE, Lozano AM. Parkinson's disease. First of two parts. N Engl J Med 1998a; 339: 1044-53.

Lang AE, Lozano AM. Parkinson's disease. Second of two parts. N Engl J Med 1998b; 339: 1130-43.

Langeveld CH, Jongenelen CA, Schepens E, Stoof JC, Bast A, Drukarch B. Cultured rat striatal and cortical astrocytes protect mesencephalic dopaminergic neurons against hydrogen peroxide toxicity independent of their effect on neuronal development. Neurosci Lett 1995; 192: 13-6.

Langston JW, Ballard PA, Jr. Parkinson's disease in a chemist working with 1-methyl-4-phenyl-1,2,5,6- tetrahydropyridine. N Engl J Med 1983; 309: 310.

Langston JW, Irwin I, Langston EB, Forno LS. Pargyline prevents MPTP-induced parkinsonism in primates. Science 1984; 225: 1480-2.

Lansbury PT, Jr. Structural neurology: are seeds at the root of neuronal degeneration? Neuron 1997; 19: 1151-4.

Laplanche JL, Delasnerie-Laupretre N, Brandel JP, Chatelain J, Beaudry P, Alperovitch A, et al. Molecular genetics of prion diseases in France. French Research Group on Epidemiology of Human Spongiform Encephalopathies. Neurology 1994; 44: 2347-51.

Lavedan C. The synuclein family. Genome Res 1998; 8: 871-80.

LaVoie MJ, Hastings TG. Peroxynitrite- and nitrite-induced oxidation of dopamine: implications for nitric oxide in dopaminergic cell loss. J Neurochem 1999; 73: 2546-54.

Lazzarini AM, Myers RH, Zimmerman TR, Jr., Mark MH, Golbe LI, Sage JI, et al. A clinical genetic study of Parkinson's disease: evidence for dominant transmission. Neurology 1994; 44: 499-506.

Le WD, Xu P, Jankovic J, Jiang H, Appel SH, Smith RG, et al. Mutations in NR4A2 associated with familial Parkinson disease. Nat Genet 2003; 33: 85-9.

Lecerf JM, Shirley TL, Zhu Q, Kazantsev A, Amersdorfer P, Housman DE, et al. Human single-chain Fv intrabodies counteract in situ huntingtin aggregation in cellular models of Huntington's disease. Proc Natl Acad Sci U S A 2001; 98: 4764-9.

Lee CS, Han ES, Jang YY, Han JH, Ha HW, Kim DE. Protective effect of harmalol and harmaline on MPTP neurotoxicity in the mouse and dopamine-induced damage of brain mitochondria and PC12 cells. J Neurochem 2000; 75: 521-31.

Lee FJ, Liu F, Pristupa ZB, Niznik HB. Direct binding and functional coupling of alpha-synuclein to the dopamine transporters accelerate dopamine-induced apoptosis. Faseb J 2001a; 15: 916-26.

Lee HJ, Khoshaghideh F, Patel S, Lee SJ. Clearance of alpha-synuclein oligomeric intermediates via the lysosomal degradation pathway. J Neurosci 2004; 24: 1888-96.

Lee HJ, Shin SY, Choi C, Lee YH, Lee SJ. Formation and removal of alpha-synuclein aggregates in cells exposed to mitochondrial inhibitors. J Biol Chem 2002a; 277: 5411-7.

Lee HS, Brown P, Cervenakova L, Garruto RM, Alpers MP, Gajdusek DC, et al. Increased susceptibility to Kuru of carriers of the PRNP 129 methionine/methionine genotype. J Infect Dis 2001b; 183: 192-196. Epub 2000 Dec 21.

Lee M, Hyun D, Halliwell B, Jenner P. Effect of the overexpression of wild-type or mutant alpha-synuclein on cell susceptibility to insult. J Neurochem 2001c; 76: 998-1009.

Lee MK, Stirling W, Xu Y, Xu X, Qui D, Mandir AS, et al. Human alpha-synuclein-harboring familial Parkinson's disease-linked Ala- 53 --> Thr mutation causes neurodegenerative disease with alpha- synuclein aggregation in transgenic mice. Proc Natl Acad Sci U S A 2002b; 99: 8968-73.

Lehericy S, Brandel JP, Hirsch EC, Anglade P, Villares J, Scherman D, et al. Monoamine vesicular uptake sites in patients with Parkinson's disease and Alzheimer's disease, as measured by tritiated dihydrotetrabenazine autoradiography. Brain Res 1994; 659: 1-9.

Lehmensiek V, Tan EM, Schwarz J, Storch A. Expression of mutant alpha-synucleins enhances dopamine transporter- mediated MPP+ toxicity in vitro. Neuroreport 2002; 13: 1279-83.

Leroy E, Boyer R, Auburger G, Leube B, Ulm G, Mezey E, et al. The ubiquitin pathway in Parkinson's disease. Nature 1998; 395: 451-2.

Levecque C, Destee A, Mouroux V, Becquet E, Defebvre L, Amouyel P, et al. No genetic association of the ubiquitin carboxy-terminal hydrolase-L1 gene S18Y polymorphism with familial Parkinson's disease. J Neural Transm 2001; 108: 979-84.

Levine MS, Klapstein GJ, Koppel A, Gruen E, Cepeda C, Vargas ME, et al. Enhanced sensitivity to N-methyl-D-aspartate receptor activation in transgenic and knockin mouse models of Huntington's disease. J Neurosci Res 1999; 58: 515-32.

Li H, Li SH, Cheng AL, Mangiarini L, Bates GP, Li XJ. Ultrastructural localization and progressive formation of neuropil aggregates in Huntington's disease transgenic mice. Hum Mol Genet 1999; 8: 1227-36.

Li H, Li SH, Johnston H, Shelbourne PF, Li XJ. Amino-terminal fragments of mutant huntingtin show selective accumulation in striatal neurons and synaptic toxicity. Nat Genet 2000a; 25: 385-9.

Li H, Li SH, Yu ZX, Shelbourne P, Li XJ. Huntingtin aggregate-associated axonal degeneration is an early pathological event in Huntington's disease mice. J Neurosci 2001; 21: 8473-81.

Li H, Wyman T, Yu ZX, Li SH, Li XJ. Abnormal association of mutant huntingtin with synaptic vesicles inhibits glutamate release. Hum Mol Genet 2003; 12: 2021-30.

Li M, Nakagomi Y, Kobayashi Y, Merry DE, Tanaka F, Doyu M, et al. Nonneural nuclear inclusions of androgen receptor protein in spinal and bulbar muscular atrophy. Am J Pathol 1998a; 153: 695-701.

Li SH, Gutekunst CA, Hersch SM, Li XJ. Interaction of huntingtin-associated protein with dynactin P150Glued. J Neurosci 1998b; 18: 1261-9.

Li SH, Lam S, Cheng AL, Li XJ. Intranuclear huntingtin increases the expression of caspase-1 and induces apoptosis. Hum Mol Genet 2000b; 9: 2859-67.

Li SH, Li XJ. Huntingtin-protein interactions and the pathogenesis of Huntington's disease. Trends Genet 2004; 20: 146-54.

Li Y, Chin LS, Levey AI, Li L. Huntingtin-associated protein 1 interacts with hepatocyte growth factor-regulated tyrosine kinase substrate and functions in endosomal trafficking. J Biol Chem 2002; 277: 28212-21. Epub 2002 May 20.

Liesi P, Paetau A, Rechardt L, Dahl D. Glial uptake of monoamines in primary cultures of rat median raphe nucleus and cerebellum. A combined monoamine fluorescence and glial fibrillary acidic protein immunofluorescence study. Histochemistry 1981; 73: 239-50.

Lilienfeld DE. An epidemiological overview of amyotrophic lateral sclerosis, Parkinson's disease and dementia of the Alzheimer type. In: Calne DB, editor. Neurodegenerative diseases. Philadelphia: Saunders, W.B., 1994: 399-425.

Lin CH, Tallaksen-Greene S, Chien WM, Cearley JA, Jackson WS, Crouse AB, et al. Neurological abnormalities in a knock-in mouse model of Huntington's disease. Hum Mol Genet 2001; 10: 137-44.

Lindvall O, Bjorklund A. The glyoxylic acid fluorescence histochemical method: a detailed account of the methodology for the visualization of central catecholamine neurons. Histochemistry 1974; 39: 97-127.

Linnik MD, Zobrist RH, Hatfield MD. Evidence supporting a role for programmed cell death in focal cerebral ischemia in rats. Stroke 1993; 24: 2002-8; discussion 2008-9.

Liou HH, Tsai MC, Chen CJ, Jeng JS, Chang YC, Chen SY, et al. Environmental risk factors and Parkinson's disease: a case-control study in Taiwan. Neurology 1997; 48: 1583-8.

Liu Y, Fallon L, Lashuel HA, Liu Z, Lansbury PT, Jr. The UCH-L1 gene encodes two opposing enzymatic activities that affect alpha-synuclein degradation and Parkinson's disease susceptibility. Cell 2002; 111: 209-18.

Lode HN, Bruchelt G, Seitz G, Gebhardt S, Gekeler V, Niethammer D, et al. Reverse transcriptase-polymerase chain reaction (RT-PCR) analysis of monoamine transporters in neuroblastoma cell lines: correlations to meta-iodobenzylguanidine (MIBG) uptake and tyrosine hydroxylase gene expression. Eur J Cancer 1995; 31A: 586-90.

Lodi R, Schapira AH, Manners D, Styles P, Wood NW, Taylor DJ, et al. Abnormal in vivo skeletal muscle energy metabolism in Huntington's disease and dentatorubropallidoluysian atrophy. Ann Neurol 2000; 48: 72-6.

Loeffen J, Smeitink J, Triepels R, Smeets R, Schuelke M, Sengers R, et al. The first nuclear-encoded complex I mutation in a patient with Leigh syndrome. Am J Hum Genet 1998; 63: 1598-608.

Logroscino G, Marder K, Graziano J, Freyer G, Slavkovich V, Lolacono N, et al. Altered systemic iron metabolism in Parkinson's disease. Neurology 1997; 49: 714-7.

Lonze BE, Riccio A, Cohen S, Ginty DD. Apoptosis, axonal growth defects, and degeneration of peripheral neurons in mice lacking CREB. Neuron 2002; 34: 371-85.

Lotharius J, Brundin P. Impaired dopamine storage resulting from alpha-synuclein mutations may contribute to the pathogenesis of Parkinson's disease. Hum Mol Genet 2002; 11: 2395-407.

Lowe J, McDermott H, Landon M, Mayer RJ, Wilkinson KD. Ubiquitin carboxyl-terminal hydrolase (PGP 9.5) is selectively present in ubiquitinated inclusion bodies characteristic of human neurodegenerative diseases. J Pathol 1990; 161: 153-60.

Luo Y, Roth GS. The roles of dopamine oxidative stress and dopamine receptor signaling in aging and age-related neurodegeneration. Antioxid Redox Signal 2000; 2: 449-60.

Luthman J, Fredriksson A, Sundstrom E, Jonsson G, Archer T. Selective lesion of central dopamine or noradrenaline neuron systems in the neonatal rat: motor behavior and monoamine alterations at adult stage. Behav Brain Res 1989; 33: 267-77.

Lyras L, Zeng BY, McKenzie G, Pearce RK, Halliwell B, Jenner P. Chronic high dose L-DOPA alone or in combination with the COMT inhibitor entacapone does not

increase oxidative damage or impair the function of the nigro-striatal pathway in normal cynomologus monkeys. J Neural Transm 2002; 109: 53-67.

MacDonald ME, Barnes G, Srinidhi J, Duyao MP, Ambrose CM, Myers RH, et al. Gametic but not somatic instability of CAG repeat length in Huntington's disease. J Med Genet 1993; 30: 982-6.

Mangiarini L, Sathasivam K, Seller M, Cozens B, Harper A, Hetherington C, et al. Exon 1 of the HD gene with an expanded CAG repeat is sufficient to cause a progressive neurological phenotype in transgenic mice. Cell 1996; 87: 493-506.

Mann VM, Cooper JM, Daniel SE, Srai K, Jenner P, Marsden CD, et al. Complex I, iron, and ferritin in Parkinson's disease substantia nigra. Ann Neurol 1994; 36: 876-81.

Mann VM, Cooper JM, Javoy-Agid F, Agid Y, Jenner P, Schapira AH. Mitochondrial function and parental sex effect in Huntington's disease. Lancet 1990; 336: 749.

Mann VM, Cooper JM, Krige D, Daniel SE, Schapira AH, Marsden CD. Brain, skeletal muscle and platelet homogenate mitochondrial function in Parkinson's disease. Brain 1992; 115: 333-42.

Manning-Bog AB, McCormack AL, Li J, Uversky VN, Fink AL, Di Monte DA. The herbicide paraquat causes up-regulation and aggregation of alpha- synuclein in mice: paraquat and alpha-synuclein. J Biol Chem 2002; 277: 1641-4.

Maraganore DM, Farrer MJ, Hardy JA, Lincoln SJ, McDonnell SK, Rocca WA. Case-control study of the ubiquitin carboxy-terminal hydrolase L1 gene in Parkinson's disease. Neurology 1999; 53: 1858-60.

Marcora E, Gowan K, Lee JE. Stimulation of NeuroD activity by huntingtin and huntingtin-associated proteins HAP1 and MLK2. Proc Natl Acad Sci U S A 2003; 100: 9578-83. Epub 2003 Jul 24.

Marder K, Tang MX, Mejia H, Alfaro B, Cote L, Louis E, et al. Risk of Parkinson's disease among first-degree relatives: A community-based study. Neurology 1996; 47: 155-60.

Marks L, Turner K, O'Sullivan J, Deighton B, Lees A. Drooling in Parkinson's disease: a novel speech and language therapy intervention. Int J Lang Commun Disord 2001; 36: 282-7.

Maroteaux L, Campanelli JT, Scheller RH. Synuclein: a neuron-specific protein localized to the nucleus and presynaptic nerve terminal. J Neurosci 1988; 8: 2804-15.

Marsden CD. Parkinson's disease in twins. J Neurol Neurosurg Psychiatry 1987; 50: 105-6.

Martin ER, Scott WK, Nance MA, Watts RL, Hubble JP, Koller WC, et al. Association of single-nucleotide polymorphisms of the tau gene with late-onset Parkinson disease. Jama 2001; 286: 2245-50.

Martin MA, Molina JA, Jimenez-Jimenez FJ, Benito-Leon J, Orti-Pareja M, Campos Y, et al. Respiratory-chain enzyme activities in isolated mitochondria of lymphocytes from untreated Parkinson's disease patients. Grupo-Centro de Trastornos del Movimiento. Neurology 1996; 46: 1343-6.

Martindale D, Hackam A, Wieczorek A, Ellerby L, Wellington C, McCutcheon K, et al. Length of huntingtin and its polyglutamine tract influences localization and frequency of intracellular aggregates. Nat Genet 1998; 18: 150-4.

Marttila RJ, Kaprio J, Koskenvuo M, Rinne UK. Parkinson's disease in a nationwide twin cohort. Neurology 1988a; 38: 1217-9.

Marttila RJ, Lorentz H, Rinne UK. Oxygen toxicity protecting enzymes in Parkinson's disease. Increase of superoxide dismutase-like activity in the substantia nigra and basal nucleus. J Neurol Sci 1988b; 86: 321-31.

Marx FP, Holzmann C, Strauss KM, Li L, Eberhardt O, Gerhardt E, et al. Identification and functional characterization of a novel R621C mutation in the synphilin-1 gene in Parkinson's disease. Hum Mol Genet 2003; 12: 1223-31.

Masliah E, Rockenstein E, Veinbergs I, Mallory M, Hashimoto M, Takeda A, et al. Dopaminergic loss and inclusion body formation in alpha-synuclein mice: implications for neurodegenerative disorders. Science 2000; 287: 1265-9.

Matsuoka Y, Vila M, Lincoln S, McCormack A, Picciano M, LaFrancois J, et al. Lack of nigral pathology in transgenic mice expressing human alpha- synuclein driven by the tyrosine hydroxylase promoter. Neurobiol Dis 2001; 8: 535-9.

Mattson MP, Goodman Y, Luo H, Fu W, Furukawa K. Activation of NF-kappaB protects hippocampal neurons against oxidative stress-induced apoptosis: evidence for induction of manganese superoxide dismutase and suppression of peroxynitrite production and protein tyrosine nitration. J Neurosci Res 1997; 49: 681-97.

Mayr-Wohlfart U, Rodel G, Henneberg A. Mitochondrial tRNA(Gln) and tRNA(Thr) gene variants in Parkinson's disease. Eur J Med Res 1997; 2: 111-3.

McGeer PL, Itagaki S, Boyes BE, McGeer EG. Reactive microglia are positive for HLA-DR in the substantia nigra of Parkinson's and Alzheimer's disease brains. Neurology 1988; 38: 1285-91.

McLaughlin BA, Nelson D, Erecinska M, Chesselet MF. Toxicity of dopamine to striatal neurons in vitro and potentiation of cell death by a mitochondrial inhibitor. J Neurochem 1998; 70: 2406-15.

McLean PJ, Kawamata H, Ribich S, Hyman BT. Membrane association and protein conformation of alpha-synuclein in intact neurons. Effect of Parkinson's disease-linked mutations. J Biol Chem 2000; 275: 8812-6.

McNaught KS, Belizaire R, Jenner P, Olanow CW, Isacson O. Selective loss of 20S proteasome alpha-subunits in the substantia nigra pars compacta in Parkinson's disease. Neurosci Lett 2002a; 326: 155-8.

McNaught KS, Jenner P. Proteasomal function is impaired in substantia nigra in Parkinson's disease. Neurosci Lett 2001; 297: 191-4.

McNaught KS, Olanow CW, Halliwell B, Isacson O, Jenner P. Failure of the ubiquitin-proteasome system in Parkinson's disease. Nat Rev Neurosci 2001; 2: 589-94.

McNaught KS, Shashidharan P, Perl DP, Jenner P, Olanow CW. Aggresome-related biogenesis of Lewy bodies. Eur J Neurosci 2002b; 16: 2136-48.

Mead S, Stumpf MP, Whitfield J, Beck JA, Poulter M, Campbell T, et al. Balancing selection at the prion protein gene consistent with prehistoric kurulike epidemics. Science 2003; 300: 640-3. Epub 2003 Apr 10.

Melo F, Carey DJ, Brandan E. Extracellular matrix is required for skeletal muscle differentiation but not myogenin expression. J Cell Biochem 1996; 62: 227-39.

Mena I. Manganese poisoning. In: Vinken PJ and Bruyn GW, editors. Intoxications of the Nervous System, part I. Amsterdam, North Holland, 1979: 217-237.

Mendell JR, Sahenk Z, Gales T, Paul L. Amyloid filaments in inclusion body myositis. Novel findings provide insight into nature of filaments. Arch Neurol 1991; 48: 1229-34.

Metzler M, Helgason CD, Dragatsis I, Zhang T, Gan L, Pineault N, et al. Huntingtin is required for normal hematopoiesis. Hum Mol Genet 2000; 9: 387-94.

Michel PP, Hefti F. Toxicity of 6-hydroxydopamine and dopamine for dopaminergic neurons in culture. J Neurosci Res 1990; 26: 428-35.

Mirza B, Hadberg H, Thomsen P, Moos T. The absence of reactive astrocytosis is indicative of a unique inflammatory process in Parkinson's disease. Neuroscience 2000; 95: 425-32.

Mitsumoto A, Nakagawa Y. DJ-1 is an indicator for endogenous reactive oxygen species elicited by endotoxin. Free Radic Res 2001; 35: 885-93.

Mitsumoto A, Nakagawa Y, Takeuchi A, Okawa K, Iwamatsu A, Takanezawa Y. Oxidized forms of peroxiredoxins and DJ-1 on two-dimensional gels increased in response to sublethal levels of paraquat. Free Radic Res 2001; 35: 301-10.

Mizuno Y, Matuda S, Yoshino H, Mori H, Hattori N, Ikebe S. An immunohistochemical study on alpha-ketoglutarate dehydrogenase complex in Parkinson's disease. Ann Neurol 1994; 35: 204-10.

Mizuno Y, Saitoh T, Sone N. Inhibition of mitochondrial NADH-ubiquinone oxidoreductase activity by 1-methyl-4-phenylpyridinium ion. Biochem Biophys Res Commun 1987; 143: 294-9.

Mochizuki H, Goto K, Mori H, Mizuno Y. Histochemical detection of apoptosis in Parkinson's disease. J Neurol Sci 1996; 137: 120-3.

Mogi M, Harada M, Kondo T, Mizuno Y, Narabayashi H, Riederer P, et al. The soluble form of Fas molecule is elevated in parkinsonian brain tissues. Neurosci Lett 1996; 220: 195-8.

Morales LM, Estevez J, Suarez H, Villalobos R, Chacin de Bonilla L, Bonilla E. Nutritional evaluation of Huntington disease patients. Am J Clin Nutr 1989; 50: 145-50.

Morikawa N, Nakagawa-Hattori Y, Mizuno Y. Effect of dopamine, dimethoxyphenylethylamine, papaverine, and related compounds on mitochondrial respiration and complex I activity. J Neurochem 1996; 66: 1174-81.

Morishima N, Nakanishi K, Takenouchi H, Shibata T, Yasuhiko Y. An endoplasmic reticulum stress-specific caspase cascade in apoptosis. Cytochrome c-independent activation of caspase-9 by caspase-12. J Biol Chem 2002; 277: 34287-94. Epub 2002 Jul 3.

Muqit MM, Feany MB. Modelling neurodegenerative diseases in Drosophila: a fruitful approach? Nat Rev Neurosci 2002; 3: 237-43.

Murphy DD, Rueter SM, Trojanowski JQ, Lee VM. Synucleins are developmentally expressed, and alpha-synuclein regulates the size of the presynaptic vesicular pool in primary hippocampal neurons. J Neurosci 2000; 20: 3214-20.

Mytilineou C, Werner P, Molinari S, Di Rocco A, Cohen G, Yahr MD. Impaired oxidative decarboxylation of pyruvate in fibroblasts from patients with Parkinson's disease. J Neural Transm Park Dis Dement Sect 1994; 8: 223-8.

Nagafuchi S, Yanagisawa H, Sato K, Shirayama T, Ohsaki E, Bundo M, et al. Dentatorubral and pallidoluysian atrophy expansion of an unstable CAG trinucleotide on chromosome 12p. Nat Genet 1994; 6: 14-8.

Nakagawa T, Zhu H, Morishima N, Li E, Xu J, Yankner BA, et al. Caspase-12 mediates endoplasmic-reticulum-specific apoptosis and cytotoxicity by amyloid-beta. Nature 2000; 403: 98-103.

Nakagawa-Hattori Y, Yoshino H, Kondo T, Mizuno Y, Horai S. Is Parkinson's disease a mitochondrial disorder? J Neurol Sci 1992; 107: 29-33.

Nakamura K, Jeong SY, Uchihara T, Anno M, Nagashima K, Nagashima T, et al. SCA17, a novel autosomal dominant cerebellar ataxia caused by an expanded polyglutamine in TATA-binding protein. Hum Mol Genet 2001; 10: 1441-8.

Nam S, Smith DM, Dou QP. Ester bond-containing tea polyphenols potently inhibit proteasome activity in vitro and in vivo. J Biol Chem 2001; 276: 13322-30. Epub 2001 Jan 26.

Narhi L, Wood SJ, Steavenson S, Jiang Y, Wu GM, Anafi D, et al. Both familial Parkinson's disease mutations accelerate alpha-synuclein aggregation. J Biol Chem 1999; 274: 9843-6.

Nasir J, Floresco SB, O'Kusky JR, Diewert VM, Richman JM, Zeisler J, et al. Targeted disruption of the Huntington's disease gene results in embryonic lethality and behavioral and morphological changes in heterozygotes. Cell 1995; 81: 811-23.

Navas P, Fernandez-Ayala DM, Martin SF, Lopez-Lluch G, De Caboa R, Rodriguez-Aguilera JC, et al. Ceramide-dependent caspase 3 activation is prevented by coenzyme Q from plasma membrane in serum-deprived cells. Free Radic Res 2002; 36: 369-74.

Neuwald AF, Hirano T. HEAT repeats associated with condensins, cohesins, and other complexes involved in chromosome-related functions. Genome Res 2000; 10: 1445-52.

Nicholls DG, Ward MW. Mitochondrial membrane potential and neuronal glutamate excitotoxicity: mortality and millivolts. Trends Neurosci 2000; 23: 166-74.

Nicklas WJ, Vyas I, Heikkila RE. Inhibition of NADH-linked oxidation in brain mitochondria by 1-methyl-4-phenyl-pyridine, a metabolite of the neurotoxin, 1-methyl-4-phenyl-1,2,5,6-tetrahydropyridine. Life Sci 1985; 36: 2503-8.

Oesch B, Westaway D, Walchli M, McKinley MP, Kent SB, Aebersold R, et al. A cellular gene encodes scrapie PrP 27-30 protein. Cell 1985; 40: 735-46.

Okada T, Shimada S, Sato K, Kotake Y, Kawai H, Ohta S, et al. Tetrahydropapaveroline and its derivatives inhibit dopamine uptake through dopamine transporter expressed in HEK293 cells. Neurosci Res 1998; 30: 87-90.

Olanow CW. Magnetic resonance imaging in parkinsonism. Neurol Clin 1992; 10: 405-20.

Olanow CW, Tatton WG. Etiology and pathogenesis of Parkinson's disease. Annu Rev Neurosci 1999; 22: 123-44.

Ona VO, Li M, Vonsattel JP, Andrews LJ, Khan SQ, Chung WM, et al. Inhibition of caspase-1 slows disease progression in a mouse model of Huntington's disease. Nature 1999; 399: 263-7.

Ormerod M, G., editor. Flow cytometry. Oxford: Oxford University Press, 2000.

Orr HT, Chung MY, Banfi S, Kwiatkowski TJ, Jr., Servadio A, Beaudet AL, et al. Expansion of an unstable trinucleotide CAG repeat in spinocerebellar ataxia type 1. Nat Genet 1993; 4: 221-6.

Osmond AP, Berthelier V, Wetzel R. Identification of aggregation foci, intracellular neuronal structures in the neocortex in Huntington's disease capable of recruiting polyglutamine. Soc Neurosci Abstr 2002; 293: 6.

Ostrerova-Golts N, Petrucelli L, Hardy J, Lee JM, Farer M, Wolozin B. The A53T alpha-synuclein mutation increases iron-dependent aggregation and toxicity. J Neurosci 2000; 20: 6048-54.

Owen F, Poulter M, Collinge J, Crow TJ. Codon 129 changes in the prion protein gene in Caucasians. Am J Hum Genet 1990; 46: 1215-6.

Pacholczyk T, Blakely RD, Amara SG. Expression cloning of a cocaine- and antidepressant-sensitive human noradrenaline transporter. Nature 1991; 350: 350-4.

Palmer MS, Dryden AJ, Hughes JT, Collinge J. Homozygous prion protein genotype predisposes to sporadic Creutzfeldt-Jakob disease. Nature 1991; 352: 340-2.

Pan KM, Baldwin M, Nguyen J, Gasset M, Serban A, Groth D, et al. Conversion of alpha-helices into beta-sheets features in the formation of the scrapie prion proteins. Proc Natl Acad Sci U S A 1993; 90: 10962-6.

Pandey S, Lopez C, Jammu A. Oxidative stress and activation of proteasome protease during serum deprivation-induced apoptosis in rat hepatoma cells; inhibition of cell death by melatonin. Apoptosis 2003; 8: 497-508.

Panov AV, Gutekunst CA, Leavitt BR, Hayden MR, Burke JR, Strittmatter WJ, et al. Early mitochondrial calcium defects in Huntington's disease are a direct effect of polyglutamines. Nat Neurosci 2002; 5: 731-6.

Parchi P, Capellari S, Chen SG, Petersen RB, Gambetti P, Kopp N, et al. Typing prion isoforms. Nature 1997; 386: 232-4.

Parchi P, Giese A, Capellari S, Brown P, Schulz-Schaeffer W, Windl O, et al. Classification of sporadic Creutzfeldt-Jakob disease based on molecular and phenotypic analysis of 300 subjects. Ann Neurol 1999; 46: 224-33.

Parchi P, Zou W, Wang W, Brown P, Capellari S, Ghetti B, et al. Genetic influence on the structural variations of the abnormal prion protein. Proc Natl Acad Sci U S A 2000; 97: 10168-72.

Parti R, Ozkan ED, Harnadek GJ, Njus D. Inhibition of norepinephrine transport and reserpine binding by reserpine derivatives. J Neurochem 1987; 48: 949-53.

Patel M, Day BJ, Crapo JD, Fridovich I, McNamara JO. Requirement for superoxide in excitotoxic cell death. Neuron 1996; 16: 345-55.

Paulson HL, Perez MK, Trottier Y, Trojanowski JQ, Subramony SH, Das SS, et al. Intranuclear inclusions of expanded polyglutamine protein in spinocerebellar ataxia type 3. Neuron 1997; 19: 333-44.

Paxinou E, Chen Q, Weisse M, Giasson BI, Norris EH, Rueter SM, et al. Induction of alpha-synuclein aggregation by intracellular nitrative insult. J Neurosci 2001; 21: 8053-61.

Payami H, Larsen K, Bernard S, Nutt J. Increased risk of Parkinson's disease in parents and siblings of patients. Ann Neurol 1994; 36: 659-61.

Peng SL, Fatenejad S, Craft J. Scleroderma: a disease related to damaged proteins? Nat Med 1997; 3: 276-8.

Perez RG, Waymire JC, Lin E, Liu JJ, Guo F, Zigmond MJ. A role for alpha-synuclein in the regulation of dopamine biosynthesis. J Neurosci 2002; 22: 3090-9.

Perez-Severiano F, Rios C, Segovia J. Striatal oxidative damage parallels the expression of a neurological phenotype in mice transgenic for the mutation of Huntington's disease. Brain Res 2000; 862: 234-7.

Perrin RJ, Woods WS, Clayton DF, George JM. Interaction of human alpha-Synuclein and Parkinson's disease variants with phospholipids. Structural analysis using site-directed mutagenesis. J Biol Chem 2000; 275: 34393-8.

Perry TL, Godin DV, Hansen S. Parkinson's disease: a disorder due to nigral glutathione deficiency? Neurosci Lett 1982; 33: 305-10.

Perry TL, Yong VW, Ito M, Foulks JG, Wall RA, Godin DV, et al. Nigrostriatal dopaminergic neurons remain undamaged in rats given high doses of L-DOPA and carbidopa chronically. J Neurochem 1984; 43: 990-3.

Perutz MF. Polar zippers: their role in human disease. Pharm Acta Helv 1995; 69: 213-24.

Perutz MF, Johnson T, Suzuki M, Finch JT. Glutamine repeats as polar zippers: their possible role in inherited neurodegenerative diseases. Proc Natl Acad Sci U S A 1994; 91: 5355-8.

Petchanikow C, Saborio GP, Anderes L, Frossard MJ, Olmedo MI, Soto C. Biochemical and structural studies of the prion protein polymorphism. FEBS Lett 2001; 509: 451-6.

Petrovitch H, Ross GW, Abbott RD, Sanderson WT, Sharp DS, Tanner CM, et al. Plantation work and risk of Parkinson disease in a population-based longitudinal study. Arch Neurol 2002; 59: 1787-92.

Petty RK, Harding AE, Morgan-Hughes JA. The clinical features of mitochondrial myopathy. Brain 1986; 109: 915-38.

Piccini P, Burn DJ, Ceravolo R, Maraganore D, Brooks DJ. The role of inheritance in sporadic Parkinson's disease: evidence from a longitudinal study of dopaminergic function in twins. Ann Neurol 1999; 45: 577-82.

Pickart CM. Mechanisms underlying ubiquitination. Annu Rev Biochem 2001; 70: 503-33.

Picklo MJ, Amarnath V, McIntyre JO, Graham DG, Montine TJ. 4-Hydroxy-2(E)-nonenal inhibits CNS mitochondrial respiration at multiple sites. J Neurochem 1999; 72: 1617-24.

Pleasure SJ, Lee VM. NTera 2 cells: a human cell line which displays characteristics expected of a human committed neuronal progenitor cell. J Neurosci Res 1993; 35: 585-602.

Pleasure SJ, Page C, Lee VM. Pure, postmitotic, polarized human neurons derived from NTera 2 cells provide a system for expressing exogenous proteins in terminally differentiated neurons. J Neurosci 1992; 12: 1802-15.

Poirier MA, Li H, Macosko J, Cai S, Amzel M, Ross CA. Huntingtin spheroids and protofibrils as precursors in polyglutamine fibrilization. J Biol Chem 2002; 277: 41032-7. Epub 2002 Aug 8.

Polidori MC, Mecocci P, Browne SE, Senin U, Beal MF. Oxidative damage to mitochondrial DNA in Huntington's disease parietal cortex. Neurosci Lett 1999; 272: 53-6.

Polymeropoulos MH, Higgins JJ, Golbe LI, Johnson WG, Ide SE, Di Iorio G, et al. Mapping of a gene for Parkinson's disease to chromosome 4q21-q23. Science 1996; 274: 1197-9.

Polymeropoulos MH, Lavedan C, Leroy E, Ide SE, Dehejia A, Dutra A, et al. Mutation in the alpha-synuclein gene identified in families with Parkinson's disease. Science 1997; 276: 2045-7.

Pratley RE, Salbe AD, Ravussin E, Caviness JN. Higher sedentary energy expenditure in patients with Huntington's disease. Ann Neurol 2000; 47: 64-70.

Presgraves SP, Ahmed T, Borwege S, Joyce JN. Terminally differentiated SH-SY5Y cells provide a model system for studying neuroprotective effects of dopamine agonists. Neurotox Res 2004; 5: 579-98.

Pruitt JN, 2nd, Showalter CJ, Engel AG. Sporadic inclusion body myositis: counts of different types of abnormal fibers. Ann Neurol 1996; 39: 139-43.

Prusiner SB. Shattuck lecture--neurodegenerative diseases and prions. N Engl J Med 2001; 344: 1516-26.

Pulst SM, Nechiporuk A, Nechiporuk T, Gispert S, Chen XN, Lopes-Cendes I, et al. Moderate expansion of a normally biallelic trinucleotide repeat in spinocerebellar ataxia type 2. Nat Genet 1996; 14: 269-76.

Quinn N, Parkes D, Janota I, Marsden CD. Preservation of the substantia nigra and locus coeruleus in a patient receiving levodopa (2 kg) plus decarboxylase inhibitor over a four-year period. Mov Disord 1986; 1: 65-8.

Radunovic A, Porto WG, Zeman S, Leigh PN. Increased mitochondrial superoxide dismutase activity in Parkinson's disease but not amyotrophic lateral sclerosis motor cortex. Neurosci Lett 1997; 239: 105-8.

Ragan CI, Wilson MT, Darley-Usmar VM, Lowe PN. Subfractionation of mitochondria, and isolation of the proteins of oxidative phosphorylation. In: Darley-Usmar VM, Rickwood D and Wilson MT, editors. Mitochondria, a practical approach. London: IRL Press, 1987: 79-112.

Rajput AH, Fenton M, Birdi S, Macaulay R. Is levodopa toxic to human substantia nigra? Mov Disord 1997; 12: 634-8.

Ramsay RR, Salach JI, Dadgar J, Singer TP. Inhibition of mitochondrial NADH dehydrogenase by pyridine derivatives and its possible relation to experimental and idiopathic parkinsonism. Biochem Biophys Res Commun 1986; 135: 269-75.

Ramsay RR, Singer TP. Energy-dependent uptake of N-methyl-4-phenylpyridinium, the neurotoxic metabolite of 1-methyl-4-phenyl-1,2,3,6-tetrahydropyridine, by mitochondria. J Biol Chem 1986; 261: 7585-7.

Reddy PH, Williams M, Charles V, Garrett L, Pike-Buchanan L, Whetsell WO, Jr., et al. Behavioural abnormalities and selective neuronal loss in HD transgenic mice expressing mutated full-length HD cDNA. Nat Genet 1998; 20: 198-202.

Redfearn ER. Isolation and determination of ubiquinone. Methods Enzymol 1967; 10: 381-384.

Reichmann H, Janetzky B, Bischof F, Seibel P, Schols L, Kuhn W, et al. Unaltered respiratory chain enzyme activity and mitochondrial DNA in skeletal muscle from patients with idiopathic Parkinson's syndrome. Eur Neurol 1994; 34: 263-7.

Reiner A, Albin RL, Anderson KD, D'Amato CJ, Penney JB, Young AB. Differential loss of striatal projection neurons in Huntington disease. Proc Natl Acad Sci U S A 1988; 85: 5733-7.

Reith ME, Xu C, Chen NH. Pharmacology and regulation of the neuronal dopamine transporter. Eur J Pharmacol 1997; 324: 1-10.

Riederer P, Sofic E, Rausch WD, Schmidt B, Reynolds GP, Jellinger K, et al. Transition metals, ferritin, glutathione, and ascorbic acid in parkinsonian brains. J Neurochem 1989; 52: 515-20.

Rigamonti D, Bauer JH, De-Fraja C, Conti L, Sipione S, Sciorati C, et al. Wild-type huntingtin protects from apoptosis upstream of caspase-3. J Neurosci 2000; 20: 3705-13.

Rigamonti D, Sipione S, Goffredo D, Zuccato C, Fossale E, Cattaneo E. Huntingtin's neuroprotective activity occurs via inhibition of procaspase-9 processing. J Biol Chem 2001; 276: 14545-8.

Ross CA. Polyglutamine pathogenesis: emergence of unifying mechanisms for Huntington's disease and related disorders. Neuron 2002; 35: 819-22.

Ross GW, Abbott RD, Petrovitch H, White LR, Tanner CM. Relationship between caffeine intake and parkinson disease. Jama 2000; 284: 1378-9.

Ross RA, Spengler BA, Biedler JL. Coordinate morphological and biochemical interconversion of human neuroblastoma cells. J Natl Cancer Inst 1983; 71: 741-7.

Ruan Q, Lesort M, MacDonald ME, Johnson GV. Striatal cells from mutant huntingtin knock-in mice are selectively vulnerable to mitochondrial complex II inhibitor-induced cell death through a non-apoptotic pathway. Hum Mol Genet 2004; 13: 669-81. Epub 2004 Feb 12.

Rukenstein A, Rydel RE, Greene LA. Multiple agents rescue PC12 cells from serum-free cell death by translation- and transcription-independent mechanisms. J Neurosci 1991; 11: 2552-63.

Sadeh M, Gadoth N, Hadar H, Ben-David E. Vacuolar myopathy sparing the quadriceps. Brain 1993; 116: 217-32.

Saggu H, Cooksey J, Dexter D, Wells FR, Lees A, Jenner P, et al. A selective increase in particulate superoxide dismutase activity in parkinsonian substantia nigra. J Neurochem 1989; 53: 692-7.

Saha AR, Hill J, Utton MA, Asuni AA, Ackerley S, Grierson AJ, et al. Parkinson's disease alpha-synuclein mutations exhibit defective axonal transport in cultured neurons. J Cell Sci 2004; 117: 1017-24.

Sakahira H, Enari M, Nagata S. Cleavage of CAD inhibitor in CAD activation and DNA degradation during apoptosis. Nature 1998; 391: 96-9.

Sambrook J, Fritsch EF, Maniatis T. Molecular cloning: A laboratory manual. New York: Cold Spring Harbor Laboratory Press, 1989.

Sanberg PR, Fibiger HC, Mark RF. Body weight and dietary factors in Huntington's disease patients compared with matched controls. Med J Aust 1981; 1: 407-9.

Sanchez I, Mahlke C, Yuan J. Pivotal role of oligomerization in expanded polyglutamine neurodegenerative disorders. Nature 2003; 421: 373-9.

Sanchez I, Xu CJ, Juo P, Kakizaka A, Blenis J, Yuan J. Caspase-8 is required for cell death induced by expanded polyglutamine repeats. Neuron 1999; 22: 623-33.

Sanchez-Ramos J, Overvik E, Ames BN. A marker of oxyradical-mediated DNA damage (8-hydroxy-2'deoxyguanosin) is increased in nigro-striatum of Parkinson's disease brain. Neurodegeneration 1994; 3: 197-204.

Sandri G, Panfili E, Ernster L. Hydrogen peroxide production by monoamine oxidase in isolated rat-brain mitochondria: its effect on glutathione levels and Ca2+ efflux. Biochim Biophys Acta 1990; 1035: 300-5.

Sapp E, Schwarz C, Chase K, Bhide PG, Young AB, Penney J, et al. Huntingtin localization in brains of normal and Huntington's disease patients. Ann Neurol 1997; 42: 604-12.

Sarkozi E, Askanas V, Engel WK. Abnormal accumulation of prion protein mRNA in muscle fibers of patients with sporadic inclusion-body myositis and hereditary inclusion-body myopathy. Am J Pathol 1994; 145: 1280-4.

Sarkozi E, Askanas V, Johnson SA, Engel WK, Alvarez RB. beta-Amyloid precursor protein mRNA is increased in inclusion-body myositis muscle. Neuroreport 1993; 4: 815-8.

Sathasivam K, Hobbs C, Turmaine M, Mangiarini L, Mahal A, Bertaux F, et al. Formation of polyglutamine inclusions in non-CNS tissue. Hum Mol Genet 1999; 8: 813-22.

Sathasivam K, Woodman B, Mahal A, Bertaux F, Wanker EE, Shima DT, et al. Centrosome disorganization in fibroblast cultures derived from R6/2 Huntington's disease (HD) transgenic mice and HD patients. Hum Mol Genet 2001; 10: 2425-35.

Sato T, Oyake M, Nakamura K, Nakao K, Fukusima Y, Onodera O, et al. Transgenic mice harboring a full-length human mutant DRPLA gene exhibit age-dependent intergenerational and somatic instabilities of CAG repeats comparable with those in DRPLA patients. Hum Mol Genet 1999; 8: 99-106.

Satoh JI, Kuroda Y. Ubiquitin C-terminal hydrolase-L1 (PGP9.5) expression in human neural cell lines following induction of neuronal differentiation and exposure to cytokines, neurotrophic factors or heat stress. Neuropathol Appl Neurobiol 2001; 27: 95-104.

Saudou F, Finkbeiner S, Devys D, Greenberg ME. Huntingtin acts in the nucleus to induce apoptosis but death does not correlate with the formation of intranuclear inclusions. Cell 1998; 95: 55-66.

Sawa A, Wiegand GW, Cooper J, Margolis RL, Sharp AH, Lawler JF, Jr., et al. Increased apoptosis of Huntington disease lymphoblasts associated with repeat length-dependent mitochondrial depolarization. Nat Med 1999; 5: 1194-8.

Schapira AH, Cooper JM, Dexter D, Clark JB, Jenner P, Marsden CD. Mitochondrial complex I deficiency in Parkinson's disease. J Neurochem 1990a; 54: 823-7.

Schapira AH, Cooper JM, Dexter D, Jenner P, Clark JB, Marsden CD. Mitochondrial complex I deficiency in Parkinson's disease. Lancet 1989; 1: 1269.

Schapira AH, Mann VM, Cooper JM, Dexter D, Daniel SE, Jenner P, et al. Anatomic and disease specificity of NADH CoQ1 reductase (complex I) deficiency in Parkinson's disease. J Neurochem 1990b; 55: 2142-5.

Scherzinger E, Lurz R, Turmaine M, Mangiarini L, Hollenbach B, Hasenbank R, et al. Huntingtin-encoded polyglutamine expansions form amyloid-like protein aggregates in vitro and in vivo. Cell 1997; 90: 549-58.

Scherzinger E, Sittler A, Schweiger K, Heiser V, Lurz R, Hasenbank R, et al. Self-assembly of polyglutamine-containing huntingtin fragments into amyloid-like fibrils: implications for Huntington's disease pathology. Proc Natl Acad Sci U S A 1999; 96: 4604-9.

Schilling G, Becher MW, Sharp AH, Jinnah HA, Duan K, Kotzuk JA, et al. Intranuclear inclusions and neuritic aggregates in transgenic mice expressing a mutant N-terminal fragment of huntingtin. Hum Mol Genet 1999; 8: 397-407.

Schinder AF, Olson EC, Spitzer NC, Montal M. Mitochondrial dysfunction is a primary event in glutamate neurotoxicity. J Neurosci 1996; 16: 6125-33.

Schlossmacher MG, Frosch MP, Gai WP, Medina M, Sharma N, Forno L, et al. Parkin localizes to the Lewy bodies of Parkinson disease and dementia with Lewy bodies. Am J Pathol 2002; 160: 1655-67.

Schluter OM, Fornai F, Alessandri MG, Takamori S, Geppert M, Jahn R, et al. Role of alpha-synuclein in 1-methyl-4-phenyl-1,2,3,6-tetrahydropyridine-induced parkinsonism in mice. Neuroscience 2003; 118: 985-1002.

Schuelke M, Smeitink J, Mariman E, Loeffen J, Plecko B, Trijbels F, et al. Mutant NDUFV1 subunit of mitochondrial complex I causes leukodystrophy and myoclonic epilepsy. Nat Genet 1999; 21: 260-1.

Schulz-Schaeffer WJ, Giese A, Windl O, Kretzschmar HA. Polymorphism at codon 129 of the prion protein gene determines cerebellar pathology in Creutzfeldt-Jakob disease. Clin Neuropathol 1996; 15: 353-7.

Seidler A, Hellenbrand W, Robra BP, Vieregge P, Nischan P, Joerg J, et al. Possible environmental, occupational, and other etiologic factors for Parkinson's disease: a case-control study in Germany. Neurology 1996; 46: 1275-84.

Semchuk KM, Love EJ, Lee RG. Parkinson's disease and exposure to agricultural work and pesticide chemicals. Neurology 1992; 42: 1328-35.

Serpell LC, Berriman J, Jakes R, Goedert M, Crowther RA. Fiber diffraction of synthetic alpha-synuclein filaments shows amyloid- like cross-beta conformation. Proc Natl Acad Sci U S A 2000; 97: 4897-902.

Sharp AH, Loev SJ, Schilling G, Li SH, Li XJ, Bao J, et al. Widespread expression of Huntington's disease gene (IT15) protein product. Neuron 1995; 14: 1065-74.

Sharp AH, Ross CA. Neurobiology of Huntington's disease. Neurobiol Dis 1996; 3: 3-15.

Shashidharan P, Good PF, Hsu A, Perl DP, Brin MF, Olanow CW. TorsinA accumulation in Lewy bodies in sporadic Parkinson's disease. Brain Res 2000; 877: 379-81.

Shaw G, Morse S, Ararat M, Graham FL. Preferential transformation of human neuronal cells by human adenoviruses and the origin of HEK 293 cells. Faseb J 2002; 16: 869-71. Epub 2002 Apr 10.

Shelbourne PF, Killeen N, Hevner RF, Johnston HM, Tecott L, Lewandoski M, et al. A Huntington's disease CAG expansion at the murine Hdh locus is unstable and associated with behavioural abnormalities in mice. Hum Mol Genet 1999; 8: 763-74.

Shen XM, Zhang F, Dryhurst G. Oxidation of dopamine in the presence of cysteine: characterization of new toxic products. Chem Res Toxicol 1997; 10: 147-55.

Shenkar R, Navidi W, Tavare S, Dang MH, Chomyn A, Attardi G, et al. The mutation rate of the human mtDNA deletion mtDNA4977. Am J Hum Genet 1996; 59: 772-80.

Sherer TB, Betarbet R, Stout AK, Lund S, Baptista M, Panov AV, et al. An in vitro model of Parkinson's disease: linking mitochondrial impairment to altered alpha-synuclein metabolism and oxidative damage. J Neurosci 2002; 22: 7006-15.

Sherer TB, Kim JH, Betarbet R, Greenamyre JT. Subcutaneous rotenone exposure causes highly selective dopaminergic degeneration and alpha-synuclein aggregation. Exp Neurol 2003; 179: 9-16.

Sherman MY, Goldberg AL. Cellular defenses against unfolded proteins: a cell biologist thinks about neurodegenerative diseases. Neuron 2001; 29: 15-32.

Shimada H, Hirai K, Simamura E, Pan J. Mitochondrial NADH-quinone oxidoreductase of the outer membrane is responsible for paraquat cytotoxicity in rat livers. Arch Biochem Biophys 1998; 351: 75-81.

Shimizu K, Ohtaki K, Matsubara K, Aoyama K, Uezono T, Saito O, et al. Carrier-mediated processes in blood--brain barrier penetration and neural uptake of paraquat. Brain Res 2001; 906: 135-42.

Shimura H, Hattori N, Kubo S, Mizuno Y, Asakawa S, Minoshima S, et al. Familial Parkinson disease gene product, parkin, is a ubiquitin-protein ligase. Nat Genet 2000; 25: 302-5.

Shimura H, Hattori N, Kubo S, Yoshikawa M, Kitada T, Matsumine H, et al. Immunohistochemical and subcellular localization of Parkin protein: absence of protein in autosomal recessive juvenile parkinsonism patients. Ann Neurol 1999; 45: 668-72.

Shimura-Miura H, Hattori N, Kang D, Miyako K, Nakabeppu Y, Mizuno Y. Increased 8-oxo-dGTPase in the mitochondria of substantia nigral neurons in Parkinson's disease. Ann Neurol 1999; 46: 920-4.

Shoffner JM, Watts RL, Juncos JL, Torroni A, Wallace DC. Mitochondrial oxidative phosphorylation defects in Parkinson's disease. Ann Neurol 1991; 30: 332-9.

Shuldiner AR. Transgenic animals. N Engl J Med 1996; 334: 653-5.

Sian J, Dexter DT, Lees AJ, Daniel S, Jenner P, Marsden CD. Glutathione-related enzymes in brain in Parkinson's disease. Ann Neurol 1994; 36: 356-61.

Simon DK, Mayeux R, Marder K, Kowall NW, Beal MF, Johns DR. Mitochondrial DNA mutations in complex I and tRNA genes in Parkinson's disease. Neurology 2000; 54: 703-9.

Simonian NA, Coyle JT. Oxidative stress in neurodegenerative diseases. Annu Rev Pharmacol Toxicol 1996; 36: 83-106.

Singer TP, Salach JI, Castagnoli N, Jr., Trevor A. Interactions of the neurotoxic amine 1-methyl-4-phenyl-1,2,3,6-tetrahydropyridine with monoamine oxidases. Biochem J 1986; 235: 785-9.

Singleton AB, Farrer M, Johnson J, Singleton A, Hague S, Kachergus J, et al. alpha-Synuclein locus triplication causes Parkinson's disease. Science 2003; 302: 841.

Sofic E, Lange KW, Jellinger K, Riederer P. Reduced and oxidized glutathione in the substantia nigra of patients with Parkinson's disease. Neurosci Lett 1992; 142: 128-30.

Sofic E, Riederer P, Heinsen H, Beckmann H, Reynolds GP, Hebenstreit G, et al. Increased iron (III) and total iron content in post mortem substantia nigra of parkinsonian brain. J Neural Transm 1988; 74: 199-205.

Song C, Perides G, Liu YF. Expression of full-length polyglutamine-expanded Huntingtin disrupts growth factor receptor signaling in rat pheochromocytoma (PC12) cells. J Biol Chem 2002; 277: 6703-7.

Soto-Otero R, Mendez-Alvarez E, Hermida-Ameijeiras A, Munoz-Patino AM, Labandeira-Garcia JL. Autoxidation and neurotoxicity of 6-hydroxydopamine in the presence of some antioxidants: potential implication in relation to the pathogenesis of Parkinson's disease. J Neurochem 2000; 74: 1605-12.

Spencer MD, Knight RS, Will RG. First hundred cases of variant Creutzfeldt-Jakob disease: retrospective case note review of early psychiatric and neurological features. Bmj 2002; 324: 1479-82.

Spillantini MG, Crowther RA, Jakes R, Hasegawa M, Goedert M. alpha-Synuclein in filamentous inclusions of Lewy bodies from Parkinson's disease and dementia with lewy bodies. Proc Natl Acad Sci U S A 1998; 95: 6469-73.

Spillantini MG, Schmidt ML, Lee VM, Trojanowski JQ, Jakes R, Goedert M. Alpha-synuclein in Lewy bodies. Nature 1997; 388: 839-40.

Stefanis L, Larsen KE, Rideout HJ, Sulzer D, Greene LA. Expression of A53T mutant but not wild-type alpha-synuclein in PC12 cells induces alterations of the ubiquitin-dependent degradation system, loss of dopamine release, and autophagic cell death. J Neurosci 2001; 21: 9549-60.

Storch A, Ludolph AC, Schwarz J. HEK-293 cells expressing the human dopamine transporter are susceptible to low concentrations of 1-methyl-4-phenylpyridine (MPP+) via impairment of energy metabolism. Neurochem Int 1999; 35: 393-403.

Strong TV, Tagle DA, Valdes JM, Elmer LW, Boehm K, Swaroop M, et al. Widespread expression of the human and rat Huntington's disease gene in brain and nonneural tissues. Nat Genet 1993; 5: 259-65.

Sugars KL, Rubinsztein DC. Transcriptional abnormalities in Huntington disease. Trends Genet 2003; 19: 233-8.

Suh YA, Arnold RS, Lassegue B, Shi J, Xu X, Sorescu D, et al. Cell transformation by the superoxide-generating oxidase Mox1. Nature 1999; 401: 79-82.

Sun Y, Savanenin A, Reddy PH, Liu YF. Polyglutamine-expanded huntingtin promotes sensitization of N-methyl-D- aspartate receptors via post-synaptic density 95. J Biol Chem 2001; 276: 24713-8.

Sveinbjornsdottir S, Hicks AA, Jonsson T, Petursson H, Gugmundsson G, Frigge ML, et al. Familial aggregation of Parkinson's disease in Iceland. N Engl J Med 2000; 343: 1765-70.

Swerdlow RH, Parks JK, Miller SW, Tuttle JB, Trimmer PA, Sheehan JP, et al. Origin and functional consequences of the complex I defect in Parkinson's disease. Ann Neurol 1996; 40: 663-71.

Tabrizi SJ, Cleeter MW, Xuereb J, Taanman JW, Cooper JM, Schapira AH. Biochemical abnormalities and excitotoxicity in Huntington's disease brain. Ann Neurol 1999; 45: 25-32.

Tabrizi SJ, Orth M, Wilkinson JM, Taanman JW, Warner TT, Cooper JM, et al. Expression of mutant alpha-synuclein causes increased susceptibility to dopamine toxicity. Hum Mol Genet 2000a; 9: 2683-9.

Tabrizi SJ, Workman J, Hart PE, Mangiarini L, Mahal A, Bates G, et al. Mitochondrial dysfunction and free radical damage in the Huntington R6/2 transgenic mouse. Ann Neurol 2000b; 47: 80-6.

Takano H, Gusella JF. The predominantly HEAT-like motif structure of huntingtin and its association and coincident nuclear entry with dorsal, and NF-kB/Rel/dorsal family transcription factor. BMC Neurosci (www.biomedcentral.com/1471-2202/3/15) 2002; 3.

Talpade DJ, Greene JG, Higgins DS, Jr., Greenamyre JT. In vivo labeling of mitochondrial complex I (NADH:ubiquinone oxidoreductase) in rat brain using [(3)H]dihydrorotenone. J Neurochem 2000; 75: 2611-21.

Tan EK, Khajavi M, Thornby JI, Nagamitsu S, Jankovic J, Ashizawa T. Variability and validity of polymorphism association studies in Parkinson's disease. Neurology 2000; 55: 533-8.

Tanaka M, Kim YM, Lee G, Junn E, Iwatsubo T, Mouradian MM. Aggresomes formed by alpha-synuclein and synphilin-1 are cytoprotective. J Biol Chem 2004; 279: 4625-31. Epub 2003 Nov 19.

Tanaka M, Sotomatsu A, Kanai H, Hirai S. Dopa and dopamine cause cultured neuronal death in the presence of iron. J Neurol Sci 1991; 101: 198-203.

Tanaka Y, Engelender S, Igarashi S, Rao RK, Wanner T, Tanzi RE, et al. Inducible expression of mutant alpha-synuclein decreases proteasome activity and increases sensitivity to mitochondria-dependent apoptosis. Hum Mol Genet 2001; 10: 919-26.

Tanner CM, Goldman SM, Aston DA, Ottman R, Ellenberg J, Mayeux R, et al. Smoking and Parkinson's disease in twins. Neurology 2002; 58: 581-8.

Tanner CM, Ottman R, Goldman SM, Ellenberg J, Chan P, Mayeux R, et al. Parkinson disease in twins: an etiologic study. Jama 1999; 281: 341-6.

Tatton NA. Increased caspase 3 and Bax immunoreactivity accompany nuclear GAPDH translocation and neuronal apoptosis in Parkinson's disease. Exp Neurol 2000; 166: 29-43.

Tatton NA, Kish SJ. In situ detection of apoptotic nuclei in the substantia nigra compacta of 1-methyl-4-phenyl-1,2,3,6-tetrahydropyridine-treated mice using terminal deoxynucleotidyl transferase labelling and acridine orange staining. Neuroscience 1997; 77: 1037-48.

Tatton NA, Maclean-Fraser A, Tatton WG, Perl DP, Olanow CW. A fluorescent double-labeling method to detect and confirm apoptotic nuclei in Parkinson's disease. Ann Neurol 1998; 44: S142-8.

Tatton WG, Chalmers-Redman R, Brown D, Tatton N. Apoptosis in Parkinson's disease: signals for neuronal degradation. Ann Neurol 2003; 53: S61-70; discussion S70-2.

Terland O, Flatmark T, Tangeras A, Gronberg M. Dopamine oxidation generates an oxidative stress mediated by dopamine semiquinone and unrelated to reactive oxygen species. J Mol Cell Cardiol 1997; 29: 1731-8.

Thanos D, Maniatis T. NF-kappa B: a lesson in family values. Cell 1995; 80: 529-32.

The Huntington's Disease Collaborative Research Group. A novel gene containing a trinucleotide repeat that is expanded and unstable on Huntington's disease chromosomes. Cell 1993; 72: 971-83.

The Parkinson's Disease Study Group. Effects of tocopherol and deprenyl on the progression of disability in early Parkinson's disease. N Engl J Med 1993; 328: 176-83.

Thomzig A, Kratzel C, Lenz G, Kruger D, Beekes M. Widespread PrPSc accumulation in muscles of hamsters orally infected with scrapie. EMBO Rep 2003; 4: 530-3.

Tofaris GK, Layfield R, Spillantini MG. alpha-synuclein metabolism and aggregation is linked to ubiquitin-independent degradation by the proteasome. FEBS Lett 2001; 509: 22-6.

Tompkins MM, Basgall EJ, Zamrini E, Hill WD. Apoptotic-like changes in Lewy-body-associated disorders and normal aging in substantia nigral neurons. Am J Pathol 1997; 150: 119-31.

Towbin H, Staehelin T, Gordon J. Electrophoretic transfer of proteins from polyacrylamide gels to nitrocellulose sheets: procedure and some applications. Proc Natl Acad Sci U S A 1979; 76: 4350-4.

Triepels RH, van den Heuvel LP, Loeffen JL, Buskens CA, Smeets RJ, Rubio Gozalbo ME, et al. Leigh syndrome associated with a mutation in the NDUFS7 (PSST) nuclear encoded subunit of complex I. Ann Neurol 1999; 45: 787-90.

Trottier Y, Devys D, Imbert G, Saudou F, An I, Lutz Y, et al. Cellular localization of the Huntington's disease protein and discrimination of the normal and mutated form. Nat Genet 1995a; 10: 104-10.

Trottier Y, Lutz Y, Stevanin G, Imbert G, Devys D, Cancel G, et al. Polyglutamine expansion as a pathological epitope in Huntington's disease and four dominant cerebellar ataxias. Nature 1995b; 378: 403-6.

Turmaine M, Raza A, Mahal A, Mangiarini L, Bates GP, Davies SW. Nonapoptotic neurodegeneration in a transgenic mouse model of Huntington's disease. Proc Natl Acad Sci U S A 2000; 97: 8093-7.

Turrens JF. Superoxide production by the mitochondrial respiratory chain. Biosci Rep 1997; 17: 3-8.

Ungerstedt U. 6-Hydroxydopamine induced degeneration of central monoamine neurons. Eur J Pharmacol 1968; 5: 107-110.

Uversky VN, Li J, Bower K, Fink AL. Synergistic effects of pesticides and metals on the fibrillation of alpha-synuclein: implications for Parkinson's disease. Neurotoxicology 2002; 23: 527-36.

Uversky VN, Li J, Fink AL. Pesticides directly accelerate the rate of alpha-synuclein fibril formation: a possible factor in Parkinson's disease. FEBS Lett 2001; 500: 105-8.

Vachon PH, Loechel F, Xu H, Wewer UM, Engvall E. Merosin and laminin in myogenesis; specific requirement for merosin in myotube stability and survival. J Cell Biol 1996; 134: 1483-97.

Valente EM, Abou-Sleiman PM, Caputo V, Muqit MM, Harvey K, Gispert S, et al. Hereditary early-onset Parkinson's disease caused by mutations in PINK1. Science 2004; 304: 1158-60. Epub 2004 Apr 15.

Valleron AJ, Boelle PY, Will R, Cesbron JY. Estimation of epidemic size and incubation time based on age characteristics of vCJD in the United Kingdom. Science 2001; 294: 1726-8.

van den Heuvel L, Ruitenbeek W, Smeets R, Gelman-Kohan Z, Elpeleg O, Loeffen J, et al. Demonstration of a new pathogenic mutation in human complex I deficiency: a 5-bp duplication in the nuclear gene encoding the 18-kD (AQDQ) subunit. Am J Hum Genet 1998; 62: 262-8.

van der Putten H, Wiederhold KH, Probst A, Barbieri S, Mistl C, Danner S, et al. Neuropathology in mice expressing human alpha-synuclein. J Neurosci 2000; 20: 6021-9.

van Dijk JG, van der Velde EA, Roos RA, Bruyn GW. Juvenile Huntington disease. Hum Genet 1986; 73: 235-9.

van Duijn CM, Dekker MC, Bonifati V, Galjaard RJ, Houwing-Duistermaat JJ, Snijders PJ, et al. Park7, a novel locus for autosomal recessive early-onset parkinsonism, on chromosome 1p36. Am J Hum Genet 2001; 69: 629-34.

Vaughan J, Durr A, Tassin J, Bereznai B, Gasser T, Bonifati V, et al. The alpha-synuclein Ala53Thr mutation is not a common cause of familial Parkinson's disease: a study of 230 European cases. European Consortium on Genetic Susceptibility in Parkinson's Disease. Ann Neurol 1998a; 44: 270-3.

Vaughan JR, Farrer MJ, Wszolek ZK, Gasser T, Durr A, Agid Y, et al. Sequencing of the alpha-synuclein gene in a large series of cases of familial Parkinson's disease fails

to reveal any further mutations. The European Consortium on Genetic Susceptibility in Parkinson's Disease (GSPD). Hum Mol Genet 1998b; 7: 751-3.

Velier J, Kim M, Schwarz C, Kim TW, Sapp E, Chase K, et al. Wild-type and mutant huntingtins function in vesicle trafficking in the secretory and endocytic pathways. Exp Neurol 1998; 152: 34-40.

Vieregge P, Heberlein I. Increased risk of Parkinson's disease in relatives of patients. Ann Neurol 1995; 37: 685.

Vieregge P, Schiffke KA, Friedrich HJ, Muller B, Ludin HP. Parkinson's disease in twins. Neurology 1992; 42: 1453-61.

Vila M, Przedborski S. Targeting programmed cell death in neurodegenerative diseases. Nat Rev Neurosci 2003; 4: 365-75.

Voges D, Zwickl P, Baumeister W. The 26S proteasome: a molecular machine designed for controlled proteolysis. Annu Rev Biochem 1999; 68: 1015-68.

Vonsattel JP, Myers RH, Stevens TJ, Ferrante RJ, Bird ED, Richardson EP, Jr. Neuropathological classification of Huntington's disease. J Neuropathol Exp Neurol 1985; 44: 559-77.

Wadsworth JD, Hill AF, Joiner S, Jackson GS, Clarke AR, Collinge J. Strain-specific prion-protein conformation determined by metal ions. Nat Cell Biol 1999; 1: 55-9.

Wakabayashi K, Engelender S, Yoshimoto M, Tsuji S, Ross CA, Takahashi H. Synphilin-1 is present in Lewy bodies in Parkinson's disease. Ann Neurol 2000; 47: 521-3.

Ward CD, Duvoisin RC, Ince SE, Nutt JD, Eldridge R, Calne DB. Parkinson's disease in 65 pairs of twins and in a set of quadruplets. Neurology 1983; 33: 815-24.

Warner TT, Schapira AH. The role of the alpha-synuclein gene mutation in patients with sporadic Parkinson's disease in the United Kingdom. J Neurol Neurosurg Psychiatry 1998; 65: 378-9.

Weinreb PH, Zhen W, Poon AW, Conway KA, Lansbury PT, Jr. NACP, a protein implicated in Alzheimer's disease and learning, is natively unfolded. Biochemistry 1996; 35: 13709-15.

Weintraub H. The MyoD family and myogenesis: redundancy, networks, and thresholds. Cell 1993; 75: 1241-4.

Wellington CL, Ellerby LM, Hackam AS, Margolis RL, Trifiro MA, Singaraja R, et al. Caspase cleavage of gene products associated with triplet expansion disorders generates truncated fragments containing the polyglutamine tract. J Biol Chem 1998; 273: 9158-67.

Wellington CL, Singaraja R, Ellerby L, Savill J, Roy S, Leavitt B, et al. Inhibiting caspase cleavage of huntingtin reduces toxicity and aggregate formation in neuronal and nonneuronal cells. J Biol Chem 2000; 275: 19831-8.

Werner P, Cohen G. Intramitochondrial formation of oxidized glutathione during the oxidation of benzylamine by monoamine oxidase. FEBS Lett 1991; 280: 44-6.

Wersinger C, Sidhu A. Attenuation of dopamine transporter activity by alpha-synuclein. Neurosci Lett 2003; 340: 189-92.

West AB, Maraganore D, Crook J, Lesnick T, Lockhart PJ, Wilkes KM, et al. Functional association of the parkin gene promoter with idiopathic Parkinson's disease. Hum Mol Genet 2002; 11: 2787-92.

Westaway D, DeArmond SJ, Cayetano-Canlas J, Groth D, Foster D, Yang SL, et al. Degeneration of skeletal muscle, peripheral nerves, and the central nervous system in transgenic mice overexpressing wild-type prion proteins. Cell 1994; 76: 117-29.

Wexler NS, Young AB, Tanzi RE, Travers H, Starosta-Rubinstein S, Penney JB, et al. Homozygotes for Huntington's disease. Nature 1987; 326: 194-7.

Wharton D, Tzagoloff A. Cytochrome oxidase from beef heart mitochondria. Methods Enzymol 1967; 10: 245-257.

Wheeler VC, White JK, Gutekunst CA, Vrbanac V, Weaver M, Li XJ, et al. Long glutamine tracts cause nuclear localization of a novel form of huntingtin in medium spiny striatal neurons in HdhQ92 and HdhQ111 knock- in mice. Hum Mol Genet 2000; 9: 503-13.

White RJ, Reynolds IJ. Mitochondria and Na+/Ca2+ exchange buffer glutamate-induced calcium loads in cultured cortical neurons. J Neurosci 1995; 15: 1318-28.

Widdowson PS, Farnworth MJ, Simpson MG, Lock EA. Influence of age on the passage of paraquat through the blood-brain barrier in rats: a distribution and pathological examination. Hum Exp Toxicol 1996a; 15: 231-6.

Widdowson PS, Farnworth MJ, Upton R, Simpson MG, Lock EA. No changes in behaviour, nigro-striatal system neurochemistry or neuronal cell death following toxic multiple oral paraquat administration to rats

Influence of age on the passage of paraquat through the blood-brain barrier in rats: a distribution and pathological examination. Hum Exp Toxicol 1996b; 15: 583-91.

Wigley WC, Fabunmi RP, Lee MG, Marino CR, Muallem S, DeMartino GN, et al. Dynamic association of proteasomal machinery with the centrosome. J Cell Biol 1999; 145: 481-90.

Wilhelmsen KC, Weeks DE, Nygaard TG, Moskowitz CB, Rosales RL, dela Paz DC, et al. Genetic mapping of "Lubag" (X-linked dystonia-parkinsonism) in a Filipino kindred to the pericentromeric region of the X chromosome. Ann Neurol 1991; 29: 124-31.

Will RG, Ironside JW, Zeidler M, Cousens SN, Estibeiro K, Alperovitch A, et al. A new variant of Creutzfeldt-Jakob disease in the UK. Lancet 1996; 347: 921-5.

Windl O, Dempster M, Estibeiro JP, Lathe R, de Silva R, Esmonde T, et al. Genetic basis of Creutzfeldt-Jakob disease in the United Kingdom: a systematic analysis of predisposing mutations and allelic variation in the PRNP gene. Hum Genet 1996; 98: 259-64.

Wood SJ, Wypych J, Steavenson S, Louis JC, Citron M, Biere AL. alpha-synuclein fibrillogenesis is nucleation-dependent. Implications for the pathogenesis of Parkinson's disease. J Biol Chem 1999; 274: 19509-12.

Wyttenbach A, Carmichael J, Swartz J, Furlong RA, Narain Y, Rankin J, et al. Effects of heat shock, heat shock protein 40 (HDJ-2), and proteasome inhibition on protein aggregation in cellular models of Huntington's disease. Proc Natl Acad Sci U S A 2000; 97: 2898-903.

Xu J, Kao SY, Lee FJ, Song W, Jin LW, Yankner BA. Dopamine-dependent neurotoxicity of alpha-synuclein: A mechanism for selective neurodegeneration in Parkinson disease. Nat Med 2002; 8: 600-6.

Yakes FM, Van Houten B. Mitochondrial DNA damage is more extensive and persists longer than nuclear DNA damage in human cells following oxidative stress. Proc Natl Acad Sci U S A 1997; 94: 514-9.

Yamamoto A, Lucas JJ, Hen R. Reversal of neuropathology and motor dysfunction in a conditional model of Huntington's disease. Cell 2000; 101: 57-66.

Yang W, Dunlap JR, Andrews RB, Wetzel R. Aggregated polyglutamine peptides delivered to nuclei are toxic to mammalian cells. Hum Mol Genet 2002; 11: 2905-17.

Yoritaka A, Hattori N, Mori H, Kato K, Mizuno Y. An immunohistochemical study on manganese superoxide dismutase in Parkinson's disease. J Neurol Sci 1997; 148: 181-6.

Yoritaka A, Hattori N, Uchida K, Tanaka M, Stadtman ER, Mizuno Y. Immunohistochemical detection of 4-hydroxynonenal protein adducts in Parkinson disease. Proc Natl Acad Sci U S A 1996; 93: 2696-701.

Yoshida E, Mokuno K, Aoki S, Takahashi A, Riku S, Murayama T, et al. Cerebrospinal fluid levels of superoxide dismutases in neurological diseases detected by sensitive enzyme immunoassays. J Neurol Sci 1994; 124: 25-31.

Yoshino H, Nakagawa-Hattori Y, Kondo T, Mizuno Y. Mitochondrial complex I and II activities of lymphocytes and platelets in Parkinson's disease. J Neural Transm Park Dis Dement Sect 1992; 4: 27-34.

Yu PH, Zuo DM. Enhanced tolerance of neuroblastoma cells towards the neurotoxin 6-hydroxydopamine following specific cell-cell interaction with primary astrocytes. Neuroscience 1997; 78: 903-12.

Zanusso G, Vattemi G, Ferrari S, Tabaton M, Pecini E, Cavallaro T, et al. Increased expression of the normal cellular isoform of prion protein in inclusion-body myositis, inflammatory myopathies and denervation atrophy. Brain Pathol 2001; 11: 182-9.

Zeitlin S, Liu JP, Chapman DL, Papaioannou VE, Efstratiadis A. Increased apoptosis and early embryonic lethality in mice nullizygous for the Huntington's disease gene homologue. Nat Genet 1995; 11: 155-63.

Zeron MM, Chen N, Moshaver A, Lee AT, Wellington CL, Hayden MR, et al. Mutant huntingtin enhances excitotoxic cell death. Mol Cell Neurosci 2001; 17: 41-53.

Zeron MM, Hansson O, Chen N, Wellington CL, Leavitt BR, Brundin P, et al. Increased sensitivity to N-methyl-D-aspartate receptor-mediated excitotoxicity in a mouse model of Huntington's disease. Neuron 2002; 33: 849-60.

Zeviani M, Carelli V. Mitochondrial disorders. Curr Opin Neurol 2003; 16: 585-94.

Zhuchenko O, Bailey J, Bonnen P, Ashizawa T, Stockton DW, Amos C, et al. Autosomal dominant cerebellar ataxia (SCA6) associated with small polyglutamine expansions in the alpha 1A-voltage-dependent calcium channel. Nat Genet 1997; 15: 62-9.

Zigas V, Gajdusek DC. Kuru: clinical study of a new syndrome resembling paralysis agitans in natives of the Eastern Highlands of Australian New Guinea. Med J Aust 1957; 44: 745-54.

Zigova T, Willing AE, Tedesco EM, Borlongan CV, Saporta S, Snable GL, et al. Lithium chloride induces the expression of tyrosine hydroxylase in hNT neurons. Exp Neurol 1999; 157: 251-8.

Zimmermann K, Turecek PL, Schwarz HP. Genotyping of the prion protein gene at codon 129. Acta Neuropathol (Berl) 1999; 97: 355-8.

Ziv I, Melamed E, Nardi N, Luria D, Achiron A, Offen D, et al. Dopamine induces apoptosis-like cell death in cultured chick sympathetic neurons--a possible novel pathogenetic mechanism in Parkinson's disease. Neurosci Lett 1994; 170: 136-40.

Zuccato C, Ciammola A, Rigamonti D, Leavitt BR, Goffredo D, Conti L, et al. Loss of huntingtin-mediated BDNF gene transcription in Huntington's disease. Science 2001; 293: 493-8.

Appendix 1

Western blotting

5 X dissociation buffer

- 6ml glycerol
- 2g SDS
- 5mg bromophenol blue
- 1ml 1M Tris-HCl (pH 6.5)

The ingredients were mixed in a 50ml screw top tube; 2ml double distilled H_2O were added and the mixture dissolved in a hot water bath (~80°C). The total volume of 10ml was made up with double distilled H_20. β-mercaptoethanol was added after protein estimation because it interferes with the BCA protein determination assay.

Electrophoresis buffer

- 28.8g glycine
- 6g Tris (Trizma base)
- 2g sodium dodecylsulfate (SDS)

Make up to a final volume of 2 litres with double distilled H_2O.

Towbin's blotting buffer (25mM Tris, 192mM glycine, 20% methanol)

- 7.57g Tris
- 36.04g glycine
- 500ml methanol

Make up to a final volume of 2.5 litres with H_2O, adjust pH to 8.3 and refridgerate.

Gel recipes for one pair of mini-gels (0.75mm spacers) using the BioRad Mini-Protean system

	STACKING		SEPARATING	
	3%	10%	12.5%	15%
3.75mM Tris-HCl (pH 8.6)	-	920µl	920µl	920µl
0.5M Tris-HCl (pH 6.5)	500µl	-	-	-
40% acrylamide-bis (37.5:1)[1]	450µl	2.5ml	3.1ml	3.7ml
Urea	1.8g	3.25g	3.25g	3.25g
20% SDS	25µl	46µl	46µl	46µl
Double distilled H_2O	3.25ml	4.1ml	3.5ml	2.9ml
TEMED[1]	3µl	6µl	6µl	6µl
10% ammonium persulfate	25µl	44µl	44µl	44µl

[1] from BioRad

Appendix 2.

α-synuclein cell culture models

A number of studies have investigated the effects of wild-type, G209A or G88C α-synuclein over-expression *in vitro* (Table A1). Studies differ in the cell lines used, the vector used for transfection and the mode of transfection, i.e. transient, stable or stable and inducible (see section 1.1.7.4). The literature on over-expression of wild-type, or G209A or G88C mutant, α-synuclein revealed variable results. The following tables differentiate the effects of α-synuclein, either wild-type or mutant, transfection on processes that are relevant in PD, i.e. viability, oxidative stress, the UPS and aggregate formation, and mitochondrial function (for a summary see Tables A2 and A3).

Cell type	Transfection	Reference	α-synuclein	Number
Mouse hypothalamic GT1-7	Stable	(Hsu et al., 2000)	Wild-type	1
SH-SY5Y	Stable	(Kanda et al., 2000),	Wild-type	2
			G209A, G88C	3
BE(2)-M17 neuroblastoma	Stable	(Ko et al., 2000),	Wild-type	4
			G88C	5
PC-12 cells	Stable, doxy-cycline switch	(Tanaka et al., 2001)	G88C	6
PC-12 cells	Stable	(Stefanis et al., 2001)	Wild-type	7
			G209A	8
SH-SY5Y	Stable	(Junn and Mouradian, 2002),	Wild-type,	9
			G209A, G88C	10
human foetal dopaminer-gic neurones, SH-SY5Y	Transient	(Xu et al., 2002)	Wild-type,	11
	Stable, inducible		G88C, G209A	12
HEK293	Transient	(Engelender et al., 1999)	Wild-type	13
SH-SY5Y	Transient	(Kalivendi et al., 2004)	Wild-type	14
COS-7	Transient	(Lee et al., 2004)	Wild-type	15
Differentiated SH-SY5Y	Transient	(Lee et al., 2004)	Wild-type	16
SH-SY5Y	Transient	(Lee et al., 2004)	Wild-type	17
SH-SY5Y	Transient	(Kalivendi et al., 2004)	Wild-type	18
primary cortical rat neurones	Transient	(Saha et al., 2004)	Wild-type	19
			G88C, G209A	20
TSM1 neuronal	Stable	(da Costa et al., 2000)	Wild-type	21
			G209A	22
HEK293 stably trans-fected with synphilin-1	Transient	(Tanaka et al., 2004)	Wild-type	23
			G88C, G209A	24
MN9D (murine mesencephalic)	Stable	(Jensen et al., 2003)	Wild-type,	25
			G88C, G209A	26
SK-NM-C	Stable, inducible	(Lee et al., 2001c)	Wild-type,	27
BE-M17 neuroblastoma	Stable	(Ostrerova-Golts et al., 2000)	Wild-type,	28
			G88C, G209A	29

Table A1. Cell culture models of α-synuclein over-expression.

Process	Effect	Cell line and reference number (see Table 3.3)
Viability	→	SH-SY5Y (2), PC-12 (7)
	↓	BE-M17 neuroblastoma (28)
Susceptibility to staurosporine	↑	SK-NM-C (27)
	↓	TSM1 neuronal (21)
Oxidative stress	↑	Mouse hypothalamic GT1-7 (1)
	→	SH-SY5Y (14)
Susceptibility to H_2O_2	→	SH-SY5Y (2)
	↓	SK-NM-C (27)
Aggregates	↑	Mouse hypothalamic GT1-7 (1), BE-M17 neuroblastoma (28), COS-7 (15), differentiated SH-SY5Y (16)
UPS and aggregates	→	PC-12 (7), SH-SY5Y (17), HEK293 with synphilin (23)
MRC function	→	SH-SY5Y (18)
	↓	Mouse hypothalamic GT1-7 (1)
Susceptibility to MPP+	→	SH-SY5Y (2)
	↑	SH-SY5Y (18)
	↓	MN9D (murine mesencephalic) (25)
Susceptibility to rotenone	↑	COS-7 (15), differentiated SH-SY5Y (16)
Susceptibility to dopamine	↑	SH-SY5Y (9), human foetal dopaminergic neurones and SH-SY5Y (11)

Table A2. Effect of wild-type α-synuclein over-expression in cell culture models.

↑: increase. ↓: decrease. →: no change.

Process	Effect	Cell line and reference number (see Table 3.3)
Viability	→	BE-M17 neuroblastoma (5)
	↓	PC-12 (6,8), HEK293 with synphilin (24), BE-M17 neuroblastoma (29)
Susceptibility to H_2O_2	↑	SH-SY5Y (3)
Susceptibility to menadione	↑	BE-M17 neuroblastoma (5)
UPS	↓	PC-12 (6,8),
Aggregates	↑	HEK293 with synphilin (24); BE-M17 neuroblastoma (29)
Susceptibility to MPP+	↑	MN9D (murine mesencephalic) (25)
Susceptibility to dopamine	↑	SH-SY5Y (10), human foetal dopaminergic neurones and SH-SY5Y (12)

Table A3. Effect of mutant α-synuclein over-expression in cell culture models.

↑: increase. ↓: decrease. →: no change.

Appendix 3.

Sequences of pIND.α-syn and pIND.G209A-α-syn constructs amplified from DNA extracts of WTsyn cell lines, or MUTsyn cell lines respectively.

WTsyn 1: ATGATCATGCAGTCGACGCGAACA-GC-GCTACGTATCATGATAGTCCTAGCTCATAC-AC-T-G-
TGAGCGTCGTTCAGTA-CTAGCTGATCGAA-CACC-GTCACA-CGCA-CTCATC-CGGCCAT--A-TC-G--A-T-GTCT-
A--TCGTCGATGATC-ACTATT-A-GTCAC-TCAC-CG-A-TAC--T-CGTTGCTCGAAT-T-ATGTCACGTTG-
CGCGTGACTGGTGC-ATGTCGCA-T-AT-ATGATCT-CCTGCTTCGACT-A--AGT-C--TGAT-T-A--TC--GAT-ATG-AC-
AT-ACTGTACC-GTCGGCAG--CG-AGATCA-G-TATACGATACAT-GATG-AC-TGTCGCTCT-CAAT-
GACGTATGTG-CTCG--TC-GC-ATCACGCGA-AGAT-A-G-T-GCATGTCGACTCA----CGCT-A-T--C-GGCG-TG-
CGTG-CACTGTATGAG-C--TGTCA-CG-C-GT-T--ATTA-CATGTT-TT-T-GT-A-GA-GA-G-C-CGCCACGT-T-
GAATGGA-GA-TACC-C-ACAGAG-CC---C---G---CTTCTTTTTTGGAAATTT-
TTTCAACAAGTTACCGAGAAAGAAGAACTCACACACAGCTAGCGTTTAAACTTAAGCTTGGTACCGACAGTGTG
GTGTAAAGGAATTCATTAGCCATGGATGTATTCATGAAAGGACTTTCAAAGGCCAAGGAGGGAGTTGTGGCTG
CTGCTGAGAAAACCAAACAGGGTGTGGCAGAAGCAGCAGGAAAGACAAAAGAGGGTGTTCTCTATGTAGGCTC
CAAAACCAAGGAGGGAGTGGTGCATGGTGTGGCAACAGTGGCTGAGAAGACCAAAGAGCAAGTGACAAATGT
TGGAGGAGCAGTGGTGACGGGTGTGACAGCAGTAGCCCAGAAGACAGTGGAGGGAGCAGGGAGCATTGCAG
CAGCCACTGGCTTTGTCAAAAAGGACCAGTTGGGCAAGAATGAAGAAGGAGCCCCACAGGAAGGAATTCTGGA
AGATATGCCTGTGGATCCTGACAATGAGGCTTATGAAATGCCTTCTGAGGAAGGGTATCAAGACTACGAACCTG
AAGCCTACCCA-TA-CGACG-TCCCAGACTACGCTTGATCA-CTAGTCCAGTGTGGTGGAATTCTGCAGATAT-C-
CAGCACACGTG--CGGGCGTC-TCGA

WTsyn 2: TAGTCA-CC--TA-GT-CAGTGCGTA-GCT-A-GCA-CGCATCA--G-T-C-TGCA-TAC--TACATC-
ATCGACT-G--CT-G-AG-T-GGACGTA-TATCA-TCGT-A--T-ATGTC-AC-TGCAGTACATATTAATA-T-
CACGTCGTGCTC-A-CTGCGAGTGA--GTC-ACAT-T-GCA-CTATCTCA-C-TC-AT-CATC-GTCAGAAGTACA-TC--
TCTC-GACAG-T-CG-TCG-ATGTATC-TAGAT--GTACACGTGTCGTCATATGGCACATGA-T--ATCATGCAT-A-TG-
T--C-ATCTGATGC-ATCT-CTTATCTCTG-CGCG--T-TGCTAGTACATTATATCTGTCG-C-GCCTG-CG-CGCT-G-
TCGCT-G-CT-C-A-TG-CGTCGT--CAC-GTGTTCG-CC-TGCG-TCGCCCATCTCGCTTG-CGTTTT-TT-T-G--G-GC-
GA-T-C-GTCC-C-T-G-GGG-GG--G--G-CC-C-AGGCCC-CC-T-C-C-G-C-
CTTCTTTTGAGAAAATTTCTTTCAACAAGTTACCGAGAAAGAAGAACTCACACACAGCTAGCGTTTAAACTTAAG
CTTGGTACCGACAGTGTGGTGTAAAGGAATTCATTAGCCATGGATGTATTCATGAAAGGACTTTCAAAGGCCAA
GGAGGGAGTTGTGGCTGCTGCTGAGAAAACCAAACAGGGTGTGGCAGAAGCAGCAGGAAAGACAAAAGAGGG
TGTTCTCTATGTAGGCTCCAAAACCAAGGAGGGAGTGGTGCATGGTGTGGCAACAGTGGCTGAGAAGACCAAA
GAGCAAGTGACAAATGTTGGAGGAGCAGTGGTGACGGGTGTGACAGCAGTAGCCCAGAAGACAGTGGAGGGA
GCAGGGAGCATTGCAGCAGCCACTGGCTTTGTCAAAAAGGACCAGTTGGGCAAGAATGAAGAAGGAGCCCCA
CAGGAAGGAATTCTGGAAGATATGCCTGTGGATCCTGACAATGAGGCTTATGAAATGCCTTCTGAGGAAGGGT
ATCAAGACTACGAACCTGAAGCCTACCCA-TA-CGACG-TCCCAGACTACGCTTGATCA-
CTAGTCCAGTGTGGTGGAATTCTGCAGATAT-C-CAGCATCAGTG-GCGGACAC--T-GAG

WTsyn 3: CAGTC-GTGCTAG-CATTTC-A-CGA--GTCT-GACT-G-ACT--TCCGT--C-T-CTC----T--A----T-CA-G-T---
GATGCTAGTTC-TGGAGTCA--TCAT-TCGCATACT-CTC--A-G-TAGTAGCTTC-T-CATGCTGCACG-CT-CTCCT-C-
CA--CG-AC-TA-C-GA-TCGCTT--CAGTCT-CTACT-AC-ACT-C--TCGT-T----TC--AGG-ATC-TC-AT-CGCCTACA-
CTC-T-AG-TCG-TTCTCA-T-TATTC-AGATAA-T-CT--C--GCCACTC--CGCT--AC-TA-GT--CTCA--TCTGC-A-
CATACTA-CGAT-A---C-TG-TGTC-ACACA---TCG-T-A-TA-C-TATA-TATCGC--CATCG-ATGAG-C--TGCAATCT-T-
ATCT-GTGAGTCAGGAT-AAGTCTA-CACCCATCGTC-CGCCCCCG---GCCCGCC-GC-CGCG-G-GCCCA--CC---A-
G-G-A-CTTCTTTGTAGAAAATTT-
TTTTCACAAGTTACCGAGAAAGAAGAACTCACACACAGCTAGCGTTTAAACTTAAGCTTGGTACCGACAGTGTG
GTGTAAAGGAATTCATTAGCCATGGATGTATTCATGAAAGGACTTTCAAAGGCCAAGGAGGGAGTTGTGGCTG
CTGCTGAGAAAACCAAACAGGGTGTGGCAGAAGCAGCAGGAAAGACAAAAGAGGGTGTTCTCTATGTAGGCTC
CAAAACCAAGGAGGGAGTGGTGCATGGTGTGGCAACAGTGGCTGAGAAGACCAAAGAGCAAGTGACAAATGT
TGGAGGAGCAGTGGTGACGGGTGTGACAGCAGTAGCCCAGAAGACAGTGGAGGGAGCAGGGAGCATTGCAG
CAGCCACTGGCTTTGTCAAAAAGGACCAGTTGGGCAAGAATGAAGAAGGAGCCCCACAGGAAGGAATTCTGGA
AGATATGCCTGTGGATCCTGACAATGAGGCTTATGAAATGCCTTCTGAGGAAGGGTATCAAGACTACGAACCTG
AAGCCTACCCA-TA-CGACG-TCCCAGACTACGCTTGATCA-CTAGTCCAGTGTGGTGGAATTCTGCAGATAT-C-
CAGCACCAGTG-TCGGGGGTA-T-GA

MUTsyn 1: TATCATCATGCT-CGTGTAACGTCA-T-C-AG-TCAT-CA-GT-CAT-A--TCT-C-TCACTCGTGCATTG-
TATGCGATGCATG-CATA-TCTGTAC-TGAT-GCTAG--CCGACG-TC-GT-A-CGTCGTAGCA-TA-TCATACATGAC-
ACGAGATT-ATGCT-CG-ATTT-GTATAA-T-TATCATCATATA-
GTCTACGTATGCATAATATCGATCAGTCAGTCTCGATGACTCGCGCGCCTGTTCATGTAGTCG-AGCATATA-
TCTCGCA-TGG-TCGTCGATCTCTTATGTCATCAACGT-TCGCTAGCACTCT-ATC--T-GCTCTTATATCT-AG-T-GC-
ATG-ATAGCGAGCA-CTGATGT-G--C-CGA-TC-GTCGCAC-GC-AGA-CTGGCA---TG-TGTCTAG-TC---TCACT-G-
CT---GACC-G-TCGCAGCAC-GC-TTAGTCA-TATATTAGAAGATCTCTC-TTA-
ATTATATTGTAGTCATTCAGAGATT-CTCCACATCT-CAGTAGT-CG-
TGCCGCGAGGGGGACGGGGGGGGGGCACTTCTTTTG-GATATTTT-
TTTCAACAAGTTACCGAGAAAGAAGAACTCACACACAGCTAGCGTTTAAACTTAAGCTTGGTACCGACAGTGTG
GTGTAAAGGAATTCATTAGCCATGGATGTATTCATGAAAGGACTTTCAAAGGCCAAGGAGGGAGTTGTGGCTG
CTGCTGAGAAAACCAAACAGGGTGTGGCAGAAGCAGCAGGAAAGACAAAAGAGGGTGTTCTCTATGTAGGCTC
CAAAACCAAGGAGGGAGTGGTGCATGGTGTGACAACAGTGGCTGAGAAGACCAAAGAGCAAGTGACAAATGTT
GGAGGAGCAGTGGTGACGGGTGTGACAGCAGTAGCCCAGAAGACAGTGGAGGGAGCAGGGAGCATTGCAGC
AGCCACTGGCTTTGTCAAAAAGGACCAGTTGGGCAAGAATGAAGAAGGAGCCCCACAGGAAGGAATTCTGGAA
GATATGCCTGTGGATCCTGACAATGAGGCTTATGAAATGCCTTCTGAGGAAGGGTATCAAGACTACGAACCTGA
AGCCTACCCA-TA-CGACG-TCCCAGACTACGCTTGATCA-CTAGTCCAGTGTGGTGGAATTCTGCAGATAT-C-
CAGCAGCAGTG-GCGGG-GCTCTCGAG

MUTsyn 2: AGTCATCTCAGTATC-
GACTCTCAGTGCTATGAGCTGCGTATGCTTCGATCATCGTATTTGCATCGAGTCGTTAGATCTCGTACGACTCA
TGACGTCG-TCTATCACGTCG-TCTACATGGAG-C-GATC-

GTCGCACTGCACTTCTTGTAGCAGCATCTTAATCCTGCAGATAT-GTAGCATCATCTAA-TAGC-

ATGTCTCACTCACCTTCGCAGATCGCTGTAGTTATCTATGAT-CGT-G-TA-CTC-TA-CATAGTA-TGTAC-

TTGTATTCGTATCGGTGTAT-ATACACGTGTACTACGTATCTATCTCCA-CTACATACA-CGCACACGCATCAG-

CAGTC-ATACGA-CTGTCGTCATCATATATAAGTAGCATGATTCGATATCAGTATAGAT-

GCTGCAGTGTTTGAATATATGGCTACGTAG-TAT-GTCTATCTATCTATTATGGATGACGGTATGAC-

GAGCGCGCACCGACCGCACGGATACC-CGAGAAGGGACAG-G-G-G-TC-T-CTTT-G-GAAA-TTTT-TT-

AACAAGTTACCGAGAAAGAAGAACTCACACACAGCTAGCGTTTAAACTTAAGCTTGGTACCGACAGTGTGGTGT

AAAGGAATTCATTAGCCATGGATGTATTCATGAAAGGACTTTCAAAGGCCAAGGAGGGAGTTGTGGCTGCTGCT

GAGAAAACCAAACAGGGTGTGGCAGAAGCAGCAGGAAAGACAAAAGAGGGTGTTCTCTATGTAGGCTCCAAAA

CCAAGGAGGGAGTGGTGCATGGTGTGACAACAGTGGCTGAGAAGACCAAAGAGCAAGTGACAAATGTTGGAG

GAGCAGTGGTGACGGGTGTGACAGCAGTAGCCCAGAAGACAGTGGAGGGAGCAGGGAGCATTGCAGCAGCC

ACTGGCTTTGTCAAAAAGGACCAGTTGGGCAAGAATGAAGAAGGAGCCCCACAGGAAGGAATTCTGGAAGATA

TGCCTGTGGATCCTGACAATGAGGCTTATGAAATGCCTTCTGAGGAAGGGTATCAAGACTACGAACCTGAAGC

CTACCCA-TA-CGACG-TCCCAGACTACGCTTGATCA-CTAGTCCAGTGTGGTGGAATTCTGCAGATAT-C-

CAGCAGCAGTG-GCGGGCGCT-T-GAGT

MUTsyn 3: CCCCCCCCCCCCCCCCCCCCCCCCCCCCCCCCCCCACCCCCTCCCCCCCCGCCC-

CTCCCTCCCCCCCACCCCCCCCCCCCATC-CTCCATCCCCCCCCCCCCCC-TCCTCC-CCC-

GCCCCCCCCCCCCCCCCCCCCCCCCCCCCCTCCCCCCT-

TCCCCCCCCTCTCCCCCCCCCCCCCCCCCCCCCCCCCCCCCCCCCCCCTCAGCCCCCACC-CTCCTTTTG-

GAAATTTT-TTTC-

ACAAGTTACCGAGAAAGAAGAACTCACACACAGCTAGCGTTTAAACTTAAGCTTGGTACCGACAGTGTGGTGTA

AAGGAATTCATTAGCCATGGATGTATTCATGAAAGGACTTTCAAAGGCCAAGGAGGGAGTTGTGGCTGCTGCT

GAGAAAACCAAACAGGGTGTGGCAGAAGCAGCAGGAAAGACAAAAGAGGGTGTTCTCTATGTAGGCTCCAAAA

CCAAGGAGGGAGTGGTGCATGGTGTGACAACAGTGGCTGAGAAGACCAAAGAGCAAGTGACAAATGTTGGAG

GAGCAGTGGTGACGGGTGTGACAGCAGTAGCCCAGAAGACAGTGGAGGGAGCAGGGAGCATTGCAGCAGCC

ACTGGCTTTGTCAAAAAGGACCAGTTGGGCAAGAATGAAGAAGGAGCCCCACAGGAAGGAATTCTGGAAGATA

TGCCTGTGGATCCTGACAATGAGGCTTATGAAATGCCTTCTGAGGAAGGGTATCAAGACTACGAACCTGAAGC

CTACCCA-TA-CGACG-TCCCAGACTACGCTTGATCA-CTAGTCCAGTGTGGTGGAATTCTGCAGATAT-C-

CAGCAC-AGGT-GCAGA

Appendix 4.

Publications (excluding abstracts and reviews)

Orth M, Tabrizi SJ, Schapira AHV. Sporadic inclusion body myositis is not linked to Methionine homozygosity of codon 129 of the prion protein. Neurology. 2000;55(8):1235.

Tabrizi SJ*, **Orth M***, Wilkinson JM, Taanman JW, Warner TT, Cooper JM, Schapira AHV. Expression of mutant α-synuclein causes increased susceptibility to dopamine toxicity. Hum Mol Gen 2000; 9:2683-9. ***equal first authors**.

Orth M, Schapira AHV. Prion codon 129 homozygosity and sporadic inclusion body myositis. Neurology 2001; 57: 368.

Orth M, Cooper JM, Bates GP, Schapira AHV. Inclusion formation in Huntington's disease R6/2 mouse muscle cultures. J Neurochem. 2003 Oct;87(1):1-6.

Orth M, Tabrizi SJ, Cooper JM, Schapira AHV. Alpha-synuclein expression in HEK293 cells enhances the mitochondrial sensitivity to rotenone. Neurosci Lett. 2003 Nov 6;351(1):29-32.

Orth M, Tabrizi SJ, Tomlinson C, Messmer K, Korlipara LVP, Schapira AHV, Cooper JM. G209A mutant alpha-synuclein expression specifically enhances dopamine induced oxidative stress. Neurochem Int 2004;45:669-676.

Human Molecular Genetics, 2000, Vol. 9, No. 18 2683–2689

Expression of mutant α-synuclein causes increased susceptibility to dopamine toxicity

Sarah J. Tabrizi[1,+], Michael Orth[1,+], J. Max Wilkinson[2], Jan-Willem Taanman[1], Thomas T. Warner[1], J. Mark Cooper[1] and Anthony H.V. Schapira[1,3,§]

[1]University Department of Clinical Neurosciences, [2]Renal Unit, Royal Free and University College Medical School and [3]Institute of Neurology, University College London, London NW3 2PF, UK

Received 12 July 2000; Revised and Accepted 1 September 2000

Mutations of the α-synuclein gene have been identified in autosomal dominant Parkinson's disease (PD). Transgenic mice overexpressing wild-type human α-synuclein develop motor impairments, intraneuronal inclusions and loss of dopaminergic terminals in the striatum. To study the mechanism of action through which mutant α-synuclein toxicity is mediated, we have generated stable, inducible cell models expressing wild-type or PD-associated mutant (G209A) α-synuclein in human-derived HEK293 cells. Increased expression of either wild-type or mutant α-synuclein resulted in the formation of cytoplasmic aggregates which were associated with the vesicular (including monoaminergic) compartment. Expression of mutant α-synuclein induced a significant increase in sensitivity to dopamine toxicity compared with the wild-type protein expression. These results provide an explanation for the preferential dopaminergic neuronal degeneration seen in both the PD G209A mutant α-synuclein families and suggest that similar mechanisms may underlie or contribute to cell death in sporadic PD.

INTRODUCTION

Parkinson's disease (PD) is characterized by the loss of dopaminergic neurons in the substantia nigra pars compacta and by the formation of Lewy bodies in a proportion of surviving neurons. The identification of mutations in several different genes in familial parkinsonism (1–4), increased concordance amongst identical twins when studied with fluoro-dopa positron emission tomography (5), or if onset is before 50-years-old (6), and the increased familial frequency of PD (7) all support the proposition that there may be a significant genetic contribution to the aetiology of this disease. Mutations in the α-synuclein gene have now been identified in several PD families (1,2,8), although they are not common causes of either familial (9) or sporadic PD (10,11). The presence of α-synuclein has also been demonstrated in Lewy bodies in the brains of sporadic PD patients (12) suggesting the possibility that aggregation of this protein may be relevant to disease pathogenesis. In a recent report, transgenic mice overexpressing wild-type human α-synuclein developed deficits in motor performance, α-synuclein containing neuronal intranuclear and intracytoplasmic inclusions and loss of dopaminergic terminals in the striatum, proportional to the degree of α-synuclein expression (13). We have developed stable, inducible human-derived cell lines expressing wild-type or mutant (G209A) α-synuclein to investigate the morphological and biochemical consequences of wild-type and mutant protein expression.

RESULTS

There was only very weak expression of α-synuclein in the pIND.α-syn- or pIND.α-syn/G209A-transfected cells in the absence of ponasterone A (Fig. 1A) and likewise no or only weak expression in the pIND.zero cells. This suggests that the background expression of pIND.α-syn and pIND.α-syn/G209A cells is the result of the host gene and not due to leakage of the introduced gene constructs. Furthermore, the level of α-synuclein expression (wild-type or mutant) was proportional to the concentration of ponasterone A used with the inducible cell lines (Fig. 2). Thus, the production of α-synuclein protein by these cell lines was tightly controlled by ponasterone A.

Treatment of the pIND.α-syn or pIND.α-syn/G209A cell lines with 5 μM ponasterone A for 48 h led to the formation of intracellular aggregates containing α-synuclein (Fig. 1B–D). No difference in the number or location of aggregates formed was observed between cells expressing wild-type or mutant α-synuclein (Fig. 1C and D). α-synuclein did not co-localize with markers for the cell nucleus, Golgi, mitochondria or lysosomes (Fig. 1C–F and H). Neither the wild-type (data not shown) nor mutant α-synuclein deposits stained for ubiquitin (Fig. 1G). However, co-localization of both wild-type (data not shown) and mutant α-synuclein was observed with vesicle-associated membrane protein (VAMP), indicating that α-synuclein was associated with intracellular vesicles (Fig. 1I). Staining for vesicular monoamine transporter (VMAT 1) showed that a proportion of vesicles were positive for both this protein and α-synuclein (Fig. 1J).

The expression of wild-type or mutant α-synuclein did not cause any significant level of excess cell death (Fig. 3). This

+These authors contributed equally to this work
§To whom correspondence should be addressed. Tel: +44 207 830 2012; Fax: +44 207 431 1577; Email: schapira@rfhsm.ac.uk

suggests that in the time-frame of expression used (96 h) neither wild-type nor mutant α-synuclein proteins were toxic.

In view of the likely co-localization of α-synuclein with dopamine-containing vesicles and the known toxicity of dopamine through its production of reactive oxygen species (14,15), we investigated the effect of wild-type and mutant α-synuclein expression on dopamine toxicity. Following treatment with ponasterone A (5 μM) for 48 h before and during the 48 h of dopamine exposure, pIND.zero cell lines showed a significant increase in cell death with 0.75 and 1 mM dopamine ($P = 0.0002$

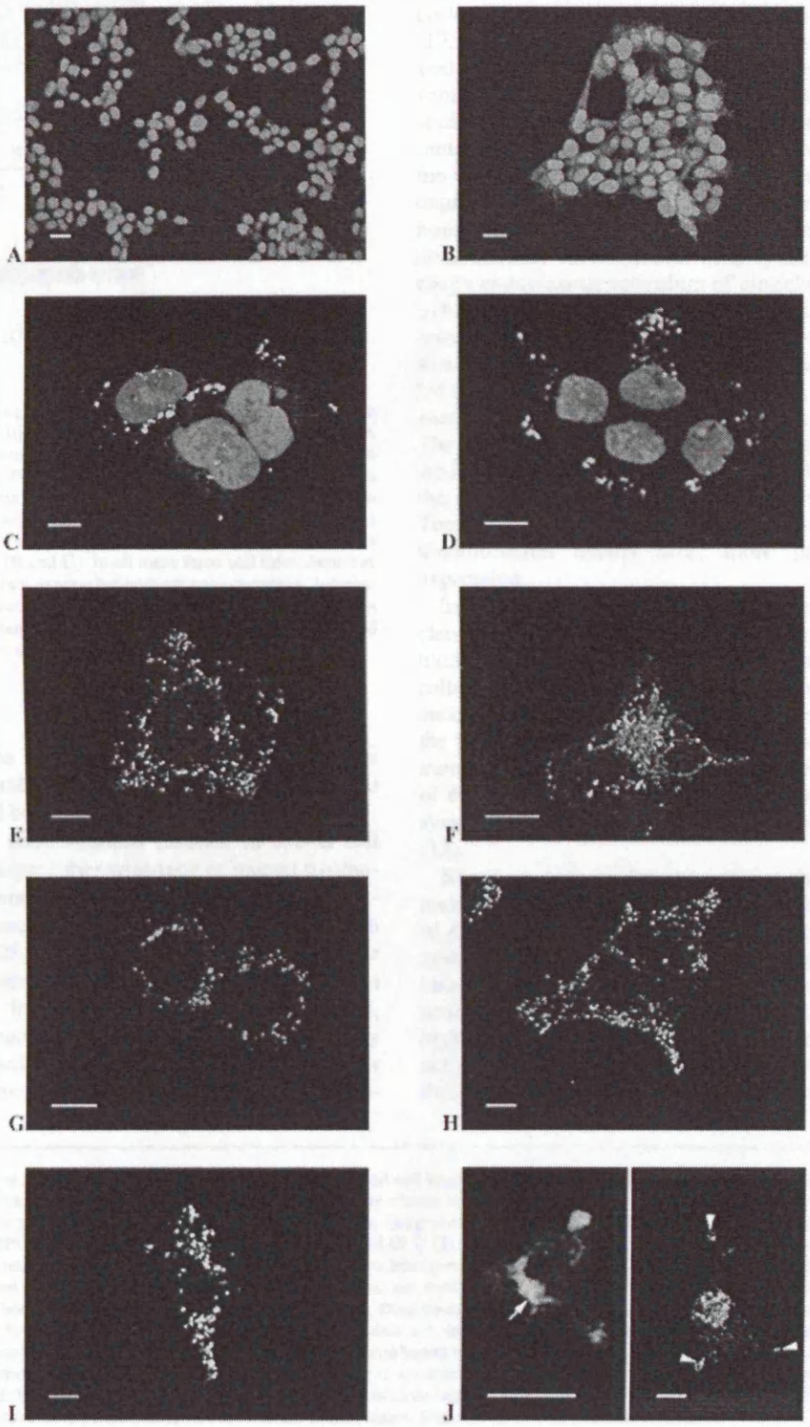

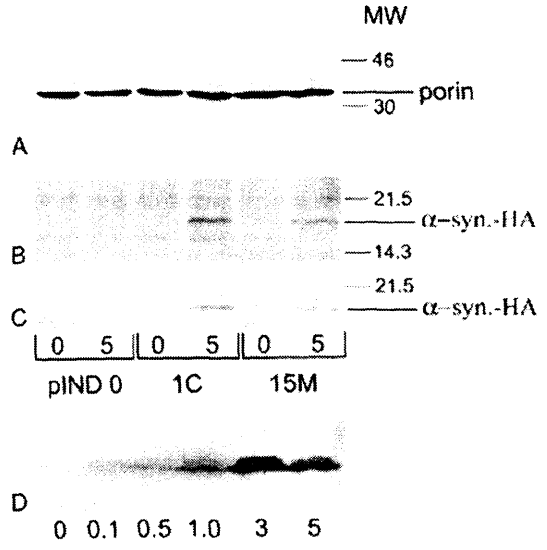

Figure 2. Western blots showing the induction of α-synuclein expression with ponasterone A. pIND (pIND.0), pIND.α-syn (IC) and pIND.α-syn/G209A (15M) transfected cell lines were grown, cell extracts prepared and western blots performed as described. Porin immunoreactivity was equal in all lanes and indicated equivalent protein loading (**A**). Both α-synuclein and HA antibodies detected a band representing the α-synuclein–HA complex at ~20 kDa with 5 μM ponasterone A in the wild-type and mutant α-synuclein cell lines but not in the pIND.zero lines (**B** and **C**). In all these three cell lines there was no detectable α-synuclein protein expression without ponasterone A. Increasing concentrations of ponasterone A (0.1, 0.5, 1.0, 3.0 and 5 μM) resulted in greater expression of the mutant protein (**D**). Similar results were obtained with the wild-type pIND.α-syn cell lines (data not shown).

for both) confirming the toxicity of dopamine in these cells (Fig. 3). These concentrations of dopamine are equivalent to those reported in the cell bodies of dopaminergic neurons (16).

Increasing dopamine concentrations resulted in excess cell death in the lines expressing either wild-type or mutant α-synuclein. At 0.5 mM dopamine both wild-type and mutant α-synuclein expression caused increased cell death compared with pIND.zero lines ($P = 0.05$ and $P = 0.007$, respectively) but there was no significant difference in susceptibility between the two α-synuclein lines. At higher concentrations of dopamine, however, mutant α-synuclein expression caused significantly greater cell death than wild-type ($P = 0.0003$ and $P = 0.02$ for 0.75 and 1 mM dopamine, respectively). There was no significant difference in cell toxicity between pIND.zero and wild-type α-synuclein lines at these concentrations.

DISCUSSION

α-synuclein has been shown to bind to vesicles, be transported by the fast component of axonal transport in rat optic nerve and co-localize with synaptophysin in the presynaptic terminal (17,18). The G88C mutant form of α-synuclein had decreased vesicle binding compared with the mutant G209A or wild-type forms in this rat model. Our fluorescent immunocytochemical studies showed that, in human cultured cells, wild-type and mutant forms of human α-synuclein are also associated with the vesicular component within cells, including those vesicles expressing the monoamine transporter. Overexpression of human wild-type α-synuclein in a transgenic mouse model demonstrated accumulation of α-synuclein aggregates in the rough endoplasmic reticulum of cingulate cortex neurons (13) indicating that α-synuclein aggregates may also be located outside vesicles. In some cells of our model, increased expression of wild-type or mutant α-synuclein with ponasterone A led to diffuse, as opposed to aggregated, protein deposits. Why some cells did and others did not form aggregates was unclear. The observation that α-synuclein aggregates were not ubiquinated in our cell system was surprising. However, it may be that the time-scale for ubiquitination to be detected was too brief. Terminally differentiated cells are needed to assess whether ubiquitination occurs after more prolonged α-synuclein expression.

In our model, neither wild-type nor mutant G209A α-synuclein expression resulted in cell death. In a transient transfection model of G209A mutant α-synuclein expression in HEK293 cells, however, excess cell death was observed (19). The difference in these results may lie in the level of protein expression—the transient transfections perhaps producing greater levels of mutant protein. Nevertheless, our results are in accord with those of the mouse model of overexpression of human wild-type α-synuclein in which there was no evidence of excess cell death (13).

Based on our results, we suggest that at least part of the toxicity of mutant α-synuclein is mediated via its enhancement of dopamine toxicity. The mice overexpressing human wild-type α-synuclein developed intraneuronal inclusions, but no increased cell death of tyrosine hydroxylase (TH)-positive neurons (13). However, at 12 months, those mice with the highest α-synuclein expression levels had reduced striatal TH activity, decreased density of TH-positive terminals and a deficit in motor performance. Thus long-term wild-type α-

Figure 1. Immunocytochemical localization of α-synuclein in HEK293-derived cell lines. HEK293-derived cell line ECR293 was transfected with pIND, pIND.α-syn or pIND.α-syn/G209A. Wild-type or mutant α-synuclein clonal lines were chosen where >70% of cells expressed the induced protein. Immunocytochemistry was performed with antibodies to α-synuclein (**A–D**, green fluorescence), the Golgi network (**E**), MitoTracker (**F**), ubiquitin (**G**), lysosomes (**H**), vesicle-associated membrane protein (VAMP) (**I**) and vesicular monoamine transporter (VMAT 1) (**J**). The cell nucleus was stained with propidium iodide as described. Nuclei were clearly visible but there was negligible background expression of α-synuclein (green fluorescence) in HEK293 cells with the wild-type or mutant constructs (A). Induction with ponasterone A increased expression of both wild-type (data not shown) and G209A mutant α-synuclein (B) with the formation of cytoplasmic but no nuclear aggregates for both wild-type (C) and mutant (D) α-synuclein. Dual staining with green fluorescence for the Golgi network (E) and lysosomes (H) showed separate localization for mutant (red fluorescence) and wild-type (data not shown) α-synuclein. Co-staining with the MitoTracker (red fluorescence) showed that α-synuclein was not localized in the mitochondria (F). This was confirmed with the COI subunit of cytochrome oxidase (data not shown). Dual labelling studies indicated that neither the mutant α-synuclein (red) nor wild-type α-synuclein (data not shown) aggregates stained for ubiquitin (green) (G). α-synuclein (red) did co-localize with VAMP (green) (I) as shown by the merged fluorescence (yellow) and with VMAT-1 (red) with green fluorescence for α-synuclein (J) although this was not exclusive to the distribution of either of the vesicle stains. Bars: (A and B) 20 μm; (C–J) 10 μm.

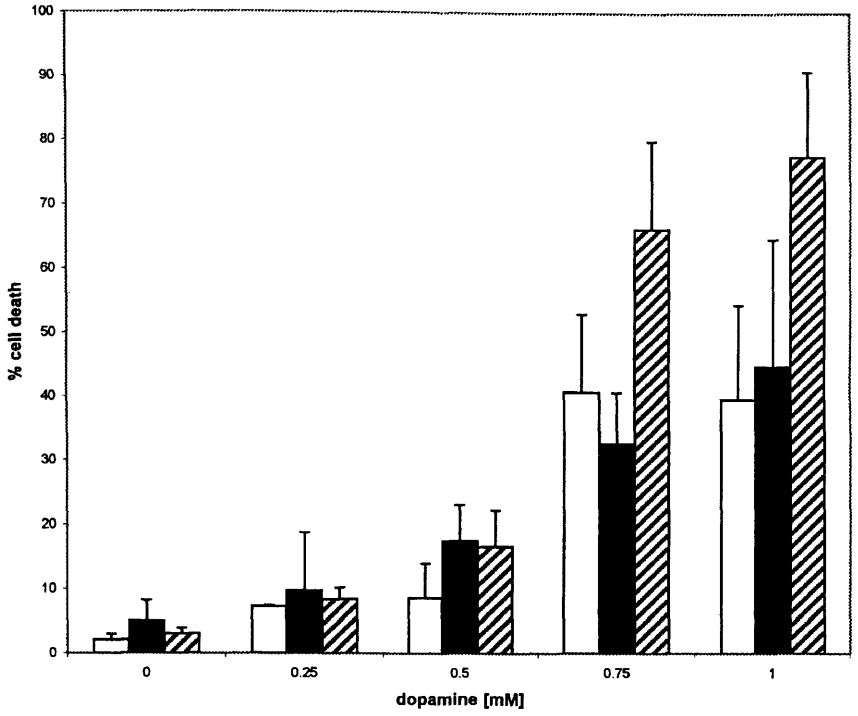

Figure 3. Cell death in pIND.zero (open bars), pIND.α-syn (black bars) and pIND.α-syn/G209A (hatched bars) cell lines with increasing concentrations of dopamine. Incubations and quantitation of cell death were undertaken as described. In the absence of dopamine, there was no significant cell death in any cell line with 5 μM ponasterone A treatment over 96 h. All concentrations of dopamine used resulted in a significant increase in cell death. At 0.75 and 1.0 mM dopamine, the degree of cell death was significantly greater in the mutant α-synuclein cell line than in either the pIND.zero or pIND.α-syn lines ($P = 0.0003$ and $P = 0.02$, respectively).

synuclein overexpression is toxic. Our model would predict that overexpression of mutant G209A α-synuclein in such mice would induce a more rapid and intense loss of striatal TH-positive terminals and loss of dopamine-containing neurons, with an earlier onset of motor dysfunction. In this context, it is interesting to note that those families with the G209A mutation develop PD at a much earlier mean age than those with idiopathic PD and also have a more accelerated course with death an average 9.7 years after onset (20). Our results are also consistent with the *Drosophila* model of wild-type and mutant α-synuclein expression in which there is aggregate formation, relative selective dopaminergic cell loss and locomotor dysfunction (21). Furthermore, expression of human G209A mutant but not wild-type α-synuclein selectively led to apoptosis of dopamine neurons in rat primary mesencephalic cultures (22). Both the mutant and wild-type forms of human α-synuclein enhanced the toxicity of 6-hydroxydopamine. Similar results were also seen at low concentrations of the pre-aggregated fibrillogenic 61–95 kDa fragment of α-synuclein in the same model system (23).

At present the mechanism by which mutant α-synuclein increases dopamine toxicity is not known. α-synuclein is highly expressed in human brain presynaptic terminals (24) and in rat substantia nigra pars compacta (25), and is also a major component in the Lewy bodies of dopamine-containing neurons in PD brains (12). Thus, α-synuclein is expressed at sites of high dopamine content and it may function to modulate dopamine release (26).

Dopamine-induced cell death has been confirmed in a number of systems (27–29). Dopamine is unstable and is readily oxidized to the dopamine quinone and generates superoxide and hydrogen peroxide. Dopamine can also covalently modify free cysteine, cysteine in glutathione and cysteinyl residues in protein (30). Sulphydryl groups on cysteines are often associated with active sites on proteins and thus their modification could alter function irreversibly. Interestingly, the formation of *S*-cysteinyl dopamine on protein is associated with the loss of monoaminergic striatal terminals in dopamine-induced toxicity (31). Thus, dopamine toxicity may be mediated via increased reactive oxygen species generation and by direct protein modification.

In our expression model, the synergistic toxic effect of mutant α-synuclein and dopamine occurs relatively rapidly. Dopamine-mediated free radical and sulphydryl group damage may increase the predisposition for mutant α-synuclein to form aggregates, a suggestion supported by the finding that α-synuclein aggregation was increased by ferric ion or by ferrous ion in the presence of hydrogen peroxide (32). However, during the time course of our experiments, increased aggregation of wild-type or mutant α-synuclein was not observed at light microscopic level in our cell system. The toxicity of dopamine may be increased by failure to compartmentalize it within vesicles. The

damaging effects of dopamine would therefore be increased if mutant α-synuclein interfered with the function of the monoamine transporter, thereby increasing intracytoplasmic concentrations and the potential for cell damage sufficient to cause cell death. This hypothesis would be consistent with the results of our study, the defective modulation of dopamine release and significant decrease in striatal dopamine levels in α-synuclein knockout mice (26), as well as the observations described above in the G209A PD families. A defect of dopamine compartmentalization could promote a slow but progressive loss of striatal terminals and nigral neurons. The overexpression of wild-type α-synuclein might lead to a similar effect, but over a longer period—such as seen in the human wild-type α-synuclein transgenic mice described above (13).

The relevance of these data for patients with idiopathic PD without α-synuclein mutations might lie in the potential for wild-type α-synuclein to be the target protein for a variety of pathogenetic pathways including dopamine toxicity, oxidative stress and possibly mitochondrial dysfunction. The gradual accumulation of auto-oxidation products may promote α-synuclein aggregation, Lewy body formation and cell death over prolonged periods.

MATERIALS AND METHODS

Generation of cell model

Total RNA was isolated as described by Chomczynski and Sacchi (33) from lymphoblasts from a male PD patient with the G209A α-synuclein mutation (a kind gift from M. Polymeropoulos, NIH, Bethesda, MD) and control lymphoblasts with wild-type α-synuclein (from ECACC, Wiltshire, UK). cDNA was generated by RT–PCR using the cDNA Cycle kit (Invitrogen, Groningen, The Netherlands) according to the manufacturer's instructions. The High Fidelity system (Roche/Boehringer, Mannheim, Germany) was used for all subsequent PCR. Full-length α-synuclein cDNA was amplified using 5′-CATTCGACGACAGTGTGGTGT-3′ (nucleotides 16–37) as a forward primer and 5′-CTGCTGAT-GGAAGACTTCGAG-3′ (nucleotides 586–607) as a reverse primer. In a subsequent PCR, the open reading frame of α-synuclein and its 31 nucleotide 5′ untranslated region was amplified using 5′-AAGGTACCGACAGTGTGGTGTAAAGGAAT-3′ as a forward primer (nucleotides 26–44 with a 5′ *Kpn*I site) and 5′-AATGATCAAGCGTAGTCTGGGACGTCGTATGGGTAGG-CTTCAGGTTCGTAGTCTTAC-3′ as a reverse primer [nucleotides 456–478 with a 3′ haemagglutinin (HA) epitope coding sequence and *Bcl*I site]. Both mutated G209A and wild-type α-synuclein amplified fragments were restricted with *Kpn*I and *Bcl*I and ligated into the *Kpn*I and *Bam*HI sites of pIND (Invitrogen). The correct sequence was confirmed by Big Dye automated sequencing (ABI 310; Perkin Elmer, Warrington, UK). HEK293 cells with stable transfection of the pVgRxR plasmid (ECR 293; Invitrogen) were grown at 37°C in a humidified atmosphere containing 5% CO_2 in growth medium consisting of Dulbecco's modified Eagle's medium (DMEM) and 4.5 μg/l glucose, 10% fetal calf serum, 50 U/ml penicillin, 50 μg/ml streptomycin, 400 μg/ml Zeocin, 50 μg/ml uridine and 110 μg/ml sodium pyruvate. ECR293 cells were transfected with 5 μg of pIND constructs containing either no insert or inserts encoding wild-type α-synuclein with a C-terminal HA epitope (pIND.α-syn) or G209A mutant α-synuclein with a C-terminal HA epitope (pIND.α-syn/G209A) using the Escort (Sigma, Poole, UK) lipofection method according to the manufacturer's instructions. Twenty-four hours post-transfection, stable clones were selected in the presence of 400 μg/ml G418 and stable cell lines generated from individual clones. All cells resistant to G418 following transfection with pIND were used as a control cell line (pIND.zero cells). Clonal cell lines transfected with either pIND.α-syn or pIND.α-syn/G209A were treated with 5 μM ponasterone A for 48 h and screened by immunocytochemistry for the expression of α-synuclein–HA construct using an antibody to HA (1:200 dilution; Boehringer). DNA was extracted from each cell line and the α-synuclein insert was amplified using pIND multiple cloning site forward and reverse sequencing primers (Invitrogen) and sequenced as above to confirm the correct sequence.

Immunocytochemistry

Cells were harvested with Versene (1:5000; Gibco BRL, Paisley, UK) and plated out on glass coverslips in a 35 mm dish with 2 ml of medium. They were allowed to settle for 24 h before induction of α-synuclein expression with 5 μM ponasterone A. After 48 h of protein expression the coverslips were washed in phosphate-buffered saline (PBS). Cells were fixed for 20 min in 4% (w/v) paraformaldehyde and then for 15 min at –20°C in methanol. All the following incubations took place in a humid chamber at 37°C. Fixation was followed by blocking with 10% normal goat serum in PBS for 1 h followed by incubation with the primary antibody for 3 h. After three washes in PBS, primary antibodies raised in mouse were developed for 1 h with respective goat anti-mouse Alexa 488 conjugates (1:200; Molecular Probes, Eugene, OR) whereas the rabbit or goat primary antibodies were detected with goat anti-rabbit or donkey anti-goat Alexa 568 conjugates, respectively (1:1000; Molecular Probes). After three washes in PBS, coverslips were mounted on glass slides in Citifluor with 1 μg/ml DAPI. Dual labelling consisted of an incubation with the rabbit or goat primary antibody and the appropriate fluorescent secondary antibody, followed by a mouse monoclonal antibody and anti-mouse fluorescent secondary antibody. The following primary antibodies were used: α-synuclein either mouse monoclonal antibody (mAb) (1:200; Zymed, San Francisco, CA) or rabbit polyclonal antibody (1:2000; Chemicon, Temecula, CA), HA (mAb anti-HA, 1:200; Roche/Boehringer), cytochrome *c* oxidase (mAb anti-COX I subunit, 1:200; Molecular Probes), lysosomes (mAb anti-lysosomal associated membrane protein 1, 1:400; PharMingen, San Diego, CA), Golgi (mAb anti-Golgi zone, 1:200; Chemicon), VAMP (mAb), anti-VAMP (1:200; Chemicon), VMAT 1 (goat polyclonal antibody, anti-VMAT 1, 1:50; Santa Cruz Biotechnology, Santa Cruz, CA) and ubiquitin (mAb anti-ubiquitin, 1:300; Chemicon). In addition, cells were labelled with propidium iodide (1 μg/ml) and Mitotracker (CMXRos-H_2, 3 μM; Molecular Probes). Slides were evaluated with a krypton–argon laser (MRC 600; BioRad, Hercules, CA) attached to an Olympus BH2-RFCA fluorescence microscope.

Western blotting

Cells were plated at 40% confluency and allowed to settle for 24 h before the addition of ponasterone A (0–5 μM). After 48 h the cells were scraped, washed in PBS and solubilized in 100 mM Tris–HCl, 8% (w/v) SDS, 24% (w/v) glycerol, 0.5%

(v/v) mercaptoethanol, pH 6.9, containing a cocktail of protease inhibitors. Samples were heated at 37°C for 10 min, centrifuged at 16 060 *g* for 10 min, separated on a 15% polyacrylamide gel containing SDS and transferred to PVDF membrane (Immobilon-P; Millipore, Bedford, MA) following standard techniques (34). Equal protein loading was verified by comparison with a gel stained with Coomassie in parallel. Blots were blocked using 10% (w/v) proprietary milk powder, incubated with anti-HA rat mAb (1:3000; Boehringer) as primary and sheep anti-rat Ig–horseradish peroxidase (HRP) (Fab fragments, 1:3000; Boehringer) as the secondary antibody. Blots were also incubated with anti-α-synuclein mAb (1:4000; Zymed) and anti-porin (1:25 000; Calbiochem, Nottingham, UK) mouse monoclonal antibodies as primary and rabbit anti-mouse HRP (1:3000; BioRad) as secondary antibody. All blots were developed by chemiluminescence detection (NEN, Life Science Products, Boston, MA).

Cell death experiments

Cells were harvested with Versene (1:5000; Gibco BRL), counted with a haemocytometer and plated out at a density of ~62 500 cells/well of a 12-well plate. After 1 day, 5 μM ponasterone A was added. After 48 h the medium was replaced with phenol-red free medium containing ponasterone A (0–5 μM) and dopamine (0–1000 μM) for 48 h. The supernatant of each well was aspirated, the cells washed with PBS and harvested by the addition of Versene and 10% (v/v) Triton X-100. Pairs of supernatant and cells of the same well were stored at –80°C until assayed for lactate dehydrogenase (LDH) spectrophotometrically (35) or using a LDH Cytotoxicity Detection kit (TaKaRa Biomedicals, Tokyo, Japan). The ratio of LDH activity in the supernatant to the total LDH activity was taken as the percentage of cell death. Protein was determined with the BCA kit (Pierce, Rockford, IL) using bovine serum albumin as standard.

ACKNOWLEDGEMENTS

The authors would like to thank V. Georgiadis for help with the western blot. This study was supported by grants from the Parkinson's Disease Society (UK), the Medical Research Council, the Wellcome Trust, the British Medical Association and the Deutsche Forschungsgemeinschaft.

REFERENCES

1. Polymeropoulos, M.H., Lavedan, C., Leroy, E., Ide, S.E., Dehejia, A., Dutra, A., Pike, B., Root, H., Rubenstein, J., Boyer, R. *et al.* (1997) Mutation in the α-synuclein gene identified in families with Parkinson's disease. *Science*, **276**, 2045–2047.
2. Kruger, R., Kuhn, W., Muller, T., Woitalla, D., Graber, M., Kosel, S., Przuntek, H., Epplen, J.T., Schols, L. and Riess, O. (1998) Ala30Pro mutation in the gene encoding alpha-synuclein in Parkinson's disease. *Nature Genet.*, **18**, 106–108.
3. Kitada, T., Asakawa, S., Hattori, N., Matsumine, H., Yamamura, Y., Minoshima, S., Yokochi, M., Mizuno, Y. and Shimizu, N. (1998) Mutations in the parkin gene cause autosomal recessive juvenile parkinsonism. *Nature*, **392**, 605–608.
4. Leroy, E., Boyer, R., Auburger, G., Leube, B., Ulm, G., Mezey, E., Harta, G., Brownstein, M.J., Jonnalagada, S., Chernova, T. *et al.* (1998) The ubiquitin pathway in Parkinson's disease. *Nature*, **395**, 451–452.
5. Piccini, P., Burn, D.J., Ceravolo, R., Maraganore, D. and Brooks, D.J. (1999) The role of inheritance in sporadic Parkinson's disease: evidence from a longitudinal study of dopaminergic function in twins. *Ann. Neurol.*, **45**, 577–582.
6. Tanner, C.M., Ottman, R., Goldman, S.M., Ellenberg, J., Chan, P., Mayeux, R. and Langston, J.W. (1999) Parkinson's disease in twins: an etiologic study. *J. Am. Med. Assoc.*, **281**, 341–346.
7. Gasser, T. (1998) Genetics of Parkinson's disease. *Ann. Neurol.*, **44**, S53–S57.
8. Markopolou, K., Wzolek, Z.K., Pfeiffer, R.F. and Chase, B.A. (1999) Reduced expression of the G209A α-synuclein allele in familial parkinsonism. *Ann. Neurol.*, **46**, 374–381.
9. Vaughan, J.R., Farrer, M.J., Wszolek, K., Gasser, T., Durr, A., Agid, Y., Bonifati, V., De Michele, G., Volpe, G., Lincoln, S. *et al.* (1998) Sequencing of the α-synuclein gene in a large series of cases of familial Parkinson's disease fails to reveal any further mutations. *Hum. Mol. Genet.*, **7**, 751–753.
10. Warner, T.T. and Schapira, A.H.V. (1998) The role of alpha-synuclein gene mutation in patients with sporadic Parkinson's disease in the UK. *J. Neurol. Neurosurg. Psychiatry*, **65**, 378–379.
11. Farrer, M., Wavrant-De Vrieze, F., Crook, R., Boles, L., Perez-Tur, J., Hardy, J., Johnson, W.G., Steele, J., Maraganore, D., Gwinn, K. and Lynch, T. (1998) Low frequency of α-synuclein mutations in familial Parkinson's disease. *Ann. Neurol.*, **43**, 394–397.
12. Spillantini, M.G., Schmidt, M.L., Lee, V.M., Trojanowski, J.Q., Jakes, R. and Goedert, M. (1997) Alpha-synuclein in Lewy bodies. *Nature*, **388**, 839–840.
13. Masliah, E., Rockenstein, E., Vienbergs, I., Mallory, M., Hashimoto, M., Takeda, A., Sisk, Y.S.A. and Mucke, L. (2000) Dopaminergic loss and inclusion body formation in α-synuclein mice: implications for neurodegenerative disorders. *Science*, **287**, 1265–1269.
14. Tse, D.C., McCreery, R.L. and Adams, R.N. (1976) Potential oxidative pathways of brain catecholamines. *J. Med. Chem.*, **19**, 37–40.
15. Graham, D.G. (1978) Oxidative pathways for catecholamines in the genesis of neuromelanin and cytotoxic quinones. *Mol. Pharmacol.*, **14**, 633–643.
16. Jonsson, G. (1971) Quantitation of fluorescence of biogenic monoamines. *Prog. Histochem. Cytochem.*, **2**, 299–344.
17. Jensen, P.H., Nielsen, M.S., Jakes, R., Dotti, C.G. and Goedert, M. (1998) Binding of alpha-synuclein to brain vesicles is abolished by familial Parkinson's disease mutation. *J. Biol. Chem.*, **273**, 26292–26294.
18. Murphy, D.D., Rueter, S.M., Trojanowski, J.Q. and Lee, V.M.Y. (2000) Synucleins are developmentally expressed, and alpha-synuclein regulates the size of the presynaptic vesicular pool in primary hippocampal neurons. *J. Neurosci.*, **20**, 3214–3220.
19. Ostrerova, N., Petrucelli, L., Farrer, M., Mehta, N., Choi, P., Hardy, J. and Wolizin, B. (1999) α-synuclein shares physical and functional homology with 14-3-3-proteins. *J. Neurosci.*, **19**, 5782–5791.
20. Golbe, LI.., Farrell, T.M. and Davis, P.H. (1988) Case-control study of early life dietary factors in Parkinson's disease. *Arch. Neurol.*, **45**, 1350–1353.
21. Feany, M.B. and Bender, W.W. (2000) A *Drosophilia* model of Parkinson's disease. *Nature*, **404**, 394–398.
22. Zhou, W.B., Hurlbert, M.S., Schaack, K., Prasad, K.N. and Freed, C.R. (2000) Overexpression of human alpha-synuclein causes dopamine neuron death in rat primary culture and immortalized mesencephalon-derived cells. *Brain Res.*, **866**, 33–43.
23. Forloni, G., Bertani, H., Calella, A.M., Thaler, F. and Invernizzi, R. (2000) α-synuclein and Parkinson's disease: selective neurodegenerative effect of α-synuclein fragment on dopaminergic neurons *in vitro* and *in vivo*. *Ann. Neurol.*, **47**, 632–640.
24. Irizarry, M.C., Kim, T.W., McNamara, M., Tanzi, R.E., George, J.M., Clayton, D.F. and Hyman, B.T. (1996) Characterization of the precursor protein of the non A beta component of senile plaques (NACP) in the human central nervous system. *J. Neuropathol. Exp. Neurol.*, **55**, 889–895.
25. Kholodilov, N.G., Neystat, M., Oo, T.F., Larsen, K.E., Sulzer, D. and Burne, R.E. (1999) Increased expression of rat synuclein in the substantia nigra pars compacta identified by mRNA differential display in a model of developmental target injury. *J. Neurochem.*, **73**, 2586–2599.
26. Abeliovich, A., Schmitz, Y., Fariñas, I., Choi-Lundberg, D., Ho, W.S., Castillo, P.E., Shinsky, N., Verdugo, J.M.G., Armanini, M., Ryan, A. *et al.* (2000) Mice lacking α-synuclein display functional deficits in the nigrostriatal dopamine system. *Neuron*, **25**, 239–252.
27. Lai, C.T. and Yu, P.H. (1997) Dopamine and L-dopa induced cytotoxicity towards catecholaminergic neuroblastoma. *Biochem. Pharmacol.*, **53**, 363–371.
28. Ziv, I., Melamed, E., Nardi, N., Lurie, D., Achiron, A., Offen, D. and Barzilai, A. (1994) Dopamine induces apoptosis-like cell death in cultured sympathetic neurons—a possible novel pathogenetic mechanism in Parkinson's disease. *Neurosci. Lett.*, **170**, 136–140.
29. Alexander, T., Sortwell, C.E., Sladek, C.D., Roth, R.H. and Steece-Collier, K. (1997) Comparison of neurotoxicity following repeated administration of

L-dopa, D-dopa and dopamine to embryogenic mesencephalic dopamine neurons in cultures derived from Fischer 344 and Sprague-Dawley donors. *Cell Transplant.*, **6**, 309–315.
30. LaVoie, M.J. and Hastings, T.G. (1999) Peroxynitrite and nitrite induced oxidation of dopamine: implications for nitric oxide in dopaminergic cell loss. *J. Neurochem.*, **73**, 2546–2554.
31. Hastings, T.G., Lewis, D.A. and Zigmond, M.J. (1996) Role of oxidation in the neurotoxic effects of intrastriatal dopamine injections. *Proc. Natl Acad. Sci. USA*, **93**, 1956–1961.
32. Hashimoto, M., Hsu, L.J., Xia, Y., Takeda, A., Sisk, A., Sundsmo, M. and Masliah, E. (1999) Oxidative stress induces amyloid-like aggregate formation of NACP-α-synuclein *in vitro*. *Neuroreport*, **106**, 717–721.
33. Chomczynski, P. and Sacchi, N. (1987) Single-step method of RNA isolation by acid guanidinium thiocyanate-phenol-chloroform extraction. *Anal. Biochem.*, **162**, 156–159.
34. Towbin, H., Staehelin, T. and Gordon, J. (1979) Electrophoretic transfer of protein form polyacrylamide gels to nitrocellulose sheets: procedure and some applications. *Proc. Natl Acad. Sci. USA*, **76**, 4350–4354.
35. Clark, J.B. and Nicklas, W.J. (1970) The metabolism of rat brain mitochondria; preparation and characterisation. *J. Biol. Chem.*, **245**, 4724–4731.